Recipient dendritic cells dictate allograft fate

by

Sherrie Jill Divito

B.A. The College of Wooster, 2003

Submitted to the Graduate Faculty of

School of Medicine in partial fulfillment

of the requirements for the degree of

Doctor of Philosophy

University of Pittsburgh

2009

UNIVERSITY OF PITTSBURGH

SCHOOL OF MEDICINE

This dissertation was presented

by

Sherrie Jill Divito

It was defended on

June 12th, 2009

and approved by

Fadi Lakkis MD, Professor, Departments of Surgery and Immunology

Adriana Larregina MD, PhD, Associate Professor, Departments of Dermatology and Immunology

Russell Salter PhD, Professor, Department of Immunology

Donna Beer Stolz, PhD, Associate Professor, Department of Cell Biology and Physiology

Dissertation Advisor: Adrian Morelli MD, PhD, Associate Professor, Department of Surgery

Copyright © by Sherrie J. Divito

2009

RECIPIENT DENDRITIC CELLS DICTATE ALLOGRAFT FATE

Sherrie J. Divito, PhD

University of Pittsburgh, 2009

Organ transplantation is a life-saving and increasingly common procedure, as it often serves as the only treatment available for end-stage organ disease. Although the constant development of new and more effective immunosuppressive drugs has revolutionized the prevention and treatment of acute graft rejection, these drugs have significant toxicity, greatly increase patient susceptibility to neoplasms and infection and exert little impact on chronic rejection.

A major obstacle to developing improved therapeutics is a lack of understanding the mechanisms by which the adaptive immune response is initiated, and how cellular therapies impact this response. Previous research has provided a mechanistic scaffold, however numerous gaps, often filled with assumptions rather than data, remain. In this dissertation, I demonstrate that contrary to current dogma, dendritic cell (DC)-based therapies simply serve as a source of alloantigen, and therefore have comparable efficacy to alternative cellular therapies. Further, I show that contradictory to the current paradigm of direct pathway T cell priming, recipient antigen-presenting cells (APC) stimulated via CD40 ligation by indirect pathway $CD4^+$ T cells is requisite for a direct pathway response and allograft rejection. Conversely, I did validate the assumption that donor passenger APC are required for the direct pathway T cell response, but further show that they are also required for the indirect pathway T cell response, indicating that donor APC serve as a source of alloantigen for presentation by recipient APC. Finally, through investigating the role of recipient APC in cardiac allograft rejection, I identified that the recently described population of inflammatory monocyte-derived DC play a crucial role as effector cells

that mediate a DTH-like response within cardiac allografts during acute rejection, while at the same time, inhibiting T cell effector responses within the graft and systemically.

Overall, our data provide essential puzzle pieces to understanding the processes of acute allograft rejection and insight into the utility of DC-based therapies for transplantation.

TABLE OF CONTENTS

PREFACE ..... **XVI**

1.0 INTRODUCTION **1**

1.1 DENDRITIC CELLS **1**

1.1.1 Conductors of the adaptive immune response **1**

1.1.2 Types of DC **3**

1.1.2.1 Conventional DC **4**

1.1.2.2 Plasmacytoid DC **4**

1.1.2.3 Inflammatory DC **5**

1.1.3 DC can induce T cell tolerance **8**

1.1.3.1 Basics of Treg **8**

1.1.3.2 Apoptotic cell uptake induces tolerogenic DC **9**

1.1.4 Mechanisms of donor Ag re-processing **12**

1.1.5 Tolerogenic DC as therapeutics **13**

1.1.6 Vitamin D_3 renders DC maturation-resistant **15**

1.2 ORGAN TRANSPLANTATION **18**

1.2.1 Types of allograft rejection **19**

1.2.2 Pharmacologic immunosuppression **20**

1.3 IMMUNE MECHANISMS OF ALLOGRAFT REJECTION 21

1.3.1 Ischemia-reperfusion injury 21

1.3.2 Innate immune response 23

1.3.3 Adaptive immune response 24

1.3.3.1 Pathways of allorecognition 24

1.3.3.2 Anti-donor T cell effector response 27

1.4 CELLULAR THERAPIES IN TRANSPLANTATION 29

1.4.1 Types and history of cellular therapies 29

1.4.2 Effects of DST on allograft transplantation 30

1.4.3 Effects of apoptotic splenocytes on allograft transplantation 31

1.4.3.1 Apoptotic leukocytes promote allograft survival 31

1.4.3.2 Apoptotic leukocytes down-regulate the T cell alloresponse 32

1.4.3.3 Apoptotic leukocytes decrease the B cell alloresponse 33

1.4.3.4 Apoptotic leukocytes mitigate chronic rejection 34

1.4.4 Comparing DST to apoptotic leukocyte therapy 34

1.4.5 DC therapies in transplantation 35

1.5 SPECIFIC AIMS 36

1.5.1 Specific Aim 1 (Chapter 2): To investigate the in vivo mechanism(s) by which tolerogenic DC therapy prolongs allograft survival 36

1.5.2 Specific Aim 2 (Chapter 3): To examine the necessity of donor "passenger" APC in priming the anti-donor T cell response 37

1.5.3 Specific Aim 3 (Chapter 4): To investigate the role of inflammatory monocytes in transplant rejection 37

2.0 RECIPIENT APC RE-PROCESS THERAPEUTIC DC AND LINK ALLO-RECOGNITION PATHWAYS TO PROLONG ALLOGRAFT SURVIVAL 39

2.1 INTRODUCTION 39

2.2 RESULTS 40

2.2.1 Vitamin D_3 treated bm-DC are maturation-resistant and exhibit normal survival. 40

2.2.2 VD_3-DC prolong cardiac allograft survival similarly to alternative cellular therapies 42

2.2.3 Donor-derived MR-DC rapidly die in vivo 44

2.2.4 Apoptotic MR-DC derived fragments are internalized, re-processed into allopeptides and presented by recipient DC briefly in vivo 46

2.2.5 Recipient DC down-modulate indirectly alloreactive T cells 49

2.2.6 Therapeutic DC fail to directly tolerize anti-donor T cells 53

2.2.7 Therapeutic DC inhibit the immune response to cardiac allografts 56

2.2.8 Indirect $CD4^+$ T cell help is required for the direct pathway response and cardiac allograft rejection 59

2.3 DISCUSSION 63

3.0 DONOR APC ARE REQUIRED TO ELICIT THE ANTI-DONOR T CELL RESPONSE 69

3.1 INTRODUCTION 69

3.2 RESULTS 71

3.2.1 Donor passenger APC emigrate from cardiac allograft tissue 71

3.2.2 Cardiac allograft tissue expresses MHC class I and II 72

3.2.3 Donor passenger APC are required for an anti-donor T cell response . 74
3.3 DISCUSSION 76
4.0 INFLAMMATORY MONOCYTES DIFFERENTIATE INTO TIP-DC BUT INHIBIT T CELL RESPONSES IN CARDIAC ALLOGRAFT TRANSPLANTATION .. 78
4.1 INTRODUCTION 78
4.2 RESULTS 80
4.2.1 Composition of graft-infiltrating APC 80
4.2.2 Graft-infiltrating monocytes differentiate into CD11c$^+$ DC 84
4.2.3 The pDC marker, PDCA-1, is non-specifically expressed during allograft rejection 86
4.2.4 Acute rejection is associated with monocytopoiesis, monocytosis and inflammatory monocyte infiltration into secondary lymphoid organs 88
4.2.5 Graft-infiltrating inflammatory DC express TNF-α and iNOS 90
4.2.6 Inflammatory DC inhibit effector T cell responses 94
4.3 DISCUSSION 98
5.0 METHODS AND MATERIALS 101
5.1 MICE AND REAGENTS 101
5.2 HEART TRANSPLANTATION 102
5.3 GENERATION OF MR-DC 102
5.4 ISOLATION OF TCR TRANSGENIC T CELLS 103
5.5 MICROSCOPIC ANALYSIS AND IMMUNOSTAINING 104
5.6 LEUKOCYTE ISOLATION FROM TISSUE 105
5.6.1 From cardiac allografts 105

5.6.2 From bone marrow and spleen 106
5.6.3 From blood 106
5.7 FLOW CYTOMETRY 106
5.7.1 Surface staining 106
5.7.2 Additional stains 107
5.8 MLC AND ELISPOT ASSAY 109
5.9 QUANTIFICATION OF DONOR DC BY PCR ANALYSIS 109
5.10 ASSAY FOR ANTIGEN PRESENTATION 110
5.11 ELISA 110
5.12 NITRITE DETECTION 111
5.13 STATISTICAL ANALYSIS 111
6.0 SUMMARY 112
6.1 CELLULAR THERAPIES IN TRANSPLANTATION 112
6.1.1 Caveats to cellular therapy research 112
6.1.2 Caveats to clinical implementation of cellular therapies 113
6.2 PRIMING THE ANTI-DONOR T CELL RESPONSE 113
6.2.1 Caveats to our proposed model 115
6.2.2 Future directions 115
6.3 INFLAMMATORY DC IN TRANSPLANTATION 115
6.4 FINAL STATEMENT 116
APPENDIX A. ACTIVATED INFLAMMATORY INFILTRATE IN HSV-1-INFECTED CORNEAS WITHOUT HERPES STROMAL KERATITIS 117

APPENDIX B. A NOVEL P40-INDEPENDENT FUNCTION OF IL-12P35 IS REQUIRED FOR PROGRESSION AND MAINTENANCE OF HERPES STROMAL KERATITIS. 146

APPENDIX C. PUBLICATIONS..... 168

BIBLIOGRAPHY..... 170

LIST OF TABLES

Table 1. Characterization of monocyte subsets by surface expression. 6

Table 2. Methods of generating tolerogenic DC in vitro. 14

Table 3. Antibodies used for flow cytometry. 108

LIST OF FIGURES

Figure 1. Stages of DC maturation. 2

Figure 2. Types of DC. 3

Figure 3. Vitamin D_3 structure (a) and synthesis (b). 16

Figure 4. Pathways of allorecognition. 25

Figure 5. Models of direct pathway $CD8^+$ T cell priming. 27

Figure 6. VD_3-treated bone marrow-derived DC are maturation-resistant. 41

Figure 7. VD_3 treatment does not affect DC viability in vitro. 42

Figure 8. Donor-derived MR-DC prolong cardiac allograft survival. 43

Figure 9. Donor-derived MR-DC are short-lived in vivo. 45

Figure 10. Apoptotic bodies derived from donor MR-DC are internalized by recipient DC. 46

Figure 11. Recipient DC re-process therapeutic DC into alloAg for presentation via the indirect pathway. 47

Figure 12. Donor MR-DC-derived alloAg is presented only briefly in vivo 48

Figure 13. Donor-derived MR-DC induce defective activation of indirect pathway $CD4^+$ T cells. 50

Figure 14. Indirect pathway presentation results in peripheral deletion and Treg outgrowth. 52

Figure 15. Model for direct pathway experimentation. 53

Figure 16. MR-DC fail to directly prime anti-donor T cells in vivo. 55

Figure 17. Therapeutic DC fail to directly induce T cell anergy or Treg. 56

Figure 18. Allograft histology from non-treated and MR-DC treated mice. 57

Figure 19. Donor-derived MR-DC therapy decreases T cell responses within the graft and systemically..... 58

Figure 20. CD40 ligation of recipient APC by indirect $CD4^+$ helper T cells is required for allograft rejection. 60

Figure 21. CD40 ligation of recipient APC by indirect $CD4^+$ helper T cells is required for direct pathway priming. 62

Figure 22. Proposed model for mechanism of action of donor-derived MR-DC. 67

Figure 23. Donor passenger APC emigrate from cardiac allograft tissue rapidly following transplantation. 72

Figure 24. Cardiac allograft tissue up-regulates expression of MHC class II. 73

Figure 25. Cardiac allograft tissue up-regulates expression of MHC class I..... 74

Figure 26. Donor passenger APC are required for a direct pathway T cell response. 75

Figure 27. DC comprise the majority of recipient APC infiltrating cardiac allograft tissue. 82

Figure 28. Graft-infiltrating DC are inflammatory monocyte-derived. 83

Figure 29. Graft-infiltrating inflammatory DC derive from two subsets of inflammatory monocytes. 85

Figure 30. Graft-infiltrating inflammatory DC express PDCA-1 in response to the inflammatory milieu. 87

Figure 31. Inflammatory monocytes emigrate from bone marrow into circulation and secondary lymphoid organs..... 89

Figure 32. Graft-infiltrating inflammatory DC produce TNF-α..... 91

Figure 33. CD11b^{hi}Ly6C^{hi} inflammatory DC produce iNOS. 92

Figure 34. Inflammatory DC mediate a DTH-like response that requires indirect CD4^{+} T cell help..... 94

Figure 35. T cell responses in allografts are more robust in the absence of inflammatory monocytes. 95

Figure 36. T cell responses in secondary lymphoid organs are more robust in the absence of inflammatory monocytes. 97

Figure 37. Model for generating MR-DC. 103

Figure 38. Proposed model for mechanism of direct pathway T cell priming. 114

PREFACE

I would like to thank Dr. Louis Falo Jr and Dr. Geetha Chalasani for generously donating the CD11c-DTR-eGFP mice and 2C TCRtg mice, respectively, used in this study. I would also like to acknowledge the work of the histopathology lab that performed the H&E staining and iNOS immunohistochemistry presented herein and Greg Gibson for assisting with confocal microscopy work.

I would like to thank my thesis committee, Drs. Beer-Stolz, Lakkis, Larregina and Salter for guidance throughout the passed two and half years. I would also like to thank Geetha and Geza for intellectual contributions to this study, Dr. Ahearn for always listening and smiling no matter how crazy I sounded, and a huge thank you to JoAnne for being an ear, a shoulder and a mentor when I was most in need!!

Of course much thanks to Bill for all the sectioning, last minute ordering, food and jokes!!! And grazi to Angela for all the laughs-I have learned from you the greatest lesson . . . never to work with exosomes!

To Adrian, thank you so much for giving me a home when I was so very much in need, for being an excellent scientific mentor, a collaborator, a comedian and a friend. Thanks to you and Adriana, Angela and Bill for making my graduate school experience a great one!!!

Finally and most importantly, to my family,

Thank you mom and dad for always supporting me and believing in me, for sharing all the great moments in my life and all the “black cloud” moments too. To my brothers and new sisters, for always supporting me, and always making me laugh! Your Chrisms and Brian Boitano impressions can’t be beat.

This dissertation is a testament to your unwavering support, I could not have achieved this without any of you. Much love and thanks.

P.S. one down, one to go.

Abbreviations used in this dissertation:

Ab, antibody

Ag, antigen

alloAb, alloantibody

alloAg, alloantigen

APC, antigen-presenting cells

bm, bone marrow

bm-DC, bone marrow-derived DC

CVA, chronic vascular arteriopathy

d, day

DC, dendritic cells

DC1c, DC1-maturation cocktail

DST, donor-specific transfusion

DTH, delayed-type hypersensitivity

ECP, extracorporeal photophoresis

FSC, forward scatter

GIL, graft-infiltrating leukocyte

h, hour

IL, interleukin

IFN, interferon

iNOS, inducible nitric oxide synthase

i.p., intraperitoneal

i.v., intravenous

L, ligand

LN, lymph node

LPF, low-power fields

mAb, monoclonal Ab

MDSC, myeloid-derived suppressor cells

MΦ, macrophages

MHC, major histocompatibility complex

MLC, mixed lymphocyte culture

MR-DC, maturation-resistant DC

MST, mean survival time

NGS, normal goat serum

NO, nitrite

IDO, indoleamine-2,3-dioxygenase

PD-1, programmed cell death-1

pDC, plasmacytoid DC

PMN, polymorphonuclear cells

ROI, reactive oxygen intermediaries

SSC, side scatter

TCRtg, TCR transgenic

$T_h1/2$, T helper type 1 or 2 response

Tip-DC, TNF-α and iNOS-producing DC

TLR, toll-like receptor

TNF, tumor necrosis factor

Treg, regulatory T cells

UV-B, ultraviolet B light

VD_3-DC, vitamin D_3-treated DC

VDR, vitamin D receptor

vWF, von Willebrand factor

WT, wild-type

1.0 INTRODUCTION

1.1 DENDRITIC CELLS

1.1.1 Conductors of the adaptive immune response

Dendritic cells (DC) are a heterogeneous population of hematopoietic-derived antigen-presenting cells (APC) that orchestrate the adaptive immune response to self and foreign antigen (Ag). DC are defined by surface expression of major histocompatibility complex (MHC) class II and the integrin and complement receptor CD11c[1]. DC respond to both endogenous and exogenous danger signals such as pathogen-associated molecular patterns on microorganisms, products secreted by activated macrophages, (MΦ) and parenchymal cells and stimulatory signals from activated T cells[1]. Further, they are the only APC capable of priming naïve T cells and as such, they serve as a crucial link between innate and adaptive immunity[1,2].

In the periphery, DC exist in 3 different stages of activation/maturation: immature, semi-mature or quiescent, and mature or activated (Fig. 1). In the steady-state, quiescent DC have high phagocytic ability and low surface expression of MHC:peptide complexes and the co-stimulatory molecules CD80 and CD86[1-3]. DC mature upon Ag uptake and exposure to pro-inflammatory stimuli. During maturation, DC decrease phagocytic ability and increase expression of MHC class I and II loaded with peptide, co-stimulatory molecules CD40, CD80 and CD86, as well as

the chemokine receptor CCR7[3]. Maturing DC migrate through afferent lymphatics to secondary lymphoid organs, where CCR7 interacts with CCL19 and CCL21, allowing DC entrance into T cell-dependent areas for interaction with Ag-specific T cells[2,4]. MHC:peptide complex presented by DC binds the T cell receptor (TCR) (signal 1) and DC expressed co-stimulatory molecules, CD80 and CD86, bind CD28 (signal 2) on the T cell. This induces secretion of the pro-inflammatory cytokine Interluekin (IL)-2, which is a potent agonist for T cell proliferation[5]. Additionally, there is interaction between CD40 on the DC and CD40Ligand (CD40L) (CD154) on the T cell which further enhances DC and T cell stimulation[6]. Mature DC also secrete pro-inflammatory mediators (signal 3) which help direct the immune response, such as IL-12p70, which polarizes T cells toward a T helper cell type 1 (T_h1) response[1-3].

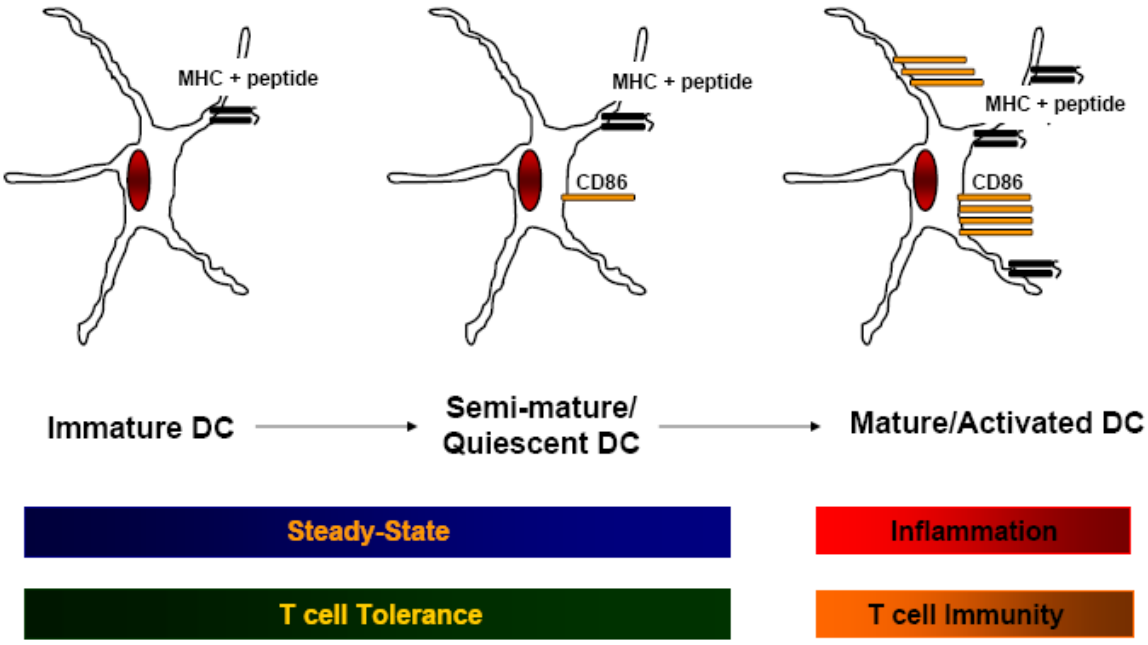

Figure 1. Stages of DC maturation.

DC can exist as either immature (express low levels of MHC:peptide complex without co-stimulatory molecules CD80 or CD86), semi-mature or quiescent (express low levels of MHC:peptide complex along with low levels of co-stimulatory molecules), or mature or activated (express high levels of MHC:peptide complex and high levels of co-stimulatory molecules).

Notably, activated T cells up-regulate expression of CTLA-4 (CD152), an inhibitory receptor that binds CD80/CD86 with higher affinity than CD28[7]. Ligation of CTLA-4 decreases IL-2 production and IL-2 receptor expression, and impedes cell cycle progression[7]. This serves as one example of a system of checks and balances to prevent uncontrolled immunity.

1.1.2 Types of DC

DC derive from multiple lineages[1-3,8]. Classically, they are divided into conventional DC plasmacytoid DC (pDC) and inflammatory DC (Fig. 2).

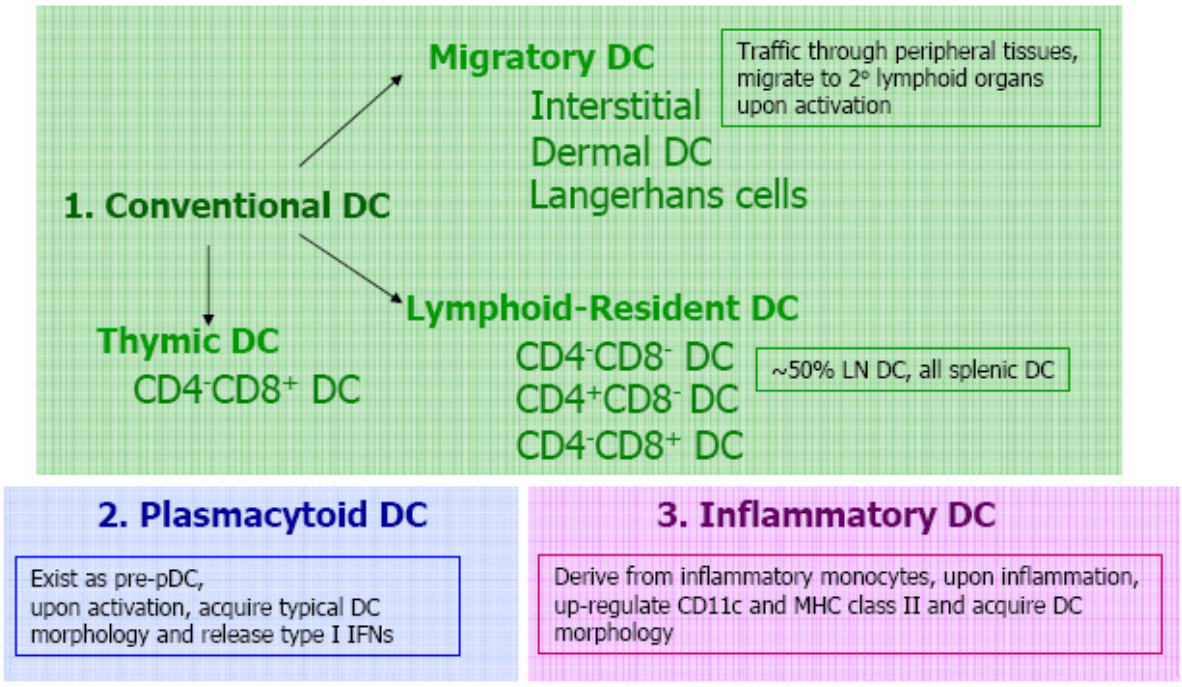

Figure 2. Types of DC.

1.1.2.1 Conventional DC

Conventional DC have typical DC morphology in the steady-state[9] and are divided by location into lymphoid-resident and migratory DC. In mice, lymphoid-resident (spleen and lymph nodes) DC include $CD8\alpha^+$ DC, $CD4^+CD8^-$ DC and $CD4^-CD8^-$ DC[10]. $CD8^-$ DC are immature and are located primarily in the splenic marginal zone and to a lesser extent, throughout the splenic red pulp, although upon stimulation, they migrate to T cell areas. $CD8\alpha^+$ DC constitute 20-30% of the $CD11c^{hi}$ DC population, reside in the T cell area, and are semi-mature. They also constitute the majority of APC in thymus[10,11].

Migratory DC consist of tissue interstitial DC, dermal DC and Langerhans cells, which patrol skin and peripheral tissues for foreign Ag. Upon stimulation, these DC carry Ag from the periphery through lymphatics to draining lymph nodes[12].

1.1.2.2 Plasmacytoid DC

Pre-pDC circulate through blood and lymphoid tissue and acquire typical DC morphology (become pDC) after activation by microbial infection or inflammation, at which time they release high amounts type I IFNs, suggesting an important role in the immune response to viral pathogens[13]. Conversely, significant work supports a role for pDC in tolerance, given the ability of pDC to produce indoleamine-2,3-dioxygenase (IDO), a potent anti-inflammatory molecule[14-18]. Mouse pDC are typically defined by low forward scatter (FSC, measure of size) and low side scatter (SSC, measure of cellular complexity) and surface expression of $CD11c^{int}CD11b^-CD45RA^+Ly6C^+PDCA\text{-}1^{+}$[13]. However, there is currently no specific marker for pDC, thus complicating study of these cells.

1.1.2.3 Inflammatory DC

Inflammatory DC derive from monocytes in vivo. Therefore, a brief review of monocytes follows.

Monocytes are bone marrow (bm)-derived leukocytes[19] that in the steady-state, constitute 4-6% of blood cells in mice and 10% in humans, and have a brief half-life, lasting only 1 d in mice[20] and 3 d in humans[21]. Monocytes express surface CD115 (M-CSF receptor), CD11b and F4/80 and have low SSC[22]. To date, three subsets of monocytes have been identified in mice, and are typically defined by their expression of Ly6C. Two subsets are considered inflammatory monocytes, so named because they migrate to sites of inflammation; these subsets express $Ly6C^{hi}$ and $Ly6C^{int}$. The third subset is comprised of resident monocytes that are characterized as $Ly6C^{low}$. Additional phenotypic differences between the three monocyte subsets are presented in Table 1. Recent evidence supports the ability of $Ly6C^{hi}$ inflammatory monocytes to differentiate into $Ly6C^{int}$ and $Ly6C^{low}$ monocytes[23], although this is a point of contention in the literature[24]. Whereas inflammatory monocytes differentiate into inflammatory DC in response to inflammatory stimuli, resident monocytes are believed to replace conventional DC and MΦ under steady-state conditions, but are not believed to play a role during inflammation, and as such will not be further discussed in this dissertation.

Table 1. Characterization of monocyte subsets by surface expression.

	Inflammatory monocytes		Resident monocytes
Ly6C (Gr-1) expression	$Ly6C^{hi}$	$Ly6C^{int}$	$Ly6C^{low}$
Surface phenotype	$CD115^{+}$ $CD11b^{+}$ $F4/80^{+}$ $CD62L^{+}$	$CD115^{+}$ $CD11b^{+}$ $F4/80^{+}$	$CD115^{+}$ $CD11b^{+}$ $F4/80^{+}$ $CD62L^{-}$
Chemokine receptor expression	$CCR2^{hi}$ CX_3CR1^{low}	$CCR2^{hi}$ CX_3CR1^{low} $CCR7^{+}$ $CCR8^{+}$	$CCR2^{low}$ CX_3CR1^{hi}

Most studies of inflammatory monocytes have focused on the $Ly6C^{hi}$ subset for two reasons. First, $Ly6C^{int}$ cells comprise only 10% of all monocytes[25]. Second, a commonly used antibody (Ab) to identify inflammatory monocytes, Gr1, recognizes both Ly6C and Ly6G, the latter expressed by granulocytes. Granulocytes in turn also express intermediate levels of Ly6C, and since granulocytes comprise a much larger population of cells than $Ly6C^{int}$ monocytes, studies of $Gr\text{-}1^{int}$ monocytes are confounded by potentially contaminating granulocytes.

Recent work unearthed inflammatory monocytes as complex entities capable of participating in immune responses in diverse ways. Circulating inflammatory monocytes extravasate across blood vessels into sites of inflammation, up-regulate CD11c, CD86 and MHC class II expression and differentiate into inflammatory DC, a phenomenon dependent on the local presence of granulocyte macrophage colony-stimulating factor (GM-CSF)[24,26-28]. Inflammatory DC in turn participate as innate effector cells that facilitate microbial clearance during bacterial, viral and parasitic infections[24,29-32]. Following infection with *L. monocytogenes*, inflammatory DC are recruited transiently into the spleen, where they secrete high levels of TNF-α, express

inducible nitric oxide synthase (iNOS) that generates nitric oxide (NO) radicals and release reactive oxygen intermediates (ROI)[29]. These inflammatory DC are fundamental to clearing infection, as their absence results in uncontrolled bacterial replication in the host[29]. Due to their ability to produce TNF-α and iNOS, these inflammatory DC are termed TNF-α and iNOS-producing-DC or Tip-DC.

Secondly, inflammatory DC can take up Ag in the periphery, migrate to draining lymph nodes (LN)[33], and present Ag to T cells[28]. According to work by Randolph's group, Gr-1^{int} monocytes have greater allostimulatory capacity in vitro compared to Gr-1^{hi} monocytes, and in vivo Gr-1^{int} monocytes are the main monocyte cell trafficking to draining LN[25]. In viral and immunization models, inflammatory DC recruited to LN produce IL-12p70 and drive T cells toward a T_h1 type response[34] and during skin and lung inflammation, inflammatory DC are recruited to inflamed tissues, where they present Ag to CD8$^+$ T cells and promote immunopathology[35,36]. Notably, the role of inflammatory DC in T cell responses varies with experimental model, as Tip-DC infiltrating *L. monocytogenes* infected spleen did not affect T cell priming[29].

Finally, inflammatory monocytes can replenish MΦ and DC resident cell compartments in skin[37], the digestive tract[38] and lung[39-41], following damage or emigration of resident APC.

Contrarily, there is data suggesting that inflammatory monocytes can expand in spleen and LN of tumor-bearing mice and differentiate into myeloid-derived suppressor cells (MDSC) that have been shown to mediate development of tumor induced regulatory T cells (Treg) and T cell anergy, partly through release of IL-10 and TGF-β[42-44]. Further, inflammatory monocyte-derived MDSC have been shown to impair T cell responses, particularly CD8$^+$ T cell responses, via molecular mechanisms involving ROI and NO[42,43,45-48]. *Clearly, the roles played by*

inflammatory monocytes in immune responses are diverse and complex, thus warranting further investigation.

1.1.3 DC can induce T cell tolerance

Although most T cells recognizing self-peptides with high affinity are eliminated centrally in the thymus through negative selection[49], a percentage of self-reactive T cells escape thymic deletion and access the periphery. An efficient mechanism in the periphery is therefore necessary to prevent activation of self-reactive T cells and avoid autoimmunity.

Quiescent DC expressing MHC:peptide complex (signal 1) with low levels of co-stimulatory signals (signal 2) provide sub-threshold stimulation to auto-reactive T cells, resulting in defective T cell activation[8,50,51]. Incomplete T cell activation results in poor cellular proliferation followed by deletion, anergy and likely differentiation/expansion of Treg cells, all mechanisms leading to T cell hypo-responsiveness or tolerance[8,50].

1.1.3.1 Basics of Treg

There are multiple types of $CD4^+$ regulatory T cells (Treg) in vivo. Naturally occurring Treg arise in the thymus, express surface CD25 (IL-2Receptor) and the transcription factor FoxP3, and inhibit T cell proliferation by a contact-dependent mechanism[52]. Two additional Treg subsets are detected in the periphery: T_r1 Treg release IL-10, while T_h3 Treg release TGF-β, both immunosuppressive cytokines[52]. Overall, Treg are thought to be important for inhibiting effector T cell priming and/or effector responses in vivo, although this remains a complicated area of research. Specifically in the setting of transplantation, most biologists agree that achieving donor-specific tolerance will require both effector T cell deletion and Treg induction.

1.1.3.2 Apoptotic cell uptake induces tolerogenic DC

Over the past decade, the central role of DC in maintaining peripheral tolerance has become increasingly appreciated[53-55]. Normal cell turnover occurring daily in our bodies generates billions of dead cells without stimulating inflammation. Other conditions that induce apoptosis such as moderate ultraviolet-B light (UV-B) irradiation, certain viral infections and malignant tumors are also accompanied by a lack of inflammation. This was originally attributed to rapid clearance of apoptotic cells, thus preventing release of their toxic cellular components into the micro-environment. However, Voll and colleagues demonstrated that internalization of apoptotic cells "actively" suppresses the inflammatory response by delivering inhibitory signals to phagocytes[56]. It was further shown that endocytosis of early apoptotic cells by immature DC prevents DC activation in both humans and rodents, as the APC fail to up-regulate expression of MHC class II and the co-stimulatory molecules CD80, CD86, CD40 and in humans CD83, despite subsequent stimulation with DC-activating factors such as LPS, CD40 ligation, TNF-α and monocyte-conditioned medium[57-61]. This inhibitory effect of apoptotic cells was not simply a result of the process of phagocytosis, as activation of immature DC was not impaired after ingestion of control latex beads that were similar in size to apoptotic cell fragments[59].

Self-Ag derived from apoptotic cells resulting from steady-state cell turnover is constantly sampled by quiescent DC that migrate constitutively from peripheral tissues to lymph nodes and spleen[62,63]. In support of this idea, it was reported that ingestion of apoptotic cells causes DC to increase levels of CCR7, indicating that the DC acquire the ability to home to draining secondary lymphoid organs in response to the chemokine MIP-3β[61,64]. In vivo, Huang et al. demonstrated that intestinal DC that have internalized apoptotic cell fragments derived from

intestinal epithelial cells migrate to mesenteric LN, independently of DC-maturation stimuli derived from intestinal bacterial flora[65].

There is accumulated evidence supporting that DC that have phagocytosed early apoptotic cells and thus express MHC:Ag complex in the absence of co-stimulation exhibit a decreased capacity to stimulate Ag-specific TCR transgenic T cells, allogeneic T cells[59,60] and even T cell clones (which do not require co-stimulation)[57].

Using mice expressing model Ag controlled by tissue-specific promoters, it has been shown that in the steady state, constitutively migrating DC transport and process tissue-specific Ag from periphery to LN and spleen. These migrating semi-mature DC silence rather than stimulate self-reactive T cells[66,67]. A similar mechanism seems to operate when foreign-Ag are delivered directly to DC in secondary lymphoid organs by i.v. administration of early apoptotic cells. After i.v. injection of OVA-loaded dying cells in mice, DC cross-present OVA-peptides and induce abortive proliferation and deletion of OVA-specific $CD8^+$ T cells and subsequent T cell tolerance to OVA-challenge[68]. Although macrophages phagocytose apoptotic cells more efficiently than DC, only the latter APC cross-present efficiently the apoptotic cell-derived peptides to $CD8^+$ T cells[69]. In this regard, it has been shown that DC, unlike macrophages, cross-present Ag derived from salmonella-infected apoptotic cells to $CD8^+$ T cells[70]. Ag derived from apoptotic cells can also be presented through MHC class II molecules to $CD4^+$ T cells. In fact, murine bone marrow-derived (bm-)DC present Ag from internalized apoptotic cells to $CD4^+$ T cells 1-10,000 times better than pre-processed peptide[71].

In autoimmunity, Ag presentation in the absence of pro-inflammatory secondary signals, co-stimulation or cytokines results in T cell tolerization[72,73]. In the transplantation setting, human monocyte-derived DC loaded with allogeneic apoptotic cells down-regulates specifically the

anti-donor T cell response in vitro[74]. More importantly in vivo, i.v. administration of donor splenocytes in early stages of apoptosis induced by UV-B irradiation leads to defective activation of donor-reactive TCR transgenic $CD4^+$ T cells and their peripheral deletion[75]. When combined with blockade of the CD40-CD154 pathway, systemic administration of donor apoptotic splenocytes promoted expansion of donor-specific $CD4^+$ Treg in mice[75]. These findings have important implications for transplantation since, although opinions vary, induction of donor-specific tolerance will ultimately depend on both deletion of alloreactive T cells and generation/expansion of Treg.

Phagocytosis of apoptotic cells induces additional immunosuppressive changes in DC that may contribute to tolerance induction. Phagocytosis of apoptotic cells decreases activation of NF-κB, a transcription factor required for DC maturation/activation and synthesis of several pro-inflammatory cytokines, in DC and MΦ. This may explain why DC that have interacted with early apoptotic cells secrete significantly lower levels of IL-1α, IL-1β, IL-6, IL-12p70, IL-23 and TNF-α[57,76-78], a phenomenon that is maintained even in the presence of LPS[76]. Interestingly, phagocytosis of apoptotic cells does not interfere with secretion of TGF-β1 by mouse DC[76] and even increases production of IL-10 by human DC[57], both immunosuppressive cytokines. The effect of apoptotic cells on cytokine production by DC is at least partly due to altered cytokine mRNA transcription or stabilization[76].

Following internalization of cells in early apoptosis, macrophages increase secretion of additional anti-inflammatory mediators including prostaglandin E2 (PGE2), platelet-activating factor (PAF), IL-1 receptor-antagonist and hepatocyte growth factor, although these molecules have not been fully explored in DC[79-81]. More recently, other inhibitory mediators have been discovered to have pervasive anti-inflammatory effects on immune responses, including the

tryptophan catabolizing enzyme IDO and the cell surface receptor programmed cell death (PD)-1 and its ligands PD-L1 and PD-L2[14,16,18,59,82-87]. The contribution of these mediators to tolerance induction by DC following phagocytosis of apoptotic cells remains to be fully explored, but regardless, the potential to harness similar mechanisms in the setting of transplantation and autoimmunity is indeed promising.

1.1.4 Mechanisms of donor Ag re-processing

Ag re-processing refers to uptake of donor MHC class I or II, or minor histocompatibility Ag, from donor cells by recipient APC and processing it into allopeptides for presentation by recipient self:MHC. Re-processing of self-Ag is an important mechanism for maintaining peripheral tolerance in the steady-state. It could also play a key role during immunization (vaccination for infectious disease or cancer) and negative vaccination (for therapy of transplantation or autoimmune disorders). Thus, understanding the mechanisms by which donor Ag re-processing occurs in vivo is important for translational/clinical research of DC-based therapies in transplantation.

Internalization of apoptotic cells is one mechanism by which donor Ag is transferred between cells for re-processing by recipient phagocytes. There is evidence that apoptotic cells dock on the surface of DC and macrophages through binding to the $\alpha_v\beta_5$ integrin, that recruits the CrkII-Dock180 molecular complex and in turn triggers Rac1 activation and phagosome formation[88,89]. Once internalized, the apoptotic cells are processed within MHC class II rich compartments (MHC class II^+ $LAMP^+$ $H\text{-}2M^+$ cytoplasmic vesicles) for presentation as peptides loaded in MHC class II molecules to $CD4^+$ T cells[71]. Alternatively, apoptotic cell-derived Ag can be routed out of the endosomal compartment into the lumen of the endoplasmic reticulum for

loading into MHC class I for cross-presentation to $CD8^+$ T cells[69,90]. The ultimate mechanism by which apoptotic cell-derived Ag are shuttled into the endoplasmic reticulum is unknown, however the ability of lactacystin, a 26S proteasome inhibitor to partially block cross-presentation of apoptotic cell-derived Ag in DC suggests that both classical and non-classical MHC class I pathways participate in this process[69].

In addition to apoptotic cell uptake, there is evidence that when administered i.v., exosomes (nanovesicles) carrying donor MHC molecules on their surface are re-processed by recipient DC and down-regulate the anti-donor response to prolong cardiac allograft survival in rats[91,92], and our own data demonstrate that donor-derived exosomes significantly prolong cardiac allograft survival in an Ag-specific manner in mice (unpublished data). Further, living cells can exchange plasma membrane fragments containing intact MHC molecules, a process termed "nibbling"[93,94]. Interestingly, even $CD4^+$ T cells have been shown to acquire intact MHC:peptide complex and act as potent APC[95]. Whether these other forms of donor-Ag uptake and re-processing occur upon DC or cellular therapy administration remain to be explored.

1.1.5 Tolerogenic DC as therapeutics

The ability of DC to tolerize T cells in an Ag-specific manner, coupled with the ability to propagate large numbers of DC in vitro, has heralded the use of tolerogenic DC as therapeutics for transplantation and autoimmunity. Tolerogenic DC are in an immature or quiescent state, in that they express low MHC:peptide complexes and low or absent co-stimulation (Fig. 1), and are impaired in their ability to produce the T_h1-driving cytokine IL-12p70. A number of methods, including culture-conditioning with different cytokines or growth factors, treatment with various pharmacologic agents or genetic engineering (Table 2)[9], have been developed to increase DC

tolerizing potential and/or render tolerogenic DC resistant to maturation (maturation resistant, MR-DC), to combat the risk of in vivo maturation of the administered DC and thus patient sensitization.

Table 2. Methods of generating tolerogenic DC in vitro.

Cytokines, Growth Factors	Pharmacologic Mediators	Genetic Engineering
↓GM-CSF ↑ IL-10 ↑ TGFβ1 ↑ VEGF	*Immunosuppressive or anti-inflammatory drugs:* Cyclosporine Rapamycin Tacrolimus Deoxyspergualin Mycophenolate mofetil Sanglifehrin A Corticosteroids Aspirin 1α,25-dihydroxyvitamin D_3 N-acetyl-L-cysteine Cyclic AMP inducers Glucosamine Cobalt protoporphyrin ILT receptor ligands	*Recombinant viral vectors or naked DNA:* CD95L (FasL) CTLA4-Ig IL-10 TGFβ1 IDO Soluble TNFR CCR7 Dominant-negative IκB kinase *ODNs:* NF-κB-specific decoy *RNA interference:* RELB IL-12

These pharmacologic or genetic manipulations affect DC differentiation and function by various mechanisms[9]. Some tolerogenic DC express high levels of co-inhibitory molecules such as PD-L1 on their surface, or have a lower net ratio of co-stimulatory to co-inhibitory molecule expression (i.e. CD86:PD-L1). Secretion of inhibitory cytokines/mediators also is variable, as some tolerogenic DC release IL-10, which has been shown to inhibit T cell expansion[96]. Further, tolerogenic DC can induce activation-induced cell death through FasL expression or induce Treg through IDO expression[15,97]. Although tolerogenic DC phenotypes and their effect on T cells have been well characterized in vitro, the actual mechanisms by which tolerogenic DC achieve their effects in vivo are still unknown.

Despite the promise of DC-based therapies to induce donor-specific tolerance in transplantation, there are a number of potential obstacles for clinical use, namely the time and cost of generating tolerogenic DC, and as previously alluded to, the risk of patient sensitization. It is therefore essential to elucidate mechanism of action and compare efficacy to other cellular and pharmacologic therapeutics prior to initiating clinical studies.

1.1.6 Vitamin D_3 renders DC maturation-resistant

The active form of vitamin D_3, 1α,25-dihydroxyvitamin D_3 (1α,25$(OH)_2D_3$), (Fig. 3a) is a secosteroid hormone known for its importance in calcium, phosphorus and bone metabolism, but also is now appreciated as a potent modulator of the immune system[98-100]. Physiologically, photosynthesis in the skin provides the majority of vitamin D_3, although diet provides a small amount as well (Fig. 3b). Exposure to UV light (270-300 nm) induces the skin to catalyze conversion of 7-dehydroxycholesterol to pre-vitamin D_3, which then spontaneously isomerizes to vitamin D_3. Vitamin D_3 is hydroxylated in the liver by D_3-25-hydroxylase (CYP2D25) into 25-hydroxyvitamin D_3, then again in the proximal convoluted tubule cells of the kidney by 25$(OH)D_3$-1-α-hydroxylase (CYP27B1) into 1α,25$(OH)_2D_3$, the active form of the hormone[101].

a.

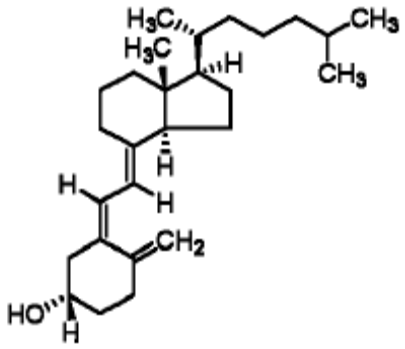

b.

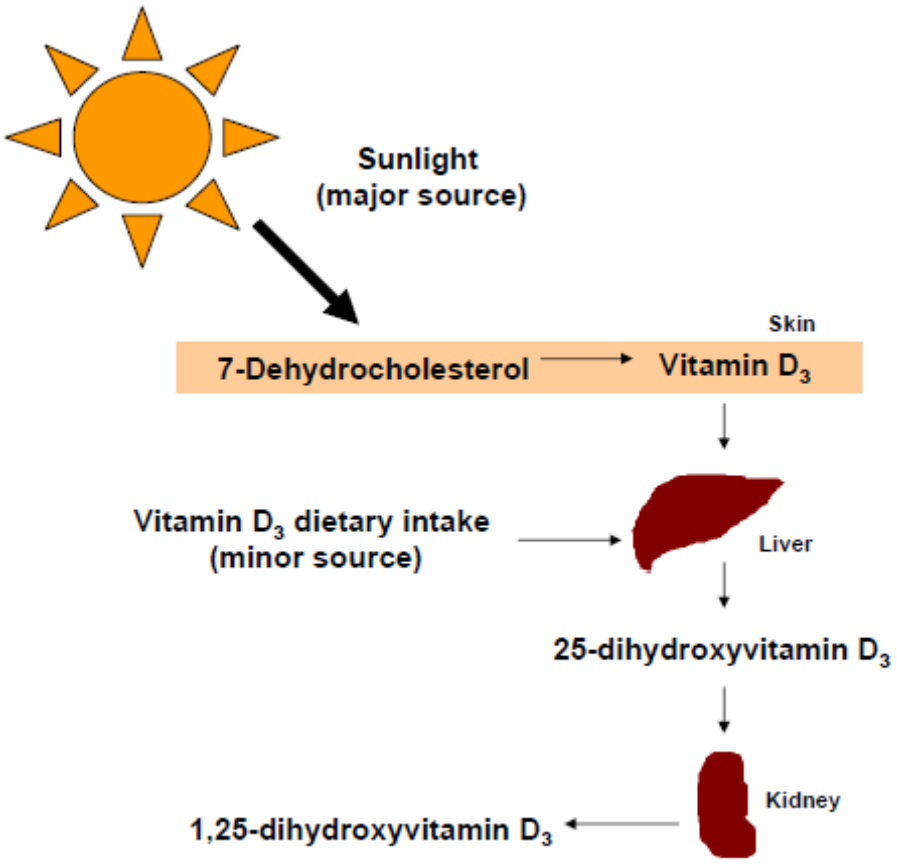

Figure 3. Vitamin D_3 structure (a) and synthesis (b).

1α,25$(OH)_2D_3$ binds the vitamin D receptor (VDR), a nuclear hormone receptor and agonist-activated transcription factor[102]. VDR binds to specific DNA sequence elements on vitamin D_3 responsive genes, such as cyp24, and affects the rate of RNA polymerase II-mediated transcription[103]. Treatment with 1α,25$(OH)_2D_3$ inhibits NFκB p65 phosphorylation and nuclear translocation[104] in myeloid but not plasmacytoid DC[105], and the inhibition of NFκB in part helps explain the effects of 1α,25$(OH)_2D_3$ on the immune response, which are multiple and diverse.

In general, $1\alpha,25(OH)_2D_3$ stimulates the innate immune response. It induces differentiation of promyelocytes to monocytes[106] and myeloid stem cells and peripheral blood monocytes toward a MΦ phenotype[107]. Further, it increases tumor cell cytotoxicity, phagocytosis and mycobactericidal activity of monocytes/MΦ[108]. When exposed to $1\alpha,25(OH)_2D_3$ in culture, human monocytes have increased expression of mannose receptor and CD32, correlating with their increased endocytic capacity[109,110].

Conversely, $1\alpha,25(OH)_2D_3$ negatively affects the adaptive immune response. It limits lymphocyte proliferation, immunoglobulin production and the amount of IL-1, IL-2, IL-6, TNF-α and β, and IFN-γ mRNA transcripts of leukocytes in culture[111-114]. Interestingly, mice lacking VDR have subcutaneous LN hypertrophy although mesenteric LN and spleen are unaffected, and DC in these hypertrophied LN have increased expression of MHC class II, CD40, and CD80/CD86[115], suggesting that $1\alpha,25(OH)_2D_3$ maintains DC in an immature state under physiologic conditions. Monocytes and DC are particularly sensitive to $1\alpha,25(OH)_2D_3$ as they express VDR constitutively[116,117]. When bound to ligand, the VDR inhibits all stages of DC life cycle including differentiation, maturation, activation and survival[109,110,118,119]. $1\alpha,25(OH)_2D_3$ prevents up-regulation of MHC class II and T cell co-stimulatory molecules CD40, CD80, CD86, and in humans CD83, and release of IL-12p70[110,119]. On human myeloid DC, $1\alpha,25(OH)_2D_3$ treatment increases expression of CCL22[105], a chemoattractant for Treg, immunoglobulin-like transcript 3, an inhibitory receptor shown to anergize T cells[120,121] and IL-10[110,122]. In vitro, $1\alpha,25(OH)_2D_3$ induces apoptosis of mature DC[110], but at low doses does not affect DC morphology or survival[109,119].

DC treated with $1\alpha,25(OH)_2D_3$, VD_3-DC, have decreased T cell allostimulatory capacity[110,123], and T cells stimulated by VD_3-DC in primary mixed lymphocyte cultures (MLC)

become hypo-responsive to control (not exposed to VD_3) DC[109] and have increased expression of CTLA-4 with decreased CD40L expression and IFN-γ production[110].

1α,25$(OH)_2D_3$ treatment exerts beneficial effects on various autoimmune diseases including experimental autoimmune encephalomyelitis[124,125], systemic lupus erythematosus[126,127] and type 1 diabetes[128-130] and prolongs allograft survival in murine models[131-133]. In cardiac transplant patients, it reduces dependence on pharmacologic immunosuppression[134]. However, administration of 1α,25$(OH)_2D_3$ has the potentially deleterious side effect of hyercalcemia, and further non-specifically shuts down the immune response, increasing susceptibility to infection and malignancies. Therefore, treatment of patients with in vitro generated VD_3-DC is a promising alternative. Notably, VD_3-DC are pro-tolerogenic in vivo, as their adoptive transfer (i.v.) significantly prolongs skin allograft survival in mice[115,123]. Overall, VD_3 is inexpensive, exists in good supply and is already FDA approved. Further, VD_3-DC have been extensively studied. As such, we will utilize VD_3-DC as prototypic tolerogenic DC to study the mechanisms by which DC-based therapies down-regulate the anti-donor response to prolong allograft survival.

1.2 ORGAN TRANSPLANTATION

Organ transplantation is becoming an increasingly important and common surgical procedure, as transplantation surgery often serves as the only life-saving treatment available for end-stage organ disease. Although the constant development of new and more effective immunosuppressive drugs along with better knowledge of their therapeutic application have revolutionized the prevention and treatment of acute graft rejection, these drugs have significant

toxicity and greatly increase patient susceptibility to malignant neoplasias and infections. Further, the implementation of immunosuppressive agents has exerted little impact on the incidence of chronic rejection, and therefore overall long-term graft survival has only improved modestly. Novel cell-based therapies that are able to down-regulate the immune response against donor Ag, without inducing generalized immune-suppression and its harmful side-effects, represent a promising avenue of research in transplantation.

Allograft rejection is an extremely complex process, and there are gaps in our knowledge of the mechanisms mediating rejection, which represent a substantial barrier to developing effective therapeutic strategies.

1.2.1 Types of allograft rejection

Allografts are grafted organs/tissues/cells transplanted between genetically disparate, MHC-mismatched individuals of the same species. The targeted Ag are called alloantigens (alloAg), and derive from MHC or minor histocompatibility antigens that are recognized by the adaptive immune response as non-self, or tissue incompatible[135]. Allorecognition describes recognition of the allogeneic Ag by the recipient, and alloresponse refers to the effector mechanisms recruited in the reaction to the transplanted tissue/organ[135].

Allografts are threatened by three types of rejection that are defined by the tempo of onset and histopathology. Hyperacute rejection occurs within minutes to hours (usually within 48 h) after transplantation surgery and is mediated by deposition of pre-formed circulating antibodies against Ag on graft vascular endothelial cells and the consequent activation of complement and coagulation cascades, resulting in intravascular thrombosis, ischemia and necrosis. This results from pre-sensitization of the recipient, by previous blood transfusion, organ

transplant, or pregnancy and in 1% of the general population for no known reason. Hyperacute rejection is largely preventable due to screening for antibodies against non-self HLA phenotypes and cross-matching, and subsequent pre-transplantation plasmaphoresis if necessary, and experience transplanting into pre-sensitized recipients[136,137].

Acute rejection begins within weeks or months (5 days to 3 months is typical), or in rare cases even years, following transplantation, and constitutes the main immediate threat to allograft survival. It is mediated by both innate and adaptive immune responses, however the advent of immunosuppressive drugs renders acute rejection largely preventable. Histopathology reveals diffuse interstitial $CD4^+$ and $CD8^+$ T cell infiltrate with activated or memory phenotype[138].

Chronic rejection develops in months or typically years post-transplantation and is the most common cause of graft loss one year after transplantation[139,140]. It results from both immune and non-immune factors. Typical features of chronic rejection include steady decline of organ function, interstitial fibrosis, chronic inflammatory infiltrate (i.e. lymphocytes, plasma cells), atrophy and gradual loss of parenchymal cells and chronic vascular arteriopathy (CVA), the latter a condition manifested by endothelitis, intimal proliferation, elastic fiber disruption, fibrosis and leukocyte infiltration of medium- and small-size arteries of the graft[140]. Unfortunately, current immunosuppression protocols are ineffective at preventing or treating chronic rejection.

1.2.2 Pharmacologic immunosuppression

The development and introduction of immunosuppressive drugs in the 1980s has greatly reduced the risk of acute rejection. Steroids, calcineurin inhibitors such as tacrolimus and cyclosporine

that block TCR-dependent T cell activation, and lymphocyte-depleting antibodies are currently employed in the clinic to prevent or mitigate acute rejection with great success. However, these agents non-specifically suppress the immune system, thus greatly increasing patient susceptibility to opportunistic infections and various cancers. Further, currently employed immunosuppressive regimens offer little protection against chronic rejection, and have significant toxicity. Clinical trials of newer pharmacologic agents such as rapamycin, an mTOR (mammalian target of rapamycin) inhibitor that blocks the cell cycle downstream of IL-2 signaling, and antibody mediated co-stimulation blockade are underway, although results so far are disappointing. Clearly, generation of therapeutics capable of donor Ag-specific suppression is necessary to reduce dependence on chronic pharmacologic agents.

1.3 IMMUNE MECHANISMS OF ALLOGRAFT REJECTION

The diversity and robustness of the alloresponse constitute major challenges to preventing graft rejection. Both the innate and adaptive immune responses are contributory. Mechanisms of graft damage include contact-dependent T cell cytotoxicity, granulocyte activation by T_h1 or T_h2 cytokines, NK cell mediated cytotoxicity, delayed-type hypersensitivity like reaction and alloAb and complement activation[141].

1.3.1 Ischemia-reperfusion injury

Ischemia-reperfusion injury refers to tissue damage resulting from the return of blood supply to tissue after a period of ischemia. This injury is Ag-independent and is responsible for initiating

the events associated with rejection. Land et al. developed the "injury hypothesis" by showing that intra-operative treatment of cadaver-derived renal allografts with a free-radical scavenger reduced the incidence of acute rejection and improved long-term graft outcome[142]. Tissue injury up-regulates pro-inflammatory mediators, inducing a robust innate immune response that in turn further promotes inflammation[143]. The innate immune response occurs prior to and independently of the adaptive immune response[144-146], as RAG-deficient cardiac transplant recipients experience comparable cellular infiltration, chemokine receptor expression and pro-inflammatory cytokine expression with wildtype (WT) recipients 1 day post-transplantation[146].

Innate immune cells express non-rearranged pattern recognition receptors that recognize not only conserved pathogen-derived molecules, as originally appreciated[147], but also self-derived molecules released from damaged or stressed tissue[148]. For example, signaling through toll-like receptor 4 (TLR4) expressed on hematopoietic-derived phagocytes, and activated by products of necrotic cells or extracellular matrix disruption, is required for optimal inflammatory responses to liver damage by ischemia-reperfusion injury[149-152]. However, except in cases of weakly immunogenic situations, TLR signaling is not required for graft rejection[153,154]. Interestingly, in humans, studies of lung transplant patients and kidney transplant recipients that are heterozygous for either of two TLR4 functional polymorphisms associated with LPS hyporesponsiveness both showed a reduced incidence of acute allograft rejection[155,156]. This is likely due to abundance of various redundant danger signals. Levels of high-mobility group box 1 (HMGB1), another danger signal, are increased following liver ischemia-reperfusion injury as early as 1 h following transplantation, and neutralization of HMGB1 decreases markers of liver inflammation[157]. Likewise, inhibiting signals of receptor for advanced glycation end products (RAGE), the receptor for HMGB1, prolongs survival of fully allogeneic cardiac allografts[158].

Notably, danger signals seem to persist within allografts long after transplantation, as T cell-deficient mice transplanted with mismatched skin or cardiac allografts that are allowed to heal for 50 days, rapidly reject their grafts upon T cell reconstitution[159,160]. If homeostatic proliferation is taken into account using a model devoid of secondary lymphoid organs but containing a normal T cell compartment, allografts display histological evidence of chronic rejection, but are not acutely rejected[161].

1.3.2 Innate immune response

Polymorphonuclear cells (PMN), or neutrophils, rapidly infiltrate allografts following surgery and ischemia/reperfusion injury. Neutrophils have numerous cytotoxic and pro-inflammatory mechanisms, including release of pro-inflammatory cytokines and chemoattractants, and production of reactive oxygen and nitrogen species. In a rat liver model of ischemia-reperfusion injury, depletion of neutrophils abrogates tissue damage[162] and neutralization of KC/CXCL1, a potent neutrophil chemoattractant, decreases PMN infiltration and prolongs graft survival[163].

NK cells are also important contributors to allograft rejection. Based on the 'missing self' hypothesis, NK cells recognize cells lacking expression of self-MHC class I molecules. NK cells are not sufficient to reject solid organ allografts, as $Rag^{-/-}$ or SCID mice, that lack T and B cells, fail to reject skin or heart allografts[159,164]. NK cells do however contribute to tissue damage and amplify graft inflammation through release of the pro-inflammatory cytokines IFN-γ and TNF-α, and through contact-mediated cytotoxicity[165]. Further, NK cell depletion in $CD28^{-/-}$ mice, whose T cells are unable to receive co-stimulation, prolongs fully MHC-mismatched cardiac allograft survival[166], suggesting that NK cells influence the adaptive immune response[167].

MΦ are also believed to be important for rejection, although their importance may be organ or model dependent. MΦ contribute to an inflammatory response in multiple ways. They phagocytose necrotic debris, secrete pro-inflammatory cytokines, produce reactive nitrogen and oxygen species and present Ag to effector T cells[168]. In rat renal allografts, MΦ begin infiltrating allografts within 24 h following surgery and proliferate in situ[169], and in human acute renal rejection, MΦ accumulate in significant numbers[170]. Also in a rat renal transplant model, liposomal clodronate administration 1 d post-transplantation, which depletes the majority of MΦ, reduces allograft damage[171], although liposomal clodronate also depletes some types of monocytes and DC. The production of iNOS in particular seems important for allograft rejection, as its neutralization prolongs cardiac allograft survival in mice[172,173]. Interestingly, recent data supports the ability of inflammatory monocyte-derived Tip-DC to produce iNOS in various bacterial infections. *The role of inflammatory monocytes and Tip-DC in allograft transplantation has not been investigated.*

1.3.3 Adaptive immune response

1.3.3.1 Pathways of allorecognition

There are two pathways by which the donor-reactive T cells recognize alloAg: the direct and the indirect (Fig. 4)[174]. By the direct pathway, recipient T cells recognize intact donor MHC molecules expressed by donor APC transplanted along with the allograft (i.e. donor DC, macrophages, endothelial cells)[175]. Ischemia-reperfusion injury and surgical trauma activate donor DC inducing their migration as “passenger leukocytes” to recipient secondary lymphoid organs, where they prime donor-reactive T cells[58]. The precursor frequency of direct pathway T

cells is extremely high, roughly 1-10%[176] of the T cell pool. This direct T cell alloreactivity likely results from cross-reactivity between intact allogeneic MHC molecules and self-MHC-foreign peptide complexes[175].

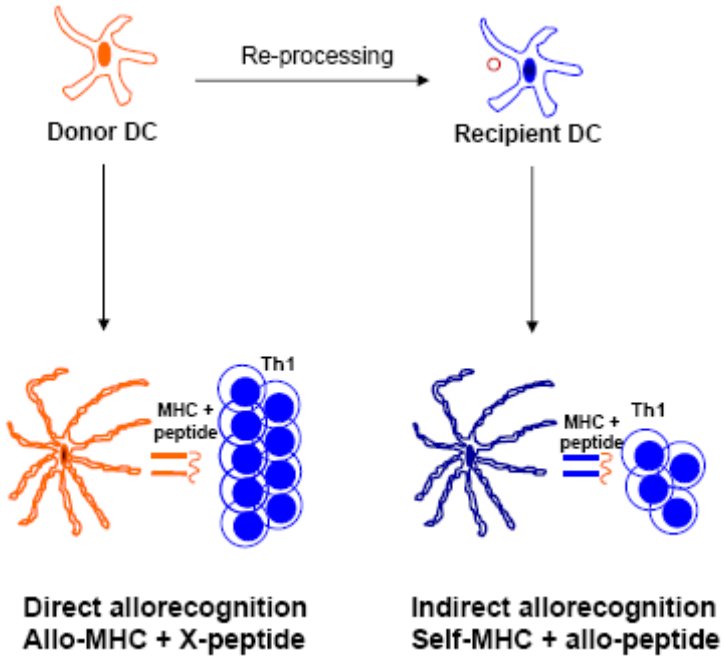

Figure 4. Pathways of allorecognition.

In the direct pathway, donor DC directly interact with anti-donor T cells. In this case, T cells recognize alloMHC:peptide complexes on the surface of donor DC. In the indirect pathway, recipient DC re-process donor alloAg derived from donor APC into allopeptide for presentation by self-MHC to anti-donor T cells.

By the indirect pathway, recipient T cells recognize self-MHC molecules presenting donor-derived allopeptides on recipient APC[177,178]. The precursor frequency of indirect pathway T cells is extremely low (1:100,000-200,000), the same as that for any other conventional/nominal Ag. It is unknown whether recipient APC mobilized into the graft acquire alloAg then traffic to secondary lymphoid organs to prime indirect pathway T cells, or whether alloAg derived from the graft, either in the form of passenger leukocytes or soluble Ag, enters

secondary lymphoid organs and is taken up by lymphoid resident DC for presentation. Either way, recipient APC internalize donor Ag and re-process it into peptide for presentation by self-MHC to indirect pathway T cells.

Recently, a third "semi-direct" pathway has been identified in mouse models. By the semi-direct pathway, intact donor MHC molecules are acquired by recipient APC and are presented intact to direct pathway T cells[179].

The semi-direct pathway is one proposed model challenging the existing paradigm that direct pathway T cells are primed independently of recipient APC and the indirect pathway (Fig. 5a,d). Alternatively, the 4-cell hypothesis suggests that indirect pathway $CD4^+$ helper T cells stimulated by recipient APC provide unlinked bystander help to direct pathway $CD8^+$ T cells stimulated by donor APC (Fig. 5b,c). Indirect $CD4^+$ T cells could also provide CD40-mediated stimulation of recipient APC that in turn might stimulate the direct pathway response through an unknown mechanism (Fig. 5b), or via interaction between a B cell receptor, if the recipient APC were a B cell, with donor MHC:alloAg on the surface of donor APC (Fig. 5c).

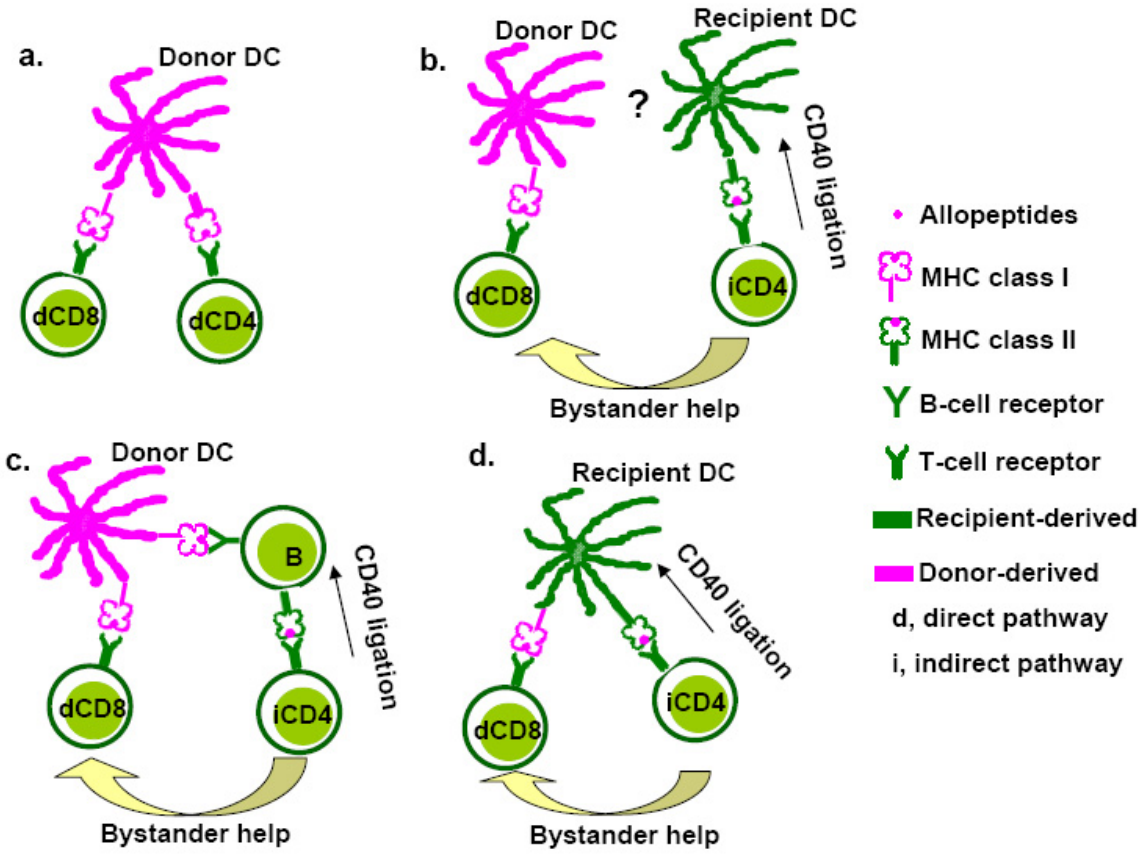

Figure 5. Models of direct pathway CD8$^+$ T cell priming.

1.3.3.2 Anti-donor T cell effector response

T cells are both necessary and sufficient for allograft rejection of almost all tissues. Acute graft rejection is considered T cell dependent, as several studies demonstrate that mice lacking T cells accept fully MHC-mismatched allografts, but that T cell reconstitution results in rejection. Due to the high precursor frequency of direct pathway T cells (approximately 1000 fold greater than indirect pathway T cells), it is assumed that the direct pathway is the more significant contributor of acute rejection[180-182]. However, as the supply of donor APC within the graft wanes over time, the contribution of the direct pathway decreases. Human studies confirm that the

direct pathway response is strongest in the period immediately following transplantation. Comparatively, alloAg is shed from the graft continuously, and due to epitope spreading[183], the significance of the indirect pathway increases[184]. As such, it is considered the main mediator of chronic rejection, which is confirmed in human studies of chronically rejected heart, kidney and lung[178,183-189].

Notably, there is evidence supporting the ability of the indirect pathway to mediate acute rejection. In human recipients of heart, kidney and liver allografts, in vitro detection of the indirect response shows strong correlation with episodes of rejection[185,190] and immunization of animals with peptide derived from allogeneic MHC (thus presented through the indirect pathway) causes allograft rejection[191,192]. Finally, using a cardiac allograft transplant model in mice, Auchincloss et al. showed that the indirect pathway is sufficient to elicit graft rejection in the absence of direct allorecognition[193]. The relative contributions of the indirect and direct pathway were evaluated in skin, cornea and retina, and results reveal that the importance of each pathway appears to be model dependent[194]. As expected, skin allografts have a pronounced direct pathway response, likely attributable to their high passenger APC load. Comparatively, cornea had a more potent indirect pathway response, again not surprising given its low level of MHC molecule expression. Such studies are yet to be performed in heart transplantation, although given the low number of passenger leukocytes, one might expect increased importance of the indirect response.

T cells contribute to allograft rejection by various mechanisms. Contact mediated cytotoxicity and release of pro-inflammatory cytokines are both potent mechanisms of allograft damage. Typically, the allograft response is T_h1, IFN-γ mediated, however both T_h1 and T_h2 effector responses can cause allograft rejection[141]. Further, T cells stimulate other immune cells

to cause damage. B cell function and the alloAb response depends on indirect pathway $CD4^+$ T cell help because B cells recognizing Ag via B cell receptors internalize, process and present antigenic peptides loaded in self-MHC to T cells, that in turn, provide the necessary help for B cell effector function and Ab class switching[195,196]. Indirect pathway T cells could also stimulate recipient MΦ or DC within the graft to release pro-inflammatory molecules in a DTH-like response. This previously has been associated with chronic rejection, however it is possible that the cytotoxic molecules released by MΦ/DC could contribute to acute rejection, particularly since one stimulated MΦ/DC could damage numerous surrounding donor cells simultaneously, while one $CD8^+$ cytotoxic T cell targets only one donor cell at a time.

1.4 CELLULAR THERAPIES IN TRANSPLANTATION

1.4.1 Types and history of cellular therapies

The concept of utilizing cellular therapies to induce allograft tolerance has its roots in the earliest studies of transplantation. Billingham, Brent and Medawar showed that infusion of donor allogeneic cells into newborn mice resulted in acceptance of skin allografts in the absence of immunosuppression[197]. More recently, Sayegh et al. demonstrated that intrathymic injection of donor allopeptides prolongs subsequent allografts of the same MHC[198], further indicating that exposure of recipients to donor Ag prior to transplantation has a tolerizing effect. Currently, there are three types of cellular therapies proposed for use in transplantation. Donor-specific transfusion (DST) refers to the transfer of donor splenocytes in mice, or peripheral blood mononuclear cells in humans, directly from donor to recipient with little manipulation. DST has

been employed in the clinic for decades and in some cases successfully decreased the anti-donor immune response and prolonged allograft survival. However, prevention of acute rejection was not universally achieved, and DST was associated with risk of recipient sensitization, thus the advent of pharmacologic immunosuppressive agents replaced DST as the main prophylactic for transplant recipients. Ironically, the negative side effects of pharmacologic immunosuppression coupled with the new goal of achieving operational tolerance, defined as long-term freedom from all immunosuppression with normal graft function, has resulted in a renewed interest in cellular therapies. Advancements in understanding peripheral tolerance mechanisms have led to development of newer cellular therapies including donor apoptotic cell therapy and tolerogenic DC therapies.

1.4.2 Effects of DST on allograft transplantation

Quezada et al showed that DST significantly prolongs skin allograft survival through peripheral deletion of indirect pathway $CD4^+$ T cells and increased numbers of Treg[199]. Brouard and Soulillou and colleagues demonstrated that infusion of splenocytes without additional immunosuppression leads to long-term survival of cardiac allografts through expansion of Treg, and that transfer of long-term survivor splenic T cells to new allograft recipients transfers long-term allograft survival in an Ag-specific manner[200]. Importantly, in the Quezada study, the injected living donor splenocytes did not directly interact with $CD4^+$ T cells[199]. This finding suggests that living splenocytes upon i.v. injection become apoptotic in vivo and are re-processed by recipient APC for indirect presentation and therefore that living donor splenocytes simply serve as a source of alloAg.

1.4.3 Effects of apoptotic splenocytes on allograft transplantation

1.4.3.1 Apoptotic leukocytes promote allograft survival

Bittencourt and colleagues demonstrated that i.v. infusion of apoptotic leukocytes enhances allogeneic bone marrow engraftment following a non-myeloablative conditioning regimen in mice[201]. The beneficial effect of apoptotic cells was independent of the stimulus used to trigger cell death. Interestingly, donor, recipient and even xenogeneic apoptotic leukocytes were capable of promoting allogeneic bone marrow engraftment, suggesting that the therapeutic effect of apoptotic cells was not donor-specific. However, since the apoptotic cells were administered simultaneously with the bone marrow graft, it is possible that the apoptotic cells had exerted a bystander pro-tolerogenic effect on recipient DC when they were presenting the donor alloAg from the graft. Further, co-administration of apoptotic leukocytes with allogeneic hematopoietic stem cells has been proven to expand Treg able to delay onset of graft versus host disease[202], and also to prevent the anti-donor humoral response[203].

Further, apoptotic cell therapy has been shown to improve bone marrow engraftment by inducing mixed chimerism, defined as the presence of donor-derived cells (normally of hematopoietic origin) in the tissues of allograft recipients[204]. Micro- and macro-chimerism refers to the detection of <1.0 and >1.0%, respectively, of donor cells in the recipient. The reason(s) that mixed chimerism correlates with a state of anti-donor hypo-response/tolerance and the consequent prolongation of graft survival has not been entirely elucidated.

A limited number of studies in murine models have proven the efficacy of apoptotic cell-based therapies for prolongation of solid organ allograft survival. Our group has demonstrated in mice that i.v. administration of donor-derived UV-B-irradiated apoptotic splenocytes seven days prior to transplantation significantly prolongs survival of heart allografts in the absence of

immunosuppression[75]. Moreover, combination of donor apoptotic splenocytes with suboptimal blockade of the CD40-CD154 pathway with a single dose of anti-CD154 monoclonal Ab (mAb) results in long-term survival of cardiac transplants for more than 100 days[75]. The therapeutic effect of donor apoptotic cells was donor-specific and required interaction of the apoptotic cells with recipient DC in secondary lymphoid organs. It also depended on the physical properties of the apoptotic leukocytes, since administration of donor necrotic cells did not affect graft survival[75]. Similarly, infusion of donor apoptotic leukocytes prolonged significantly cardiac allograft survival in a rat model[205]. In humans, there is indirect evidence suggesting that apoptotic leukocytes may have a beneficial effect in graft recipients treated with extracorporeal photophoresis (ECP), a technique by which blood leukocytes are UV-B-irradiated ex-vivo and then re-infused systemically[206]. The ultimate mechanism of action of ECP is still unknown, however it is believed that UV-B-irradiation primes leukocytes to become apoptotic when re-infused into the bloodstream with consequent anti-inflammatory effects on the immune system.

1.4.3.2 Apoptotic leukocytes down-regulate the T cell alloresponse

We demonstrated that i.v. administered donor-apoptotic cells are rapidly phagocytosed by recipient splenic DC, which present apoptotic cell-derived allopeptides in self-MHC to indirect pathway T cells[75]. Importantly, internalization of apoptotic cells did not induce maturation/activation of recipient DC in vivo, as reflected in similar expression of MHC molecules, CD40, CD80 and CD86 compared to splenic DC from non-treated mice.

Using a model of C57BL/10 (B10) mice reconstituted with 1H3.1 TCR transgenic (tg) $CD4^+$ T cells [specific for the BALB/c allopeptide $IE\alpha_{52\text{-}68}$ loaded in IA^b molecules (MHC class II of B10)], we characterized the in vivo effect of apoptotic cell-derived allopeptide presentation on indirect pathway T cells[75]. Interestingly, splenic 1H3.1 $CD4^+$ T cells proliferated in response

to injection of BALB/c apoptotic splenocytes, but did not up-regulate expression of the T cell activation markers CD25, CD44, CD69 and CD152, and secreted lower amounts of IL-2 and IFN-γ upon ex vivo re-stimulation with IEα_{52-68}, when compared to controls. Importantly, the defective activation of anti-donor 1H3.1 $CD4^+$ T cells resulted in their peripheral deletion, as their numbers decreased significantly in spleen, LN, blood and peripheral tissues, 14 days after administration of apoptotic cells. Notably, after administration of BALB/c apoptotic splenocytes, proliferating 1H3.1 $CD4^+$ T cells failed to increase levels of the anti-apoptotic protein Bcl-X_L and of receptors for IL-7 and IL-15, which are cytokines required for homeostatic survival/proliferation of T cells.

Besides inducing peripheral deletion of donor-reactive T cells, administration of donor apoptotic splenocytes in combination with suboptimal CD40-CD154 blockade promoted differentiation/expansion of donor-specific $CD4^+$ Treg[75] and long-term heart allografts of mice treated with donor apoptotic splenocytes plus anti-CD154 mAb were infiltrated with a high number of $CD4^+$ T cells expressing the Treg marker FoxP3 and containing intracellular IL-10 and TGF-β. Accordingly, adoptive transfer of $CD4^+$ T cells, from B10 mice with long-term surviving BALB/c cardiac grafts (>100 days) following treatment with BALB/c apoptotic splenocytes plus CD154 mAb, into naïve B10 recipients prolonged survival of BALB/c hearts but not third-party control grafts.

1.4.3.3 Apoptotic leukocytes decrease the B cell alloresponse

Given the dependence of B cell differentiation into plasma cells and secretion of alloAb on indirect pathway $CD4^+$ T cell help, deletion of indirect pathway $CD4^+$ T cells should indirectly reduce generation of alloAb. Indeed, we have shown in mice that therapy with donor

apoptotic splenocytes reduces significantly the level of circulating alloAb in cardiac allograft recipients[75].

1.4.3.4 Apoptotic leukocytes mitigate chronic rejection

Although the effects of cellular therapies on acute rejection are routinely studied, the effects on chronic rejection are less commonly explored. Given the detrimental outcomes from chronic rejection in the clinic, this is of importance to study in animal models. An experimental approach in mice to investigate the onset of CVA, the main feature of chronic rejection, is the model of aortic (abdominal) allografts, where the histological features of CVA develop in the transplanted aorta 30-60 days after surgery. Using this model, we found that administration of BALB/c apoptotic splenocytes to recipient B6 mice seven days before transplant of BALB/c aortic grafts, results in significant inhibition of the indirect pathway T cell response and the histopathological features of CVA[207].

1.4.4 Comparing DST to apoptotic leukocyte therapy

Although there are multiple similarities between the mechanisms of action of donor apoptotic and living splenocytes injected i.v., dead or dying cells behave in some aspects differently than living cells. Whereas donor apoptotic cells injected i.v. induce activation of donor-reactive T cells only in the spleen, DST is followed by T cell stimulation in spleen and LN[75]. This difference is likely attributable to the ability of living splenocytes to traffic actively to both spleen and LN, as opposed to the passive transport of apoptotic cells by the bloodstream into the spleen, where they are trapped mainly by marginal zone phagocytes. Further, whereas donor apoptotic cells induce defective activation of donor-reactive T cells, DST is followed by up-

regulation of the activation marker CD69 and CD44 by T cells[75]. At the same time, outcome in murine models of allograft transplantation are similar, suggesting that DST and apoptotic splenocyte therapies have comparable efficacy.

1.4.5 DC therapies in transplantation

It has been assumed that therapeutic tolerogenic DC, once administered i.v. to prospective graft recipients, interact directly with anti-donor T cells. Given the preponderance of the direct pathway in acute allograft rejection, it has further been assumed that the ability to down-modulate the direct pathway response makes DC therapies superior to alternative cellular therapies (DST and apoptotic cell therapy) in transplantation. However, the ability of DC therapies to modulate the direct and indirect pathways has never been tested, nor has a comparison of efficacy between cellular therapies been performed.

A number of different types of tolerogenic DC have been studied in mouse models of heart transplantation using a heterotopic cardiac allograft model. These tolerogenic DC therapies prolong allograft survival with a mean survival time (MST) between 20 and 50 days[208-212]. Typically, an increased percentage of Treg is observed along with decreased T cell effector responses. Although these different tolerogenic DC vary phenotypically in vitro, the similar effect on allograft survival and anti-donor T cell responses suggest similar mechanism of action in vivo.

Based on the "missing self" hypothesis, recipient NK cells would recognize as non-self and eliminate i.v. administered donor-derived therapeutic DC. Even though i.v. administered recipient-derived tolerogenic DC loaded ex vivo with alloAg would be spared from NK cell recognition, they would likely have a limited life-span in vivo and become apoptotic due to

natural turnover[213]. Supporting this concept, MST from DC therapies mirror those observed with alternative cellular therapies suggesting that contrary to current dogma, tolerogenic DC therapies, like living and dead splenocyte therapies, serve as a source of alloAg to prolong allograft survival[75,199,208-210,212,214,215].

Given the time, cost and risk of DC therapies for clinical use in transplantation, it is essential to explore the fate of tolerogenic DC in vivo, elucidate their mechanism of action and compare their efficacy to alternative cellular therapies.

1.5 SPECIFIC AIMS

1.5.1 Specific Aim 1 (Chapter 2): To investigate the in vivo mechanism(s) by which tolerogenic DC therapy prolongs allograft survival

Current dogma in transplantation assumes that therapeutic tolerogenic DC delay/prevent transplant rejection by interacting directly with donor-reactive T cells in vivo. However, this hypothesis remains untested. We demonstrate in mice that therapeutic DC failed to directly tolerize anti-donor T cells, but rather were re-processed into alloAg by quiescent recipient DC to induce Treg outgrowth and effector T cell deletion. Interestingly, therapeutic DC did impair the direct pathway response, resulting in prolonged cardiac allograft survival comparable to alternative cellular therapies. To explain this apparent paradox, we reveal that CD40 stimulation of recipient APC by indirect $CD4^+$ helper T cells was requisite for direct pathway T cell activation and cardiac allograft rejection. Therefore, recipient DC link indirect and direct pathway responses, allowing DC-based therapy prolongation of cardiac allograft survival. Our

data support utilizing safer and more practical cellular therapies coupled with agents that maintain recipient APC in a quiescent state for clinical use in transplantation.

1.5.2 Specific Aim 2 (Chapter 3): To examine the necessity of donor "passenger" APC in priming the anti-donor T cell response

Our data from specific aim 1 contradicts the paradigm that donor APC prime the direct pathway response independently of the indirect pathway. We further tested the validity of this paradigm by investigating the requirement of donor passenger APC for priming the T cell alloresponse. We observed that although cardiac allograft parenchymal and endothelial cells up-regulated robust MHC class I and II expression, donor passenger APC were required for direct pathway T cell responses in cardiac allograft and secondary lymphoid organs. Further, we have preliminary data that donor passenger APC are required for an indirect pathway T cell response as well. Therefore, donor passenger APC provide both intact MHC:peptide complexes, and a source of alloAg, for priming the T cell alloresponse.

1.5.3 Specific Aim 3 (Chapter 4): To investigate the role of inflammatory monocytes in transplant rejection

Given the crucial nature of recipient DC in transplantation, we investigated the role that inflammatory monocyte-derived DC, "inflammatory DC" play in cardiac allograft rejection. We identified two populations of inflammatory monocytes, one characterized as $CD11b^{hi}Ly6C^{hi}$ and the other as $CD11b^{hi}Ly6C^{int}$, as the main types of APC infiltrating cardiac allografts. Infiltration peaked at 7 d post-transplant, during the effector phase of the anti-donor immune response.

Accordingly, we observed that inflammatory monocytes differentiated into TNF-α and iNOS producing-DC that participated in a DTH-like response mediated by indirect pathway $CD4^+$ helper T cells. Allograft infiltration was concomitant with monocytopoiesis and monocytosis, as well as increased infiltration into secondary lymphoid organs. Egress of inflammatory monocytes out of the bone marrow depended on CCR2 expression. Interestingly, absence of inflammatory monocytes in the periphery resulted in enhanced T cell priming and effector function.

This data demonstrate a previously undocumented finding that inflammatory monocytes are capable of playing a dual role within the same disease model, one as a pro-inflammatory innate immune cell, and the other as a brake on the adaptive immune response. Further, our data suggest the exciting possibility that blood tests to detect monocytosis could be employed in the clinic to screen for acute allograft rejection, thus relinquishing dependence on risky and costly heart biopsies.

2.0 RECIPIENT APC RE-PROCESS THERAPEUTIC DC AND LINK ALLO-RECOGNITION PATHWAYS TO PROLONG ALLOGRAFT SURVIVAL

2.1 INTRODUCTION

Dendritic cells (DC) are antigen (Ag)-presenting cells (APC) capable of initiating T cell immunity or tolerance. Understanding the mechanisms by which DC promote tolerance, and the development of methods to propagate DC in vitro has enabled generation of DC-based therapies for treatment in transplantation and autoimmunity. However, in transplantation, DC-based therapy mechanism of action remains unknown. The prevailing dogma states that therapeutic donor-derived DC down-regulate the anti-donor response by directly interacting with T cells recognizing donor-MHC (direct pathway of allorecognition)[175] in lymphoid organs. Alternatively, the injected DC could function as a source of alloAg for recipient APC, which in turn down-regulate the anti-donor response elicited by T cells recognizing self-MHC molecules loaded with donor-peptide (indirect pathway of allorecognition)[177,178]. Interestingly, evidence in mice suggests that the beneficial effect on cardiac allograft survival induced by donor-specific transfusion of donor splenocytes (DST) or donor-apoptotic cell therapy may be achieved through this indirect mechanism[75,199].

Here, we investigated in vivo the mechanisms by which DC-based therapies prolong transplant survival. We demonstrate that therapeutic DC failed to directly regulate T cells, but

rather were re-processed by quiescent recipient splenic DC for indirect presentation. Therapeutic DC did impair direct pathway responses in vivo though, thus allowing prolongation of cardiac allograft survival comparable to alternative cellular therapies. These findings appear paradoxical based on the current paradigm of direct pathway priming which presumes that donor APC directly prime anti-donor T cells independently of the indirect pathway. We demonstrate however the novel finding that recipient APC activation by indirect $CD4^+$ T cells via CD154-CD40 ligation was requisite for direct pathway T cell activation and allograft rejection. We therefore conclude that recipient APC serve as a crucial link between the indirect and direct pathways and that therapeutic DC, like alternative cellular therapies, function as a source of alloAg for quiescent recipient DC to prolong allograft survival.

2.2 RESULTS

2.2.1 Vitamin D_3 treated bm-DC are maturation-resistant and exhibit normal survival

To compare the efficacy of donor-derived DC-based methods over alternative cellular therapies at prolonging allograft survival in mice, we tested as prototypic therapeutic DC, maturation-resistant (MR)-DC generated from bone marrow precursors cultured with GM-CSF, IL-4 and $1\alpha,25(OH)_2VD_3$, the active form of VD_3 which inhibits DC maturation (Fig. 6)[109,110,118,119]. We determined that 10^{-8} M VD_3 treatment of DC results in the greatest resistance to maturation with minimal effect on cell viability (data not shown), so we used this dose throughout our study. At this dose, MR-DC exhibited an immature phenotype (MHC-I/$II^{lo}CD40^{neg}CD80/86^{neg/lo}$) and, unlike control-DC, failed to up-regulate expression of MHC-I/II, CD40, CD80 and CD86

molecules, secrete IL-12p70, and stimulate proliferation of alloreactive T cells after challenge with a DC1-maturation cocktail (DC1c)[216,217] (Fig. 6), LPS or agonistic CD40 mAb (not shown). Neither IL-10 nor IL-23 were detected in culture supernatants of VD_3-treated or control-DC with or without stimulation (data not shown).

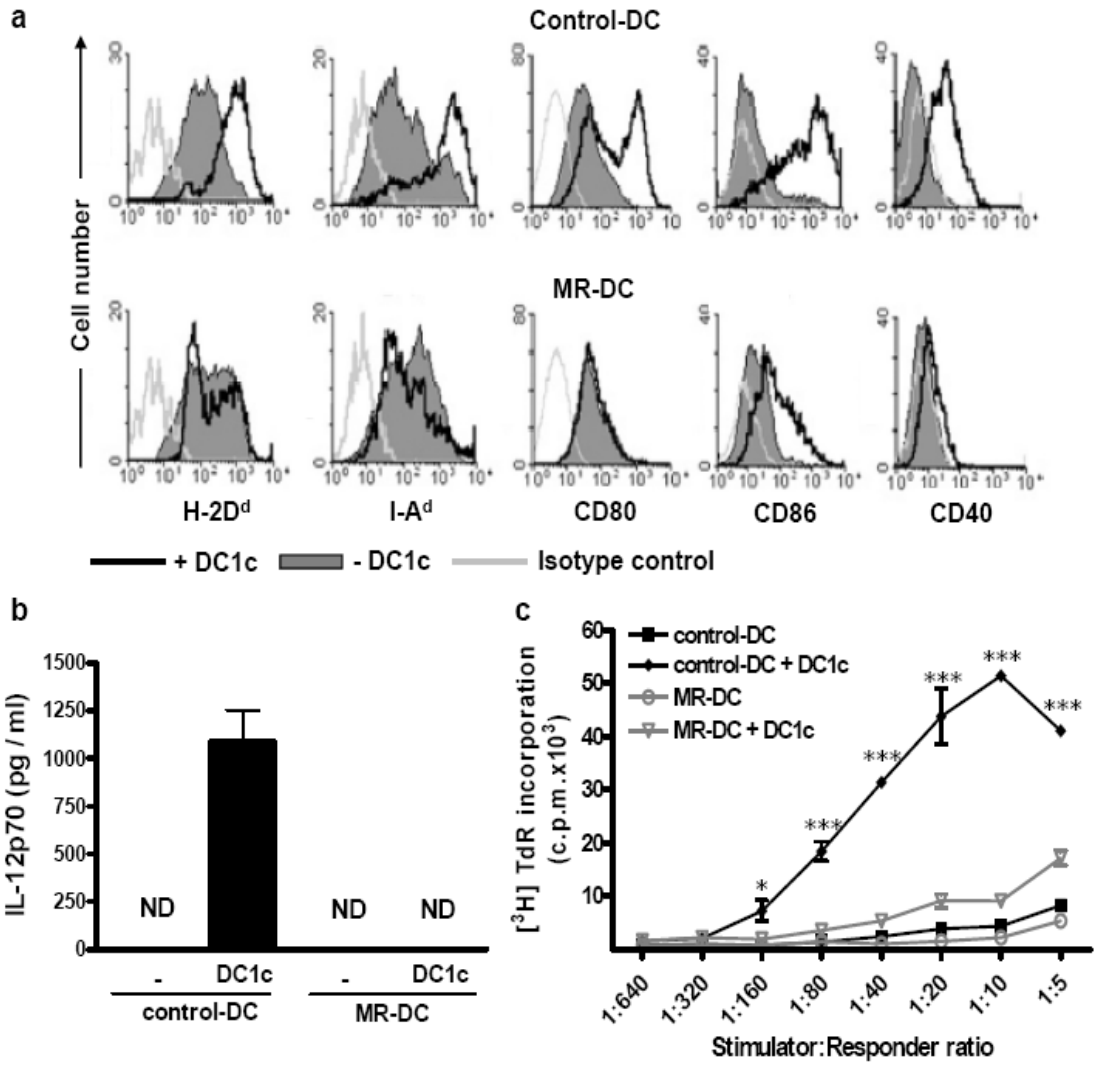

Figure 6. VD_3-treated bone marrow-derived DC are maturation-resistant.

Unlike control-DC, following challenge with DC1c, MR-DC (a) exhibited an immature phenotype (MHC-I/II^{lo}CD40^{neg}CD80/86$^{neg/lo}$) and failed to up-regulate expression of MHC-I/II, CD40, CD80 and CD86 molecules, as determined by flow cytometry, (b) secrete IL-12p70, quantified from culture supernatants by ELISA or (c) stimulate proliferation of alloreactive T

cells**.** (a,c) Representative data from 2 independent experiments is shown. (b) Combined data from 2 independent experiments is shown (mean ± SEM). * $p < 0.05$, *** $p < 0.001$.

Importantly, we confirmed that the use of VD_3 at 10^{-8} M concentration did not affect the viability of VD_3-DC (80.5% vs. 87.1% in control-DC) (Fig. 7) or expression of the chemokine receptor CCR7 (data not shown), which is required by DC for effective migration into lymph nodes, although the necessity of CCR7 for DC entry into spleen is less clear. This data indicate that, at least at the time of i.v. injection, therapeutic DC are viable and capable of migrating to lymphoid tissue.

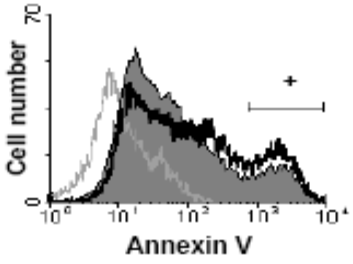

Figure 7. VD_3 treatment does not affect DC viability in vitro.

Seven days after culture, bone marrow-derived DC treated with VD_3 or not, were stained for detection of externalized phosphatidyl serine, a marker of apoptosis, by fluorochrome conjugated Annexin V, and analyzed by flow cytometry. Light gray line – unstained control, dark gray shaded region – control-DC, black line – VD_3-DC.

2.2.2 VD_3-DC prolong cardiac allograft survival similarly to alternative cellular therapies

Several studies have shown in murine models that therapy with immature, MR or alternatively-activated DC, expressing low amounts of MHC:Ag and co-stimulatory molecules, in otherwise non-immunosuppressed recipients prolongs cardiac allograft survival with mean survival times (MST) between 20-50 d[208-210,212,214,215]. Therapy with our donor-derived MR-DC 7 d prior to

transplantation prolonged survival of BALB/c hearts in B6 mice similarly to immature control-DC (MST of 52.2 vs. 53.5 d, $p>0.05$), and significantly compared to non-treated (52.2 vs. 11.5 d, $p<0.0001$) or third-party controls (21.2 d, $p=0.0317$) (Fig. 8). Surprisingly, no side-by-side comparison in cardiac transplantation of donor-derived DC therapies and alternative cellular therapies has previously been performed. Notably in our model, treatment with donor splenocytes (alive or apoptotic) prolonged cardiac allograft survival comparably to therapy with donor-derived MR-DC (56 and 45.9 vs. 52.2 d, respectively, $p>0.05$) (Fig. 8), refuting the alleged superiority of donor-derived therapeutic DC over other cellular therapies and suggesting that different donor-derived cellular therapies might share similar mechanisms of action. Given the ability of VD_3 to render DC maturation resistant, and the similar effect on allograft survival of VD_3-DC compared to other tolerogenic DC therapies, we utilized VD_3-DC as prototypic MR-DC for the remainder of studies.

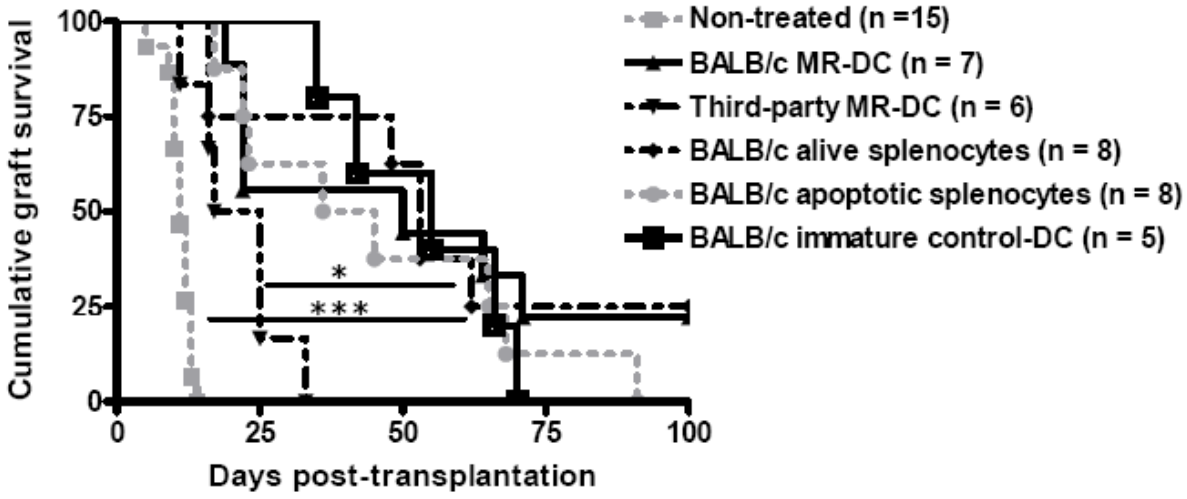

Figure 8. Donor-derived MR-DC prolong cardiac allograft survival.

Survival of BALB/c cardiac allografts in B6 recipient mice treated i.v. (or not), 7 d prior to transplantation, with $5x10^6$ donor- or third-party-derived MR-DC, $5x10^6$ donor immature control-DC or with 10^7 donor living or apoptotic splenocytes. * $p < 0.05$, *** $p < 0.001$.

2.2.3 Donor-derived MR-DC rapidly die in vivo

Given the similar MST induced by DC therapies, DST and apoptotic cell therapy, we hypothesized that once injected i.v., donor-derived MR-DC would become apoptotic due to natural turnover and/or to targeting by recipient NK cells, and thus serve as a source of alloAg for quiescent recipient DC in lymphoid organs[218].

To evaluate our hypothesis, we first analyzed trafficking of BALB/c-derived ($CD45.2^+$) MR-DC administered i.v. (10^7 DC) in B6 mice ($CD45.1^+$). Six h after injection, very few MR-DC ($CD45.2^+$) were detected in the splenic marginal zone, and between 12-48 h, within T cell areas (Fig. 9a). Due to the low numbers of BALB/c MR-DC observed by microscopy, we estimated the number of MR-DC in recipient spleen by PCR analysis for the *IgG2a*^{a} allele (encoded in the BALB/c, but not B6, genome)[219]. Using BALB/c MR-DC serially diluted in a fixed number of B6 splenocytes, we determined the PCR sensitivity to be approximately 1 BALB/c MR-DC in 10,000 B6 splenocytes[220,221] (Fig. 9b). By assaying B6 spleens 1, 6 and 24 h following BALB/c MR-DC administration ($5x10^6$ DC), we found that BALB/c DNA content decreased steadily 1 h after DC inoculation and was barely detectable 24 h later, roughly indicative of ≤10,000 BALB/c MR-DC per spleen (Fig. 9b). Treatment with depleting NK1.1 mAb increased the amount of BALB/c DNA detected 6 and 24 h following MR-DC injection, indicating that host NK cells contribute to or hasten elimination of donor-derived MR-DC.

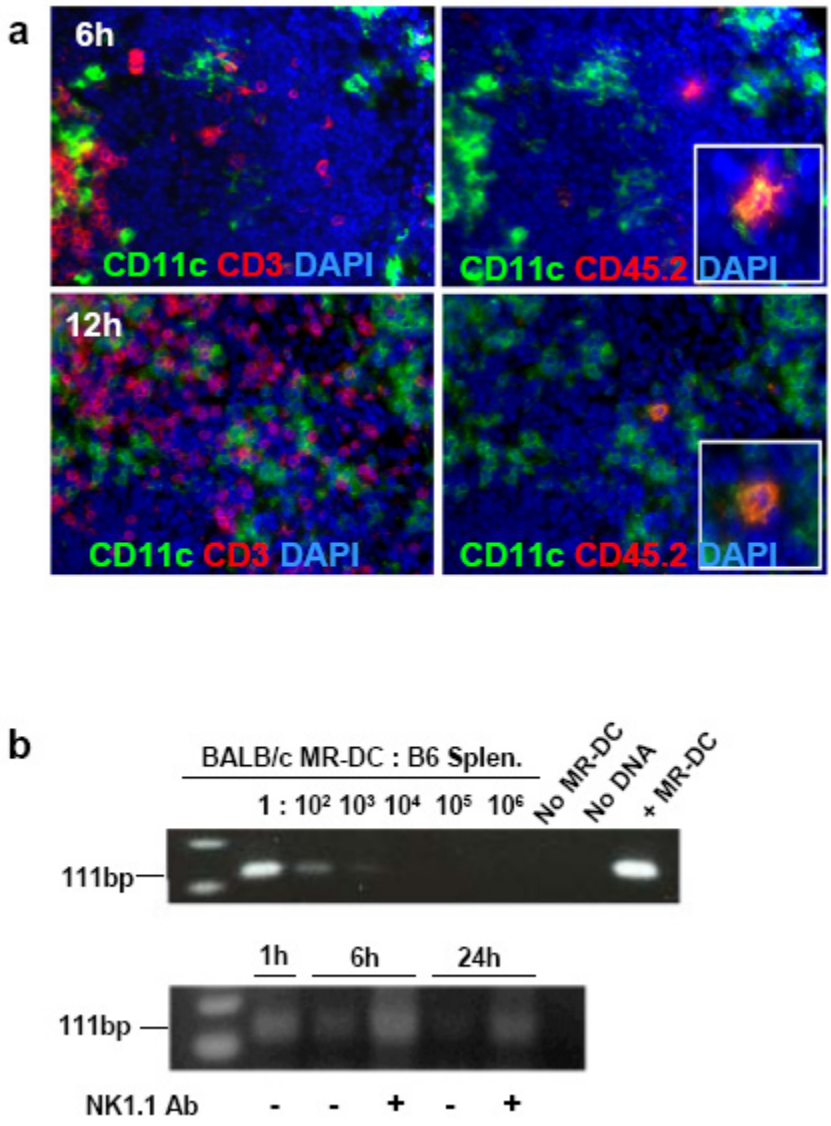

Figure 9. DC. Donor-derived MR-DC are short-lived in vivo.

(a) BALB/c MR-DC ($CD45.2^+$) migration into host B6 mice ($CD45.1^+$) with staining for CD11c, CD45.2 and CD3. (b) PCR analysis of the BALB/c *IgG2a*^{a} allele. Top: assay sensitivity. Bottom: samples taken 1, 6 or 24 h after injection of BALB/c MR-DC into B6 mice treated (+) or not (-) with depleting NK1.1 mAb. Representative images are shown.

2.2.4 Apoptotic MR-DC derived fragments are internalized, re-processed into allopeptides and presented by recipient DC briefly in vivo

Given this rapid loss of donor-derived MR-DC in vivo, we explored whether BALB/c MR-DC are internalized as apoptotic cell fragments by splenic APC. Following i.v. injection of PKH26-labeled (red) BALB/c MR-DC ($5x10^6$ DC) into CD11c-eGFP B6 mice, MR-DC-derived fragments were clearly visible inside recipient $CD11c^+$ DC (Fig. 10a). Quantification revealed that at 6, 24 and 48 h after adoptive transfer, roughly 20% of recipient $CD11c^+$ DC contained BALB/c MR-DC-derived fragments (Fig. 10b). To exclude passive transfer of PKH26 between donor and host DC and to identify apoptotic bodies, BALB/c MR-DC ($CD45.2^+$) were injected into B6 mice ($CD45.1^+$). Twelve h later, we detected BALB/c MR-DC-derived apoptotic bodies ($CD45.2^+$ $TUNEL^+$) within B6 splenic DC ($CD11c^+$ $CD45.2^-$) (Fig. 10c).

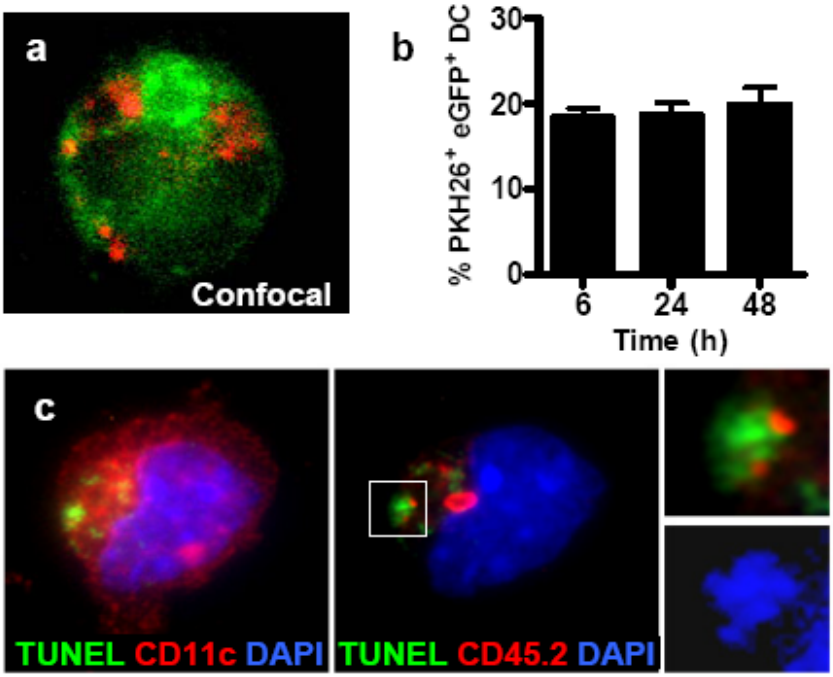

Figure 10. Apoptotic bodies derived from donor MR-DC are internalized by recipient DC.

Confocal microscopy image of recipient splenic CD11c-eGFP$^+$ cells containing intracellular fragments derived from PKH26-labeled BALB/c MR-DC (a) and the number of recipient DC containing fragments derived from donor MR-DC were quantified and averaged from 15 low power fields (b). (c) Cytospin showing a recipient splenic CD11c$^+$ DC containing phagocytosed apoptotic bodies (TUNEL$^+$) derived from CD45.2$^+$ BALB/c MR-DC. Nuclei were counter-stained with DAPI. Insets: detail of apoptotic cell fragments. (a,c) Representative data is shown, (b) Mean ± SEM is shown. n = 3 animals per group.

We next identified the subpopulation(s) of splenic APC responsible for re-processing donor-derived MR-DC and presentation of alloAg to donor-reactive T cells. BALB/c MR-DC were injected i.v. (10^7 DC) in B6 mice and 20 h later, subsets of host (H2-K^{b+}) splenic APC were isolated by FACS-sorting: (i) CD11c^{hi}CD8$^-$ DC, (ii) CD11c^{hi}CD8α^+ DC, (iii) CD11c^{int}CD45RA$^+$ plasmacytoid DC, and (iv) CD11c^{neg} cells. Each subset was used as stimulators of CFSE-labeled 1H3.1 CD4$^+$ TCRtg T cells (specific for the BALB/c IE$\alpha_{52\text{-}68}$-B6 IA^b complex) in 5 d-mixed lymphocyte culture. Only CD11c^{hi}CD8$^-$ and CD8α^+ DC induced 1H3.1 T cell proliferation (Fig. 11).

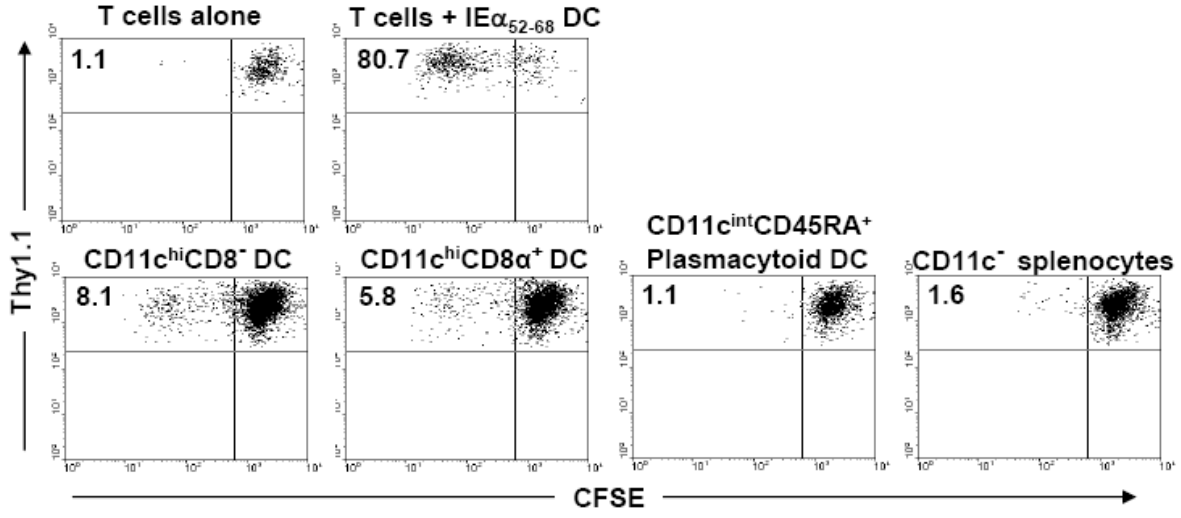

Figure 11. Recipient DC re-process therapeutic DC into alloAg for presentation via the indirect pathway.

Five d-MLC of CFSE-labeled 1H3.1 $CD4^+$ T cells stimulated with FACS-sorted splenic APC isolated from B6 mice injected 20 h earlier with BALB/c MR-DC. Representative data from two independent experiments is shown.

A recent publication showed that splenic DC undergo a limited number of divisions over 10-14 d and pass on Ag to daughter DC[222], thus we assessed the duration that recipient splenic DC present MR-DC-derived alloAg in vivo. B6 mice were injected with BALB/c MR-DC 14, 7, 3 or 1 d before adoptive transfer of CFSE-labeled responder 1H3.1 $CD4^+$ T cells. Splenic DC presentation of BALB/c allopeptides was limited in time, as only minor 1H3.1 T cell proliferation was detected following the 3 d lag period between MR-DC and 1H3.1 T cell administration (Fig. 12). Thus, systemically-injected donor-derived MR-DC rapidly become apoptotic, and are internalized, re-processed and briefly presented to indirect $CD4^+$ T cells by splenic $CD8^-$ and $CD8\alpha^+$ DC.

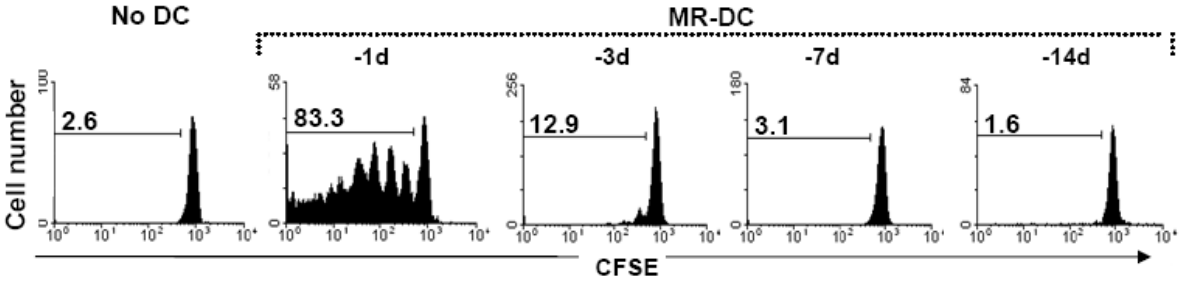

Figure 12. Donor MR-DC-derived alloAg is presented only briefly in vivo.

BALB/c MR-DC were injected on various days before CFSE-labeled 1H3.1 T cells to assess duration of alloAg presentation in vivo. Representative data from two independent experiments is shown.

2.2.5 Recipient DC down-modulate indirectly alloreactive T cells

These findings prompted us to investigate the effect of donor-derived MR-DC on the indirect T cell response in vivo, and the importance of activation status of the recipient DC that re-process injected MR-DC. B6 mice were adoptively transferred with CFSE-labeled 1H3.1 $CD4^+$ T cells ($Thy1.1^+$), then 1 d later were injected i.v. with BALB/c MR-DC alone, or to determine the influence of recipient DC maturation status, plus agonistic CD40 mAb (Fig. 13a). BALB/c MR-DC administration induced "defective activation" of 1H3.1 T cells assessed 3 d after DC injection, as demonstrated by proliferation of 1H3.1 T cells with $CD69^{lo}CD62L^{hi}$ phenotype, while 1H3.1 T cells from mice treated with MR-DC plus CD40 mAb expressed a typical activation phenotype ($CD69^+CD62L^{lo}CD127^-$) (Fig. 13b).

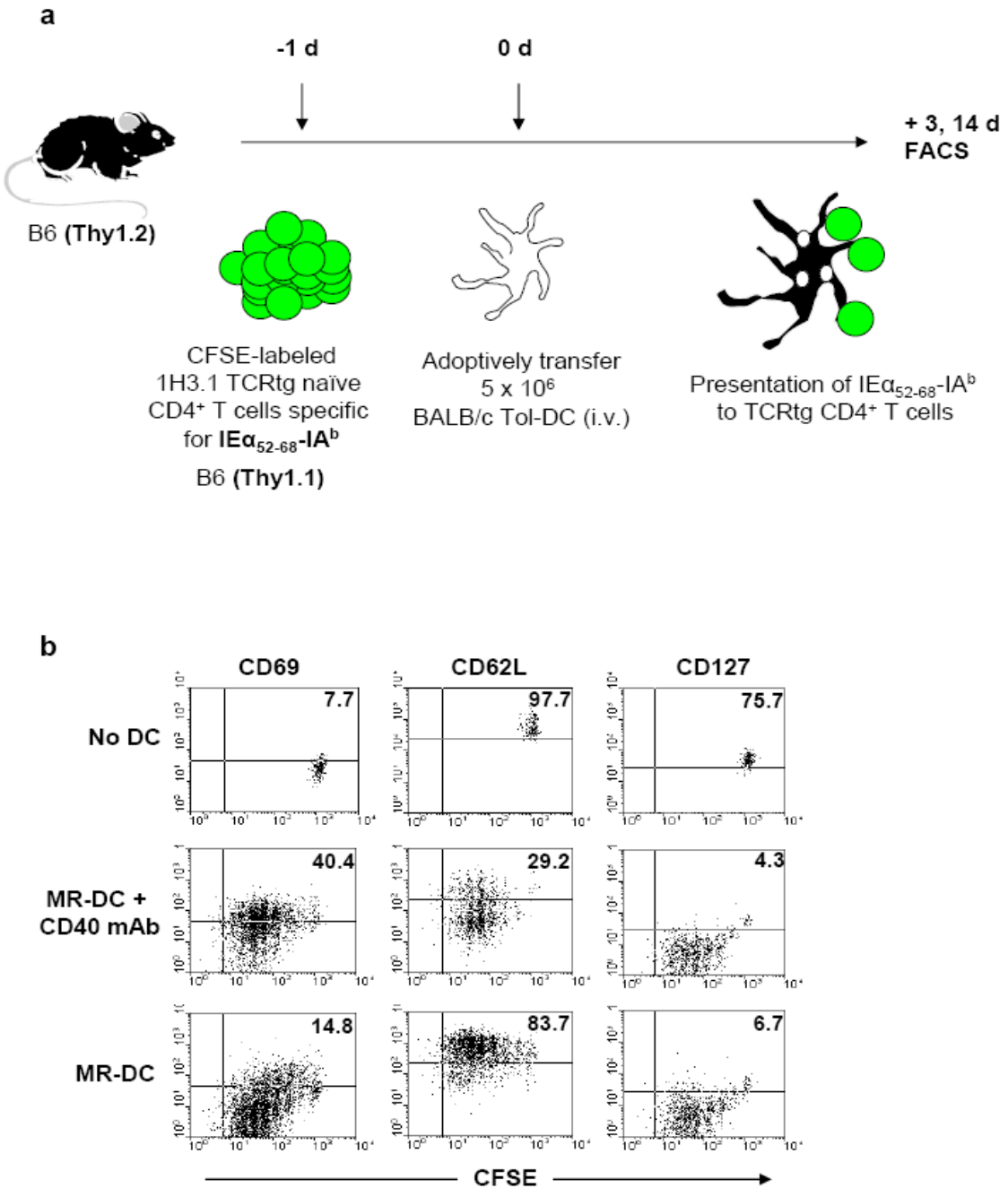

Figure 13. Donor-derived MR-DC induce defective activation of indirect pathway CD4$^+$ T cells.

(a) Recipient B6 mice were adoptively transferred with CFSE-labeled 1H3.1 CD4$^+$ T cells then treated, or not, 1 d later with BALB/c MR-DC alone or plus agonistic CD40 mAb. (b) FACS analysis showing representative dot plots gated on CD4$^+$Thy1.1$^+$ T cells of activation marker expression 3 d after MR-DC administration. Representative plots shown. n = 3 or more animals per group.

The initial expansion of defectively activated splenic 1H3.1 $CD4^+$ T cells was followed 14 d after MR-DC administration by a significant reduction in their number, compared to MR-DC plus CD40 mAb (p=0.0054) or to No DC negative controls (p=0.0329) (Fig. 14a), and ability to secrete IFN-γ in response to stimulation with $IE\alpha_{52\text{-}68}$, compared to MR-DC plus CD40 mAb (p=0.0024) (Fig. 14c), indicating that peripheral deletion of indirect $CD4^+$ T cells had occurred. This reduction in number could be attributed to 1H3.1 T cell migration to the periphery, however we were unable to detect 1H3.1 $Thy1.1^+CD4^+$ T cells in heart, kidney, liver or blood 14 d after MR-DC treatment (not shown). 1H3.1 T cell deletion in mice treated with MR-DC alone was accompanied at d 14 by a significant increase in 1H3.1 $CD4^+$ T cells expressing the regulatory T cell (Treg) marker FoxP3, compared to MR-DC plus CD40 mAb (p=0.0002) and to No DC controls (p=0.0081) (Fig. 14b). MR-DC administration did not induce immune-deviation of indirect $CD4^+$ T cells, as neither IL-4 nor IL-10 was detected in culture supernatants following stimulation with $IE\alpha_{52\text{-}68}$, 3 or 14 d after MR-DC treatment (not shown). Thus, therapy with donor-derived MR-DC utilizes the indirect pathway to promote deletion of anti-donor effector $CD4^+$ T cells and expansion of Treg.

By contrast, 1H3.1 T cell IFN-γ production remained high (Fig. 14c) and percentage $FoxP3^+$ low (Fig. 14b) in mice treated 14 d prior with donor-derived MR-DC plus agonistic CD40 mAb. These findings demonstrate that recipient DC quiescence is critical for down-regulating the indirect T cell response.

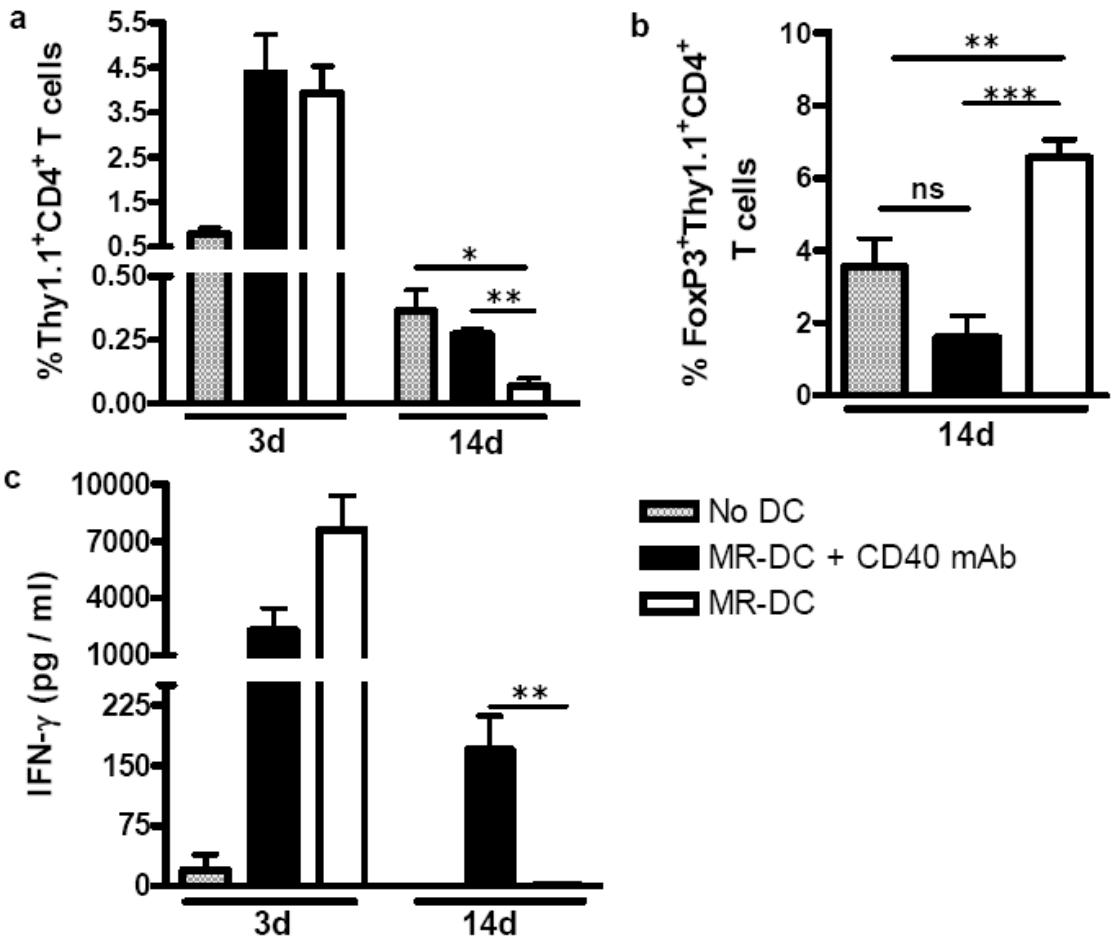

Figure 14. Indirect pathway presentation results in peripheral deletion and Treg outgrowth.

(a) Percentage 1H3.1 Thy1.1$^+$ T cells of the total splenic CD4$^+$ T cell population of B6 recipient mice, 3 and 14 d after MR-DC administration. (b) Percentage 1H3.1 CD4$^+$Thy1.1$^+$FoxP3$^+$ T cells in host spleen 14 d after MR-DC injection. (c) Amount of IFN-γ secreted by host B6 splenocytes stimulated with the BALB/c IE$\alpha_{52\text{-}68}$ allopeptide for 24 h. Data are averaged from 2 independent experiments with 3 or more animals per group (mean ± SEM). * $p < 0.05$ ** $p < 0.01$, *** $p < 0.001$.

2.2.6 Therapeutic DC fail to directly tolerize anti-donor T cells

The prevailing theory regarding prolongation of allograft survival by currently employed therapeutic DC proposes that systemically-administered DC interact directly with anti-donor T cells in lymphoid organs to induce deficient activation/proliferation of T cells leading to deletion, anergy and/or regulation. To test this hypothesis we injected i.v. $5x10^6$ BALB/c MR-DC (therapeutic dose in our cardiac transplant model) in B6 MHC-$I^{KO-/-}$ mice (Thy1.2$^+$) previously reconstituted with CFSE-labeled 2C TCRtg CD8$^+$ T cells (Thy1.1$^+$), that are specific for BALB/c H-2L^d (Fig. 15). Since host APC lack surface MHC-I molecule expression, 2C T cell priming depends upon contact with donor-derived MR-DC.

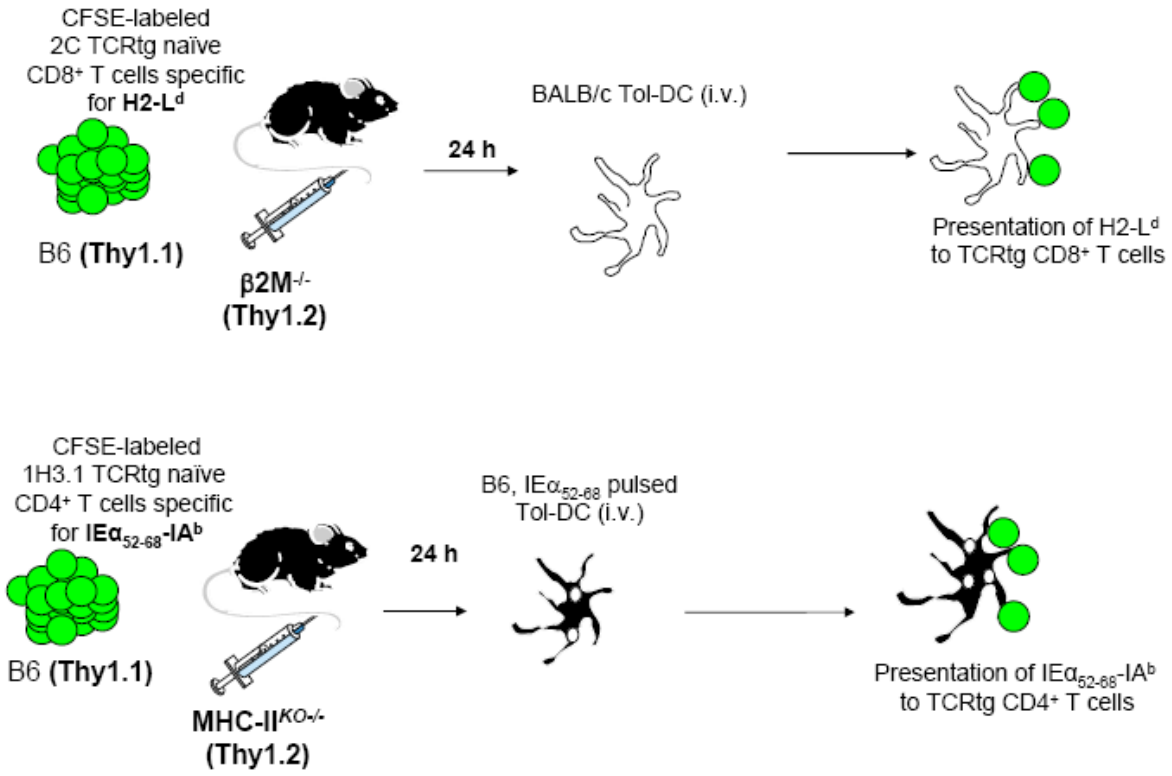

Figure 15. Model for direct pathway experimentation.

Surprisingly, no or minimal 2C T cell proliferation was detected in spleen 3 d after MR-DC administration (Fig. 16). If the number of donor MR-DC was increased 3-fold, greater proliferation of 2C cells was observed compared to therapeutic dose (p=0.0131). These results suggest that at therapeutic dose ($5x10^6$ DC), too few MR-DC home to/persist in the spleen to directly prime anti-donor $CD8^+$ T cells (Fig. 16). Administration of $5x10^6$ BALB/c LPS-matured DC triggered robust 2C T cell proliferation in these animals (p<0.0001) (Fig. 17), supporting the capability of 2C T cells to proliferate in MHC-$I^{KO-/-}$ mice, and intimating that LPS-matured DC are superior to MR-DC at homing to/surviving in recipient spleen.

To address this question with anti-donor $CD4^+$ T cells, we employed a surrogate model, where syngeneic B6 MR-DC were pulsed with the BALB/c IEα_{52-68} peptide and injected into B6 MHC-$II^{KO-/-}$ mice (Thy1.2^+) previously reconstituted with CFSE-labeled 1H3.1 $CD4^+$ T cells (Thy1.1^+) (Fig. 15). Similar to the 2C system, administration of a therapeutic dose of MR-DC carrying donor alloAg ($5x10^6$ DC) failed to directly prime anti-donor $CD4^+$ T cells (Fig. 16), while increasing the number of injected MR-DC 3-fold did induce limited $CD4^+$ T cell proliferation (p=0.0355 vs No DC group). Administration of LPS-matured DC pulsed with IEα_{52-68} induced significant 1H3.1 T cell proliferation (p=0.0201).

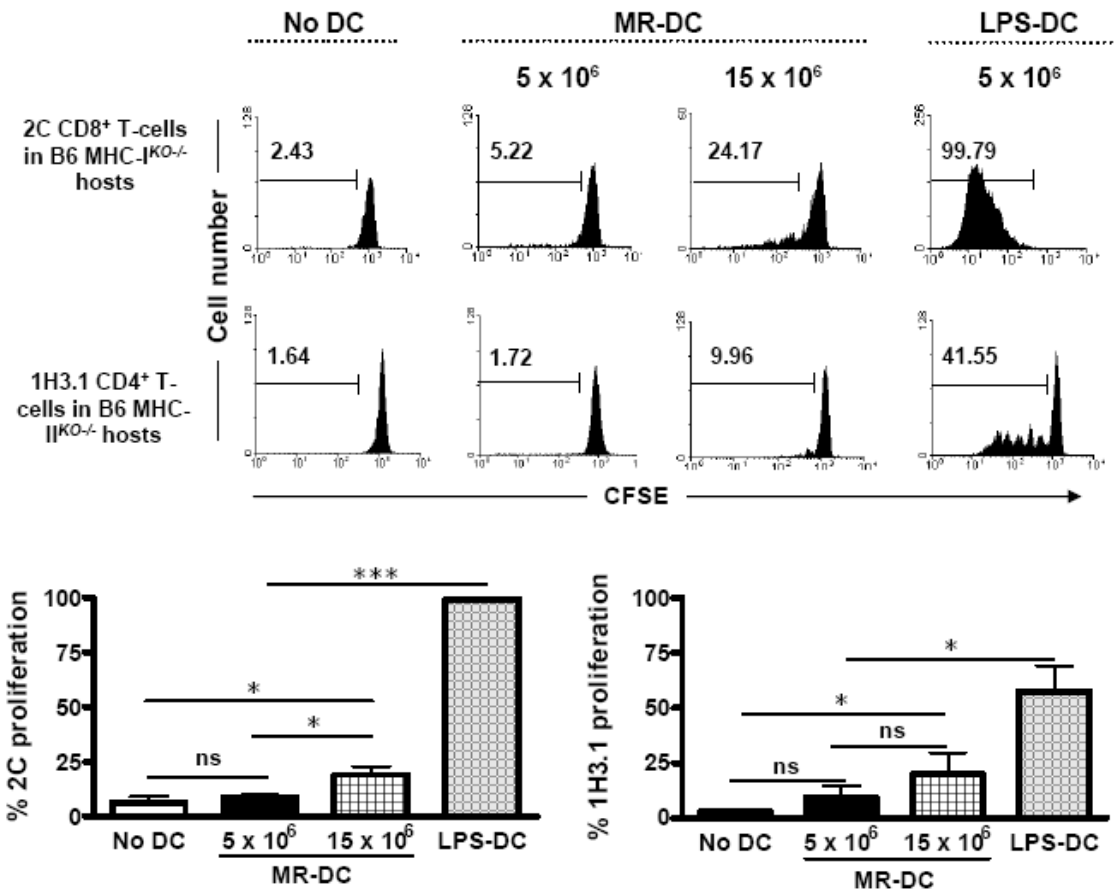

Figure 16. MR-DC fail to directly prime anti-donor T cells in vivo.

Representative histograms showing in vivo proliferation of CFSE-labeled 2C $CD8^+$ T cells and 1H3.1 $CD4^+$ T cells adoptively transferred into host MHC-$I^{KO-/-}$ or MHC-$II^{KO-/-}$ B6 mice, respectively, that were injected or not the following d with either MR-DC or LPS-matured DC bearing BALB/c alloAg. Numbers in histograms are percentages of dividing TCRtg T cells. Bars indicate mean ± SEM of percentages of T cell proliferation from 2 independent experiments with 3 or more animals per group. * $p < 0.05$, *** $p < 0.001$.

We next examined whether the lack of anti-donor $CD4^+$ T cell proliferation was due to induction of anergy or Treg. To do so, B6 MHC-$II^{KO-/-}$ mice previously reconstituted with CFSE-labeled 1H3.1 T cells were injected i.v. (or not) with B6 MR-DC pulsed with IEα_{52-68} ($5x10^6$ DC) and challenged 7 d later, or not, with B6 LPS-matured-DC loaded with IEα_{52-68}. The fact that splenic 1H3.1 $CD4^+$ T cells from B6 MHC-$II^{KO-/-}$ mice pre-treated with B6 MR-DC + IEα_{52-}

$_{68}$ proliferated vigorously in vivo in response to challenge without up-regulating FoxP3 expression, precludes anergy induction or Treg differentiation through direct contact between therapeutic MR-DC and anti-donor $CD4^+$ T cells (Fig. 17).

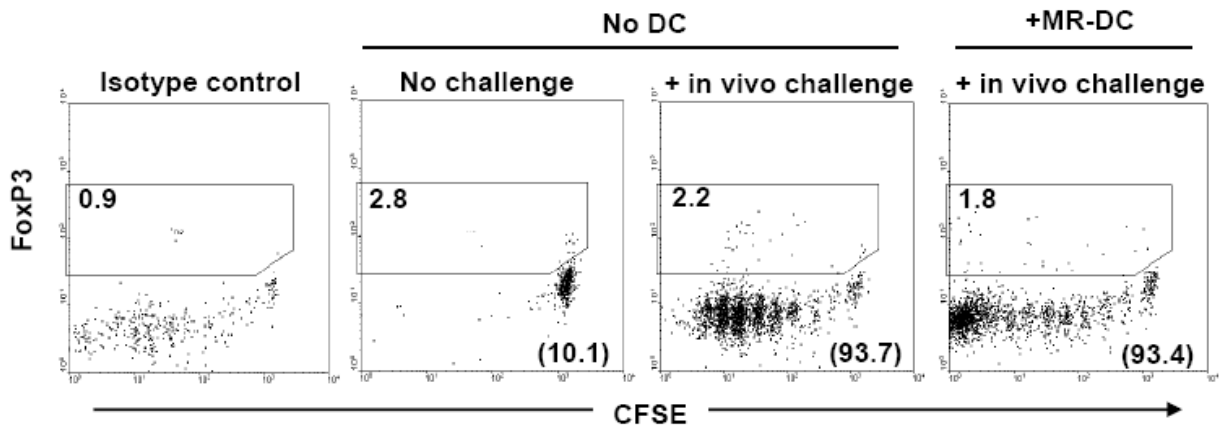

Figure 17. Therapeutic DC fail to directly induce T cell anergy or Treg.

MHC-$II^{KO-/-}$ B6 mice reconstituted with CFSE-labeled 1H3.1 $CD4^+$ T cells were injected or not with IEα_{52-68} peptide-pulsed B6 MR-DC. After 7 d, mice were challenged in vivo, or not, with IEα_{52-68} peptide-pulsed B6 LPS-matured DC. Representative dot plots show percentage proliferation (in parentheses) and FoxP3 expression (in gated region) of 1H3.1 $CD4^+$ T cells 3 d later. Two or more independent experiments were performed with at least 3 animals per group.

2.2.7 Therapeutic DC inhibit the immune response to cardiac allografts

Direct pathway T cells are classically considered the main mediators of acute cardiac allograft rejection. Given that donor-derived MR-DC therapy fails to directly interact with T cells, we wondered why direct pathway T cells did not acutely reject cardiac allografts in MR-DC treated recipients. To address this, we analyzed the effect of donor-derived MR-DC administration on the intra-graft and systemic response 7 d post-transplantation. Cardiac allografts from non-treated mice exhibited intense cellular infiltrate, hemorrhagic foci, interstitial edema and

myocardial damage whereas allografts from MR-DC treated mice showed reduced infiltrate and minimal hemorrhage (Fig. 18).

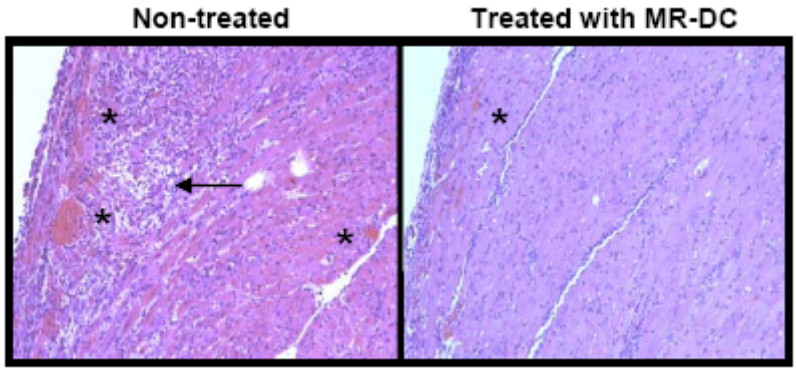

Figure 18. Allograft histology from non-treated and MR-DC treated mice.

Representative allograft histology (H&E) 7 d post-transplantation in B6 recipient mice. Asterisks indicate hemorrhagic foci, arrows point to interstitial edema. n = at least 3 animals per group.

Quantification of graft-infiltrating leukocytes (GIL) revealed significantly fewer $CD8^+$ T cells (p=0.0111) and a similar content of $CD4^+$ and $CD4^+FoxP3^+$ T cells compared to non-treated controls (Fig. 19a,b). Investigation of the systemic anti-donor T cell effector response by ELISPOT assay revealed that donor-derived MR-DC administration significantly reduced the frequency of both direct (p=0.0135) and indirect (p=0.0059) pathway IFN-γ-secreting T cells in the spleen, compared to that of non-treated recipients (Fig. 19c). Therefore, despite an inability of donor-derived MR-DC to directly interact with anti-donor T cells, the direct pathway T cell response is inhibited following DC therapy.

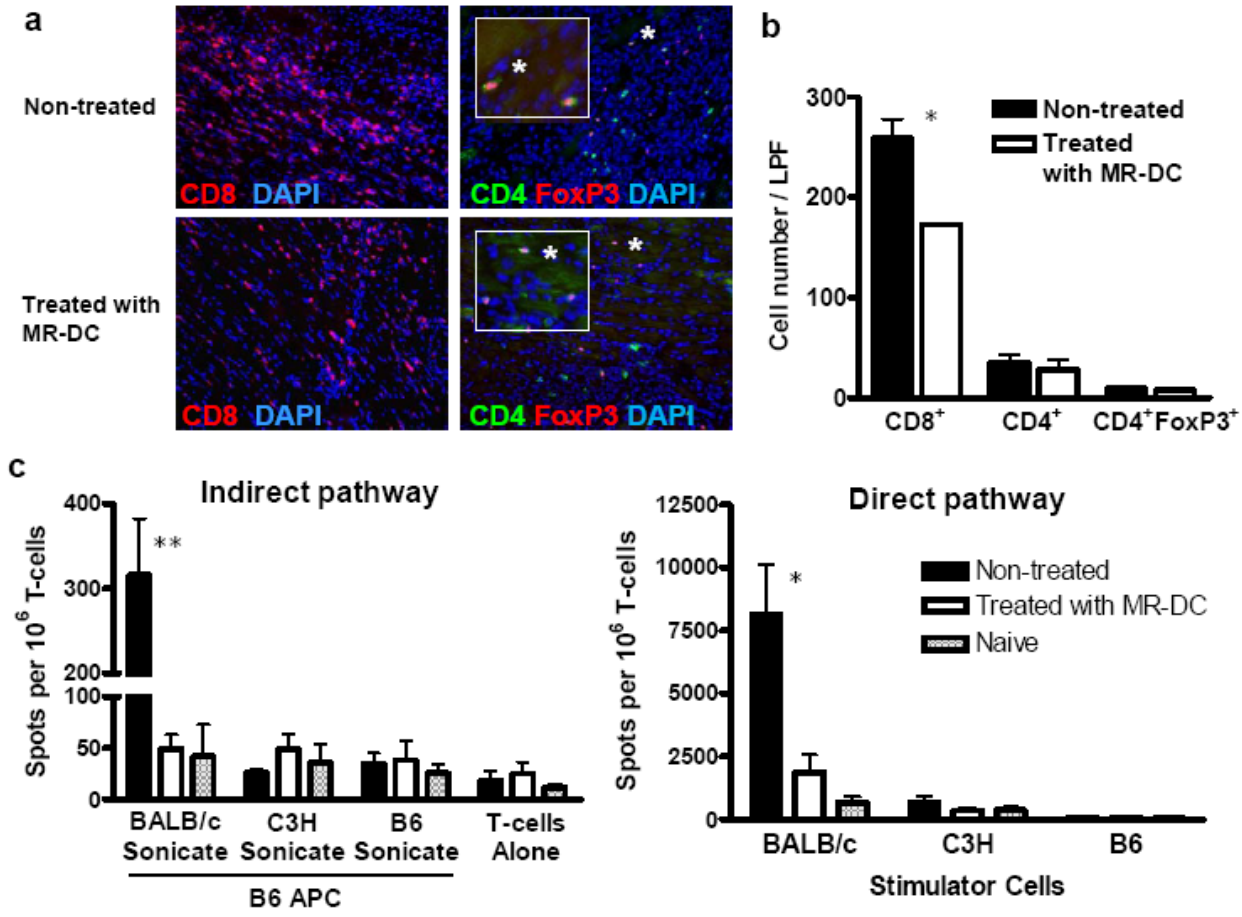

Figure 19. Donor-derived MR-DC therapy decreases T cell responses within the graft and systemically.

Representative images (a) and quantification of GIL (average of 10 low-powered fields, LPF) (b) on cardiac allograft sections. Asterisks indicate the corresponding GIL on low power image and inset. (c) Frequency of IFN-γ producing direct and indirect T cells from naïve B6 or allograft recipient B6 mice. (b,c) Data are averaged from 2 or more independent experiments with 3 or more animals per group, mean ± SEM shown. * $p < 0.05$, ** $p < 0.01$.

2.2.8 Indirect $CD4^+$ T cell help is required for the direct pathway response and cardiac allograft rejection

The prevailing paradigm regarding initiation of the anti-donor adaptive immune response assumes that donor APC prime direct pathway T cells, independently of the indirect pathway (Fig. 5). However, we demonstrate that DC therapies inhibit the direct pathway response without directly interacting with anti-donor T cells. We therefore hypothesized that induction of a direct pathway response in a cardiac allograft model may require recipient APC and/or indirect pathway T cells, which are modulated by MR-DC therapy. To address this, we transplanted BALB/c hearts into B6 MHC-$II^{KO-/-}$ mice previously reconstituted with 10^7 polyclonal syngeneic $CD4^+$ T cells. Notably, recipients, which cannot stimulate indirect $CD4^+$ T cells, universally accepted their allografts through 50 days post-transplantation (Fig. 20a). We then bypassed the need for $CD4^+$ T cell help via CD40-CD154 ligation by treating MHC-$II^{KO-/-}$ recipients with agonistic CD40 mAb 3 d after transplantation. All allografts were rejected, with a MST of 28.5 d (p=0.0027). Histologic analysis of the grafts 7 d post-transplant showed sub-pericardial leukocytic infiltrate but otherwise healthy myocardium in non-treated mice, while heavy infiltrate, hemorrhage and interstitial edema were detected in CD40 mAb treated recipients (Fig. 20b). By 50 d post-transplant, non-treated recipient allografts demonstrated healthy cardiac tissue with only mild infiltrate, while addition of agonistic CD40 mAb resulted in severe infiltrate and hemorrhage, myocardial damage, interstitial fibrosis and vasculopathy.

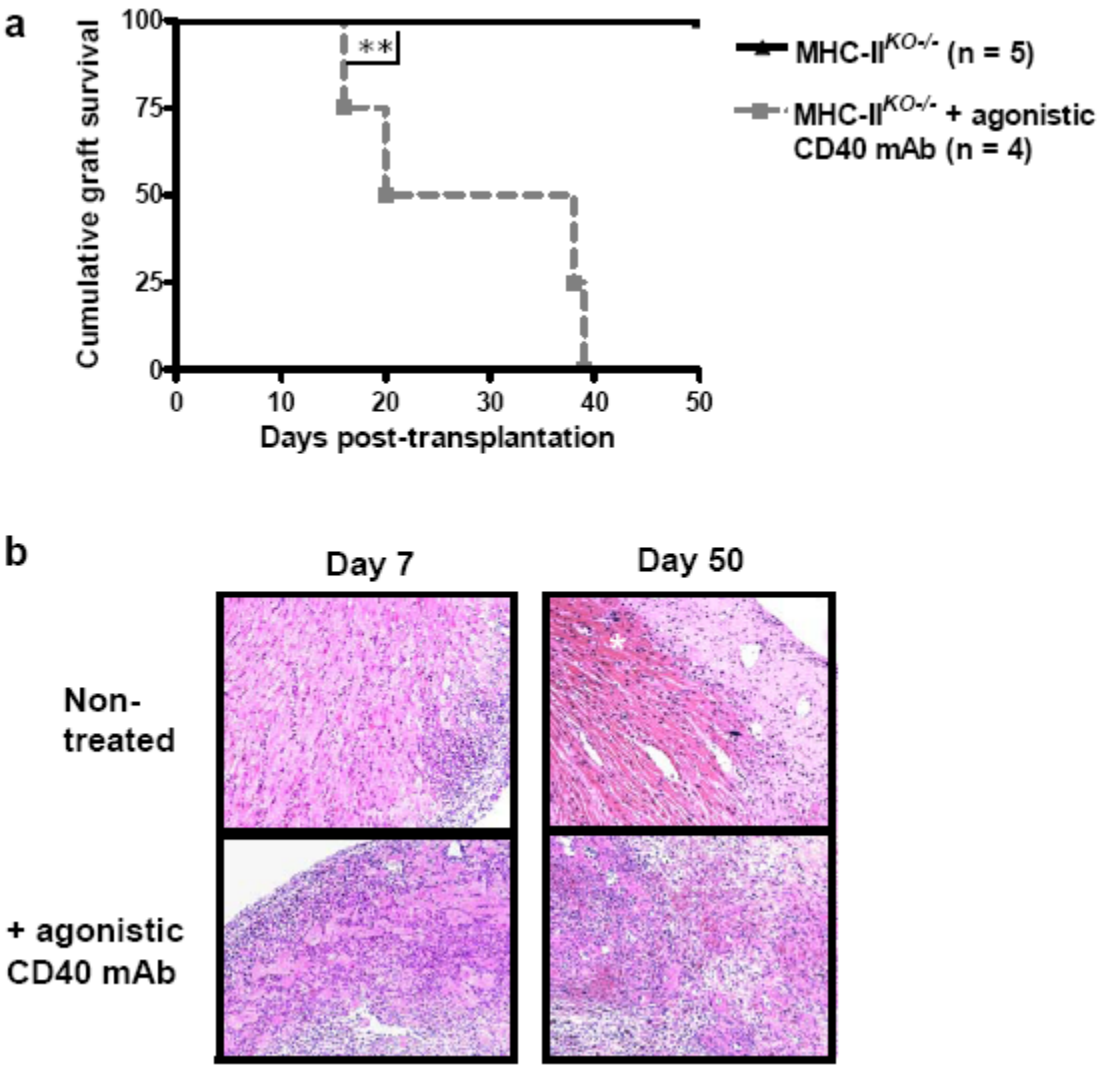

Figure 20. CD40 ligation of recipient APC by indirect CD4$^+$ helper T cells is required for allograft rejection.

MHC-II$^{KO-/-}$ recipient mice were reconstituted with 10^7 naïve syngeneic polyclonal CD4$^+$ T cells, and treated i.p., or not, with agonistic CD40 mAb on d 3 post-transplant. (a) Survival of BALB/c cardiac allografts. (b) Representative images of histology 7 and 50 d post-transplantation. n = 3 or more animals per group. ** $p < 0.01$.

Both CD4$^+$ and CD8$^+$ T cells were observed infiltrating cardiac allografts, although more robustly in CD40 mAb treated recipient mice, 7 d post-transplant (Fig. 21a). In spleens, CD40 mAb treatment roughly doubled the total number of splenic CD4$^+$ (p=0.0705) and CD8$^+$ T cells

(p=0.0023) compared to non-treated allograft recipients (Fig. 21b), suggesting that CD40 mAb treatment had induced T cell priming and proliferation. We then investigated the direct pathway effector response by performing IFN-γ ELISPOTs 7 d post-transplant. The ratio of splenic $CD4^+$:$CD8^+$ T cells was comparable between non-treated and CD40 mAb treated recipients (Fig. 21c), so equivalent numbers of $CD4^+$ and $CD8^+$ T cells were plated in both groups. In the absence of indirect $CD4^+$ T cell help, non-treated MHC-$II^{KO-/-}$ recipients lacked a direct pathway effector response, while addition of CD40 mAb into MHC-$II^{KO-/-}$ recipients induced a robust direct pathway response (p=0.0169) (Fig. 21d). Splenic $CD4^+$ and $CD8^+$ T cell number and effector frequency were unaltered in naïve wildtype mice treated with CD40 mAb (not shown). Therefore, indirect $CD4^+$ T cells function as helper cells, providing CD40 ligation to recipient APC, that is necessary for priming a direct pathway effector response and allograft rejection.

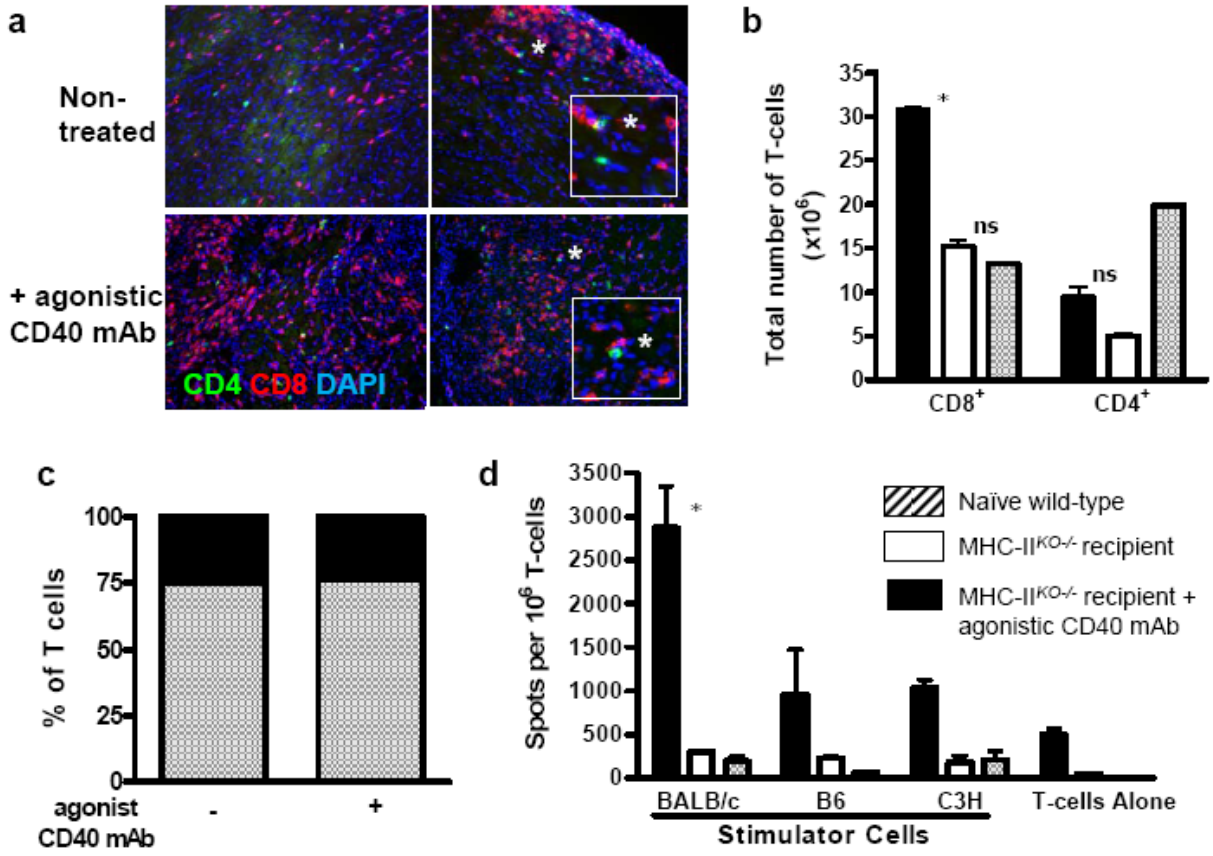

Figure 21. CD40 ligation of recipient APC by indirect $CD4^+$ helper T cells is required for direct pathway priming.

MHC-$II^{KO-/-}$ recipient mice were reconstituted with 10^7 naïve syngeneic polyclonal $CD4^+$ T cells, and treated i.p., or not, with agonistic CD40 mAb on d 3 post-transplant. (a) Representative images of graft-infiltrating $CD4^+$ and $CD8^+$ T cells 7 d post-transplantation. Asterisks indicate corresponding graft-infiltrating leukocytes on low power image and inset. (b) Total number of splenic $CD4^+$ and $CD8^+$ T cells in recipient mice. (c) Ratio of $CD4^+$:$CD8^+$ T cells. (d) Frequency of IFN-γ producing direct pathway T cells 7 d post-transplant. (c,d) Representative data is shown from two independent experiments (mean ± SD), n = 3 or more per group. * $p < 0.05$.

2.3 DISCUSSION

Neither the in vivo mechanisms by which in vitro-generated therapeutic DC promote allograft survival nor their efficacy compared to other cell-based therapies have been explored. Our data show for the first time that VD_3 generated donor-derived MR-DC prolonged cardiac allograft survival with similar efficacy to donor immature control-DC, DST or donor-apoptotic cell therapy, and comparably to previously described immature, MR or alternatively-activated DC generated by various pharmacologic and/or genetic manipulations[208,209,212,214,215,223]. Importantly, maintaining therapeutic cells in a quiescent state is essential, as we demonstrate that treatment with mature-DC induced potent direct T cell stimulation, and others have reported that treatment with mature-DC induces allograft rejection[224], thus highlighting a major risk of DC therapies for transplantation.

Mechanistically, we observed that donor-derived MR-DC survived only briefly in vivo, at least partly due to targeting by recipient NK cells, and likely also by natural turnover, given that both donor-derived MR-DC and recipient-derived MR-DC pulsed with alloAg failed to directly tolerize anti-donor T cells in vivo, yet both equally prolong allograft survival[212,214]. Thus, therapeutic DC quickly become apoptotic in vivo. Despite the immunoregulatory effects of apoptotic cells, apoptosis of even tolerogenic therapeutic cells presents an additional risk of patient sensitization, as an increase in the ratio between apoptotic cells and phagocytes can promote inflammation and immunity. DC incubated with an excess of apoptotic cells results in DC maturation and efficient Ag presentation to both MHC class I- and class II-restricted T cells[225] and immunization with DC exposed to high numbers of apoptotic cells results in priming of tumor-specific cytotoxic T cells and protection against tumor challenge in mice[226]. Our data

showing that increasing the dose of MR-DC three-fold directly induced robust allo-reactive T cell proliferation supports this concept.

The ability of splenic-resident DC to capture and present circulating apoptotic cell-derived Ag to down-regulate the T cell response has received great attention, but the individual contribution of each splenic DC subset to this process is incompletely understood. Intravenous administration of apoptotic leukocytes generated by osmotic shock are internalized exclusively by splenic $CD8\alpha^+$ DC, while UV-B-induced apoptotic leukocytes are captured mainly by splenic $CD8^-$ DC of the marginal zone and to a lesser extent by $CD8\alpha^+$ DC of the T cell areas[76]. Intriguingly, i.v. treatment of naïve recipients with splenic DC isolated from mice pretreated (i.v., 24-26 hours before) with donor UV-B-induced apoptotic cells, prolongs heart allograft survival in those treated mice, but that depletion of $CD8\alpha^+$ DC from the transferred inoculum abrogates the effect[75], suggesting that presentation of donor alloAg by splenic $CD8\alpha^+$ DC is necessary for the beneficial effect of donor apoptotic cells in allograft survival. In our model, we found that both splenic $CD11c^{hi}CD8\alpha^+$ and $CD8^-$ DC re-processed and presented MR-DC-derived alloAg to indirectly alloreactive T cells. The stage of apoptosis of i.v. injected cells could be relevant in this regard. Dying cells may be capable of actively migrating to T cell areas for internalization by $CD8\alpha^+$ DC, whereas apoptotic cells unable to actively traffic are captured by marginal zone $CD8^-$ DC. Alternatively, $CD8^-$ DC could capture apoptotic MR-DC-derived Ag and migrate to T cell areas where they either up-regulate $CD8\alpha$ expression or transfer alloAg to $CD8\alpha^+$ DC.

Additionally, other cells may phagocytose MR-DC-derived fragments to impact the immune response. Plasmacytoid DC were shown to be tolerogenic in mice[227-231], although Dalgaard and colleagues showed that pDC do not phagocytose apoptotic or necrotic cells in

vitro[232]. In our model, pDC did not capture, re-process and/or present MR-DC-derived alloAg to T cells. We did observe internalization of donor MR-DC-derived fragments by F4/80$^+$ splenic MΦ (data not shown), a major phagocyte of apoptotic cells, and interestingly, splenic B cells can process and present self-Ag to T cells[233], although its unknown whether they phagocytose apoptotic cells. However, as neither MΦ nor B cells are capable of priming naïve T cells, we did not observe T cell stimulation in our ex vivo assay of CD11c$^-$ cells for MR-DC-derived alloAg presentation. Notably, this does not rule out bystander regulation by splenic MΦ or B cells that have phagocytosed MR-DC, or an effect on memory T cells in sensitized animal models.

MR-DC-derived alloAg presentation via the indirect pathway is only brief in vivo, but similar to observations in the literature for DST and donor-apoptotic cell therapy[75,199,200], triggered defective activation and deletion of effector T cells and survival/outgrowth of FoxP3$^+$CD4$^+$ T cells. However, as an additional level of complexity, we demonstrate that the quiescent state of recipient DC is crucial for tolerance, as activated recipient DC presenting MR-DC-derived alloAg induced robust T cell stimulation. This supports our previous findings that donor apoptotic cell treated mice fail to prolong allograft survival if recipient DC are activated in situ by agonistic CD40 mAb[75]. Interestingly, the specific signals received during activation seem to dictate DC function rather than simply the stage of maturation, as administration of TNF-α-stimulated DC pulsed with self-Ag protects against autoimmune encephalomyelitis in mice, partly through release of IL-10, while treatment with LPS or CD40-ligated DC has no beneficial effects[234]. Given the potent pro-inflammatory milieu resulting from transplant surgery, it seems likely that in the clinical setting, agents aimed at maintaining recipient APC in a quiescent state, will be necessary for successful implementation of cellular therapies.

Based on our findings, we developed a proposed model (Fig. 22) for tolerogenic DC mechanism of action. Notably, this model encompasses an important paradox: donor-derived MR-DC fail to directly interact with donor-reactive T cells, yet down-regulate the direct pathway T cell response in allograft recipients. This could occur through (i) indirect pathway Treg-mediated suppression of direct pathway T cell function, or (ii) deletion of indirect pathway $CD4^+$ T cell help that is required for induction of direct pathway $CD8^+$ T cells. In support of the former, it has been shown that indirect Treg mediate linked suppression in a mouse skin graft model[235], and that Treg attenuate anti-donor $CD8^+$ T cell priming in lymphoid organs and prevent rejection upon homing to the graft[236]. In agreement with the latter theory, the limited number of passenger donor DC mobilized from the cardiac graft may render direct pathway $CD4^+$ T cell help inconsequential, necessitating indirect $CD4^+$ T cell help for induction of direct pathway T cells. It was previously shown in an allogeneic skin transplant model that indirect $CD4^+$ T cells are capable of providing help to direct $CD8^+$ T cells[237], and that WT cardiac allografts transplanted into $CD80/86^{KO-/-}$ recipient mice results in long-term survival that is abrogated with treatment of agonistic CD28 Ab[238], indicating that indirect pathway co-stimulation is requisite for acute allograft rejection.

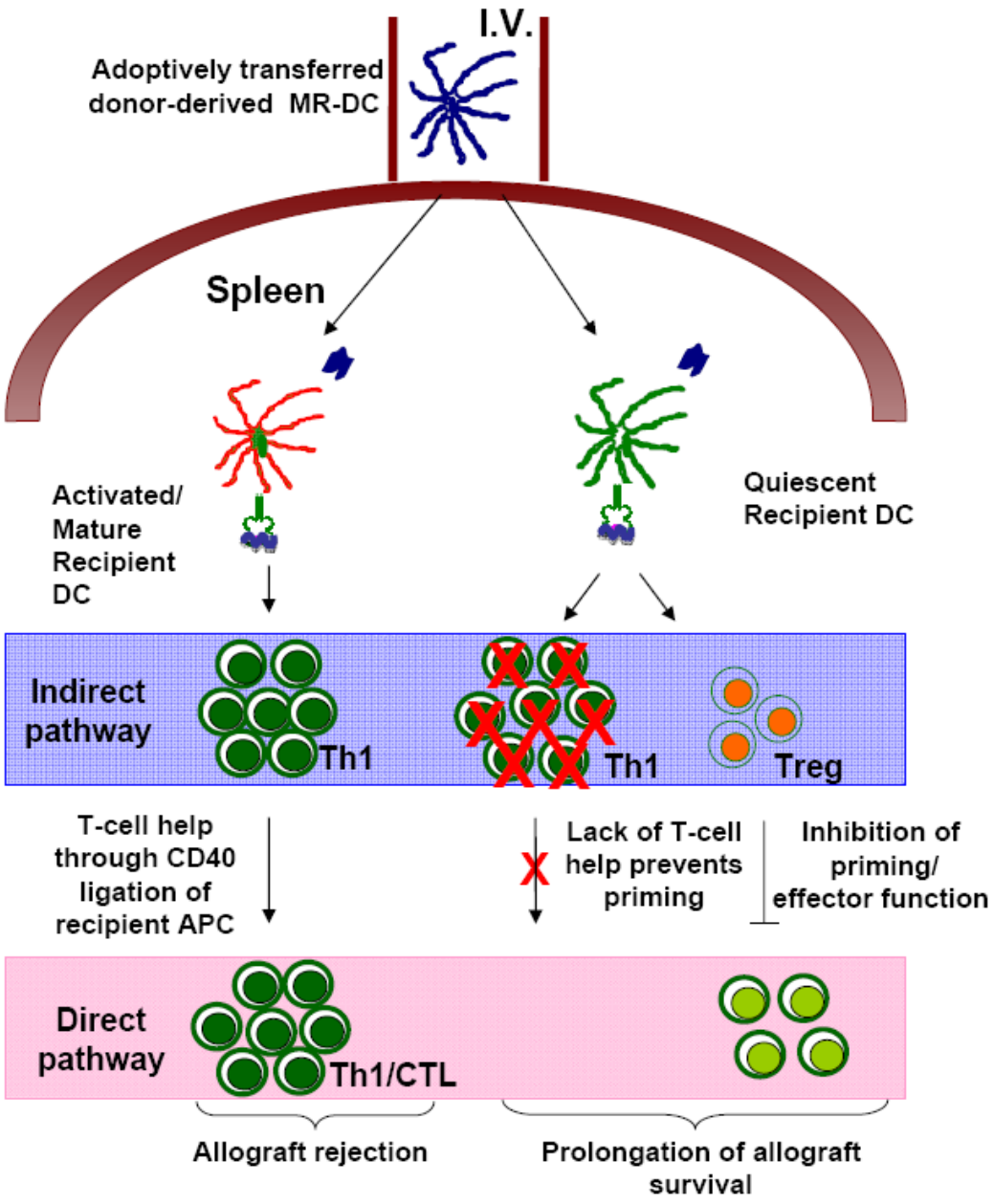

Figure 22. Proposed model for mechanism of action of donor-derived MR-DC.

Donor-derived cells and Ag are depicted in blue and recipient cells in green. Donor-derived MR-DC administered systemically undergo apoptosis. Upon entering recipient spleen, apoptotic MR-DC are internalized and re-processed by recipient $CD11c^{hi}$ DC for presentation via the indirect pathway (donor allo-peptides loaded in self-MHC molecules) to donor-reactive T cells. Activated recipient DC induce T cell stimulation, while quiescent DC promote deletion of effector T cells and Treg outgrowth. Deletion of indirect $CD4^+$ T cells reduces the helper T cell cooperation necessary for priming direct pathway T cells. Indirect $CD4^+$ Treg generated by MR-DC therapy may also inhibit priming and/or function of direct pathway T cells.

We investigated this latter hypothesis and demonstrate that, contrary to the current paradigm, (Fig. 5a) recipient APC and indirect $CD4^+$ T cell help are requisite for direct pathway T cell priming and cardiac allograft rejection. Further, our data indicate that indirect pathway $CD4^+$ T cells provide help through CD40 ligation of recipient APC rather than through bystander mechanisms. The activated recipient APC could in turn i) modulate donor APC through B cell receptor:donor MHC interaction if the recipient APC is a B cell (Fig. 5c) or ii) express intact donor MHC:Ag on its surface for presentation to and modulation of direct pathway T cells, recently dubbed "semi-direct" presentation (Fig. 5d). There is emerging evidence supporting the latter[179], however, this complex area of research requires further investigation.

Our findings indicate that in mice, currently employed DC-based therapies have similar mechanism of action[75,199] and efficacy as other safer and more clinically practical cellular therapies. Comparing efficacy in larger animal models is yet to be performed, and our study does not preclude generation of a tolerogenic DC capable of mediating direct T cell suppression and superior efficacy. However, our data support providing alloAg from alternative cellular sources, coupled with agents that prevent recipient APC activation for use in transplantation.

3.0 DONOR APC ARE REQUIRED TO ELICIT THE ANTI-DONOR T CELL RESPONSE

3.1 INTRODUCTION

Donor passenger APC are typically regarded as the primary stimulators of the anti-donor T cell response and allograft rejection. This is largely supported by "parking" studies where donor organs are transplanted into one recipient, then several days later re-transplanted into a naïve recipient, presumably after all donor passenger APC have emigrated out of the grafted organ. In rat, kidney parking prior to transplantation achieves 'tolerance' that is reversible upon infusion of donor DC into the recipient[181,239-241]. Likewise, prolongation of cardiac allograft survival is observed in rats following donor APC depletion or in mice using donors that are Flt3Ligand$^{-/-}$ and therefore lack donor DC[242-245]. However, these results seem to be strain and experimental model dependent. Soulillou's group showed that depletion of donor passenger APC by graft parking or treatment with cyclosporine only mildly prolonged cardiac allograft survival and that although graft infiltrate and cytokine transcript levels were reduced at 5 d post-transplant, by the time of rejection, Ab deposition (a marker of the indirect pathway cellular response) and transcript levels had reached that of unmodified controls[246], indicating that depleting donor passenger APC only mildly delayed the alloresponse. Further, due to methodological limitations,

these studies did not distinguish effects on the direct versus the indirect pathway, nor on the intragraft versus systemic alloresponse.

More recent studies have attempted to utilize donor organs lacking expression of MHC class I or II[247,248], however the role of donor passenger APC versus donor non-hematopoietic cell MHC expression cannot be discriminated, and further the indirect pathway response is also affected due to the absence of alloAg.

We therefore investigated the role of donor passenger APC in priming both the direct and indirect pathway responses, both systemically and within the graft. We determined that, similar to previous observations by Larsen et al.[249], donor passenger APC rapidly emigrated out of cardiac allograft through the vasculature. We further show that following transplantation, allograft parenchymal and endothelial cells robustly expressed MHC class I and II. To test whether anti-donor T cells could be primed by MHC class I or II expressed on non-hematopoietic allograft tissue in the absence of donor passenger APC, we eliminated donor passenger APC from the graft without affecting parenchymal and endothelial cell up-regulation of MHC class I and II by total body irradiating donor mice 3 day prior to organ harvest. We observed that in the absence of donor passenger APC, a direct pathway T cell response failed to occur in either secondary lymphoid organs or within the allograft. Further, preliminary experiments suggest that the absence of donor passenger APC also attenuated priming of an indirect pathway T cell response in secondary lymphoid organs, although to less extent than the direct pathway response. We therefore conclude that donor passenger APC do serve as a source of alloAg that is requisite for priming the anti-donor T cell response.

3.2 RESULTS

3.2.1 Donor passenger APC emigrate from cardiac allograft tissue

To evaluate the hypothesis that donor passenger APC are requisite for a T cell alloresponse, we first characterized the fate of donor passenger APC in vivo, by immunofluorescently staining cardiac allograft tissue. We identified donor passenger APC by expression of donor MHC class II, IA^d. We observed a surprisingly high number of donor passenger APC present in naïve donor (BALB/c) hearts (Fig. 23a,c). Expression of CD11c was much lower or even undetectable on naïve donor APC by this method. Following transplantation, donor APC numbers in cardiac allografts rapidly diminished (between naïve and 2 d, p=0.0043, between naïve and 3 d, p=0.0328) (Fig. 23a,c) and donor APC were observed emigrating through cardiac vessels (Fig. 23b). Notably, by averaging the number of IA^{d+} cells per low power field, we did observe an increased number of IA^{d+} cells at 7 d post-transplant (Fig. 23c). Since donor passenger APC had already exited allograft tissue by this time, we wondered whether alternative cell populations up-regulated expression of MHC class II during the effector phase (day 7) of the immune response.

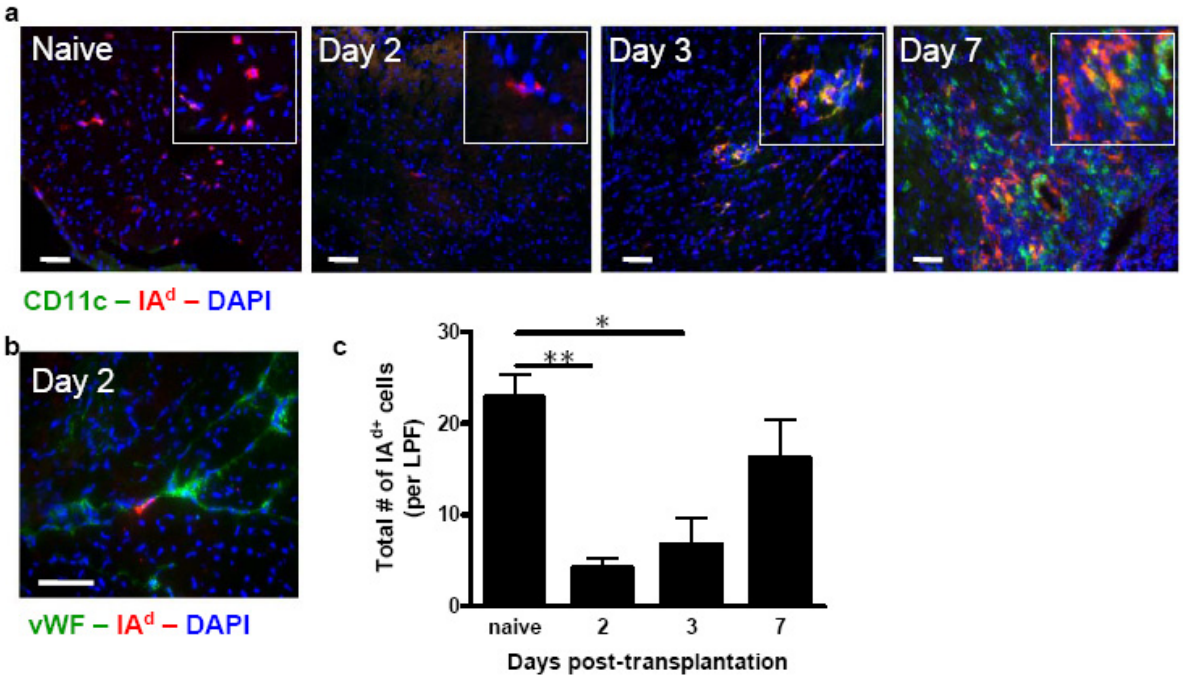

Figure 23. Donor passenger APC emigrate from cardiac allograft tissue rapidly following transplantation.

(a) Immunofluorescent staining for CD11c and donor MHC class II, IA^d on naïve donor hearts and cardiac allografts 2, 3 and 7 d post-transplant was performed. Inserts show enlarged images. (b) Immunofluorescent staining for IA^d and von Willebrand factor, vWF, an endothelial marker 2 d post-transplant. (a,b) Nuclei are counterstained with DAPI. Bars indicate 50 μm. (c) The total number of IA^{d+} cells per low power field averaged from 10 images from naïve donor hearts and cardiac allografts 2, 3 and 7 d post-transplant is graphed. (a,b) Representative images are shown. (c) Mean ± SD is shown. n = 3 or more animals per group. * $p < 0.05$, ** $p < 0.01$.

3.2.2 Cardiac allograft tissue expresses MHC class I and II

By staining for IA^d and the endothelial marker von Willebrand Factor (vWF), we observed that naïve cardiac tissue and allograft tissue 2 d post-transplant failed to express IA^d (Fig. 24). However, up-regulation of MHC class II was noted by 3 d post-transplant, and significant expression of MHC class II was observed 7 d post-transplant by endothelial and parenchymal

cells. In fact, overall expression of MHC class II was more robust at 7 d post-transplant than in naïve cardiac tissue prior to donor passenger APC emigration.

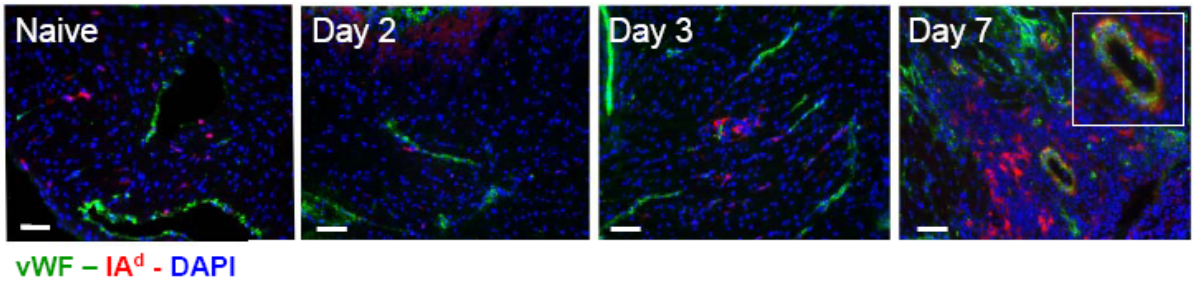

Figure 24. Cardiac allograft tissue up-regulates expression of MHC class II.

Naïve donor hearts and cardiac allograft sections were immunofluoresently stained for IA^d and von Willebrand factor 2, 3 and 7 d post-transplant. Nuclei were counterstained with DAPI. Bars indicate 50 μM. Inset shows enlarged image from 7 d post-transplant. Representative images are shown. n = 3 or more animals per group.

We next evaluated expression of MHC class I, H2D^d, on cardiac allograft tissue. We observed very low expression of H2D^d in naïve donor hearts, but up-regulated expression by 2 d post-transplant (Fig. 25). Interestingly, H2D^d expression was visualized in patches at 2 and 3 d post-transplant. By 7 d post-transplant, there was significant expression of MHC class I by both parenchymal and endothelial cells in the graft. High power imaging revealed that parenchymal cells were actually fibroblasts rather than myocardial cells (Fig. 25).

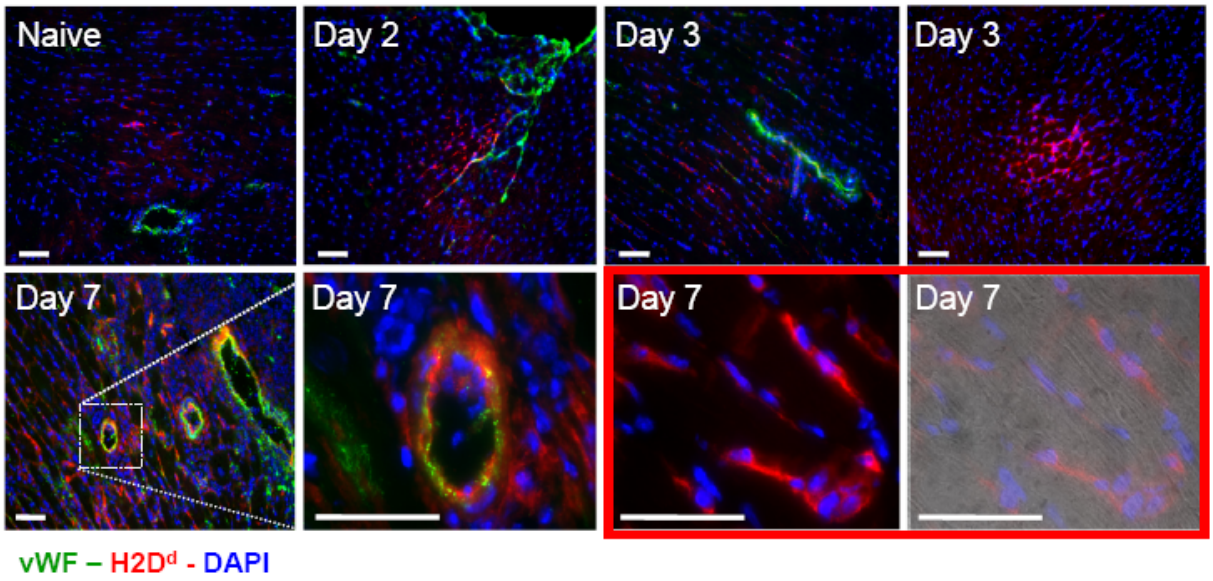

Figure 25. Cardiac allograft tissue up-regulates expression of MHC class I.

Naïve donor hearts and cardiac allografts were immunofluorescently stained for von Willebrand factor and donor MHC class I, H2D^d, 2, 3 and 7 d post-transplant. Nuclei were counterstained with DAPI. Representative images are shown. n = 3 or more animals per group. Bars indicate 50 μM, except images within the red box, where bars indicate 100 μM.

3.2.3 Donor passenger APC are required for an anti-donor T cell response

Given the robust expression of MHC class I and II within graft tissue, we wondered whether donor passenger APC were necessary for priming the anti-donor T cell response, or whether sufficient alloAg was expressed by graft tissue for T cell priming. To evaluate this, we total body irradiated donor BALB/c mice 3 d prior to organ harvest. This eliminated all donor hematopoietic cells and thus all passenger APC. However, non-hematopoietic organ tissue was unaffected, and thus capable of up-regulating MHC class I and II expression upon transplantation. Seven days post-transplant, we performed IFN-γ ELISPOT assay to evaluate the direct pathway T cell effector response. We observed in both the heart allograft and recipient

spleen, that in the absence of donor passenger APC, a direct pathway effector T cell response failed to develop (heart, p=0.0328; spleen, p=0.0403) (Fig. 26). This data indicate that graft parenchymal and endothelial tissue can neither directly prime alloreactive T cells in the graft or provide intact MHC:peptide complex to recipient APC for semi-direct T cell priming.

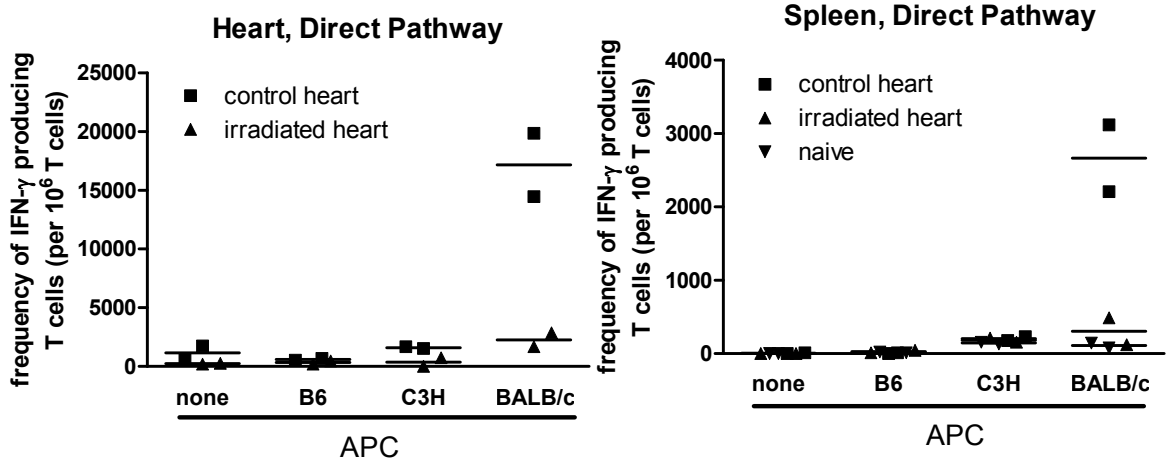

Figure 26. Donor passenger APC are required for a direct pathway T cell response.

IFN-γ ELISPOT assay was performed 7 d post-transplant on T cells isolated from recipient spleen or cardiac allograft tissue from WT control recipients or recipients that received donor hearts from irradiated mice. T cells were stimulated with donor BALB/c APC, or with syngeneic B6 APC, third-party C3H APC or nothing as controls. Naïve splenic T cells were also included as controls. Black bars, unmodified donors; open bars, irradiated donors; striped bars, naïve splenic T cells. Mean is shown. n = 2 mice per group. * $p < 0.05$.

We previously showed (chapter 2) that recipient APC and indirect pathway T cell help is required for a direct pathway response. Figure 26 suggests that either donor passenger APC are directly required for a direct pathway response, or potentially, that donor passenger APC are required for an indirect pathway response and therefore by attenuating the indirect pathway response, we have effectively prevented a direct pathway response. We therefore evaluated in preliminary experiments the indirect pathway T cell effector response by IFN-γ ELISPOT assay

7 d post-transplant in recipient mice transplanted with hearts from irradiated donor or unmodified controls. To our surprise, the indirect pathway T cell response was undetectable in cardiac allograft tissue of either irradiated or unmodified WT recipients (data not shown). In recipient spleen, the indirect pathway T cell response was markedly reduced in recipients of irradiated donor organs (data not shown). This suggests that recipient APC do not acquire alloAg from allograft parenchymal or endothelial tissue for presentation via the indirect pathway, but rather acquire alloAg from donor passenger APC.

3.3 DISCUSSION

Our data demonstrating that donor passenger APC rapidly emigrate out of cardiac allograft tissue supports findings by Larson et al. who showed similarly that donor APC migrate from cardiac tissue to the white pulp of recipient spleen for interaction with T cells[249]. Interestingly, our data indicate that alloAg presented via the indirect pathway derives from donor passenger APC, rather than recipient graft-infiltrating APC taking up alloAg from non-hematopoietic graft tissue expression, or from soluble Ag or apoptotic graft cells circulating through secondary lymphoid organs. Since splenic resident recipient DC acquire alloAg from donor passenger APC that have migrated to spleen, and that direct pathway priming requires activated recipient APC (Chapter 2), it follows that naïve anti-donor T cells could not be primed by allograft parenchymal or endothelial cells despite robust expression of MHC class I and II. This data supports findings by Lakkis et al. who demonstrated in a mouse model of cardiac transplantation that T cell priming requires secondary lymphoid organs (spleen or LN)[250].

One caveat to this work is that by preventing the indirect pathway response in our irradiated donor model, we potentially negated the indirect $CD4^+$ T cell help necessary for a direct pathway response. To evaluate this possibility, recipient mice of irradiated donor hearts could be treated with agonistic CD40 mAb to bypass the need for indirect pathway $CD4^+$ T cell help. Further exploration of these preliminary studies are required, but if true, this data provide novel insight into the interactions between donor and recipient APC and thus between the direct and indirect pathway T cell responses. This remains an intriguing area of research for our lab and the transplantation community.

4.0 INFLAMMATORY MONOCYTES DIFFERENTIATE INTO TIP-DC BUT INHIBIT T CELL RESPONSES IN CARDIAC ALLOGRAFT TRANSPLANTATION

4.1 INTRODUCTION

Traditionally, transplantation biologists have emphasized the central role of donor 'passenger' dendritic cells (DC) as initiators of the anti-donor response. However, we recently showed in a cardiac allograft transplant model in mice, that activated recipient DC are requisite for a T cell alloresponse and acute allograft rejection. It is yet unknown which recipient DC subset(s) participate in this response, whether these DC function in the graft itself or within secondary lymphoid organs and whether their role is limited to Ag presentation or if they contribute additional effector functions. To further elucidate the contributions of recipient DC to the anti-graft immune response, we investigated the involvement of inflammatory monocyte-derived DC, "inflammatory DC" in acute cardiac allograft rejection in a mouse model.

Inflammatory monocytes have become increasingly appreciated as key players in various models of infection and inflammation over the past few years. By definition, both $CD11b^{+}Ly6C^{hi}$ and $CD11b^{+}Ly6C^{int}$ monocytes are inflammatory monocytes, since both migrate to inflammatory sites, although to date, research has primarily focused on the characterization and functional analysis of $CD11b^{+}Ly6C^{hi}$ monocytes. Pamer's group first described the ability of $CD11b^{+}Ly6C^{hi}$ monocytes to infiltrate *Listeria monocytogenes* infected spleen, and differentiate

into tumor necrosis factor-α (TNF-α) and inducible nitric oxide synthase (iNOS)-producing (Tip-) DC, that were necessary for effective bacterial clearance[29]. Inflammatory monocytes have also been shown to take up Ag in peripheral tissues, migrate to draining LN and present Ag to T cells[33]. Further, in viral infection and immunization models, inflammatory monocytes produce IL-12p70 and skew T cells toward a T_h1 response[34]. However, the ability of inflammatory monocytes to modulate T cell responses is apparently model dependent, as Tip-DC were not required to elicit T cell responses to *L. monocytogenes* infection[29]. Comparatively, in studies of tumor-bearing mice, inflammatory monocytes have been shown to expand in spleen and LN into myeloid-derived suppressor cells that mediate development of Treg and T cell anergy, and impair T cell responses[42-48,251,252].

In light of these studies, it is clear that inflammatory monocytes are dynamic cells, capable of playing diverse and complex roles in an immune response. To our knowledge, the role of inflammatory monocytes in organ transplantation has not been investigated. In this study, we discovered that the vast majority of cardiac allograft-infiltrating recipient APC were inflammatory monocyte, $CD11b^{hi}Ly6C^{hi}$ and $CD11b^{hi}Ly6C^{int}$, derived DC, that infiltrated into the allograft most robustly during the effector phase of the alloresponse. Allograft infiltration was associated with monocytopoiesis and monocytosis similar to the "left shift" of granulocytes, and emigration of inflammatory monocytes out of the bone marrow into circulation required CCR2 expression. Interestingly, this monocytosis may prove a safer and more practical means of diagnosing or screening for acute rejection episodes, thus relinquishing the current dependence on routine heart biopsies, a risky procedure.

Within cardiac allografts, inflammatory DC differentiated into Tip-DC and served as effector cells in a DTH-like response, explaining previous reports that $CCR2^{-/-}$ recipient mice

have modestly improved cardiac allograft survival[253]. Notably, this DTH-like effector response depended on indirect (recognize self-MHC presenting allopeptide) $CD4^+$ T cell help via CD40-CD40 ligation. Therefore, cellular therapies aimed at deleting indirect $CD4^+$ T cells effectively attenuate the DTH-like response in cardiac allografts.

Surprisingly, despite this pro-inflammatory response within cardiac allografts, T cell responses within allografts and within secondary lymphoid organs were actually enhanced in the absence of $CD11b^{hi}Ly6C^{hi}$ inflammatory monocytes, suggesting that $CD11b^{hi}Ly6C^{hi}$ monocytes inhibit T cell responses in WT mice. As such, inflammatory monocytes apparently are capable of serving dual roles as both pro- and anti-inflammatory mediators within the same disease model, a finding not previously described. Our data further illustrate the diversity and complexity of inflammatory monocytes, and offer a new intriguing dual functionality of these enigmatic cells.

4.2 RESULTS

4.2.1 Composition of graft-infiltrating APC

Previously, characterization of cardiac allograft infiltrate has been performed by immunofluorescence staining, yielding only estimated quantification by microscopy. We performed flow cytometry on graft-infiltrating leukocytes (GIL) isolated from cardiac allografts to better quantify and characterize the recipient APC infiltrate. BALB/c $CD45.2^+$ hearts were transplanted into B6 $CD45.1^+$ recipients, then 2, 3 or 7 d later, hearts were harvested and digested with collagenase for 1 h at 37^o C. Single cell suspensions were generated and GIL were enriched by lympholyte M density gradient. By this method, we observed that the vast majority

of graft-infiltrating APC were $CD11c^+$ DC, with few $F4/80^+$ MΦ or $CD19^+$ B cells (Fig. 27a,b). Notably, massive accumulation of $CD11c^+$ cells did not occur at 2 or 3 d post-transplant, as initially anticipated, but rather at 7 d post-transplant (Fig. 27b), during the effector phase of the anti-donor immune response. Immunofluorescence staining of allograft sections revealed that recipient ($H2D^{dneg}$) $CD11c^+$ DC migrated into cardiac allograft tissue from the periphery of the graft at 3 d post-transplant and infiltrated deeper within myocardial tissue by 7 d post-transplant (Fig. 27c).

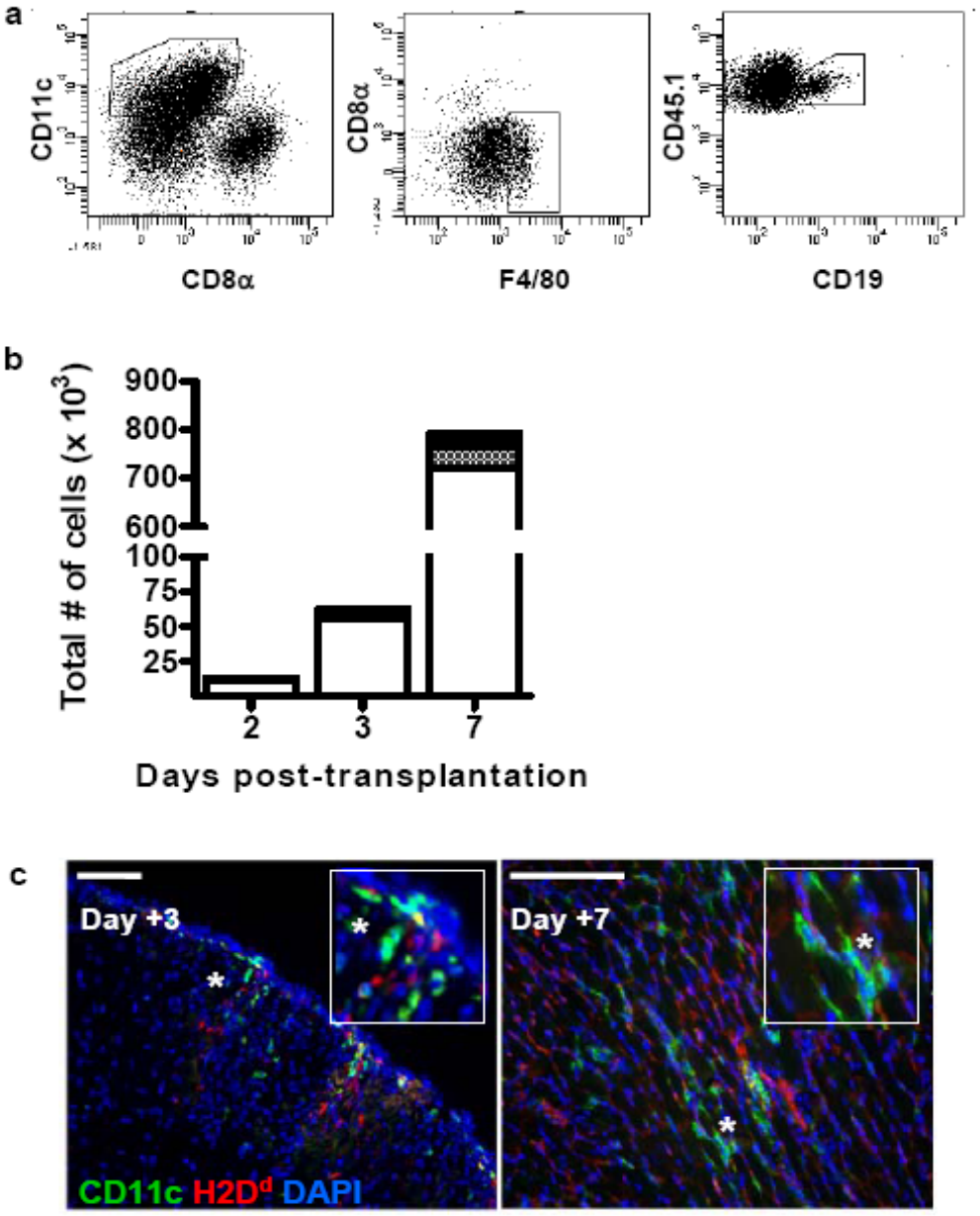

Figure 27. DC comprise the majority of recipient APC infiltrating cardiac allograft tissue.

GIL were isolated from CD45.2$^+$ cardiac allografts transplanted into CD45.1$^+$ recipient mice. (a) Representative dot plots of graft-infiltrating APC are shown with staining for CD45.1 (recipient), CD11c, CD8α, F4/80 and CD19. (b) These populations were quantified at 2, 3 and 7 d post-transplant and the total number is graphed. (c) Cardiac allograft sections were immunofluorescently stained for CD11c and donor MHC class I, H2D^d. Nuclei were counterstained with DAPI. Insets show enlarged images, and asterisks demonstrate corresponding regions on insets and images. Representative images are shown. n = 3 or more animals per group.

Graft-infiltrating CD11c^{+} DC were CD8α^{-} (Fig. 27a) and composed of two distinct subpopulations based on expression of CD11c and CD11b: CD11c^{hi}CD11b^{hi}FSC^{hi}SSC^{hi} cells that constitute the majority of DC and CD11c^{int}CD11b^{-}FSC^{low}SSC^{low} (p=0.0029) (Fig. 28a,b). The high expression of CD11b and larger FSC/SSC suggested that the majority of graft-infiltrating DC are inflammatory monocyte-derived. This assertion was confirmed by immunofluorescence staining of cardiac allograft sections that revealed that the majority of CD11c^{+} DC co-expressed the monocyte marker CD115 (M-CSF receptor) (Fig. 28c).

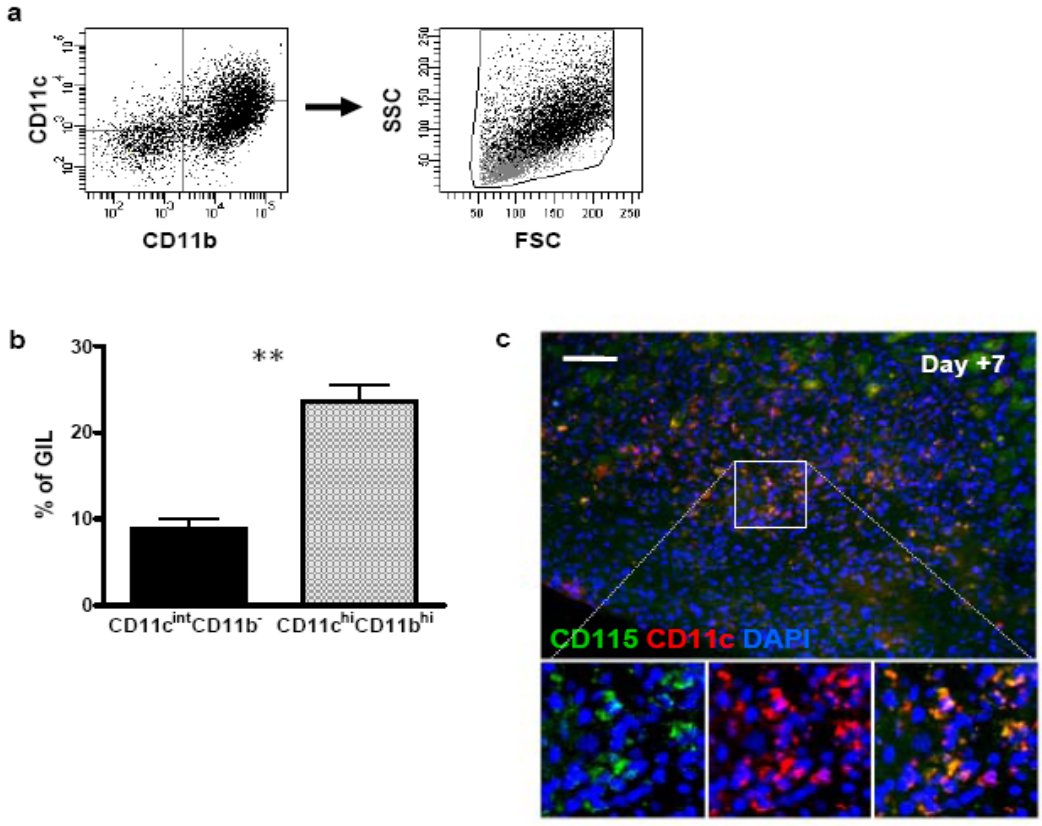

Figure 28. Graft-infiltrating DC are inflammatory monocyte-derived.

Graft-infiltrating APC were stained for CD11c and CD11b. (a) Representative dot plots showing two populations of CD11c^{+} cells: CD11c^{int}CD11b^{-} (gray) and CD11c^{hi}CD11b^{hi} (black), shown on FSC/SSC. (b) Quantification of two DC populations showing mean ± SD. (c) Cardiac allograft sections were immunofluorescently stained for CD115, a monocyte marker and CD11c. Nuclei were counterstained with DAPI. Representative images are shown. n = 3 animals. ** $p < 0.01$.

4.2.2 Graft-infiltrating monocytes differentiate into CD11c^{+} DC

Employing CD45 congenic models, we found that 7 d post-transplant, all GIL isolated from cardiac allografts were of recipient origin (not shown), therefore further analysis at d 7 post-transplant was performed using WT non-congenic BALB/c to B6 strain combination.

We further investigated the origin of graft-infiltrating CD11c^{+} DC by performing FACS analysis for co-expression of Ly6C and CD11b. To do so, staining for Ly6G, a granulocyte marker, was concomitantly performed to allow separation of Ly6C^{+}Ly6G^{-} inflammatory monocytes from the Ly6C^{+}Ly6G^{+} contaminating granulocytes (Fig. 29a). As a result, two populations were identified: one characterized as CD11b^{hi}Ly6C^{hi}, and the second as CD11b^{hi}Ly6C^{int}. These populations each comprised approximately 20% of the total graft-infiltrate 7 d post-transplant, or roughly 1x10^{6} cells per allograft (Fig. 29b,c). Consistent with recent literature, the CD11b^{hi}Ly6C^{hi} population required CCR2 expression for migration into allografts, while the CD11b^{hi}Ly6C^{int} population infiltrated cardiac allografts independently of CCR2 expression (Fig. 29a,b,c).

Notably, upon migration into cardiac allografts, both infiltrating monocyte populations, CD11b^{hi}Ly6C^{hi} and CD11b^{hi}Ly6C^{int}, expressed CD11c and IA^{b} (recipient MHC class II) (Fig. 29d), although CD11b^{hi}Ly6C^{int} monocytes expressed higher levels of CD11c and slightly higher levels of IA^{b} compared to CD11b^{hi}Ly6C^{hi} monocytes.

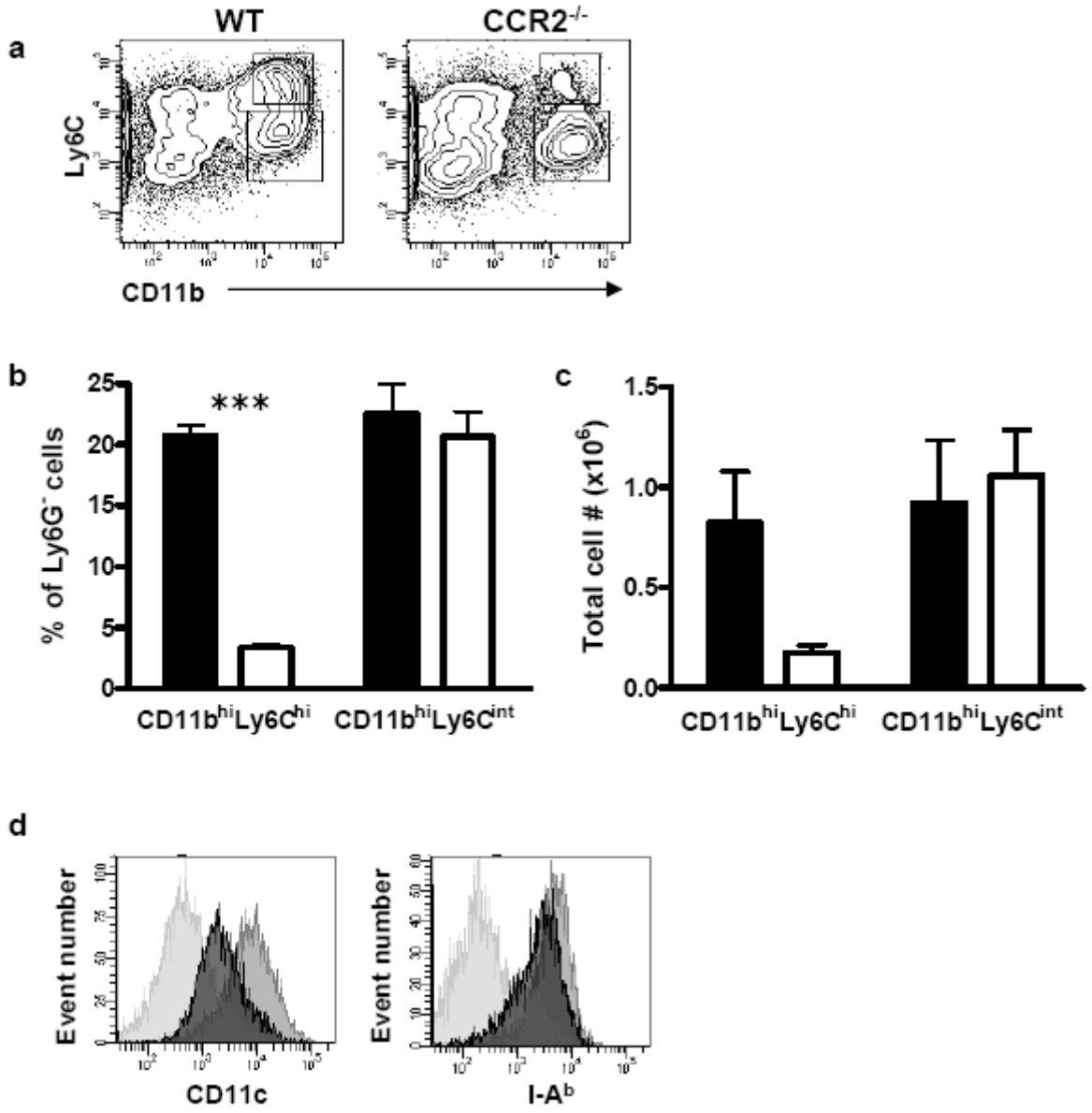

Figure 29. Graft-infiltrating inflammatory DC derive from two subsets of inflammatory monocytes.

GIL from WT and CCR2$^{-/-}$ recipient mice were stained for Ly6G, Ly6C, CD11b, CD11c and MHC class II, IA^{b} and analyzed by flow cytometry. (a) Representative dot plots showing all Ly6G^{-} graft-infiltrating leukocytes are shown. Regions depict CD11b^{hi}Ly6C^{hi} and CD11b^{hi}Ly6C^{int} populations. (b) Percentage of total GIL and (c) total cell number of the two inflammatory monocyte populations within cardiac allografts. Black bars, WT recipients; open bars, CCR2$^{-/-}$ recipients. Mean ± SD is shown. (d) Representative histograms of CD11c expression and IA^{b} expression on CD11b^{hi}Ly6C^{hi} monocytes (dark gray), CD11b^{hi}Ly6C^{int} monocytes (medium gray) and a negative population (light gray). n = 4 or more animals per group. *** $p < 0.001$.

4.2.3 The pDC marker, PDCA-1, is non-specifically expressed during allograft rejection

Ochando et al. recently described that recipient-derived plasmacytoid DC (pDC) comprised the majority of cardiac allograft-infiltrating DC in a mouse model[254]. This conclusion was based primarily on positive staining for PDCA-1, a marker often considered specific for pDC. However, work by Blasius et al. clearly demonstrated that under inflammatory conditions, PDCA-1 expression can be up-regulated by numerous cell types[255]. Notably, pDC are better characterized by the expression pattern $CD11c^{int}CD11b^{-}$ and $FSC^{low}SSC^{low}$. As previously mentioned, in our hands, the majority of $CD11c^{+}$ DC were $CD11c^{hi}CD11b^{hi}FSC^{hi}SSC^{hi}$ (Fig. 28a,b), suggesting that these graft-infiltrating DC are not pDC. We therefore investigated PDCA-1 expression by graft-infiltrating DC to clarify this point. Interestingly, in WT BALB/c allografts transplanted into WT B6 recipients, $CD11c^{hi}CD11b^{+}$ cells expressed PDCA-1 while $CD11c^{int}CD11b^{-}$ cells did not (p=0.0120) (Fig. 30a,b). Consistent with the report that PDCA-1 is up-regulated as a result of inflammation, we observed a significant increase in PDCA-1 expression by graft-infiltrating $CD11c^{+}$ DC between 3 and 7 d post-transplant (7 d vs 2 d, p=0.122; 7 d vs 3 d, p=0.0053) (Fig. 30b). Further, robust PDCA-1 expression by allograft endothelium and non-hematopoietic cells was visualized by immunofluorescence microscopy of allograft sections at 7 d post-transplant (Fig. 30c). Interestingly, the few $CD11b^{hi}Ly6C^{hi}$ inflammatory DC infiltrating cardiac allografts in $CCR2^{-/-}$ recipient mice failed to up-regulate PDCA-1 expression (p=0.0181) (Fig. 30b).

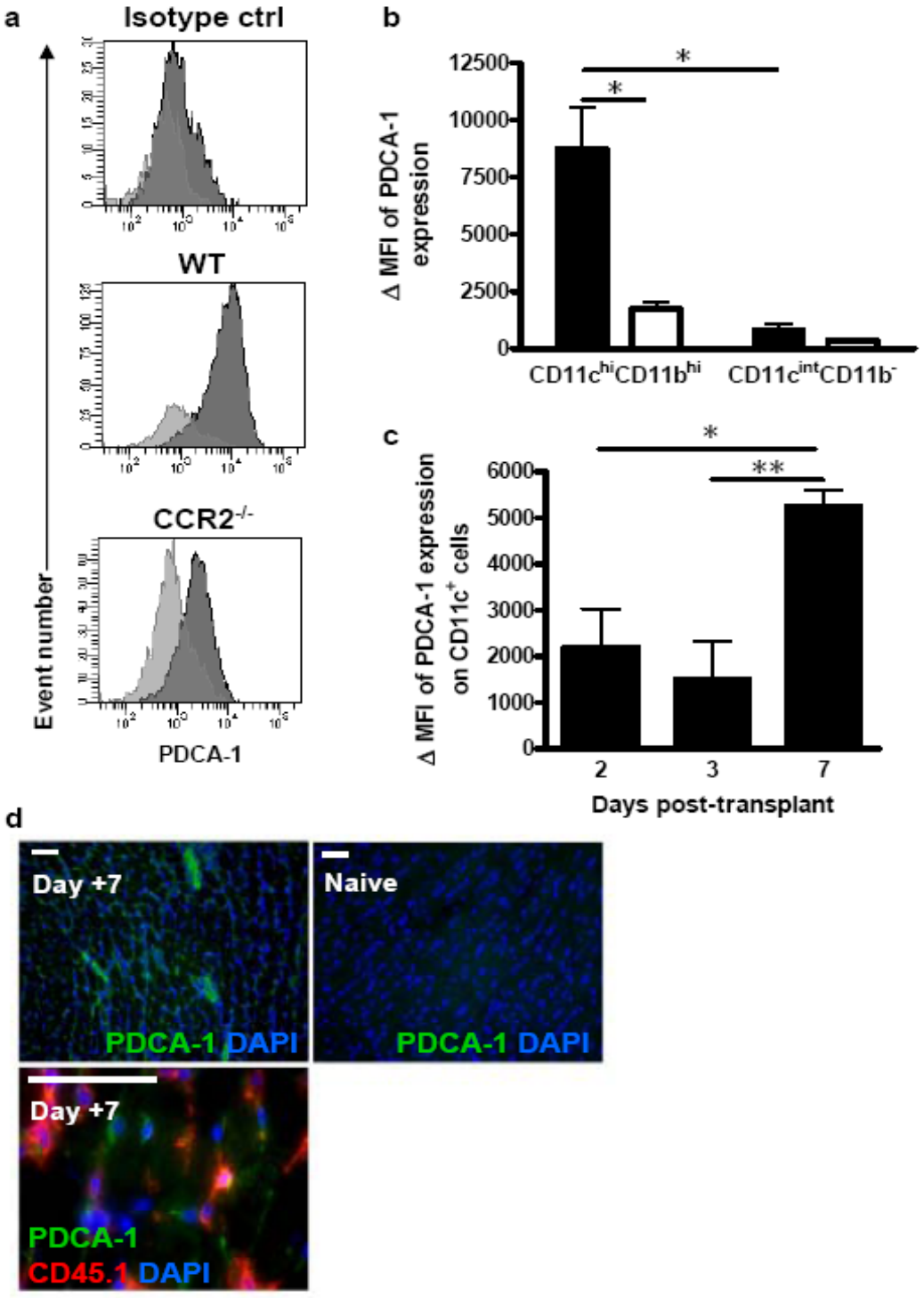

Figure 30. Graft-infiltrating inflammatory DC express PDCA-1 in response to the inflammatory milieu.

(a) Representative histograms showing expression of PDCA-1 by graft-infiltrating $CD11c^{hi}CD11b^{hi}$ (dark gray) and $CD11c^{int}CD11b^{-}$ (light gray) from WT and $CCR2^{-/-}$ recipient mice at 7 d post-transplant. (b) Change in MFI (stained – isotype control) of the two graft-infiltrating DC populations in WT and $CCR2^{-/-}$ mice at 7 d post-transplant. (c) Change in MFI of all $CD11c^{+}$ cells at 2, 3 and 7 d post-transplant. (d) Representative images of PDCA-1 expression by immunofluorescence staining of naïve donor ($CD45.2^{+}$) heart or allograft tissue ($CD45.2^{+}$) at 7 d post-transplant. Mean ± SD shown. n = 3 or more animals per group. * $p < 0.05$, ** $p < 0.01$.

4.2.4 Acute rejection is associated with monocytopoiesis, monocytosis and inflammatory monocyte infiltration into secondary lymphoid organs

Similar to previous observations, we detected only inflammatory monocytes in naïve mouse bone marrow, and that inflammatory monocytes constituted roughly 6% of total blood cells. In our cardiac transplant model, acute allograft rejection was associated with both monocytopoiesis and monocytosis compared to naïve controls ($CD11b^{hi}Ly6C^{hi}$, bone marrow (bm), p=0.0006; blood p=0.0003; $CD11b^{hi}Ly6C^{int}$, bm, p=0.0033; blood, p=0.0004) (Fig. 31a,b). Similarly to previous reports in infection models of *Listeria monocytogenes* and *Leishmania major*, $CCR2^{-/-}$ recipient mice had a significantly increased population of $CD11b^{hi}Ly6C^{hi}$ cells in bm, but few $CD11b^{hi}Ly6C^{hi}$ monocytes in blood or spleen 7 d post-transplant ($CCR2^{-/-}$ vs WT recipients, blood, p<0.0001; spleen, p=0.0181; $CCR2^{-/-}$ recipients vs naïve WT, blood, p=0.0414; spleen, p=0.9105) (Fig. 31a,b), indicating that CCR2 expression is necessary for egress out of the bm into the circulation and peripheral tissues. The percentage of $CD11b^{hi}Ly6C^{int}$ monocytes was unaltered in bm of $CCR2^{-/-}$ recipients compared to WT recipients, and although a significant reduction in the percentage of these monocytes was observed in blood, there was no reduction in the spleen of $CCR2^{-/-}$ recipients (bm, p=0.6975; blood, p=0.0008; spleen, p=0.3324), suggesting

that CCR2 expression contributes to egress of CD11b^{hi}Ly6C^{int} out of the bm, but that these cells proliferate in situ.

In bm, blood and spleen, neither CD11b^{hi}Ly6C^{hi} nor CD11b^{hi}Ly6C^{int} cells expressed CD11c or IA^{b}, indicating that differentiation into inflammatory DC occurred only within cardiac allografts (data not shown).

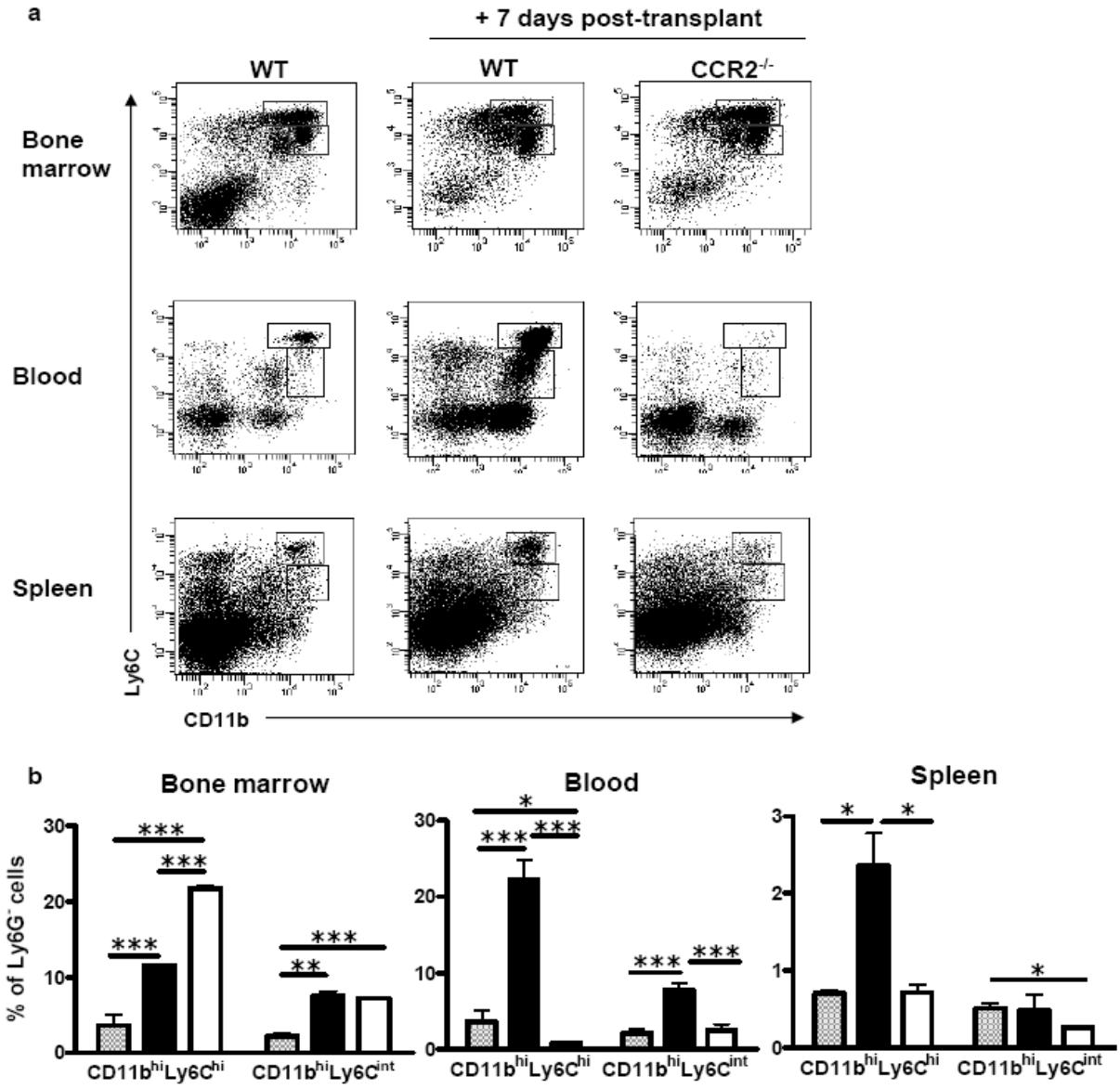

Figure 31. Inflammatory monocytes emigrate from bm into circulation and secondary lymphoid organs.

Single cell suspensions were stained for Ly6G, Ly6C and CD11b from bone marrow, blood and spleen of WT and $CCR2^{-/-}$ recipient mice or naïve WT mice. (a) Representative dot plots showing all Ly6G- cells. Two regions are gated revealing two distinct populations: $CD11b^{hi}Ly6C^{hi}$ and $CD11b^{hi}Ly6C^{int}$. (b) Percentage of the two inflammatory monocyte populations of the total leukocyte population per tissue. Gray bars, naïve control mice; black bars, WT recipient mice; open bars, $CCR2^{-/-}$ recipient mice. Mean ± SD shown. n = 3 or more animals per group. * $p < 0.05$,** $p < 0.01$, *** $p < 0.001$.

4.2.5 Graft-infiltrating inflammatory DC express TNF-α and iNOS

Differentiation of $CD11b^{hi}Ly6C^{hi}$ inflammatory monocytes into TNF-α and iNOS producing-DC (Tip-)DC has been recently described in bacterial infection models. Given the massive influx of inflammatory DC during the effector phase of cardiac allograft rejection, we explored whether these inflammatory DC were in fact Tip-DC. After excluding granulocytes by FACS analysis, we determined that both $CD11b^{hi}Ly6C^{hi}$ and $CD11b^{hi}Ly6C^{int}$ cells produced significant amounts of TNF-α (~9% and 6%, respectively) following 4 h ex vivo stimulation with CD40 ligation (Fig. 32a). The $Ly6C^{hi}$ population produced only slightly more TNF-α than the $Ly6C^{int}$ population (p=0.1695) (Fig. 32b). Gating on all living cells revealed that all TNF-α producing cells expressed CD11b (Fig. 32c). The majority of these cells were $Ly6C^{+}$ inflammatory DC, while a smaller population of granulocytes also contributed to TNF-α production (not shown). Notably, $CCR2^{-/-}$ recipient mice, which contain graft-infiltrating granulocytes and $CD11b^{hi}Ly6C^{int}$ inflammatory DC, still had significantly reduced levels of TNF-α compared to WT recipients (p=.0276) (Fig. 32c,d).

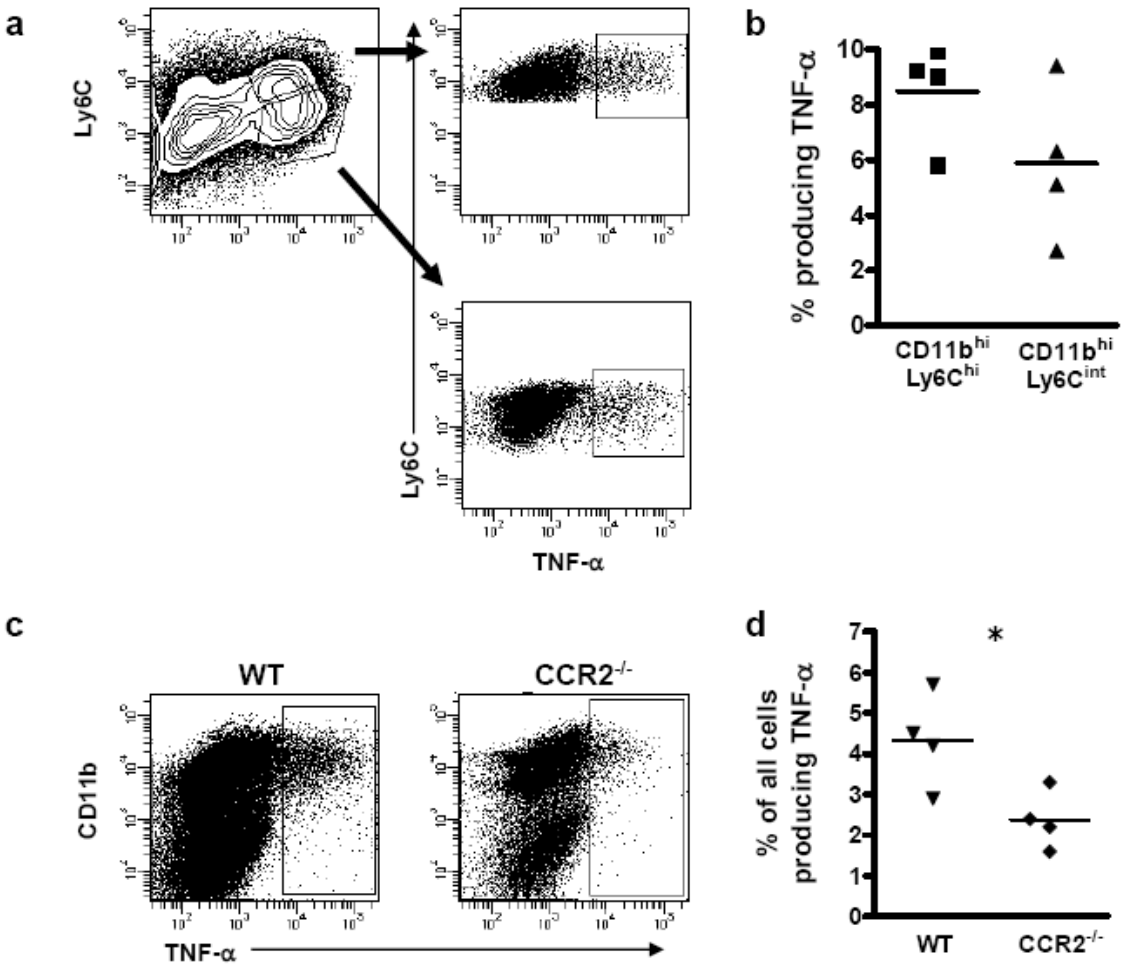

Figure 32. Graft-infiltrating inflammatory DC produce TNF-α.

Graft-infiltrating leukocytes from WT and CCR2$^{-/-}$ recipient mice were cultured for 4 h in the presence of brefeldin-A and agonistic CD40 mAb. Cells were then stained for Gr-1, Ly6C, CD11b and TNF-α and analyzed by flow cytometry. Gr-1 was used to gate out granulocytes. (a) Representative contour plot showing all non-granulocytic cells reveals two populations of inflammatory DC. Each population is then shown in a dot plot for TNF-α production. (b) The percentage of TNF-α producing cells of each inflammatory DC population is shown. (c) Representative dot plots showing TNF-α production by all graft-infiltrating leukocytes in WT and CCR2$^{-/-}$ recipient mice. (d) Percentage of total graft-infiltrating leukocytes in WT and CCR2$^{-/-}$ recipient mice producing TNF-α is shown. n = 4 or more mice per group. * $p < 0.05$.

Additionally, a high number of iNOS-expressing cells were detected in cardiac allografts in WT recipient mice by immunohistochemistry, while cardiac allografts transplanted into CCR2$^{-/-}$ recipient mice had only minimal iNOS expression (Fig. 33a), and quantification of nitrite (a by-product of iNOS activity) by GIL in culture revealed significantly reduced levels of nitrite produced by GIL from CCR2$^{-/-}$ recipient mice compared to WT recipients (p=.0274) (Fig. 33b). Since CCR2$^{-/-}$ mice contain normal numbers of graft-infiltrating CD11b^{hi}Ly6C^{int} inflammatory DC but significantly reduced numbers of CD11b^{hi}Ly6C^{hi} inflammatory DC, these data suggest that CD11b^{hi}Ly6C^{hi} inflammatory DC are either the main producers of iNOS in cardiac allografts, or that iNOS expression is indirectly dependent on CD11b^{hi}Ly6C^{hi} inflammatory DC infiltration. To confirm that inflammatory DC are the main producers of iNOS, we performed immunofluorescence staining of cardiac allografts in WT recipient mice. By this method, we visualized that all iNOS producing cells co-expressed CD11c (Fig. 33c).

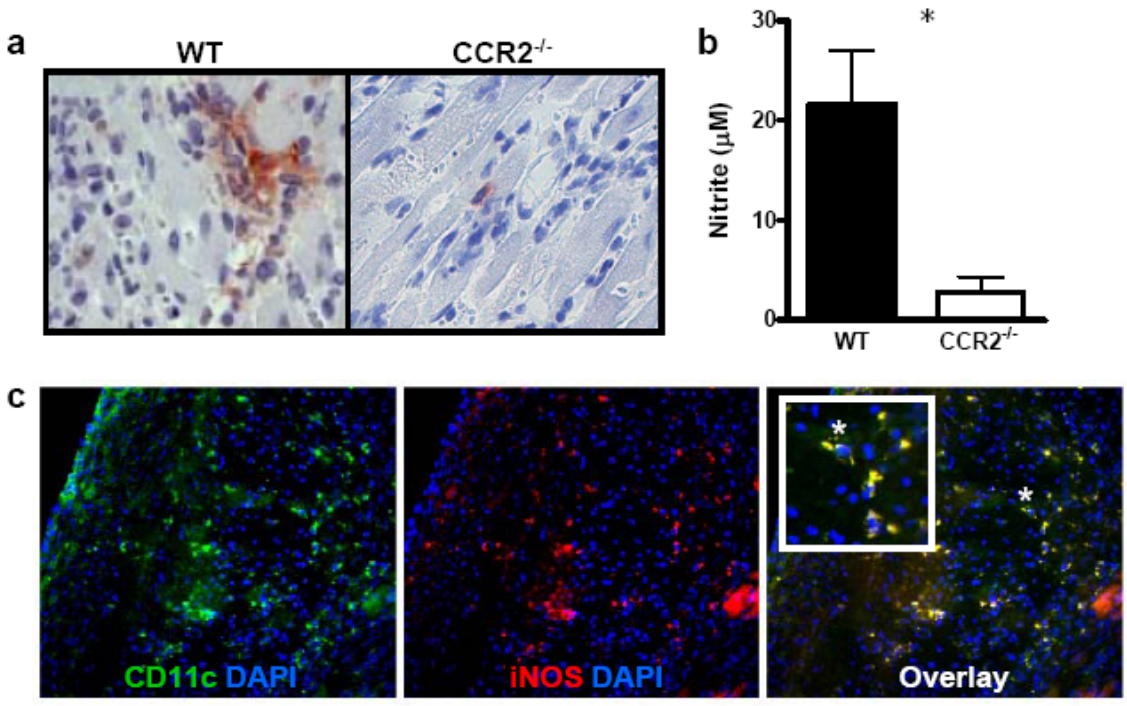

Figure 33. CD11b^{hi}Ly6C^{hi} inflammatory DC produce iNOS.

(a) Representative images of cardiac allograft tissue from WT and CCR2$^{-/-}$ recipient mice stained by immunohistochemistry for iNOS. (b) Nitrite production was quantified in 72 h culture supernatants of single cell suspensions of GIL from WT and CCR2$^{-/-}$ recipient mice. Mean ± SD shown. (c) Representative images of cardiac allograft tissue from WT recipient mice immunofluorescently stained for CD11c and iNOS. Nuclei were counterstained with DAPI. n = 3 or more animals per group. * $p < 0.05$.

Release of TNF-α and iNOS by inflammatory DC suggests that these DC participate in a DTH-like reaction. Valujskikh et al. previously published data suggesting that indirectly alloreactive T cells mediate a DTH-like response in cardiac allografts that contributes to allograft rejection[184], however, the mechanism by which this occurs has never been elucidated. We observed in mice lacking MHC class II expression, MHC-II$^{KO-/-}$ mice, previously reconstituted with polyclonal syngeneic CD4$^+$ T cells, that cardiac allografts lacked detectable expression of iNOS by immunohistochemistry (Fig. 34), indicating that indirect CD4$^+$ T cell interaction with recipient inflammatory DC is necessary for the DTH-like response. Comparatively, treatment of such recipients with agonistic CD40 mAb in vivo 2 d post-transplantation resulted in marked up-regulation of iNOS expression throughout cardiac allografts (Fig. 34), suggesting that CD40-CD154 ligation provided by indirect CD4$^+$ helper T cells is requisite for the DTH-like response. In further support of this conclusion, we found that WT recipient mice pre-treated with tolerogenic maturation-resistant (MR-)DC therapy, which we have previously shown to delete indirect CD4$^+$ effector T cells thus abrogating CD4$^+$ T cell help, had significantly reduced iNOS expression throughout cardiac allografts (Fig. 34).

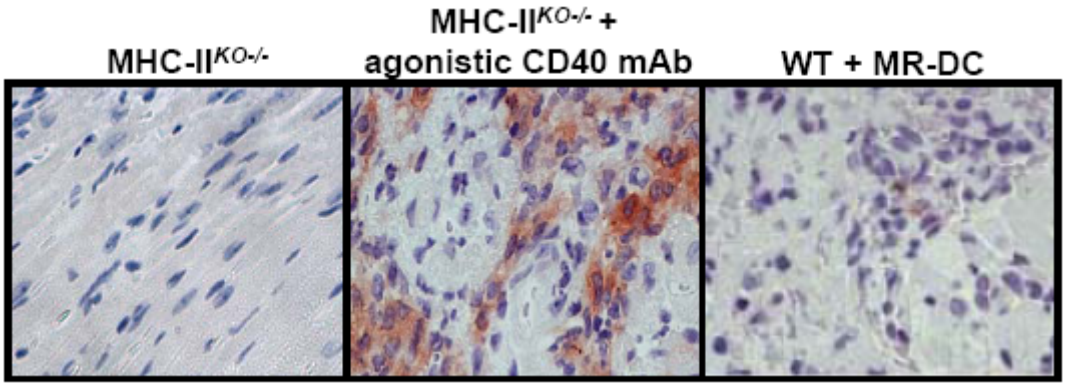

Figure 34. Inflammatory DC mediate a DTH-like response that requires indirect CD4$^+$ T cell help.

Representative images of cardiac allograft tissue stained by immunohistochemistry for iNOS are shown. Recipient mice include MHC class-II$^{KO-/-}$ mice reconstituted with 10^7 polyclonal syngeneic CD4$^+$ T cells prior to transplantation, the same mice treated with agonistic CD40 mAb i.p. 2 d post-transplantation, or WT recipient mice pre-treated 7 d prior to cardiac transplantation with $5x10^6$ donor-derived MR-DC. n = 3 or more animals per group.

4.2.6 Inflammatory DC inhibit effector T cell responses

Recent publications have demonstrated a role for inflammatory DC in T cell priming and T_h1 skewing. However, Abdi et al. previously showed that CCR2$^{-/-}$ recipient mice had only slightly prolonged cardiac allograft survival compared to WT recipients (MST 12 d vs 8)[253], and given that we now show that CCR2$^{-/-}$ recipients have significantly reduced inflammatory DC infiltration into cardiac allografts, resulting in significantly reduced TNF-α and iNOS production, both potent pro-inflammatory mediators, we hypothesized that T cell alloresponses in our model likely occur independently of inflammatory DC infiltration/activity.

Surprisingly, we observed a significantly increased CD8$^+$ T cell infiltrate in cardiac allografts of CCR2$^{-/-}$ recipient mice compared to WT recipients (p=.0136), although CD4$^+$ T cell infiltrate appeared to be unaffected (Fig. 35a). Intracellular cytokine staining demonstrated that

the same frequency of $CD8^+$ and $CD4^+$ T cells were capable of producing IFN-γ in $CCR2^{-/-}$ recipients compared to WT recipients (Fig. 35b,c), therefore, the overall number of $CD8^+$ effector T cells was increased in allografts in $CCR2^{-/-}$ recipient mice, suggesting that inflammatory DC inhibit the T cell alloresponse.

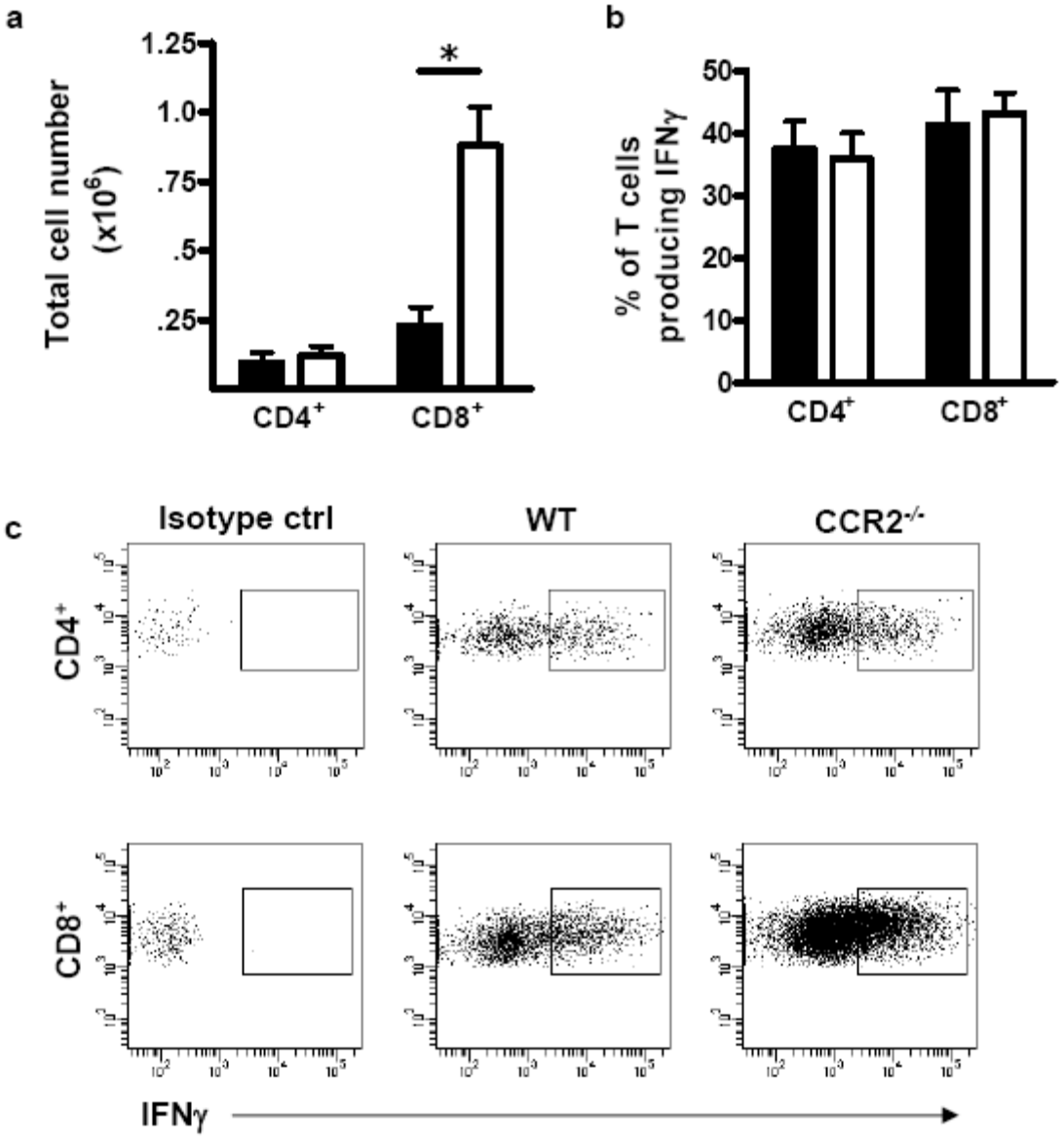

Figure 35. T cell responses in allografts are more robust in the absence of inflammatory monocytes.

(a) The number of graft-infiltrating T cells in WT and CCR2$^{-/-}$ recipient mice was quantified from flow cytometry following staining for CD3, CD4 and CD8. (b) The percentage of graft-infiltrating T cells from WT and CCR2$^{-/-}$ recipient mice producing IFN-γ was determined by intracellular cytokine staining following 5 h culture with brefeldin A and PMA/ionomycin. Mean ± SEM is shown. (c) Representative plots of IFN-γ production by CD4^{+} and CD8^{+} T cells are shown. Black bars, WT recipient ; open bars, CCR2$^{-/-}$ recipient mice. n = 4 or more mice per group. * $p < 0.05$.

This inhibition could be mediated solely within the allograft and/or within secondary lymphoid organs. Therefore we next analyzed the T cell response in spleens of WT and CCR2$^{-/-}$ recipient mice. The number of both CD4^{+} and CD8^{+} T cells was significantly increased in CCR2$^{-/-}$ recipient mice compared to WT recipients, as was the frequency of IFN-γ producing effector CD4^{+} and CD8^{+} T cells (Fig. 36a,b,c). Further, neither IL-4 nor IL-5 was detected in heart or spleen in preliminary experiments (data not shown). Therefore, the absence of CD11b^{hi}Ly6C^{hi} inflammatory monocytes increases type 1 T cell responses systemically.

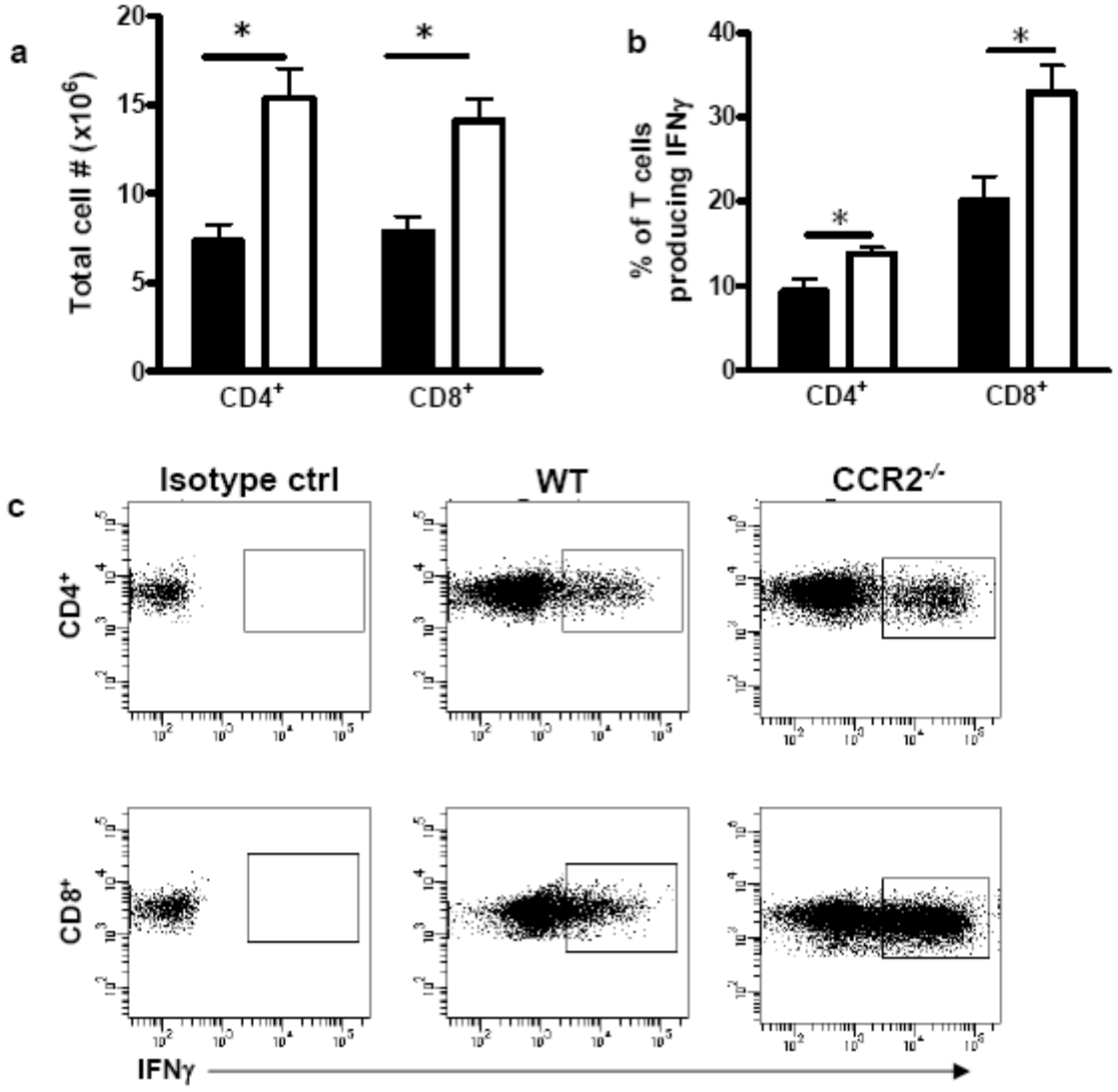

Figure 36. T cell responses in secondary lymphoid organs are more robust in the absence of inflammatory monocytes.

(a) T cells were quantified from WT and CCR2$^{-/-}$ recipient mouse spleen 7 d post-transplant by staining for CD3, CD4 and CD8 and analysis by flow cytometry. (b) The percentage of splenic T cells from WT and CCR2$^{-/-}$ recipient mice producing IFN-γ was determined by intracellular cytokine staining following 5 h culture with brefeldin A and PMA/ionomycin. Mean ± SEM is shown. (c) Representative plots of IFN-γ production by CD4^{+} and CD8^{+} T cells are shown. Black bars, WT recipient mice; open bars, CCR2$^{-/-}$ recipient mice. n = 4 or more mice per group. * $p <$ 0.05.

4.3 DISCUSSION

Recipient APC serve a crucial role in orchestrating and mediating the alloimmune response, yet few studies of recipient DC in transplantation have been performed. A major limitation has been the inability to isolate recipient leukocytes from allografts for thorough phenotypic characterization and functional analysis. Here we developed a protocol to consistently isolate GIL from cardiac allografts with good viability for analysis. In so doing, we quickly identified $CD11c^+$ DC rather than $F4/80^+$ MΦ or $CD19^+$ B cells, as the primary recipient APC infiltrating allografts. This methodology further allowed us to characterize these DC as inflammatory DC, that express PDCA-1 in response to the inflammatory milieu, rather than pDC, as previously suggested[254].

We identified two populations of inflammatory DC infiltrating cardiac allografts, one $CD11b^{hi}Ly6C^{hi}$ and one $CD11b^{hi}Ly6C^{int}$. In our hands, consistent with the literature, $Ly6C^{hi}$ cells required CCR2 expression to emigrate from bone marrow into blood. By contrast, the absence of CCR2 expression resulted in accumulation of these inflammatory monocytes within the bm[256]. Notably, a small number of $Ly6C^{hi}$ monocytes did egress from bm into blood, followed by their migration into the cardiac allografts, suggesting that escape through alternative chemokines receptors may be possible. Similar findings were observed by Randolph's group in a skin inflammation model in $CCR2^{-/-}$ mice[25].

The literature is more controversial in regards to $Ly6C^{int}$ inflammatory DC. In our model, although the percentage of $Ly6C^{int}$ cells was significantly reduced in blood of $CCR2^{-/-}$ recipients, the total number accumulating in cardiac allografts and spleen was comparable to WT recipients. It is possible that CCR2 contributes to egress from the bm, but that these $Ly6C^{int}$ monocytes proliferate in situ. Qu et al. also demonstrated that circulating $Gr\text{-}1^{int}$ inflammatory monocytes

selectively express CCR7 and CCR8, and utilize these receptors for migration into LN[25]. Further, these authors showed that Gr-1^{int} inflammatory monocytes had increased allostimulatory capacity compared to Gr-1^{hi} monocytes. Consistent with these observations, we noted higher surface expression of MHC class II on CD11b^{hi}Ly6C^{int} inflammatory DC compared to CD11b^{hi}Ly6C^{hi} inflammatory DC. Further delineation of CD11b^{hi}Ly6C^{hi} versus CD11b^{hi}Ly6C^{int} inflammatory DC in transplantation may reveal distinct roles for these two APC subsets.

Importantly, in WT recipients, there was a clear monocytopoiesis and monocytosis compared to naïve WT mice, similar to the "left shift" of granulocytes. Currently in clinical medicine, diagnosis of acute rejection requires heart biopsy, a risky procedure. Our data suggest that a simple blood draw for monocytosis could be an effective and simpler approach for diagnosing or screening acute cardiac allograft rejection in patients.

In our hands, although CD11b^{hi}Ly6C^{int} inflammatory DC produced some TNF-α and iNOS, the majority of Tip-DC in cardiac allografts were CD11b^{hi}Ly6C^{hi} cells. The contributions of iNOS and TNF-α to allograft rejection have been previously demonstrated. Increased serum concentration of nitrite correlates with the kinetics of acute allograft rejection[257] and neutralization of iNOS in rat cardiac models results in increased cardiac contractile function, decreased histologic rejection and prolonged survival[172,173]. Increased expression of TNF protein is detected in acutely rejecting cardiac allografts[258] and blocking TNF-α in vivo with neutralizing Ab prolongs cardiac allograft survival[259]. Therefore, eliminating monocytes should theoretically prolong cardiac allograft survival.

However, to our surprise, we observed that substantially decreased numbers of CD11b^{hi}Ly6C^{hi} inflammatory monocytes within recipient spleen and CD11b^{hi}Ly6C^{hi} inflammatory DC within cardiac allografts was associated with increased numbers of splenic and

graft-infiltrating effector T cells, suggesting that inflammatory monocytes/inflammatory DC actually inhibit T cell responses in WT mice. The increased T cell responses in the absence of $CD11b^{hi}Ly6C^{hi}$ inflammatory monocytes/inflammatory DC could reflect compensatory mechanisms due to the an aberrant immune response, or alternatively, inflammatory monocytes/DC could directly inhibit T cell responses, perhaps by decreasing T cell proliferation or by promoting T cell apoptosis. In tumor-bearing mice, inflammatory monocytes can expand in spleen into myeloid-derived suppressor cells (MDSC) that are capable of inducing Treg or T cell anergy, or impairing T cell responses[42-48,251,252]. Specifically, MDSC have been shown to inhibit $CD8^+$ T cells through reactive oxygen intermediaries and through nitrite[43]. We are currently investigating the mechanisms by which inflammatory monocytes/inflammatory DC inhibit T cell responses in cardiac transplantation.

Previously, inflammatory monocytes and inflammatory DC have been shown to serve either pro-inflammatory roles in infection and immunization experimental models, or anti-inflammatory suppressor roles in tumor models. We for the first time describe a dual functionality for these cells: as mediators of a DTH-like response contributing to allograft rejection, and as inhibitors of the T cell alloresponse. Further work is required to clarify the mechanisms by which inflammatory monocytes/inflammatory DC limit T cell responses and the roles and relationships of the different inflammatory APC subsets, however our study demonstrates the importance of the recipient inflammatory DC population in dictating allograft fate.

5.0 METHODS AND MATERIALS

5.1 MICE AND REAGENTS

C57BL/6 (B6), BALB/c, C3H, B6.129-H2$^{dlAb1\text{-}E\alpha}$/J (MHC-II$^{KO\text{-}/\text{-}}$), B6.FVB-Tg (Itagx-DTR/eGFP)$_{57}$Lan/J (CD11c-eGFP), B6.129P2-β_2m$^{tm1Unc/J}$ (MHC-I$^{KO\text{-}/\text{-}}$), B6.129S4-CCR2^{tm1Ifc}/J and B6.SJL-Ptprc^{a}Pepc^{b}/BoyJ (CD45.1^{+}) mice (all Thy1.2^{+}) were purchased from The Jackson Laboratory (Bar Harbor, ME). 1H3.1 TCR transgenic (tg) B6 mice (provided by C. Viret and C. Janeway, Yale University, New Heaven, CT) and 2C RAG1$^{KO\text{-}/\text{-}}$ TCRtg B6 mice (both Thy1.1^{+}), were bred at the University of Pittsburgh Animal Facility. For total body irradiation, wildtype BALB/c mice were irradiated with 1000 rad to eliminate hematopoietic cells, 3 d prior to organ harvest for transplantation. Studies were approved by the Institutional Animal Care and Use Committee.

Mouse GM-CSF and IL-4 were from PeproTech, and PKH26 and 1α,25-(OH)$_2$ vitamin D$_3$ (VD$_3$) from Sigma. The IE$\alpha_{52\text{-}68}$ peptide (ASFEAQGALANIAVDKA) was synthesized, HPLC-purified and confirmed by mass spectroscopy. Agonistic CD40 (FGK45.5; 150 μg i.p. for 3 d or on d 2-3 post-transplant) and depleting NK1.1 (PK136) mAb were from BioXCell (West Lebanon, NH). Unless otherwise specified, mAb were from BD-PharMingen (San Diego, CA).

5.2 HEART TRANSPLANTATION

Intra-abdominal cardiac transplantation and monitoring of graft survival were performed as previously described[260]. Palpation for heart beat was performed daily to determine organ survival.

5.3 GENERATION OF MR-DC

BM cells were removed from mouse femurs and tibias and depleted of erythrocytes by treatment with NH_4Cl solution. Erythroid precursors, T, B and NK cells, and granulocytes were removed by complement depletion using a cocktail of mAb (TER-119, CD3ε, B220, NK1.1, and Gr1) followed by incubation (40 min, 37°C) with low toxicity rabbit complement (Cedarlane®, Ontario, Canada). Remaining BM cells were cultured in RPMI-1640 (Mediatech, Inc., Herndon, VA) in 75 cm^2 flasks ($15x10^6$ cells/flask) with 10% heat-inactivated fetal calf serum (FCS, Life Technologies, Grand Island, NY), glutamine, non-essential amino acids, sodium pyruvate, HEPES, 2-ME, and penicillin/streptomycin, supplemented with 1000 U/ml mouse GM-CSF and 500 U/ml mouse IL-4 either with addition of 10 nM VD_3 beginning on d 2 of culture (MR-DC) or not (control-DC). Culture medium, cytokines and VD_3 were renewed every other day. Before administration, MR-DC were purified from potential contaminating mature $CD86^+$ DC by negative depletion (Dynabeads®, Invitrogen Dynal, Norway) (Fig. 37). For generation of LPS-matured DC, control-DC (d 6) were cultured with LPS (200 ng/ml) overnight. For in vitro challenge, control- and MR-DC (d 6) were treated for 48 h with a DC_1-maturation cocktail

containing IFN-γ (20 ng/ml), IL-1β (20 ng/ml), TNF-α (50 ng/ml), CpG (1 μM), and poly I:C (1 μM); or with LPS (50 ng/ml); or agonistic CD40 mAb (10 μg/ml, HM40-3).

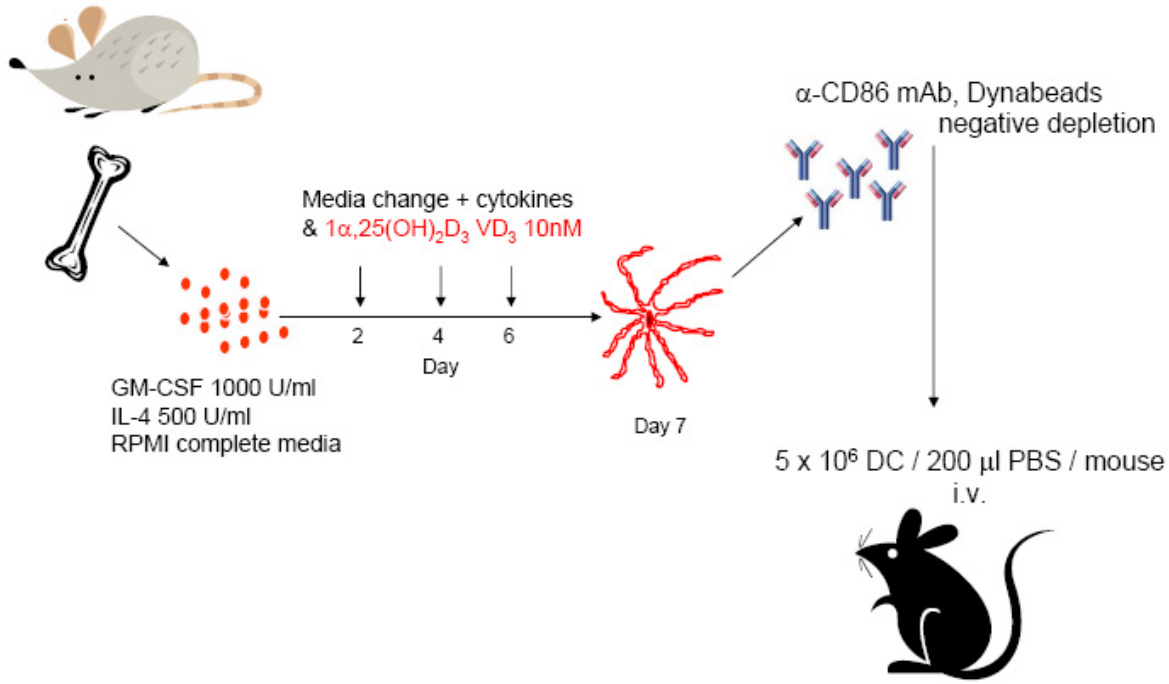

Figure 37. Model for generating MR-DC.

5.4 ISOLATION OF TCR TRANSGENIC T CELLS

T cells were purified from spleens and LN of WT, 1H3.1 or 2C mice with either CD4 or CD8 Dynabeads® negative isolation kits. After purification, T cells were stained with 7.5 μM Vybrant CFDA SE Cell Tracer (Molecular Probes Inc., Invitrogen, Eugene, OR). Three x 10^6 CFSE-labeled $CD4^+$ 1H3.1 or $CD8^+$ 2C T cells were administered i.v. to B6 mice. Ten x 10^6 polyclonal $CD4^+$ T cells were i.v injected per MHC-$II^{KO-/-}$ mice 7 d prior to transplantation, or were used unstained in culture.

5.5 MICROSCOPIC ANALYSIS AND IMMUNOSTAINING

Paraffin-embedded sections of allografts were processed for H&E or for iNOS staining by immunohistochemistry (BD Biosciences cat no. 610333 at 1:100). OCT embedded frozen tissue was sectioned by cryostat (8 μm), fixed in 95% ethanol, and treated with 5% normal goat serum (NGS), then avidin/biotin blocking kit (Vector, Burlingame, CA).

The composition of the GIL following treatment with MR-DC was analyzed by incubating sections with alexa-488-CD4 mAb and biotin-FoxP3 mAb or biotin-CD8α mAb plus Cy3-straptividin.

For trafficking studies of BALB/c MR-DC ($CD45.2^+$) in B6 mice ($CD45.1^+$), spleen sections were labeled with CD11c mAb plus Cy2-anti-hamster IgG, biotin-CD45.2 mAb plus Cy3-streptavidin and alexa-647-CD3 mAb (from BD Pharmingen, Invitrogen, eBiosciences or Jackson ImmunoResearch Laboratories, West Grove, PA).

Cystospins of splenic DC-enriched suspensions [generated by digesting spleens in 400 U/ml collagenase (30', 37°C), diluting splenocytes in ice-cold Ca^{++} free 0.01 M EDTA-PBS, and centrifuging splenocytes (1800 rpm, 20', 4°C) over 16% Histodenz gradient] from recipient $CD45.1^+$ B6 mice treated with donor-derived MR-DC were incubated with biotin-CD45.2 mAb plus Cy3-streptavidin, CD11c mAb plus Cy5 anti-hamster IgG and with FITC-TUNEL (ROCHE, Indianapolis, IN).

To detect allospecific TCRtg $CD4^+$ T cells in peripheral tissues of host B6 mice after treatment with donor-derived MR-DC, heart, liver and kidney sections were labeled with alexa-647-CD4 mAb and biotin-Thy1.1 mAb plus Cy2-streptavidin.

To visualize donor passenger APC in naïve hearts and allografts, sections were stained with biotinylated-$H2D^d$ mAb and CD11c mAb then with Cy3-streptavidin and Cy2-anti-hamster

IgG. Detection of MHC class I and II were performed by staining with biotinylated-H2D^d mAb or with biotinylated-IA^d and von Willebrand factor mAb, then with Cy3-streptavidin and Cy2-anti-rabbit IgG.

To characterize cardiac allograft infiltration of APC, allograft sections were stained with CD11c mAb and biotinylated-H2D^d mAb then with Cy2-anti-hamster IgG and Cy3-streptavidin, or alternatively with CD115 mAb, CD11c mAb and with iNOS polyclonal Ab then with alexa-488-anti-rat IgG, Cy5-anti-hamster IgG and Cy3-anti-rabbit IgG. To visualize PDCA-1 expression, sections were stained with PDCA-1 mAb and biotinylated-CD45.2 mAb, then with alexa-488-anti-rat IgG and Cy3-streptavidin.

Nuclei were counterstained with DAPI (Molecular Probes Inc.). Slides were examined with a Zeiss Axiovert 135 microscope equipped with a CCD camera.

For confocal microscopic analysis, splenic DC-enriched suspensions from host CD11c-eGFP B6 mice injected with PKH26-labeled BALB/c MR-DC, were attached to poly-L-lysine-treated slides, fixed with 4% paraformaldehyde and imaged with an Olympus 1X81 microscope (Olympus America, Inc., Melville, NY).

5.6 LEUKOCYTE ISOLATION FROM TISSUE

5.6.1 From cardiac allografts

Cardiac allografts were digested with 400 U/ml type IV collagenase for 1 h at 37^{o}C, with vortexing every 15 min. Tissue was then disaggregated through 40 μm cell strainers and treated

with red blood cell lysis buffer. Single cell suspensions were passed over a lympholyte M density gradient for 20 min at 4°C at 2000 rpm. Leukocytes at the interface were isolated and counted.

5.6.2 From bone marrow and spleen

Bone marrow cells were flushed from tibia and femur then passed through 40 μm cell strainer and treated with red blood cell lysis buffer. Spleens were flushed with culture media then treated with 400 U/ml type IV collagenase for 30 min at 37°C. Spleens were then disaggregated into single cell suspensions, passed through a 40 μm cell strainer and treated with red blood cell lysis buffer.

5.6.3 From blood

Blood was drawn undiluted from mouse heart and passed through Ficoll gradient for 20 min at room temperature at 2000 rpm. Cells at the were collected for analysis.

5.7 FLOW CYTOMETRY

5.7.1 Surface staining

Single cell suspensions were blocked with 10% NGS and incubated (30', 4°C) with mAb, and if necessary, washed and stained with secondary Ab or in the case of a biotinylated primary Ab, with fluorescently labeled streptavidin (see Table 3). Appropriate fluorochrome-conjugated

isotype-matched mAb were used as negative controls. After staining, cells were fixed in 4% paraformaldehyde, read on a LSRII flow cytometer (BD Biosciences) and analyzed using FACSDiva software (BD Biosciences).

5.7.2 Additional stains

Annexin-V staining was performed according to manufacturer's instructions (BD Biosciences).

For Treg staining, cells were first surface labeled and then permeabilized using cytofix/cytoperm solution (eBiosciences) and stained with FoxP3 mAb (eBiosciences).

For intracellular cytokine staining of T cells, GIL and splenocytes were cultured for 5 h at 250,000 cells per well, in 96-well round bottom plates with brefeldin A at 1.5 μl/ml, PMA 20 ng/ml and 100μM ionomycin. For TNF-α staining, GIL were cultured at 250,000 cells per well, in 96-well round bottom plates for 4 h with brefeldin A at 1.5 μl/ml and agonistic CD40 mAb at 10 μg/ml. After culture, cells were surface stained, permeabilized using cytofix/cytoperm solution (eBiosciences) and stained with IFN-γ, IL-4, IL-5 or TNF-α mAb.

Table 3. Antibodies used for flow cytometry.

Ag	Fluorochrome	Clone	Manufacturer
CD3	alexa-648	17A2	eBiosciences
CD4	PE-Cy5 Pacific blue	GK1.5 RM4-5	eBiosciences
CD8α	PE-Cy5 APC-Cy7 FITC	53-6.7	eBiosciences BD BD
CD11b	alexa-647	M1/70	eBiosciences
CD11c	PE-Cy5 Pacific Blue	N418	eBiosciences
CD19	FITC	MB19-1	eBiosciences
CD40	PE	1C10	eBiosciences
CD45.1	biotinylated	A20	eBiosciences
CD45RA	PE	14.8	BD
CD62L	PE	MEL-14	eBiosciences
CD69	PE	H1.2F3	BD
CD80	PE	16.10A1	eBiosciences
CD86	PE	PO3-1	eBiosciences
CD127	PE	A7R34	eBiosciences
F4/80	FITC	BM8	eBiosciences
Gr1	APC-Cy7	RB6-8C5	BD
Ly6C	FITC	AL-21	BD
Ly6G	PE	IA8	BD
PDCA-1	PE	eBio129c	eBiosciences
Thy1.1	APC	HIS51	eBiosciences
IFN-γ	PE	XMG1.2	eBiosciences
IL-4	PE	11B11	BD
IL-5	PE	JES1-39D10	BD
TNF-α	PE	MP6-XT22	eBiosciences
$H2D^d$	PE	34-2-12	BD
IA^b	PE biotinylated	AF6-120.1	BD
IA^d	PE	AMS-32.1	BD
FoxP3	PE	NRRF-30	eBiosciences
alexa-647-streptavidin			Invitrogen
alexa-700-streptavin			Invitrogen

5.8 MLC AND ELISPOT ASSAY

The allostimulatory ability of (γ-irradiated) BALB/c control- and MR-DC, untreated or following in vitro challenge with the DC_1-maturation cocktail, was tested in 3 d-MLC using B6 splenic $CD4^+$ T cells. Cell proliferation was evaluated by assessment of [^{3}H]thymidine incorporation.

For analysis of the anti-donor response via the direct pathway by ELISPOT assay, purified splenic or graft-infiltrating T cells (enrichment columns, R&D Systems, Minneapolis, Minnesota) from B6 WT or MHC-$II^{KO-/-}$ mice transplanted 7 d before with BALB/c cardiac grafts from total body irradiated or unmodified donor mice were incubated with CD3-depleted, γ-irradiated, splenic B6, BALB/c or C3H APC ($3x10^4$ splenic T cells or 5,000 graft-infiltrating T cells + $2.5x10^5$ APC / well) in 96-well ELISPOT plates coated with IFN-γ mAb. For analysis of the indirect pathway, purified recipient splenic or graft-infiltrating T cells were incubated with CD3-depleted, γ-irradiated, splenic B6 APC ($3x10^5$ splenic T cells or 25,000 graft-infiltrating T cells + $2.5x10^5$ APC / well) and sonicate (50µl / well) prepared from BALB/c, B6 or C3H splenocytes (from $2x10^7$ cells / ml). ELISPOT plates were developed 36 h later following manufacturer's instructions (BD Biosciences).

5.9 QUANTIFICATION OF DONOR DC BY PCR ANALYSIS

DNA was extracted with the DNeasy Tissue Kit (QIAGEN Inc., Valencia, CA) from spleen of B6 mice injected with BALB/c MR-DC 24 h after treatment with (or not) NK1.1 mAb (200µg, i.p.). PCR was performed using primers for $IgG2a^a$ (BALB/c and B6 mice encode for the $IgG2a^a$ and $IgG2a^b$ alleles, respectively)[219]: F 5' ACAAAGTCCCTGGTTTGGTGC; R 5'

GGCATTTGCATGGAGGACAG; 111 Kb product. For PCR, 750ng DNA was added to Illustra PuReTaq Ready-To-Go PCR beads (GE Healthcare, Buckinghamshire, UK) and run at 94^{o}C 3 min; (94^{o}C 30 s, 67.7 ^{o}C 30 s, 72^{o}C 50s) x 38 cycles, and 72^{o}C for 10 min. PCR products were run on 2% agarose gels and photographed using the Kodak 1D Imaging System.

5.10 ASSAY FOR ANTIGEN PRESENTATION

Splenic DC-enriched suspensions were labeled with FITC-H2-K^{b}, APC-CD11c, APC-Cy7-CD8α and PE-CD45RA mAb and sorted on a FACSAria flow cytometer (BD Biosciences). Each subset of FACS-sorted APC was γ-irradiated and used as stimulators of CFSE-labeled 1H3.1 CD4^{+} T cells (50,000 APC : 400,000 T cells / well) in 96 well round-bottom plates. After 5 d, T cells were FACS-assayed for CFSE-dilution. FACS-sorted splenic B6 CD11c^{hi}CD8^{-} DC pulsed with BALB/c IE$\alpha_{52\text{-}68}$ peptide were used as positive controls.

5.11 ELISA

Detection of IL-4, IL-10, IL-12p70, and IFN-γ were performed by ELISA according to manufacturers' instructions (eBiosciences, BioLegend and BD Biosciences).

5.12 NITRITE DETECTION

GIL were cultured at 200,000 cells per well in 96-well round bottom culture plates in complete RPMI media. After 72 h, culture supernatant was collected and analyzed for quantification of nitrite using the Griess Reagent System per manufacturer's instructions (Promega Corporation, Madison, WI).

5.13 STATISTICAL ANALYSIS

GraphPad Prism was used for statistical analyses. Results are expressed as mean ± SD, if one representative experiment is shown, or as mean ± SEM if data is averaged from more than one experiment. Comparison between two groups was performed by Student's t-test. Graft survivals were compared by Kaplan-Meier analysis and the log-rank test. A "*p*" value < 0.05 was considered significant.

6.0 SUMMARY

6.1 CELLULAR THERAPIES IN TRANSPLANTATION

From the initial findings that quiescent DC internalize, process and present apoptotic cell-derived Ag to T cells with regulatory effects on the immune response, cellular therapies have been a promising candidate for treatment of transplant rejection and autoimmune disorders. Our data indicates that DC therapies, like alternative cellular therapies, function as a source of alloAg for presentation by recipient DC via the indirect pathway. We therefore conclude that safer and more practical cellular therapies should be employed in the clinical setting.

6.1.1 Caveats to cellular therapy research

Most research on cellular therapies in transplantation has been conducted using young inbred mice maintained in clean or nearly pathogen-free conditions, which therefore may contain low numbers of memory T cells compared to outbred animals. Comparatively, transplant rejection in humans is mediated by both naïve and memory T cells and as such, the ability of cellular therapies to tolerize not only recipient DC but also other non-professional recipient APC capable of activating anti-donor memory T cells will likely be critical for successful therapy. Therefore, studies in murine models with memory T cells, or better yet, studies in larger animal models, must be performed.

6.1.2 Caveats to clinical implementation of cellular therapies

There are quite varied opinions on the utility of cellular therapies for the clinic[261]. First and foremost, safety is a major point of concern. What if a preparation of cellular therapuetic contained contaminating effector cells? or if a batch of tolerizing agent was ineffective? If administration of a cellular therapy had a deleterious effect, could the adoptively transferred cell be eliminated from the patient?

In reality, it is likely that cellular therapeutics would never be instituted in the clinic as a single therapy, but rather in combination with additional pharmacologic immunosuppression. This may help alleviate some of the risks associated with cellular products, however there are then issues of practicality. Realistically, cellular therapies would have a high cost due to necessary skilled personnel and facility requirements. Reproducibility between research centers may be challenging. It is also unknown how many cells each patient should receive and how often? Can sufficient numbers of cells actually be obtained for clinical use?

Despite these concerns, based on the tremendous need for donor-specific immuno-suppression/tolerance in transplantation, further investigation into this fascinating area of research is warranted.

6.2 PRIMING THE ANTI-DONOR T CELL RESPONSE

From our data, we have developed a model for anti-donor T cell priming following cardiac allograft transplantation (Fig. 38). Donor passenger APC emigrate from the cardiac allograft through the vasculature to recipient spleen, where they present directly or transfer to recipient

APC intact donor MHC:peptide complex for presentation to direct pathway T cells. Donor passenger APC also transfer alloAg that is re-processed by recipient APC into allopeptides for presentation to T cells via the indirect pathway. In return, indirect pathway $CD4^+$ helper T cells provide CD40 stimulation of recipient APC which is required for direct pathway T cell priming and allograft rejection.

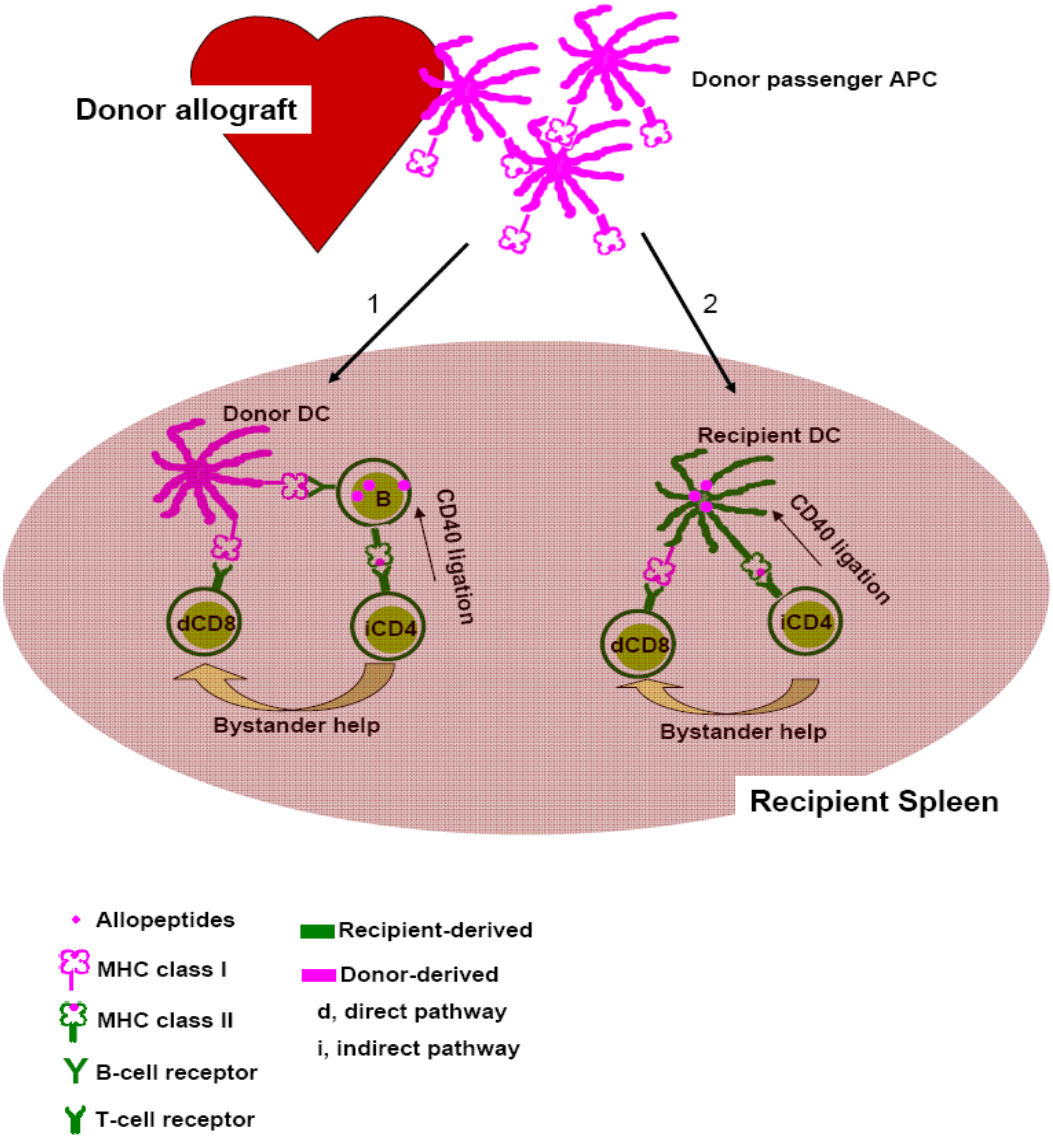

Figure 38. Proposed model for mechanism of direct pathway T cell priming.

6.2.1 Caveats to our proposed model

This work has been performed in naïve mouse models that lack memory T cells. Notably, memory T cells require less co-stimulation than do naïve T cells, and further memory T cells could circulate through the graft. As such, memory T cells may be stimulated by MHC class I or II expressed on the surface of allograft parenchymal or endothelial cells, therefore abrogating the necessity for donor passenger APC.

6.2.2 Future directions

Our data supports that either recipient APC are B cells that can interact with donor passenger APC through MHC – B cell receptor interaction or alternatively, that recipient APC acquire intact alloMHC:peptide complex and present this complex "semi-directly" to direct pathway T cells (Fig. 38). Further investigation into these mechanisms is required.

6.3 INFLAMMATORY DC IN TRANSPLANTATION

We demonstrate the novel finding that inflammatory monocytes/inflammatory DC serve two opposing roles in transplantation, one as an effector cell causing allograft tissue damage, and the other as an inhibitor of the T cell response. This epitomizes the diversity and complexity inherent in the monocyte population, and beckons further investigation. Evidence from tumor-bearing mice provides some direction as to possible inhibitory mechanisms employed by inflammatory

monocytes/inflammatory DC, and this represents an avid area of research in our lab. Further, relationship and functional comparisons between inflammatory DC subsets may reveal additional important roles for these enigmatic cells.

6.4 FINAL STATEMENT

This work provides mechanistic insight into the functionality and efficacy of therapeutic tolerogenic DC vs alternative cellular therapies, into the pathways by which anti-donor T cells are primed into effector cells that mediate allograft rejection, and into the involvement in transplant rejection of a recently described unique population of recipient DC. Overall, the data presented here formulates a strong framework for further mechanistic studies to elucidate the pathways by which the anti-donor response is stimulated, knowledge of which will lead to optimal design and implementation of therapeutics in transplantation

APPENDIX A

ACTIVATED INFLAMMATORY INFILTRATE IN HSV-1-INFECTED CORNEAS WITHOUT HERPES STROMAL KERATITIS

Sherrie J. Divito and Robert L. Hendricks

Invest Ophthalmol Vis Sci. 2008 Apr;49(4):1488-95.

I acknowledge that the Association for Research in Vision and Ophthalmology holds the copyright to this article.

Abstract

Purpose. To investigate herpes stromal keratitis (HSK) immunopathology by studying HSV-1-infected corneas that fail to develop HSK.

Methods. Plaque assay quantified HSV-1 in the tear film of infected mice. FACS analysis enumerated corneal leukocytic infiltrate, and characterized infiltrate phenotypically after staining for activation and regulatory T cell (Treg) markers and for markers of antigen presenting cell (APC) maturation. Treg cells were depleted in vivo using anti-CD25 mAb. Luminex analysis quantified the amount of cytokines and chemokines expressed in corneal tissue homogenate.

Results. Infected corneas without HSK exhibited a pronounced leukocytic infiltrate containing a significantly higher proportion and nearly identical absolute number of activated $CD4^+$ T cells at 15 days post-infection (dpi) when compared to those with HSK. Moreover, the frequency and absolute number of regulatory $CD4^+$ T cells (Tregs) was lower in non-diseased corneas, and Treg depletion did not influence HSK incidence. The frequency of mature, immunogenic DC and the ratio of mature DC to $CD4^+$ T cells were nearly identical in corneas with and without HSK. We observed a reduced population of neutrophils, and reduced expression of neutrophil chemoattractants MIP-1β and KC and the neutrophil attracting cytokine IL-6 in corneas without HSK.

Conclusions. Our findings demonstrate that HSV-1 infected corneas can retain clarity in the presence of a substantial secondary leukocytic infiltrate, that activated $CD4^+$ T cells while necessary are not sufficient for HSK development, that susceptibility to HSK is not determined by Tregs, and that clinical disease correlates with accumulation of a critical mass of neutrophils through chemoattraction.

Introduction

Herpes simplex virus type 1 (HSV-1)-induced stromal keratitis (HSK) is a blinding immunopathologic disease of the cornea characterized by recurrent bouts of destructive inflammation and progressive scarring in the corneal stroma[262]. In mice, HSV-1 infection induces a transient neutrophilic primary infiltrate that dissipates 3 – 4 days post infection (dpi). This primary PMN infiltrate contributes to control of replicating virus, and coincides with the presence of an epithelial lesion[263]. This primary neutrophilic infiltrate appears to occur in response to cytokines and chemokines produced by corneal parenchymal cells and/or cells of the innate immune system, and is independent of T lymphocytes[263-266]. A more chronic secondary leukocytic infiltrate is initiated after viral clearance from the cornea in normal mice, but does not occur in T cell-deficient mice[267-269]. The secondary infiltrate consists of neutrophils, $CD4^+$ T cells, few $CD8^+$ T cells, and antigen presenting cells (APC) consisting of $CD11c^+$ dendritic cells (DC) and $F4/80^+$ macrophages[264,267,270,271]. In most murine models of HSK, the secondary leukocytic infiltration of the cornea is orchestrated by $CD4^+$ T cells.

Activation of naïve $CD4^+$ T cells in different microenvironments can result in differentiation along pathways leading to cells with distinct cytokine profiles. The involvement in HSK of $CD4^+$ T cells expressing the Th1 cytokines IL-2 and IFN-γ has been established in mouse models[272,273]. Extravasation of neutrophils into the infected cornea is facilitated by IFN-γ, apparently through up-regulation of platelet endothelial cell adhesion molecule 1 on local vascular endothelium[274], and is regulated indirectly by IL-2[274,275], presumably through induction of chemotactic factors. $CD4^+$ Th17 T cells have also been implicated in HSK, as IL-17 induces corneal fibroblasts to produce the neutrophil chemoattractant IL-8[276], and IL-6 regulates angiogenesis through induction of vascular endothelial growth factor (VEGF) and neutrophilic

infiltration through induction of chemokines[276-280]. In contrast, HSK severity appears to be ameliorated by $CD4^+$ T cells expressing the Th2 cytokine IL-4[281], and by regulatory $CD4^+$ T cells (Tregs) at least in part through production of IL-10[282], which separately has been shown to mitigate HSK[265,283].

Several chemokines have also been implicated in the secondary leukocytic infiltrate associated with HSK, including MIG (CXCL9), IP-10 (CXCL10), macrophage inflammatory protein (MIP)-1α (CCL3), MIP-1β (CCL4), MIP-2 (CXCL2), macrophage chemotactic protein (MCP)-1 (CCL2), MIP-3α (CCL20), and keratinocyte chemoattractant (KC)[265,271,284-287]. Many of these chemokines are produced by corneal parenchymal cells and by infiltrating inflammatory cells, and the relative contribution of these cellular sources to the chemokine milieu within the infected cornea likely changes as inflammation progresses. The combined effect of cytokine and chemokine production is an inflammatory infiltrate that upon achieving a critical mass initiates neovascularization and destruction of the corneal architecture. However, in most humans who shed virus at the corneal surface and in some mice receiving a low dose HSV-1 corneal infection, HSK fails to develop, suggesting that this cycle of leukocytic infiltration and activation is interrupted at some unknown point prior to the initiation of clinical disease.

Our previous study demonstrated that susceptibility to HSK was not associated with the magnitude of the HSV-specific $CD4^+$ T cell response generated in the draining lymph nodes, or with the level of the delayed type hypersensitivity (DTH) response following HSV-1 corneal infection[288]. However, HSK development was associated with a massive DC infiltration into the infected cornea between 7-14 dpi, which was abrogated by $CD4^+$ T cell depletion. These findings suggest that susceptibility to HSK is determined by the capacity of HSV-specific $CD4^+$ T cells to infiltrate the cornea and induce DC and neutrophil infiltration. We hypothesized that corneas that

fail to develop HSK following HSV-1 infection would lack a critical mass of activated $CD4^+$ T cells. However, this study demonstrates that HSV-1 infected corneas without HSK contained as many activated $CD4^+$ T cells as those with HSK at the time of near maximal HSK severity. Corneas without HSK exhibited significantly fewer neutrophils and DC, and lower levels of known neutrophil and DC chemoattractants, suggesting that interference in the inflammatory process in these corneas occurs following $CD4^+$ T cell activation.

Materials and Methods

Animals

Female BALB/c wild type mice 6 to 8 weeks of age were purchased from The Jackson Laboratory (Bar Harbor, ME). All experimental animal procedures were reviewed and approved by the University of Pittsburgh Institutional Animal Care and Use Committee and adhered to the ARVO Statement for the Use of Animals in Ophthalmic and Vision Research.

Corneal HSV-1 infection

Corneal scarification was accomplished with a 30 gauge needle on mice that were under deep anesthesia induced by intraperitoneal (i.p.) injection of 2.0 mg ketamine hydrochloride and 0.04 mg xylazine (Phoenix Scientific; St. Joseph, MO) in 0.2 ml of HBSS (Biowhittaker; Walkersville, MD). HSV-1 strain RE was grown in Vero cells, and intact virions were isolated on Optiprep gradients according to the manufacturer's instructions (Accurate Chemical & Scientific). Virus was applied directly to the eye at 1×10^3 PFU in 3 μl RPMI (Biowhittaker).

HSK scoring system

Mice were scored for herpes stromal keratitis (HSK) by slit lamp examination on alternate days between 7 and 15 days post-infection (dpi). A standard scale ranging from 1 – 4 based on corneal opacity was used: 1^+ mild corneal haze, 2^+ moderate opacity, 3^+ complete opacity, 4^+ corneal perforation.

Quantification of infectious virus

Corneal surfaces were swabbed with sterile plastic applicators with cotton tips (Fisherbrand) at 2, 4, 6, 8, and 10 dpi, and swabs were placed in 0.5 ml sterile RPMI. Viral load was quantified using a standard plaque assay performed in duplicate. Samples were added in serial dilution to confluent Vero cells, incubated 1 hour at 37^{o}C 5% CO_2, then overlaid with 0.5% methylcellulose. Cultures were incubated 72 hours at 37^{o}C 5% CO_2, then were fixed with 20% formaldehyde, and stained with cresyl violet for 30 min each, prior to rinsing with tap water.

Flow cytometric analysis

Corneas were excised at 15 dpi and incubated in PBS-EDTA at 37^{o}C for 10 minutes, stromas were separated from overlying epithelium and digested in 84 U/cornea collagenase type 1 (Sigma-Aldrich Co., St. Louis, MO) for 2 hours at 37^{o}C, then triturated forming a single cell suspension. Suspensions were filtered through a 40-μm cell strainer cap (BD Labware; Bedford, MA) and washed. Suspensions were incubated with anti-mouse CD16/CD32 (Fcγ III/II receptor; clone 2.4G2; BD PharMingen, San Diego, CA), then stained with various leukocyte surface markers for 30 minutes on ice. The following antibodies were used: PerCP-conjugated anti-CD45 (30-F11), PE-conjugated anti-CD4 (RM4-5), anti-IA/IE (2G9), APC-Cy7-conjugated anti-CD8α (53-6.7), FITC-conjugated anti-CD69 (H1.2F3), anti-CD25 (7D4), anti-CD11c (HL3), APC-conjugated anti-F4/80, biotin-conjugated anti-CD80, pacific blue-conjugated anti-CD8α, Streptavidin-PE (all BD PharMingen); APC-conjugated anti-Gr-1 (RB6-8C5) (CALTAG; Carlsbad, CA) and pacific blue-conjugated anti-CD40 using Zenon Pacific Blue Labeling Kit (Invitrogen). All isotype antibodies were obtained from BD PharMingen. Intracellular staining for regulatory T cells was performed according to standard protocol using Foxp3 staining kit (eBiosciences). Briefly, following surface staining, cells were permeabilized using

Cytofix/Cytoperm solution for 2 hours, then stained with APC-conjugated anti-Foxp3 (FJK16s) (eBiosciences) for 30 min. After staining, cells were fixed with 1% paraformaldehyde (PFA; Electron Microscopy Services) and analyzed on a flow cytometer (FACSAria with FACSDIVA data analysis software; BD Biosciences).

Regulatory T cell depletion

Mice received by i.p. injection 100 μg anti-CD25 mAb (PC61) in 500 μl PBS 3 days prior to infection. Control mice received 100 μg HLA-DR5 in 500 μl PBS, 500 μl PBS alone, or no injection.

Multiplex bead array

Corneas with HSK were assayed individually, while two corneas without HSK were pooled per sample for assay. In both cases the results are reported as the amount of protein per cornea. Corneas obtained at 15 dpi were quartered in sterile 1X PBS then placed in 300 μl PBS + complete protease inhibitor (Complex Mini Protease Inhibitor, Roche Applied Science). Samples were sonicated (Fisher Model 100 Sonic Dismembrator, Fisher Scientific) 4 times for 15 seconds each and the sonicator tip rinsed with 75 μl PBS + protease inhibitor, yielding a final volume of 600 μl/sample. Samples were microcentrifuged twice to remove cellular debris. Bio-Plex assay from BioRad (Hercules, CA) was performed according to manufacturer's instructions or samples were sent for luminex analysis by Millipore (St. Louis, MO). The following cytokines and chemokines were assayed: IL-6, IL-10, KC, MCP-1 (CCL2), and MIP-1β (CCL4).

Statistical analyses

GraphPad Prism software was used for all statistical analyses. Where indicated, *p*-values were calculated using the Student's *t* test when comparing two groups. *p*-values less than 0.05 were considered significant. Results are presented as mean ± SEM.

Results

Corneal viral burden and clearance do not impact HSK development

An infectious dose (1 x 10^3 PFU) of HSV-1 RE produced a 50-60% HSK incidence through 15 dpi. We hypothesized that rapid clearance of replicating HSV-1 from infected corneas might be an important factor in determining HSK susceptibility. To test this, we quantified tear film viral titers using viral plaque assay and retrospectively compared viral clearance from eyes that did or did not develop HSK (Fig. 1). No significant differences were observed in either viral burden or viral clearance kinetics between diseased and non-diseased corneas.

Inflammatory infiltrate in non-diseased corneas

In all corneas that developed HSK, corneal opacity and neovascularization were apparent by 15 dpi (data not shown). At 15 dpi, corneas that developed HSK (HSK score 2.0 ± 0.1) or not (HSK score 0) were excised, and the inflammatory infiltrate was compared by staining cells from dispersed corneas for various leukocyte markers followed by flow cytometric analysis (Fig. 2A). Surprisingly, corneas without HSK exhibited a substantial leukocytic infiltrate, although the magnitude of the infiltrate was reduced relative to corneas with HSK (Fig. 2B). The majority of infiltrating cells in corneas with or without HSK were PMN, which were identified by their large size and high granularity, combined with high expression of Gr-1.

Within non-diseased corneas the total number of $CD4^+$ T cells was reduced approximately 3-fold while the frequency of activated ($CD69^+$) $CD4^+$ T cells was increased by a similar margin (Fig. 3A), resulting in virtually identical numbers of activated $CD4^+$ T cells in corneas with and without HSK (with HSK = 343 ± 7.6; without HSK = 340 ± 6.0) (Fig. 3B). The frequency of activated $CD8\alpha^+$ T cells was also dramatically higher in corneas without HSK (Fig.

3A), resulting in a significantly higher absolute number of activated $CD8\alpha^+$ T cells in corneas without HSK (with HSK = 72 ± 2.4; without HSK = 216 ± 4.5) (Fig. 3B). Thus, corneas with HSK exhibited a lower overall ratio of $CD8\alpha^+$:$CD4^+$ T cells (with HSK 0.16:1, without HSK 0.64:1) and lower ratio of activated $CD8\alpha^+$:activated $CD4^+$ T cells (with HSK 0.22:1, without HSK 0.64:1) (Table 1).

Tregs in infected corneas

$CD4^+$ T cells can be either pro-inflammatory effector T cells (Teff) or anti-inflammatory Tregs; and the two types of $CD4^+$ T cells can be distinguished phenotypically, with Tregs expressing Foxp3 usually in conjunction with CD25. We hypothesized that the large number of activated $CD4^+$ T cells in corneas without HSK would be comprised predominantly of Tregs, while those in corneas with HSK would be comprised mainly of Teff. To test this, cells from corneas with and without HSK were stained for Foxp3. Surprisingly, corneas with HSK contained a higher number of Tregs (Fig. 4) and a higher Treg:Teff ratio (1:2.75) compared to corneas without HSK (1:5.00). We also observed that extracts of corneas with HSK contained a greater amount of IL-10 than did corneas without HSK (Fig. 5), although values within both diseased and non-diseased corneas were low.

To further explore a role for Tregs in HSK susceptibility, mice were depleted of Tregs by systemic treatment with anti-CD25 mAb 3 days before HSV-1 corneal infection, thus depleting Tregs rather than Teff. Additionally, in our hands nearly all $CD4^+$, $CD25^+$ cells in infected corneas co-expressed Foxp3 (Fig. 6A), further insuring specific depletion of Tregs and not Teff. Antibody treatment reduced the frequency of $CD4^+CD25^+$ cells by 95% and of $CD4^+Foxp3^+$ (both $CD25^+$ and $^-$) Tregs in infected corneas by approximately 80% beyond 15 dpi (Fig. 6A),

but did not alter the incidence of HSK, further supporting the notion that susceptibility to HSK is not determined by Tregs. The frequency of $CD4^+$ and $CD8\alpha^+$ T cells in corneas with HSK was significantly increased by anti-CD25 treatment (Fig. 6B). However, infiltration of neutrophils was not significantly altered by Treg depletion (Fig. 6B), and HSK severity was similar in depleted and non-depleted mice (not shown).

Antigen presenting cells in infected corneas

The number of APC was reduced in corneas without HSK; with $F4/80^+$ macrophages reduced 8.90-fold and $CD11c^+$ DC reduced 5.38-fold (Fig. 2). Likewise, the amount of MCP-1 (CCL2), an APC chemoattractant, was also reduced in corneas without HSK compared to corneas with HSK (Fig. 7). Moreover, the ratio of total APC (DC + macrophages) to $CD4^+$ T cells was significantly higher in corneas with HSK than in those without HSK (Table 1); consistent with the notion that a high overall APC:$CD4^+$ ratio might predispose corneas to HSK development.

Susceptibility to HSK could be influenced by qualitative differences in APC, as macrophages and DC can be either immunogenic or tolerogenic depending on their maturation phenotype[8,50]. We compared the maturation phenotype of APC in corneas with and without HSK. A higher frequency of MHC class II positive macrophages and DC were observed in corneas without HSK (Fig. 8); whereas the frequency of macrophages and DC that expressed the co-stimulatory molecules CD80 and CD40 were comparable in corneas with and without HSK. Moreover, the level of expression of MHC class II, CD80, and CD40 was uniformly higher on DC and macrophages in corneas without HSK. Therefore, the majority of APC in corneas that failed to develop HSK exhibited a mature immunogenic phenotype. Furthermore, the ratio of MHC class II positive DC to $CD4^+$ T cells in corneas without HSK (0.25:1) was nearly identical

to that in corneas with HSK (0.27:1) (Table 1), consistent with the similar number of activated $CD4^+$ T cells in corneas with and without HSK.

Neutrophils in infected cornea

Neutrophils are considered to be the proximal mediators of corneal damage in HSK. Accordingly, the greatest reduction in the inflammatory infiltrate in corneas without HSK was observed in the Gr-1^{bright} neutrophil population (9.77-fold reduction) (Fig. 2). This dramatic reduction in neutrophil infiltration was accompanied by reduced levels of the neutrophil chemoattractants KC and MIP-1β (CCL4) and the neutrophil attracting cytokine IL - 6 in corneas that failed to develop HSK (Fig. 9).

Discussion

HSK is a potentially blinding immunopathologic response to HSV-1 corneal infection. The key to developing effective prophylaxis is to define differences in the immune response that results in protection in some mice and immunopathology in others. Scientists have been dissuaded from such studies because the immune response in lymphoid organs declines prior to HSK onset so that at the peak of the immune response one cannot predict which mice will or will not develop HSK. Moreover, the HSV-specific T cell response in the draining lymph nodes and the HSV-specific DTH response in the skin following HSV-1 corneal infection are uniform among infected mice, despite models providing 50% HSK incidence[288]. These studies suggest that HSK susceptibility is not determined at the inductive phase of the $CD4^+$ T cell response in the lymphoid organs, but rather at the effector phase of the response within the infected cornea.

Our current studies demonstrate for the first time that corneas that fail to develop HSK do nonetheless develop an inflammatory infiltrate that is significant and quantifiable using current sensitive techniques. These findings establish the feasibility of studying differences in the inflammatory milieu in corneas that do or do not develop HSK. A key finding of this study is that the number of activated $CD4^+$ T cells as assessed by expression of the CD69 recent activation marker is identical in corneas with and without HSK at the time of nearly maximal HSK severity, indicating that the mere presence of activated $CD4^+$ T cells is not causal for disease and that accumulation of activated $CD4^+$ T cells is independent of accumulation of immunogenic APC. Previous studies demonstrated a high Treg frequency in corneas with HSK, and demonstrated that these cells attenuated the severity of HSK at least in part through the production of IL-10[282], leading us to consider that the activated $CD4^+$ T cells in corneas that failed to develop HSK might contain a higher frequency of $Foxp3^+$ Tregs. However, our studies

demonstrate that both the absolute number of Tregs and the ratio of Tregs:Teff is actually higher in corneas with HSK. Moreover, an 80% reduction of the Treg population in the cornea did not influence HSK incidence. Although the remaining 20% of Tregs could theoretically be capable of preventing HSK onset, an 80% reduction in Tregs did have an effect, as depleted corneas that developed HSK had an increased number of $CD4^+$ T cells, suggesting a role for Tregs in controlling $CD4^+$ T cell expansion or corneal infiltration. Thus, Tregs might regulate the severity of HSK in agreement with previous findings[282], but they do not appear to be a determining factor for susceptibility to HSK in our model.

We observed higher levels of IL-10 in corneas with HSK than in those without HSK. While many cells produce IL-10, our finding would be consistent with the known capacity of Th1 cells (that mediate HSK) to produce IL-10 in an apparent attempt to dampen inflammatory tissue damage (reviewed in ref [289]). While the low levels of IL-10 observed in corneas with HSK were apparently below the threshold required to prevent inflammatory damage to the cornea, the even lower level in corneas without HSK demonstrates that IL-10 is not a critical factor in determining susceptibility to HSK.

An interesting characteristic of HSK is the preponderance of $CD4^+$ over $CD8\alpha^+$ T cells in the corneal infiltrate[290,291]. Consistent with the possibility that a high $CD4^+$:$CD8\alpha^+$ T cell ratio favors HSK development, we observed that corneas that failed to develop HSK exhibited significantly higher numbers of activated $CD8\alpha^+$ T cells and a significantly lower $CD4^+$:$CD8\alpha^+$ T cell ratio. Although the small numbers of $CD8\alpha^+$ T cells within HSV-1 infected corneas calls to question any significant role in determining disease onset, our data are consistent with the notion that a high ratio of $CD8\alpha^+$:$CD4^+$ T cells might limit HSK susceptibility.

We next entertained the possibility that differences in corneal APC determined HSK susceptibility. Indeed, the absolute number of macrophages and DC and the ratio of DC to $CD4^+$ T cells were significantly higher in corneas with HSK. However, since our previous study demonstrated that DC maturation within the infected cornea was important for HSK development[288], we characterized the corneal APC for maturation marker expression. Surprisingly, the frequency of mature macrophages and DC as indicated by expression of CD80 and CD40 was similar in corneas with and without HSK, and the level of expression of these molecules as indicated by the mean fluorescence intensity was actually higher on APC from corneas without HSK. Moreover, the frequency of macrophages and DC that expressed MHC class II, and the level of MHC class II expression per cell were significantly higher in corneas without HSK, while the ratio of MHC class II positive DC to $CD4^+$ T cells was nearly identical in corneas with and without HSK. We conclude from these observations that neither a lack of APC availability nor the APC stimulatory capacity is a likely explanation for failure of HSK development.

HSK corneal damage results from a second wave of infiltrating neutrophils that occurs after replicating virus is eliminated from the cornea[264,271]. Neutrophils release matrix metalloproteinases (MMP) that break down the extracellular matrix of the corneal stroma and enhance neovascularization through production of MMP and VEGF[292-296]. The most obvious difference in the inflammatory infiltrate in corneas with and without HSK was the dramatically (~10-fold) reduced neutrophil population in corneas without HSK. This reduced neutrophil infiltration was associated with a significant reduction in expression of the neutrophil chemoattractants MIP-1β and KC and the neutrophil attracting cytokine IL-6. Neutrophils produce chemoattractants when exposed to IL-6, and neutrophils are necessary for HSV-1

clearance from cornea. Further, IL-6 deficient mice eliminate HSV-1 from the cornea with normal kinetics and fail to develop HSK[280]. The combined results of these studies suggest that IL-6 is required for the second wave of neutrophil infiltration into the cornea that is associated with immunopathology, but is not required for the first wave of neutrophils into the cornea that provides protection from replicating virus.

Importantly, our work highlights the study of HSV-1 infected non-diseased corneas as a novel approach to elucidating HSK pathogenesis. Our findings support IL-6 as an important factor determining HSK susceptibility through induction of neutrophil chemoattraction into the cornea and also point to a possible local inhibitory effect of $CD8\alpha^+$ T cells within infected corneas on HSK progression.

Table 1. Ratios of T cell subsets and APC within HSV-infected corneas with and without HSK.

	With HSK	Without HSK
$CD8\alpha^+$:$CD4^+$	0.16:1	0.64:1
$CD69^+CD8\alpha^+$:$CD69^+CD4^+$	0.22:1	0.65:1
APC^*:$CD4^+$	2.13:1	0.87:1
MHC class II^+CD11c^+:$CD4^+$	0.27:1	0.25:1

*APC equals the average number of $CD11c^+$ plus $F4/80^+$ cells.

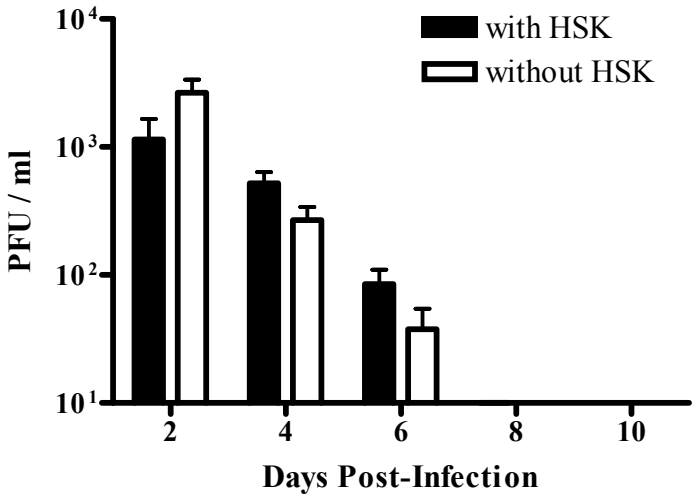

Fig. 1. Viral burden and clearance in corneal tear films were equivalent between HSV-infected corneas with and without HSK. Viral load and clearance from corneal tear films were assessed by standard plaque assay of eye swabs taken 2, 4, 6, 8 and 10 dpi. Data represents two independent experiments with at least 14 corneal samples per group.

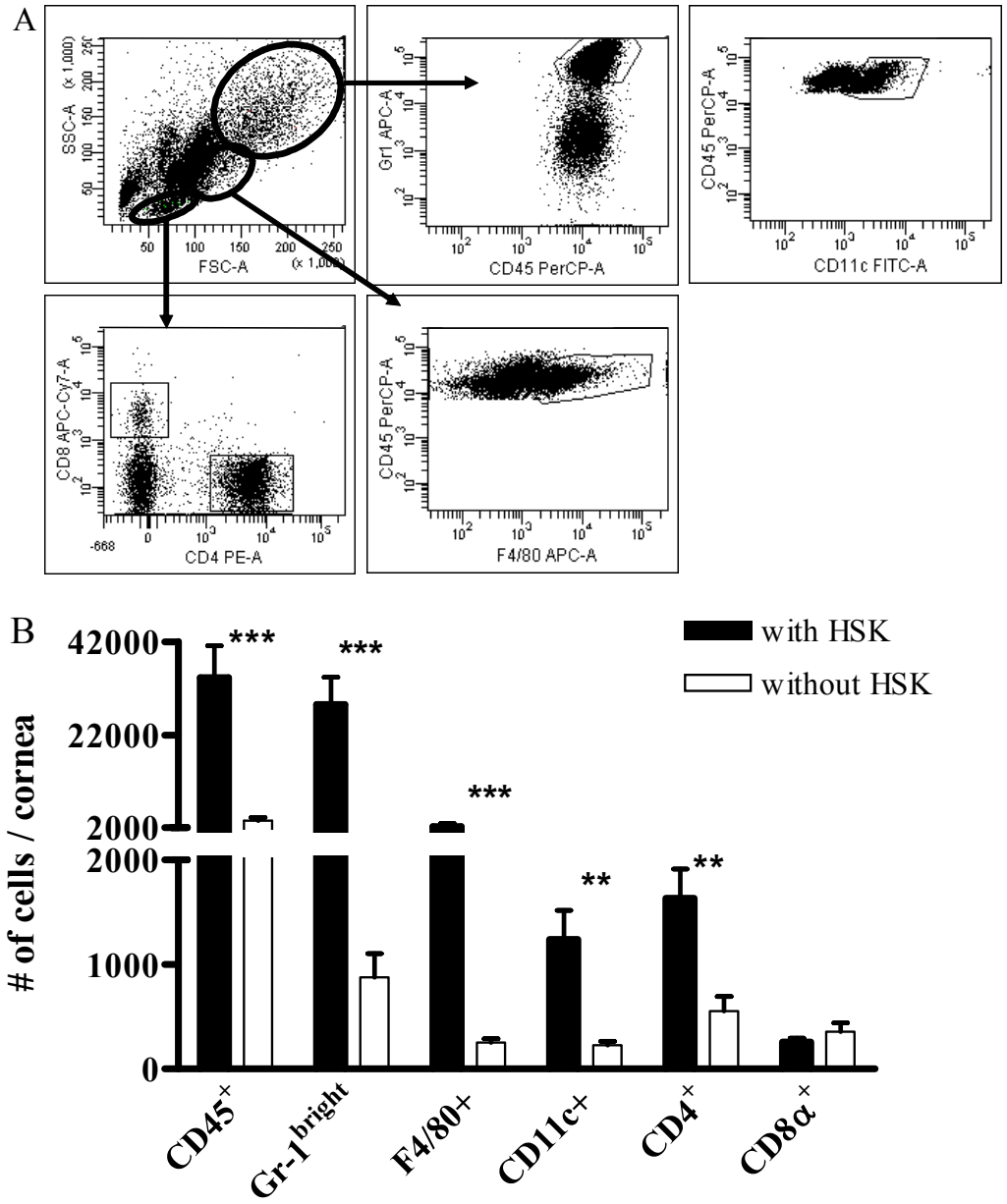

Fig. 2. Inflammatory cells infiltrate HSV-infected corneas without HSK but at reduced frequency compared to corneas with HSK. HSV-infected corneas with and without HSK at 15 dpi were disaggregated into single cell suspensions and stained with anti-CD45, CD4, CD8α, CD11c, F4/80, and Gr-1 mAb. Cells were analyzed by flow cytometry. (A) Distinct live cell populations

were identified based on FSC v. SSC, from which Gr-1^{bright} (PMNs), CD11c^{+} dendritic cells, F4/80^{+} macrophages, and CD4^{+} and CD8α^{+} T cells could be gated. Isotype controls were used to aid gating (data not shown). (B) The total number of infiltrating cells per cornea is shown. Data represent the average of at least 8 corneas per group from two or more independent experiments. ** $p < .01$; *** $p < .001$.

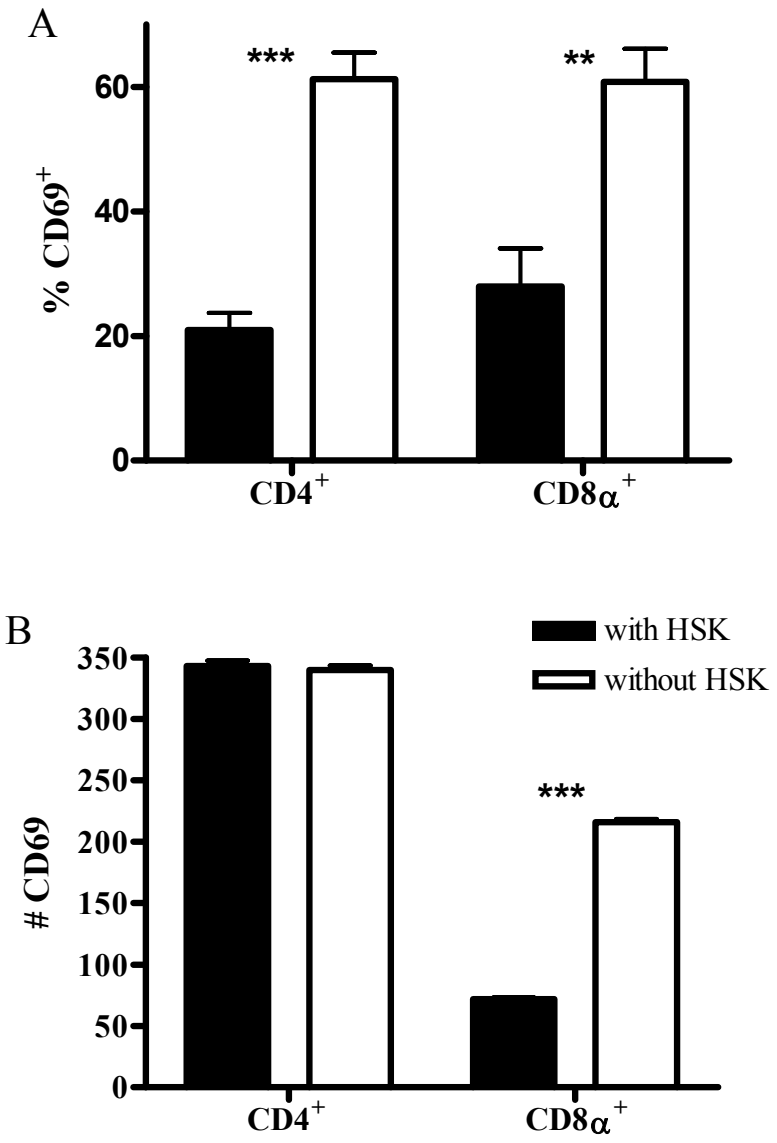

Fig. 3. T cells in HSV-infected corneas without HSK are activated. Single cell suspensions of HSV-infected corneas with and without HSK at 15 dpi were stained with anti-CD45, CD4, CD8α, and CD69 mAb. Flow cytometry was used to analyze the percent (A) and number (B) of the total $CD4^+$ and $CD8\alpha^+$ T cell populations that were $CD69^+$. Data are representative of two independent experiments with at least 7 mice per group. ** $p < .01$; *** $p < .001$.

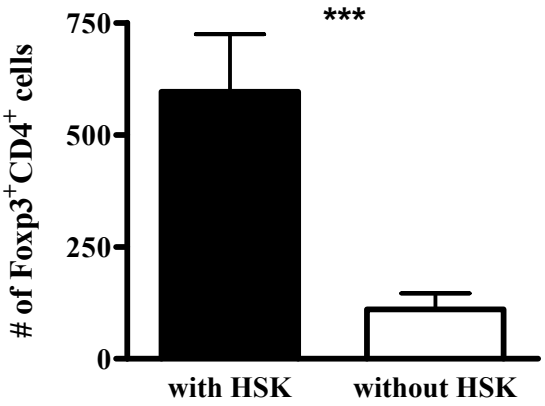

Fig. 4. Few $CD4^+$ T cells in HSV-infected non-diseased corneas are $Foxp3^+$ Tregs. Single cell suspensions of HSV-infected corneas with and without HSK at 15 dpi were stained with anti-CD45, CD4, and Foxp3 mAb. Flow cytometry was used to determine the total number of $CD4^+$ T cells per cornea, and to analyze the percent of the total $CD4^+$ T cell population that was $Foxp3^+$. Data are presented as the absolute number of $CD4^+Foxp3^+$ T cells per cornea and are representative of two independent experiments with at least 7 mice per group. *** $p < .001$.

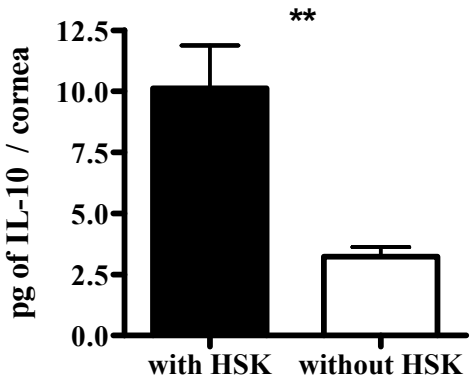

Fig. 5. Resistance to HSK is not associated with elevated levels of the inhibitory cytokine IL-10. HSV-infected corneas with and without HSK at 15 dpi were dissected and sonicated in PBS + protease inhibitor yielding a final volume of 1 diseased cornea or 2 non-diseased corneas per 600 μl. Multiplex bead array for IL-10 expression was performed on this tissue extract. Data are representative of 2 independent experiments with n values of 6 corneas with HSK and 6 samples (2 corneas pooled per sample) of corneas without HSK. ** $p < .01$.

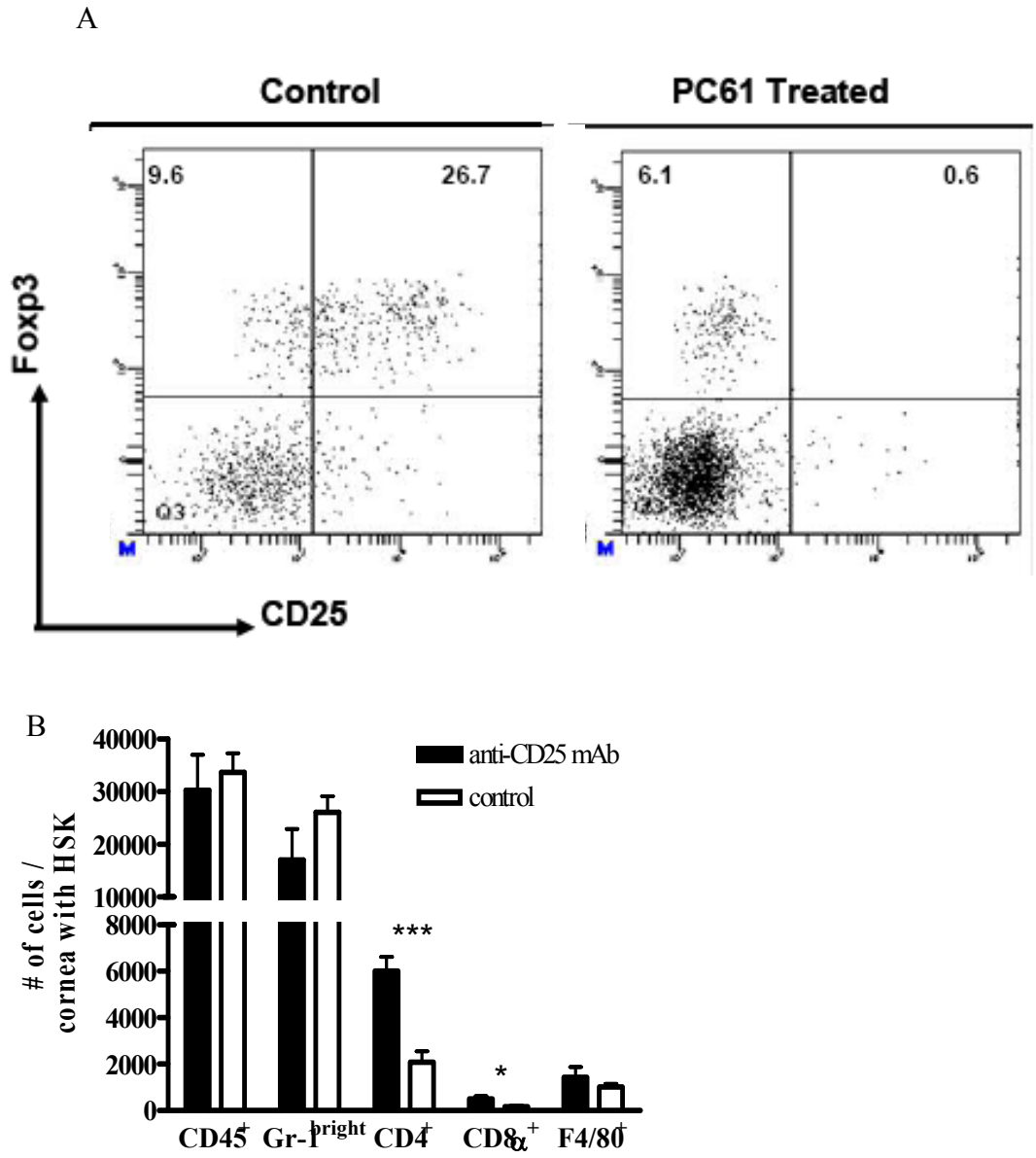

Fig. 6. Depletion of $CD4^+CD25^+$ Tregs in HSV-infected corneas affects T cell numbers in corneas but not HSK development. Mice were administered 100 μg anti-CD25 mAb (clone PC61) or anti-HLA-DR5 (control mAb) in 500 μl PBS by i.p. injection 3 days prior to infection. (A) FACS dot plots comparing depleted corneal Treg infiltrate to a non-depleted control cornea. (B) At 15 dpi, single cell suspensions of corneas that had developed HSK from both CD25 depleted and control mice were stained with anti-CD45, CD4, CD8α, Gr-1, and F4/80 mAb and

analyzed by flow cytometry to enumerate the total number of cells per cornea. Data are representative of two independent experiments with n of 14 depleted mice and 15 control mice. * $p < .05$; *** $p < .001$.

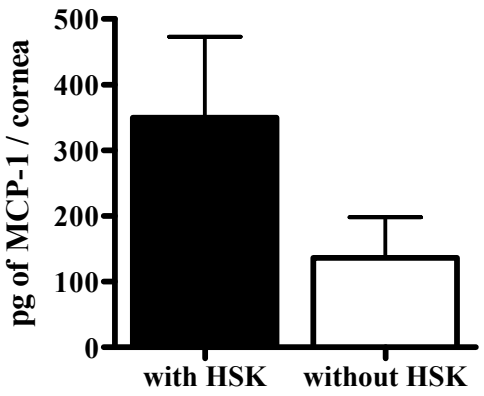

Fig. 7. HSV-infected non-diseased corneas have reduced expression of the APC and lymphocyte chemoattractant MCP-1. HSV-infected corneas with and without HSK at 15 dpi were dissected and sonicated in preparation for multiplex bead array analysis for expression of the chemokine MCP-1 (CCL2) in corneal tissue extract. Data are representative of 2 independent experiments with n values of 6 corneas with HSK and 6 samples (2 pooled corneas per sample) of corneas without HSK.

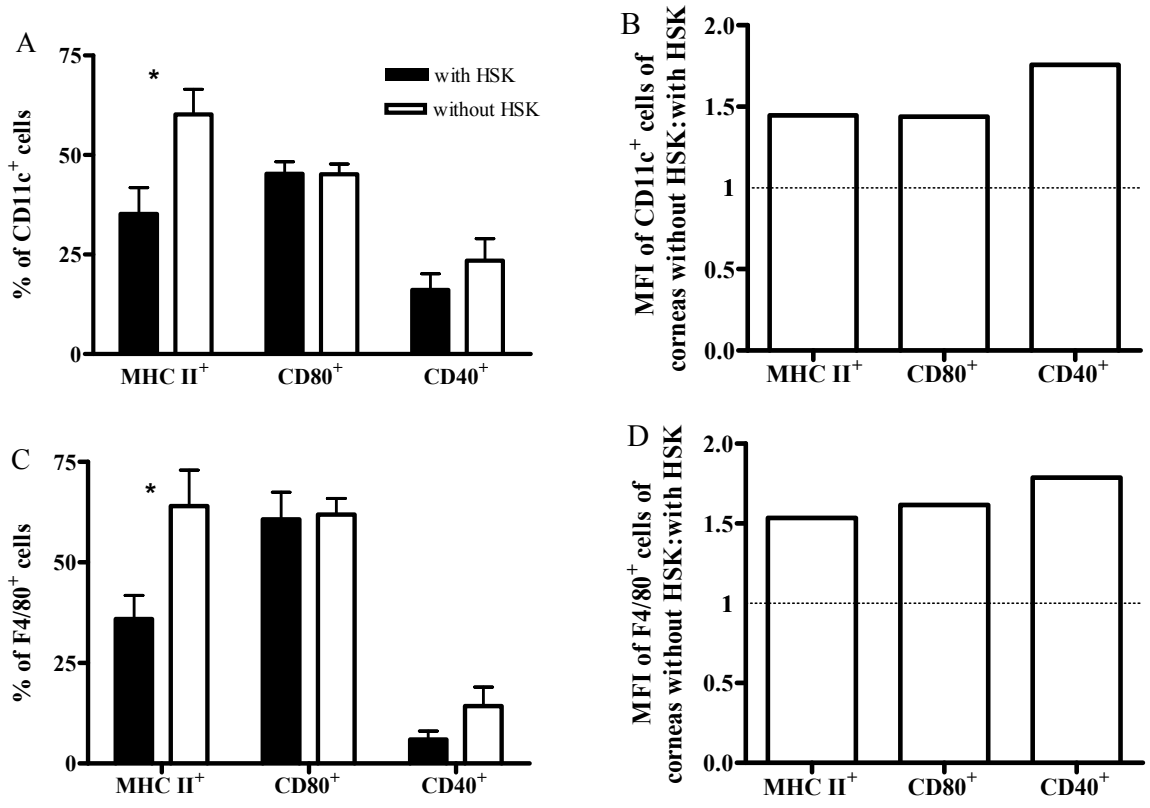

Fig. 8. $CD11c^+$ dendritic cells and $F4/80^+$ macrophages infiltrating HSV-infected non-diseased corneas are mature rather than tolerogenic. APC infiltrate was assessed at 15 dpi in HSV-infected corneas with and without HSK by flow cytometry after staining with anti-CD45, CD11c, F4/80, CD8α, MHC class II (IA/IE), CD80, and CD40 mAb, for (A and C) the frequency of APC per cornea expressing MHC class II and co-stimulatory molecules and (B and D) the amount of surface expression of MHC class II, CD80 and CD40, presented as the ratio of mean fluorescent intensity of corneas without HSK to corneas with HSK. (A and B, $CD11c^+$ cells; C and D, $F4/80^+$ cells). Data represent the average of values from two independent experiments with n of at least 7 corneas per group. * $p < .05$.

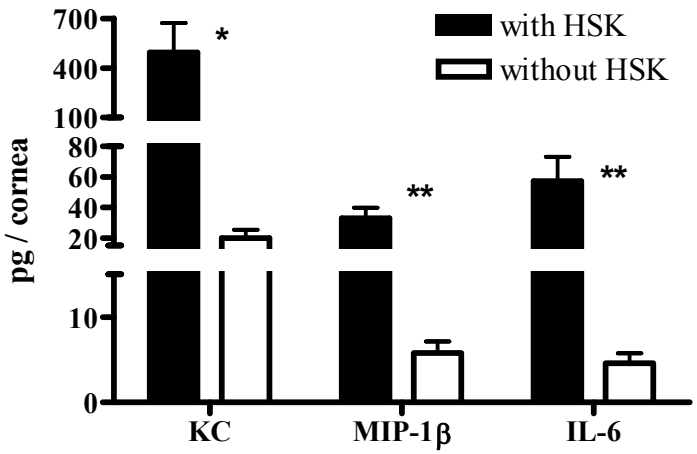

Fig. 9. HSV-infected corneas without HSK have significantly reduced neutrophil chemoattractant expression. HSV-infected corneas with and without HSK at 15 dpi were dissected and sonicated for multiplex bead array analysis of corneal tissue extract. Results for corneas without HSK were halved to estimate the amount of protein per individual cornea. Representative data from one of two independent experiments is presented with n values of 6 corneas with and 6 samples (2 pooled corneas per sample) of corneas without HSK. * $p < .05$; ** $p < .01$.

APPENDIX B

A NOVEL P40-INDEPENDENT FUNCTION OF IL-12P35 IS REQUIRED FOR PROGRESSION AND MAINTENANCE OF HERPES STROMAL KERATITIS.

Gregory M. Frank*, Sherrie J. Divito*, Dawn Maker, Min Xu, and Robert L. Hendricks

* These authors contributed equally to this work.

Abstract

Purpose: Interleukin (IL)-12p40 can couple with IL-12p35 or p19 chains to form the molecules IL-12p70 and IL-23, respectively that promote T_H1 cytokine responses. IL-12p35 can bind to EBI3 to form an anti-inflammatory molecule IL-p35, but a proinflammatory function of IL-12p35 independent of IL-12p40 has not been described. Here we demonstrate such a function in a mouse model of herpes stromal keratitis (HSK), a $CD4^+$ T_H1 cell dependent corneal inflammation.

Methods: Corneas of wild type (WT), IL-12p40$^{-/-}$, IL-12p35$^{-/-}$, and IL-12p35$^{-/-}$p40$^{-/-}$ (double knockout) mice were infected with the RE strain of HSV-1, and HSK was monitored based on corneal opacity, neovascularization, leukocytic infiltrate, and cytokine/chemokine levels.

Results: All mouse strains developed moderate HSK by 11 days post infection (dpi). However, from 11-21 dpi HSK progressed in WT and IL-12p40$^{-/-}$ mice, but regressed in IL-12p35$^{-/-}$, and IL-12p35$^{-/-}$p40$^{-/-}$ mice. HSK regression was characterized by reductions in neutrophils and CD4^{+} T cells and attenuation of blood vessels, which was associated with reduced levels of the chemokines KC (CXCL3), Mip-2 (CXCL2), and MCP-1 (CCL2) and the angiogenic factor vascular endothelial growth factor (VEGF).

Conclusion: HSK development does not require IL-12p40 and is thus independent of IL-12p70 and IL-23. However, late HSK progression does require a previously unrecognized IL-12p40-independent, proinflammatory function of IL-12p35.

Introduction

The IL-12 cytokine family, consisting of the heterodimers IL-12, IL-23, IL-27, and IL-35, has received increased attention due to its diverse and complex functions in immunity. IL-12 consists of a p40 and a p35 subunit[297] and stimulates the differentiation and activation of naïve $CD4^+$ T cells toward a T_H1 phenotype, promoting IFN-γ production[298]. The role of IL-12 in disease has been confounded by the discovery of IL-23, which consists of the same p40 subunit coupled to a unique p19 subunit[299]. IL-23 promotes both proliferation of effector/memory T_H1 cells and also the maintenance of T_H17 cells whose signature cytokine is IL-17[300]. Interestingly, homodimerization of p40 yields a unique molecule capable of anti-inflammatory function through blockade of the IL-12Rβ1[301,302] but also of pro-inflammatory function as a chemoattractant for DC and macrophages[303,304]. Complicating matters further, p35 can also interact with a second binding partner, Esptein-Barr virus-induced gene-3 (EBI3), forming the inhibitory cytokine IL-35[305,306]. IL-35 promotes the proliferation of and IL-10 production by $CD4^+CD25^+$ $FoxP3^+$ natural Tregs, inhibits proliferation of $CD4^+$ $CD25^-$ effector cells, and inhibits differentiation of T_H17 cells. Thus, IL-35 is considered to be an anti-inflammatory cytokine. The final member of the family, IL-27 consists of EBI3 and p28 (IL-30) and enhances T_H1 polarization of naïve $CD4^+$ T cells[307].

Herpes stromal keratitis (HSK) is a potentially blinding HSV-1 induced immunopathologic disease of the cornea. Previous work with athymic, SCID, and T cell depleted mice demonstrated that $CD4^+$ T cells are essential for HSK initiation and progression[267,268,270,308]. $CD4^+$ T cells infiltrating diseased corneas produce the T_H1 cytokine IFN-γ that regulates HSK[273,274]. As is often the case, this predominantly T_H1 response is associated with concurrent production of the anti-inflammatory molecule IL-10[309,310]. The latter counteracts the

proinflammatory effects of T_H1 cytokines, and its over-expression in the cornea can ameliorate HSK[311]. The T_H2 cytokine IL-4 is either not detected in corneas with HSK or is detected during the late recovery stage[290,309]. The T_H17 cytokine IL-17 has been implicated in HSK in mice and humans, and was shown to induce corneal fibroblast production of chemokines that are important regulators of HSK[276,312].

The role of the primary T_H1 driving cytokine IL-12 in HSK has been investigated previously with conflicting results. IL-12p40 mRNA and protein increases in response to HSV-1 corneal infection[313] and the protein is released by inflammatory cells rather than by infected epithelial cells[314]. However, during the period of HSK development (7-22 dpi) IL-12p40 mRNA levels decrease in the cornea, and to our knowledge IL-12p70 protein levels have not been measured. Transgenic expression of IL-12p35/p40 fusion protein under the glial fibrillary acidic protein promoter (GFAP, expressed by nervous tissue) following ocular infection with the highly neurovirulent HSV-1 strain McKrae resulted in reduced viral titers in eyes and trigeminal ganglia and increased survival in mice[315]. However, another study in which the corneas of IL-12p35$^{-/-}$ and IL-12p40$^{-/-}$ mice were infected with HSV-1 McKrae found no difference in corneal viral load but reduced HSK severity among IL-12p35$^{-/-}$ mice and no HSK among IL-12p40$^{-/-}$ mice, that had survived lethal infection at 28 dpi[316]. The use of the highly neurovirulent McKrae strain of HSV-1, coupled with the study of HSK at a single time point only in animals that had survived lethal infection limits the translation of these results to human infection.

IL-23 has also recently been studied in the context of HSK. Mice deficient in p19 developed more severe lesions with higher incidence than their WT counterparts[317]. This study concluded that the lack of IL-23 resulted in a drastically increased IL-12 driven T_H1 $CD4^+$ T cell response, though no direct evidence implicating IL-12 in the enhanced HSK was provided.

Armed with recent advances in the study of the IL-12 cytokine family, we set out to elucidate the role of these cytokines in HSK using mice that are deficient in IL-12p35, IL-12p40, or double knockouts deficient in both p35 and p40 subunits. Mice received corneal infections with the RE strain of HSV-1 that does not kill Balb/c mice, but the infectious dose employed in these studies induced epithelial corneal lesions and latent infections in the trigeminal ganglion of 100% of mice, and HSK in at least 80% of mice. Our results show that neither IL-12 nor IL-23 is necessary for HSK development, but HSK progression and maintenance requires an IL-12p40-independent function of IL-12p35 that to our knowledge has not been previously recognized.

Materials and Methods

Animals

Female wild-type (WT), IL-12p35$^{-/-}$, and IL-12p40$^{-/-}$ BALB/c mice 6 to 8 weeks of age were purchased from The Jackson Laboratory (Bar Harbor, ME). The IL-12p35$^{-/-}$ and IL-12p40$^{-/-}$mice were bred through 4 generations to produce IL-12p35$^{-/-}$p40$^{-/-}$double knockout mice. IL-12p35 and IL-12p40 genes were individually genotyped to confirm knockout status using the following primers: IL-12p35 (forward 5'-CTGAATGAACTGCAGGACGA-3', reverse. 5'-ATACTTTCTCGGCAGGAGCA-3', expected size 172 base pairs) and IL-12p40 (forward 5'-CTTGGGTGGAGAGGCTATTC-3', reverse 5'-AGGTGAGATGACAGGAGATC-3', expected size 280 base pairs). All experimental animal procedures were reviewed and approved by the University of Pittsburgh Institutional Animal Care and Use Committee and adhered to the ARVO Statement for the Use of Animals in Ophthalmic and Vision Research.

Corneal HSV-1 infection

Mouse corneas were scarified using a 30 gauge needle under deep anesthesia induced by intraperitoneal (i.p.) injection of 2.0 mg ketamine hydrochloride and 0.04 mg xylazine (Phoenix Scientific, St. Joseph, MO) in 0.2 ml of HBSS (Mediatech, Inc.; Herndon, VA). Intact virions from HSV-1 strain RE grown in Vero cells were isolated on Optiprep gradients according to the manufacturer's instructions (Accurate Chemical & Scientific; Westbury, NY) and titrated as plaque forming units (pfu) on Vero cell monolayers using a standard viral plaque assay as previously described[318]. HSV-1 RE was applied to the scarified corneas in 3 μl RPMI (Lonza, Walkersville, MD) at a dose predetermined to induce 80% HSK incidence. With different viral preparations this dose ranged from $1x10^3$ to $1x10^4$ PFU (determined by a standard viral plaque

assay). We advocate using the lowest infectious dose that induces a consistently high level of corneal disease because HSK becomes less $CD4^+$ T cell-dependent at higher doses[319].

HSK scoring system

Mice were monitored for HSK on alternate days between 7 and 21 days post-infection (dpi) by slit lamp examination. A standard scale ranging from 1 – 4 based on corneal opacity was used: 1^+ mild corneal haze, 2^+ moderate opacity, 3^+ complete opacity, 4^+ corneal perforation. Disease incidence was defined as HSK score greater or equal to 2 by 15 dpi. The extent of neovascularization and peri-ocular skin disease were also recorded.

Flow cytometric analysis

Harvested corneas were incubated in PBS-EDTA at 37°C for 10 minutes then separated from overlying epithelium and digested in collagenase type 1 (Sigma-Aldrich Co., St. Louis, MO, 84U/cornea) for 2 hours at 37°C. Cells were dispersed by trituration and suspensions were filtered through 40-μm cell strainer cap (BD Labware; Bedford, MA). Suspensions were incubated with anti-mouse CD16/CD32 (Fcγ III/II receptor; clone 2.4G2; BD PharMingen, San Diego, CA), then stained with various leukocyte surface markers for 30 minutes on ice. The following markers were used: PerCP-conjugated anti-CD45 (30-F11), Pe-conjugated anti-CD4 (RM4-5), APC-Cy7-conjugated anti-CD8α (53-6.7), FITC-conjugated anti-CD69 (H1.2F3), and anti-CD25 (7D4) (all BD PharMingen), and APC-conjugated anti-Gr-1 (RB6-8C5) (Caltag; Carlsbad, CA). All isotype antibodies were obtained from BD PharMingen. Intracellular staining for Foxp3 (FJK16s) was performed following permeabilization with Cytofix/Cytoperm solution (eBiosciences, San Diego, CA) for 2 hours. After staining, cells were fixed with 1%

paraformaldehyde (PFA; Electron Microscopy Services, Chicago, IL) and analyzed on a flow cytometer (FACSAria with FACSDIVA data analysis software; BD Biosciences).

Regulatory T cell depletion

Mice received a single i.p. injection 100 μg anti-CD25 mAb (clone PC61) or control mAb (HLA-DR5) in 500 μl 1X PBS, or received PBS alone 3 days prior to infection.

Cytokine/chemokine analysis by multiplex bead array

Individual corneas were excised at 13 or 17 dpi, quartered in sterile PBS, and pieces were transferred to tubes containing 300 μl PBS + complete protease inhibitor (Complex Mini Protease Inhibitor, Roche Applied Science, Indianapolis, IN) and sonicated (Fisher Model 100 Sonic Dismembrator, Fisher Scientific, Pittsburgh, PA) 4 times for 15 seconds each. The sonicator tip was rinsed with 75 μl PBS + protease inhibitor, yielding a final volume of 600 μl/sample. To remove cellular debris, samples were microcentrifuged twice. Bio-Plex assay (BioRad, Hercules, CA) was performed according to manufacturer's instructions or samples were sent for luminex analysis by Millipore (St. Louis, MO). The following cytokines and chemokines were assayed: IL-6, KC, MCP-1, MIP-2, and RANTES.

Statistical analyses

GraphPad Prism software was used for all statistical analyses. Where indicated, *p*-values were calculated using the Student's t test when comparing two groups. *p*-values less than 0.05 were considered significant. Results are presented as mean ± SEM.

Results

Herpes Stromal Keratitis

The corneas of IL-12p35$^{-/-}$, IL-12p40$^{-/-}$, IL-12p35$^{-/-}$p40$^{-/-}$ (double knockout), and WT mice were infected with HSV-1. All four strains of mice developed moderate to severe HSK marked by increasing corneal opacity and peripheral neovascularization by 15 dpi (Fig. 1). HSK severity progressed steadily through 21 dpi in both WT and IL-12p40$^{-/-}$ mice with complete opacity, expanded neovascularization encroaching from the periphery into the central cornea, and corneal edema. In contrast, HSK severity began to regress by 15 dpi and 11 dpi in IL-12p35$^{-/-}$ mice and IL-12p35$^{-/-}$p40$^{-/-}$ mice, respectively. Disease regression in both groups of IL-12p35 deficient mice was marked by rapidly decreased peripheral opacity with thinning of peripheral vasculature and a more gradual decrease in central opacity.

Corneal Inflammatory Infiltrate

Early in HSK development (13 dpi) the infected corneas of WT, IL-12p35$^{-/-}$, IL-12p40$^{-/-}$, and IL-12p35$^{-/-}$p40$^{-/-}$ mice showed comparable infiltrates of CD4^{+} T cells and Gr1^{bright} neutrophils (Fig. 2A), which comprised the majority of the bone marrow-derived CD45^{+} cells in the cornea (data not shown). At 17 dpi, IL-12p35$^{-/-}$p40$^{-/-}$ mice exhibited a significant reduction in neutrophilic infiltrate and a reduction in the mean number of CD4^{+} T cells in the cornea that did not achieve statistical significance (Fig. 2B). The composition of the corneal infiltrate in the p35$^{-/-}$ and p40$^{-/-}$ mice at 17 dpi was not significantly different than that of WT mice. At the peak of HSK severity (21 dpi), both IL-12p35$^{-/-}$ and IL-12p35$^{-/-}$p40$^{-/-}$ mice showed significantly reduced numbers of CD4^{+} T cells and neutrophils within their corneal infiltrates relative to WT mice (Fig. 2C). In both IL-12p35$^{-/-}$ and IL-12p35$^{-/-}$p40$^{-/-}$ mice reduction in clinical HSK severity preceded changes

in the composition of the inflammatory infiltrate in the cornea by approximately 2 days. The p40$^{-/-}$ mice had a significantly higher CD4$^+$ T cell and neutrophilic corneal infiltrate than WT mice at 21 dpi, though this did not translate into a higher clinical HSK score (Fig. 1).

We hypothesized that the HSK regression would be associated with an increased frequency of CD4$^+$ CD25$^+$ FoxP3$^+$ Tregs in the corneas of p35 deficient mice. In fact, the CD4$^+$ T cell population in the corneas of IL-12p35$^{-/-}$ mice did show an increased frequency of CD25$^+$ FoxP3$^+$ cells during HSK regression at17 dpi (Fig. 3). However, an increased frequency of Tregs was not observed in the IL-12p35$^{-/-}$p40$^{-/-}$ mice despite more rapid HSK regression (Fig. 3).

nTregs do not account for HSK regression in IL-12p35$^{-/-}$ mice

To determine if the increased frequency of CD4$^+$ CD25$^+$ FoxP3$^+$ cells in infected corneas of 12p35$^{-/-}$ mice was responsible for HSK regression, we determined if in vivo depletion of CD25$^+$ cells prior to HSV-1 corneal infection would alter the course of HSK in these mice. A single treatment with 100 μg of anti-CD25 mAb or control mAb 3 days before HSV-1 corneal infection, effectively depleted CD25$^+$ Foxp3$^+$ cells from corneas through 21 dpi (Fig. 4A). However, Treg depletion did not significantly impact the course of HSK in IL-12p35$^{-/-}$ mice, with both depleted and non-depleted mice exhibiting HSK regression (Fig. 4B). As established in previous studies[282,320], Treg depletion did significantly increase the leukocytic infiltrate in infected corneas of WT mice (Fig. 4C), but did not significantly influence the size of the infiltrate in corneas of IL-12p35$^{-/-}$ mice (Fig. 4D). Thus, while CD25$^+$ Tregs do modulate HSK severity in WT mice, they do not account for HSK regression in mice lacking IL-12p35. However, it is noteworthy that there remained in the corneas of the anti-CD25 mAb-treated IL-12p35$^{-/-}$ mice a substantial population of CD4$^+$ FoxP3$^+$ cells that did not express CD25 (Fig. 4A).

These cells did not stain with anti-rat Ig, suggesting that CD25 was not simply masked by the rat anti-mouse CD25 mAb used for depletion. A contribution of these FoxP3^{+} cells to HSK regression cannot be ruled out.

IL-12p35 influences the cytokine and chemokine profile in infected corneas

To determine if HSK progression and regression was associated with different chemokine and cytokine profiles, corneas of WT, IL-12p40$^{-/-}$, IL-12p35$^{-/-}$, and IL-12p35$^{-/-}$p40$^{-/-}$ mice were excised at 17 dpi, and cytokine and chemokine proteins were quantified using a multiplex bead array assay (Fig. 5). During HSK regression (17 dpi) the corneas of both IL-12p35$^{-/-}$ and IL-12p35$^{-/-}$p40$^{-/-}$ mice exhibited significantly reduced expression of the neutrophil chemoattractants KC/CXCL3 (Fig. 5A) and MIP-2/CXCL2 (Fig. 5B), relative to those of WT mice. This correlated with a reduction in the neutrophilic infiltrate in IL-12p35$^{-/-}$p40$^{-/-}$ mice and slightly preceded their reduction in IL-12p35$^{-/-}$ mice (Fig. 2B). In conjunction with a reduced CD4^{+} T cell infiltrate, the corneas of IL-12p35$^{-/-}$ and IL-12p35$^{-/-}$p40$^{-/-}$ mice also exhibited significantly reduced levels of the chemotactic factor MCP-1/CCL2 (Fig. 5C), a chemokine that one study suggested regulates CD4^{+} T cell infiltration into infected corneas[321]. The attenuation of blood vessels in infected corneas of IL-12p35$^{-/-}$ and IL-12p35$^{-/-}$p40$^{-/-}$ mice was also associated with significantly reduced levels of the angiogenic factor VEGF (Fig. 5D). Infected corneas of IL-12p40$^{-/-}$ mice compared to infected WT corneas exhibited elevated levels of MIP-2/CXCL2 and VEGF, but similar levels of KC/CXCL3 and MCP-1/CCL2. The increased levels of MIP-2/CXCL2 and VEGF preceded the increased leukocytic infiltrate at 21 dpi (Fig. 2C), but were not associated with increased clinical HSK scores (Fig. 1). Of interest was the lack of detectable levels of IL-6 within the corneas of the IL-12p35$^{-/-}$ corneas while levels of this cytokine were

similar in WT, IL-12p40$^{-/-}$, and IL-12p35$^{-/-}$p40$^{-/-}$ mice (Fig. 5E). As mice lacking IL-12 p35 still underwent a regression of disease (Fig. 1), it appears IL-6 while important for HSK development, is not alone sufficient to promote HSK progression.

Discussion

The established regulatory role of T_H1 cytokines in HSK immunopathology strongly implicates the involvement of the IL-12 cytokine family. Indeed, a previous study using the same BALB/c WT, IL-12p40$^{-/-}$, and IL-12p35$^{-/-}$ mice employed in our study supported a role for IL-12 in HSK by showing reduced HSK in IL-12p35$^{-/-}$ mice and no HSK in IL-12p40$^{-/-}$ mice[316]. The authors concluded that IL-12 was required for HSK. Those findings stand in stark contrast to the findings in this report. In our hands IL-IL-12p40$^{-/-}$ mice developed HSK with similar kinetics and severity to that seen in WT control mice. Indeed, infected corneas of IL-12p40$^{-/-}$ mice exhibited a more robust inflammatory infiltrate at the peak of HSK (21 dpi) compared to their WT counterparts. These findings demonstrate that in our HSK model neither IL-12 nor IL-23 has a requisite role in HSK development since both molecules incorporate an IL-12p40 chain. We further establish that the IL-12p35 chain has a requisite role in the progression of HSK beyond 11 dpi that is independent of the IL-12p40 chain as indicated by the transient nature of HSK in corneas of IL-12p35$^{-/-}$ mice and IL-12p35/p40 double knockout mice. The genotype of all the mice used in these experiments was confirmed by PCR, and the pattern of HSK was observed in multiple experiments.

We surmise that a likely explanation for the differences in findings of the two studies lies in the virus used to infect the mice. Ghiasi and colleagues used the McKrae strain of HSV-1 at an infectious dose of 2 x 10^5 PFU to infect corneas. The McKrae strain is highly neurovirulent and at the dose employed only 20% of WT and IL-12p40$^{-/-}$ mice and 50% of IL-12p35$^{-/-}$ mice survived to the time of HSK evaluation. Thus, in that study HSK was evaluated only in those few mice that survived the infection, and the general health of those surviving mice was not described. Our study employed a much less neurovirulent RE strain of HSV-1 at a much lower

infectious dose that induced HSK in 80-100% of WT mice while permitting 100% survival with no clinically apparent disease other than HSK. We previously established that HSK is highly dependent on the function of $CD4^+$ T cells at the RE HSV-1 infectious dose used in these studies[319], and our model better reflects human disease where infections are rarely fatal and HSK usually occurs in otherwise healthy individuals. One interesting parallel between the two studies is the fact that the IL-12p35 chain appears to function independent of IL-12p40; in our study prolonging HSK and in the previous study enhancing the lethality of HSV-1 infection. These findings are consistent with an important role for IL-12p35 in regulating the immunopathology in the cornea and in the CNS independent of IL-12p40.

The IL-12p40 chain can form an IL-12p40 homodimer, which has been shown to inhibit T cell responses by binding to the IL-12Rβ1 chain and inhibiting binding of IL-12 and IL-23[301,302]. We considered the possibility that IL-12p35$^{-/-}$ mice might have a propensity to produce more IL-12p40 homodimer, which might account for the transient nature of HSK in these mice. This possibility was addressed by monitoring HSK in mice that lack both the p35 and p40 subunits. We observed a transient pattern of HSK in the double knockout mice that was similar to that seen in IL-12p35$^{-/-}$ mice. These findings demonstrated that HSK regression was due to the lack of the IL-12p35 subunit rather than to an altered function of the IL-12p40 subunit. The increased level of infiltrate within the IL-12p40$^{-/-}$ corneas is in agreement with the recent study in IL-23 deficient mice, where more severe HSK lesions develop over WT mice[28]. However, the observation that mice deficient in both IL-12p35 and p40 regress in HSK earlier than IL-12p35$^{-/-}$ mice suggests more complex relationships exist for p40 in the development of HSK.

We were intrigued by the dramatic increase in the frequency of $FoxP3^+$ Tregs in the infected corneas of IL-12p35$^{-/-}$ mice during HSK regression. The reduced overall $CD4^+$ T cell

population in the infected corneas of IL-12p35$^{-/-}$ mice during HSK regression, combined with the elevated frequency of Tregs among the CD4^{+} T cells would suggest a very high Treg:effector T cell ratio in the infected corneas of these mice. The cytokine TGF-β regulates the differentiation of CD4^{+} T cells into Tregs and into T_H17 cells, with co-stimulation by IL-6 favoring the latter[322,323]. We noted dramatically reduced levels of IL-6 in the corneas of IL-12p35$^{-/-}$ mice during HSK regression when compared with those of WT mice with progressive HSK. The known presence of TGF-β in the cornea[324,325] and the low levels of IL-6 in the corneas of IL-12p35$^{-/-}$ mice might provide a cytokine milieu that favors the differentiation and/or expansion of Tregs.

However, depletion of CD25^{+} cells failed to influence HSK regression in IL-12p35$^{-/-}$ mice. The possible explanation that our anti-CD25 treatment effected HSK regression by inadvertently depleting CD4^{+} effector T cells along with Tregs appears highly unlikely. In our hands the majority of CD4^{+} CD25^{+} cells in infected corneas co-express FoxP3 (not shown) suggesting that predominantly Tregs would be depleted by anti-CD25 treatment. Moreover, similar anti-CD25 mAb treatment increased CD4^{+} T cell numbers and augmented the overall leukocytic infiltrate in HSV-1 infected corneas of WT mice, suggesting that the CD4^{+} T cells that mediate HSK do not express CD25. To further corroborate this evidence, IL-12p35$^{-/-}$p40$^{-/-}$ did not exhibit any increase in Treg frequency in their corneas, despite HSK regression. Thus, although the frequency of CD4^{+} CD25^{+} FoxP3^{+} Tregs is dramatically increased in infected corneas of IL-12p35$^{-/-}$ mice during HSK regression, these cells are either inactive or their effector molecules inhibit an IL-12p35-dependent activation pathway. However as noted above, depletion of CD25^{+} cells leaves a substantial population of CD4^{+} FoxP3^{+} CD25^{-} cells in the cornea that might contribute to HSK regression.

Our findings demonstrate that IL-12p35 and p40 regulate the production of several chemokines and cytokines in corneas with HSK. Levels of the macrophage chemoattractant MCP-1/CCL2 were significantly and equivalently reduced in infected corneas of IL-12p35$^{-/-}$ and IL-12p35$^{-/-}$p40$^{-/-}$ mice at 17 dpi. This observation is consistent with a role for IL-12 in regulating production of this chemokine. A recent study does suggest a role of MCP-1 in regulating the infiltration of CD4 T cells into the HSK inflamed cornea[321], although such studies are complicated by the fact that MCP1$^{-/-}$ mice exhibit enhanced IL-12 production and increased HSK[326,327]. Together these findings suggest a regulatory circuit in which IL-12 induces MCP-1/CCL2 production, while MCP-1/CCL2 provides feedback inhibition of IL-12 production.

We also observed that IL-12p35 regulates neutrophil infiltration and production of the neutrophil chemoattractants KC/CXCL3 and MIP-2/CXCL2 as these chemokines were significantly reduced in infected corneas of IL-12p35$^{-/-}$ and IL-12p35/40$^{-/-}$ mice relative to WT mice. This function of IL-12p35 is independent of IL-12p40 since neutrophilic infiltration and levels of these chemokines were somewhat elevated in infected corneas of IL-12p40$^{-/-}$ mice. These findings are consistent with previous studies identifying KC/CXCL3, and to a greater extent MIP-2/CXCL2 as important factors for neutrophil recruitment and HSK development[265,266,328].

Several studies have established a critical role for neovascularization in HSK progression[277-280,294]. Here we demonstrate that IL-12p35 independent of IL-12p40 regulates VEGF production in corneas with HSK. In fact, IL-12p40 appears to inhibit the induction of VEGF production by IL-12p35 as corneas of IL-12p40$^{-/-}$ mice exhibit dramatically increased VEGF production whereas the IL-12p35/p40 double knockouts show reduced VEGF levels comparable to those seen in IL-12p35 single knockouts.

The current understanding of IL-12p35 synthesis indicates that this subunit is not released by cells unbound[329]. The recent description of IL-35, a IL-12p35 EBI3 heterodimeric sets the precedence for more p35 binding partners[306,329]. The exact contribution of IL-12p35 subunit to the maintenance of HSK remains unclear, but reflects an exciting development in the study of the IL-12 cytokine family in the pathogenesis of HSK immunopathology.

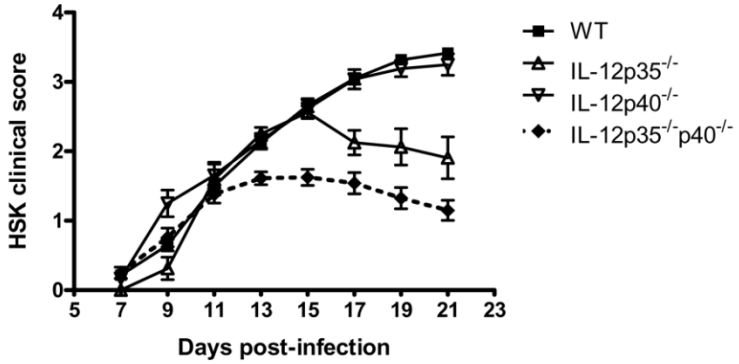

Figure 1. Mice lacking IL-12 develop HSK. IL-12p35$^{-/-}$, IL-12p40$^{-/-}$, IL-12p35$^{-/-}$p40$^{-/-}$ (double knockout), and WT mice infected with HSV-1 RE were scored for HSK by slit-lamp examination from 7 – 21 dpi. Data shown reflect n values of at least 5 mice per group and are representative of 2 or more independent experiments.

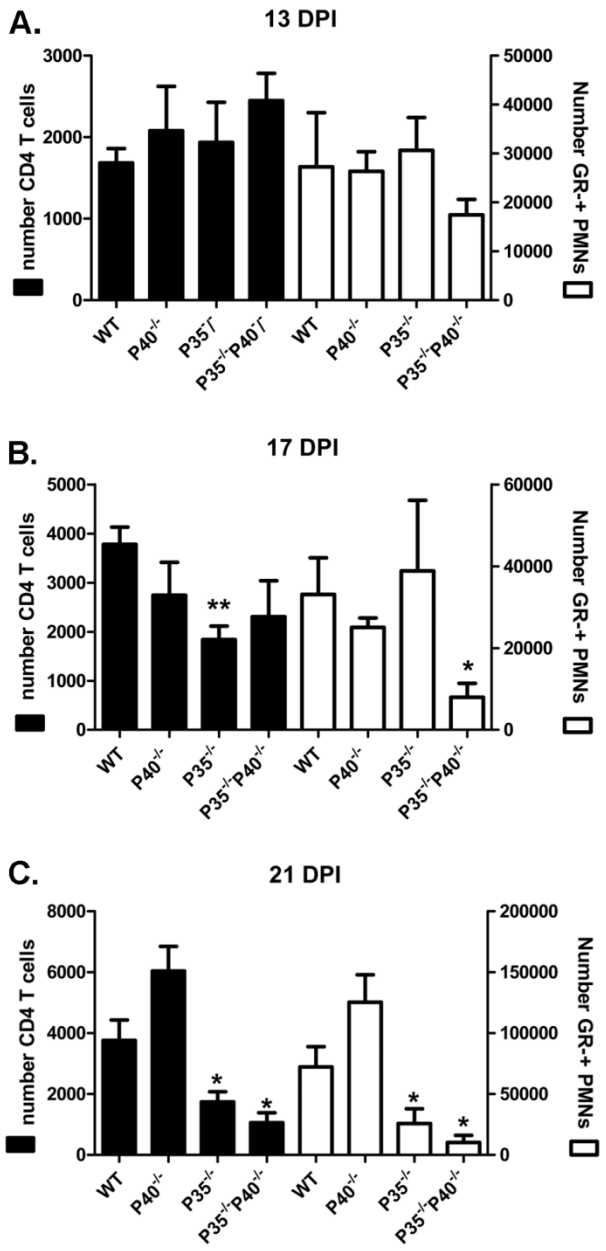

Figure 2. Mice lacking IL-12p35 have a reduced corneal leukocytic infiltrate. At 13, 17, and 21 dpi, corneas were dispersed into single cell suspensions and stained with anti-CD45, CD4, and Gr-1 mAb. Cell suspensions were analyzed by flow cytometry. Data are represented as mean ± SEM number of $CD4^+$ T cells (Left axis), and GR-1^{bright} neutrophils (Right axis). Data reflect the average of 2 independent experiments with n values of at least 4 corneas per group. * $p < .05$; ** $p < .01$.

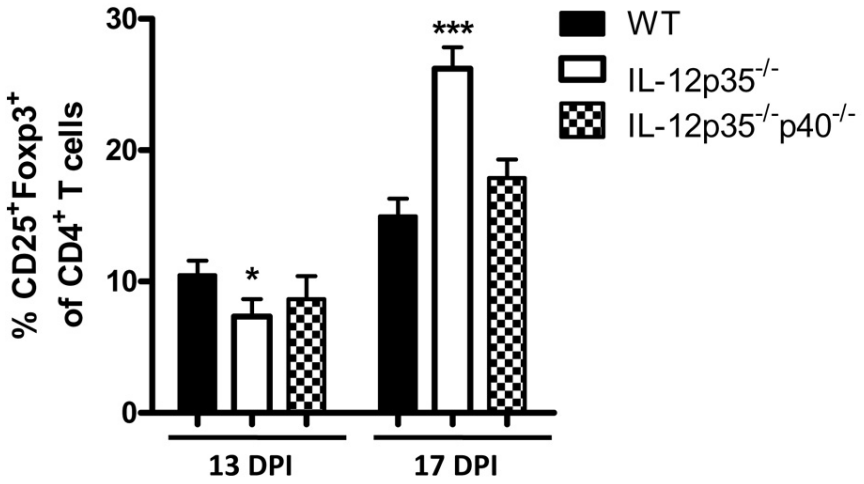

Figure 3. IL-12p35$^{-/-}$ corneas contain an increased Treg population during disease regression. Corneas were dispersed into single cell suspensions at 13 and 17 dpi and were stained with anti-CD4, CD25, and FoxP3 mAb. Corneal suspensions were analyzed by flow cytometry. Data are represented as mean % ± SEM CD25^{+}FoxP3^{+} cells in the CD4^{+} T cell population. Groups consisted of 5 or more individual corneas and results reflect the average of 2 independent experiments. * $p < .05$, *** $p < .001$.

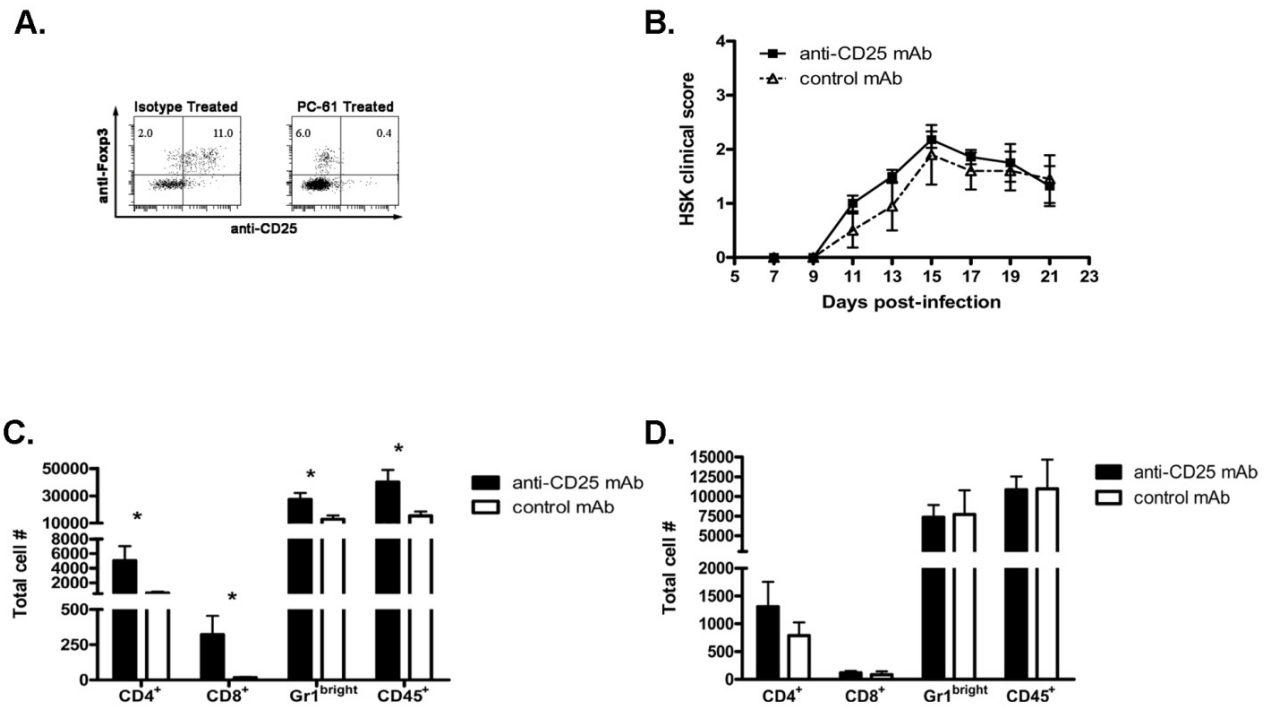

Figure 4. Regulatory T cells do not cause disease attenuation in IL-12p35$^{-/-}$ mice. IL-12p35$^{-/-}$ and WT mice were ~80% depleted of Treg cells by treatment with anti-CD25 mAb (PC61) 3 days prior to infection with HSV-1 RE (A, comparing depletion in WT mice). WT and IL-12p35$^{-/-}$ mice were followed for HSK (data not shown and B, respectively), and at 21 dpi, dispersed corneas were stained with anti-CD4, CD8, CD45, and GR-1 and analyzed by flow cytometry (WT, C and IL-12p35$^{-/-}$ D). Data are represented as mean ± SEM number of cells per cornea. Results represent the average of 2 independent experiments with an n value of at least 6 mice per group. * $p < .05$.

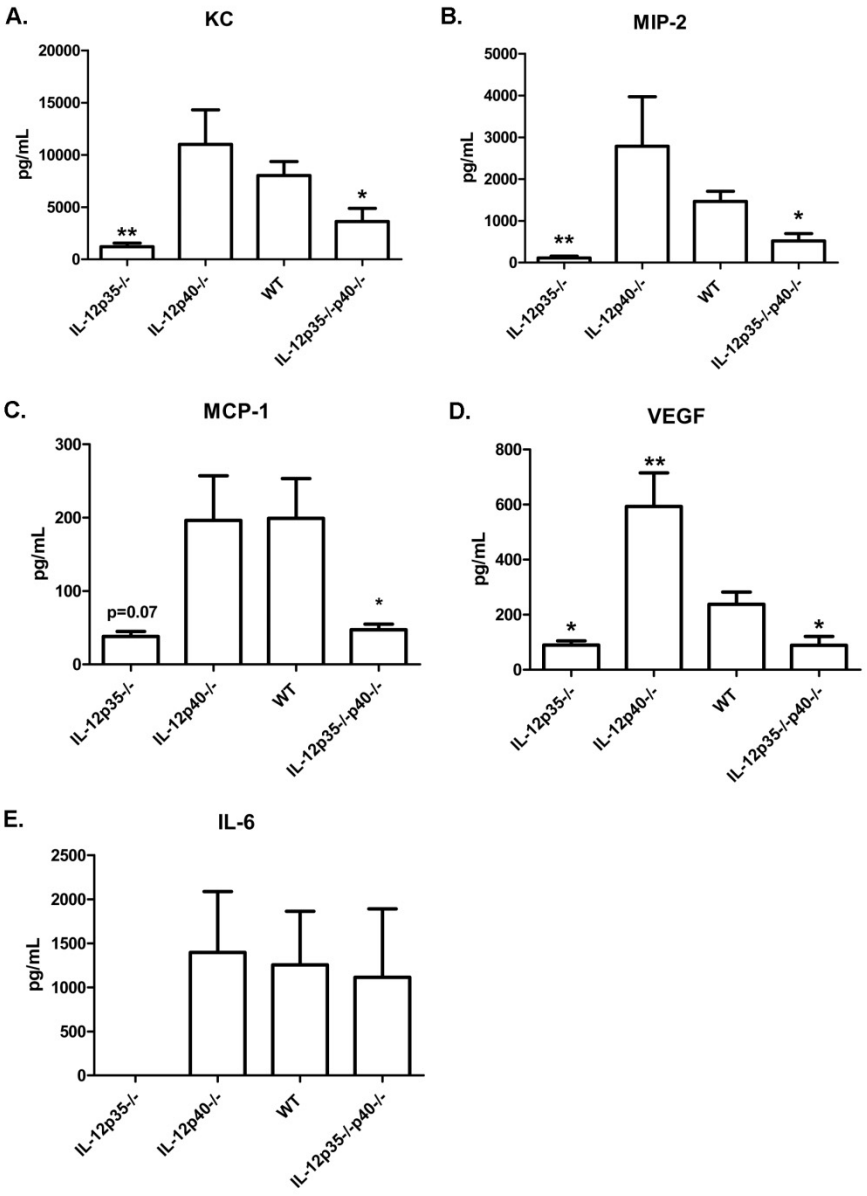

Figure 5. Absence of IL-12 alters expression of cytokines and chemoattractants in corneas. WT, IL-12p35$^{-/-}$, IL-12p40$^{-/-}$, and IL-12p35$^{-/-}$p40$^{-/-}$ corneas were harvested at 17 dpi. Corneas were homogenized by sonic dismembranation in PBS + protease inhibitor, and analyzed by multiplex bead array for cytokine and chemokine expression. Data are represented as mean ± SEM pg/ml of analyte. Groups consisted of 5 or more corneas and results were averaged between two independent experiments. * $p < .05$, ** $p < .01$.

APPENDIX C

PUBLICATIONS

Lazarevic, V., D. J. Yankura, **S. J. Divito**, and J. L. Flynn. Induction of *Mycobacterium tuberculosis*-specific primary and secondary T-cell responses in interleukin-15-deficient mice. Infect Immun. 73(5): 2910-22 2005.

Divito, S., Cherpes, T.L., and Hendricks, R.L. A triple entente: virus, neurons, and $CD8^+$ T cells maintain HSV-1 latency. Immunol Res. 36(1-3):119-26 2006.

Knicklebein, J.E., **Divito, S.**, and Hendricks, R.L. Modulation of $CD8^+$ CTL effector function by fibroblasts derived from the immunoprivileged cornea. Invest Ophthalmol Vis Sci. 48(5):2194-202 2007.

Montecalvo, A., Shufesky, Stolz, D.B., W.J., Sullivan, M.G., Wang, Z., **Divito, S.J.**, Papworth, G.D., Watkins, S.C., Robbins, P.D., Larregina, A.T., Morelli, A.E. Exosomes as a short-range mechanism to spread alloantigen between dendritic cells during T cell allorecognition. J Immunol. 180:3081-3090 2008.

Divito, S.J. and Hendricks, R.L. Activated inflammatory infiltrate in HSV-1-infected corneas without herpes stromal keratitis. Invest Ophthalmol Vis Sci. 49(4):1488-95 2008.

Perone, M.J., Bertera, S., Shufesky, W.J., **Divito, S.J.**, Montecalvo, A., Mathers, A.R., Larregina, A.T., Pang, M. Seth, N., Wucherpfennig, K.W., Trucco, M., Baum, L.G., Morelli, A.E. Suppression of autoimmune diabetes by soluble galectin-1. J Immunol. 182(5):2641-2653 2009.

Divito, S.J. and Morelli, A.E. Apoptotic cells in the treatment of transplant rejection. In P. Vandenabeele and D. Krysko (Ed.), Phagocytosis of dying cells: from molecular mechanisms to human diseases. Springer. 319-346 2009.

Wang, Z., Shufesky, W.J., Montecalvo, A., **Divito, S.J.**, Larregina, A.T., Morelli, A.E. In situ-targeting of dendritic cells with donor-derived apoptotic cells restrains indirect allorecognition and ameliorates allograft vasculopathy. PlosONE 4(3):e4940 2009.

Divito, S.J., Haught, J.M., English J.C. 3rd, Ferris, L.K. An extensive case of dermonecrotic arachnidism. Submitted.

Divito, S.J., Montecalvo, A., Wang, Z., Shufesky, B., Erdos, GA., Larregina, A.T., Morelli, A.E. Quiescent recipient dendritic cells (DC) re-process therapeutic tolerogenic donor-derived DC to prolong allograft survival. Submitted.

Divito, S.J., Wang, Z., Nakao, A., Shufesky, B., Montecalvo, A., Larregina, A.T., Morelli, A.E. Inflammatory monocytes and DC serve as mediators and suppressors of allograft damage. Submitted.

Divito, S.J., Sattar, A., Sander, C., Butterfield, L., Kirkwood, J.M. Serum IL-2, IFN-a and IL-17 predict survival in patients with Stage IV melanoma. Submitted.

Frank G.M.*, **Divito, S.J.***, Maker, D., Xu, M., Hendricks, R.L. A novel p40-independent function of IL-12p35 is required for progression and maintenance of herpes stromal keratitis. Submitted.
*Co-first authors

BIBLIOGRAPHY

1. Banchereau, J. et al. Immunobiology of dendritic cells. *Annu Rev Immunol* **18**, 767-811 (2000).
2. Banchereau, J. & Steinman, R.M. Dendritic cells and the control of immunity. *Nature* **392**, 245-52 (1998).
3. Cella, M., Sallusto, F. & Lanzavecchia, A. Origin, maturation and antigen presenting function of dendritic cells. *Curr Opin Immunol* **9**, 10-6 (1997).
4. Cyster, J.G. Chemokines and the homing of dendritic cells to the T cell areas of lymphoid organs. *J Exp Med* **189**, 447-50 (1999).
5. Lenschow, D.J., Walunas, T.L. & Bluestone, J.A. CD28/B7 system of T cell costimulation. *Annu Rev Immunol* **14**, 233-58 (1996).
6. Grewal, I.S. & Flavell, R.A. CD40 and CD154 in cell-mediated immunity. *Annu Rev Immunol* **16**, 111-35 (1998).
7. Walunas, T.L., Bakker, C.Y. & Bluestone, J.A. CTLA-4 ligation blocks CD28-dependent T cell activation. *J Exp Med* **183**, 2541-50 (1996).
8. Steinman, R.M., Hawiger, D. & Nussenzweig, M.C. Tolerogenic dendritic cells. *Annu Rev Immunol* **21**, 685-711 (2003).
9. Morelli, A.E. & Thomson, A.W. Tolerogenic dendritic cells and the quest for transplant tolerance. *Nat Rev Immunol* **7**, 610-21 (2007).

10. Vremec, D., Pooley, J., Hochrein, H., Wu, L. & Shortman, K. CD4 and CD8 expression by dendritic cell subtypes in mouse thymus and spleen. *J Immunol* **164**, 2978-86 (2000).

11. Corcoran, L. et al. The lymphoid past of mouse plasmacytoid cells and thymic dendritic cells. *J Immunol* **170**, 4926-32 (2003).

12. Henri, S. et al. The dendritic cell populations of mouse lymph nodes. *J Immunol* **167**, 741-8 (2001).

13. Colonna, M., Trinchieri, G. & Liu, Y.J. Plasmacytoid dendritic cells in immunity. *Nat Immunol* **5**, 1219-26 (2004).

14. Mellor, A.L. et al. Cutting edge: induced indoleamine 2,3 dioxygenase expression in dendritic cell subsets suppresses T cell clonal expansion. *J Immunol* **171**, 1652-5 (2003).

15. Mellor, A.L. et al. Specific subsets of murine dendritic cells acquire potent T cell regulatory functions following CTLA4-mediated induction of indoleamine 2,3 dioxygenase. *Int Immunol* **16**, 1391-401 (2004).

16. Mellor, A.L., Keskin, D.B., Johnson, T., Chandler, P. & Munn, D.H. Cells expressing indoleamine 2,3-dioxygenase inhibit T cell responses. *J Immunol* **168**, 3771-6 (2002).

17. Munn, D.H. et al. Expression of indoleamine 2,3-dioxygenase by plasmacytoid dendritic cells in tumor-draining lymph nodes. *J Clin Invest* **114**, 280-90 (2004).

18. Munn, D.H. et al. Prevention of allogeneic fetal rejection by tryptophan catabolism. *Science* **281**, 1191-3 (1998).

19. Fogg, D.K. et al. A clonogenic bone marrow progenitor specific for macrophages and dendritic cells. *Science* **311**, 83-7 (2006).

20. van Furth, R. & Cohn, Z.A. The origin and kinetics of mononuclear phagocytes. *J Exp Med* **128**, 415-35 (1968).

21. Reuter, S. & Lang, D. Life span of monocytes and platelets: importance of interactions. *Front Biosci* **14**, 2432-47 (2009).

22. Tacke, F. & Randolph, G.J. Migratory fate and differentiation of blood monocyte subsets. *Immunobiology* **211**, 609-18 (2006).

23. Sunderkotter, C. et al. Subpopulations of mouse blood monocytes differ in maturation stage and inflammatory response. *J Immunol* **172**, 4410-7 (2004).

24. Auffray, C., Sieweke, M.H. & Geissmann, F. Blood monocytes: development, heterogeneity, and relationship with dendritic cells. *Annu Rev Immunol* **27**, 669-92 (2009).

25. Qu, C. et al. Role of CCR8 and other chemokine pathways in the migration of monocyte-derived dendritic cells to lymph nodes. *J Exp Med* **200**, 1231-41 (2004).

26. Agger, R. et al. Characterization of murine dendritic cells derived from adherent blood mononuclear cells in vitro. *Scand J Immunol* **52**, 138-47 (2000).

27. Nikolic, T., de Bruijn, M.F., Lutz, M.B. & Leenen, P.J. Developmental stages of myeloid dendritic cells in mouse bone marrow. *Int Immunol* **15**, 515-24 (2003).

28. Randolph, G.J., Inaba, K., Robbiani, D.F., Steinman, R.M. & Muller, W.A. Differentiation of phagocytic monocytes into lymph node dendritic cells in vivo. *Immunity* **11**, 753-61 (1999).

29. Serbina, N.V., Salazar-Mather, T.P., Biron, C.A., Kuziel, W.A. & Pamer, E.G. TNF/iNOS-producing dendritic cells mediate innate immune defense against bacterial infection. *Immunity* **19**, 59-70 (2003).

30. Leon, B., Lopez-Bravo, M. & Ardavin, C. Monocyte-derived dendritic cells formed at the infection site control the induction of protective T helper 1 responses against Leishmania. *Immunity* **26**, 519-31 (2007).

31. Copin, R., De Baetselier, P., Carlier, Y., Letesson, J.J. & Muraille, E. MyD88-dependent activation of B220-CD11b+LY-6C+ dendritic cells during Brucella melitensis infection. *J Immunol* **178**, 5182-91 (2007).

32. Robben, P.M., LaRegina, M., Kuziel, W.A. & Sibley, L.D. Recruitment of Gr-1+ monocytes is essential for control of acute toxoplasmosis. *J Exp Med* **201**, 1761-9 (2005).

33. Palframan, R.T. et al. Inflammatory chemokine transport and presentation in HEV: a remote control mechanism for monocyte recruitment to lymph nodes in inflamed tissues. *J Exp Med* **194**, 1361-73 (2001).

34. Nakano, H. et al. Blood-derived inflammatory dendritic cells in lymph nodes stimulate acute T helper type 1 immune responses. *Nat Immunol* **10**, 394-402 (2009).

35. Le Borgne, M. et al. Dendritic cells rapidly recruited into epithelial tissues via CCR6/CCL20 are responsible for CD8+ T cell crosspriming in vivo. *Immunity* **24**, 191-201 (2006).

36. Aldridge, J.R., Jr. et al. TNF/iNOS-producing dendritic cells are the necessary evil of lethal influenza virus infection. *Proc Natl Acad Sci U S A* **106**, 5306-11 (2009).

37. Ginhoux, F. et al. Langerhans cells arise from monocytes in vivo. *Nat Immunol* **7**, 265-73 (2006).

38. Varol, C. et al. Monocytes give rise to mucosal, but not splenic, conventional dendritic cells. *J Exp Med* **204**, 171-80 (2007).

39. Jakubzick, C. et al. Blood monocyte subsets differentially give rise to CD103+ and CD103- pulmonary dendritic cell populations. *J Immunol* **180**, 3019-27 (2008).

40. Landsman, L. & Jung, S. Lung macrophages serve as obligatory intermediate between blood monocytes and alveolar macrophages. *J Immunol* **179**, 3488-94 (2007).

41. Landsman, L., Varol, C. & Jung, S. Distinct differentiation potential of blood monocyte subsets in the lung. *J Immunol* **178**, 2000-7 (2007).

42. Huang, B. et al. Gr-1+CD115+ immature myeloid suppressor cells mediate the development of tumor-induced T regulatory cells and T-cell anergy in tumor-bearing host. *Cancer Res* **66**, 1123-31 (2006).

43. Mazzoni, A. et al. Myeloid suppressor lines inhibit T cell responses by an NO-dependent mechanism. *J Immunol* **168**, 689-95 (2002).

44. Movahedi, K. et al. Identification of discrete tumor-induced myeloid-derived suppressor cell subpopulations with distinct T cell-suppressive activity. *Blood* **111**, 4233-44 (2008).

45. Bronte, V. et al. Identification of a CD11b(+)/Gr-1(+)/CD31(+) myeloid progenitor capable of activating or suppressing CD8(+) T cells. *Blood* **96**, 3838-46 (2000).

46. Gabrilovich, D.I., Velders, M.P., Sotomayor, E.M. & Kast, W.M. Mechanism of immune dysfunction in cancer mediated by immature Gr-1+ myeloid cells. *J Immunol* **166**, 5398-406 (2001).

47. Gallina, G. et al. Tumors induce a subset of inflammatory monocytes with immunosuppressive activity on CD8+ T cells. *J Clin Invest* **116**, 2777-90 (2006).

48. Kusmartsev, S., Nefedova, Y., Yoder, D. & Gabrilovich, D.I. Antigen-specific inhibition of CD8+ T cell response by immature myeloid cells in cancer is mediated by reactive oxygen species. *J Immunol* **172**, 989-99 (2004).

49. Brocker, T., Riedinger, M. & Karjalainen, K. Targeted expression of major histocompatibility complex (MHC) class II molecules demonstrates that dendritic cells can induce negative but not positive selection of thymocytes in vivo. *J Exp Med* **185**, 541-50 (1997).

50. Steinman, R.M. & Nussenzweig, M.C. Avoiding horror autotoxicus: the importance of dendritic cells in peripheral T cell tolerance. *Proc Natl Acad Sci U S A* **99**, 351-8 (2002).

51. Schwartz, R.H. A cell culture model for T lymphocyte clonal anergy. *Science* **248**, 1349-56 (1990).

52. Feng, G., Chan, T., Wood, K.J. & Bushell, A. Donor reactive regulatory T cells. *Curr Opin Organ Transplant* (2009).

53. Guery, J.C. & Adorini, L. Dendritic cells are the most efficient in presenting endogenous naturally processed self-epitopes to class II-restricted T cells. *J Immunol* **154**, 536-44 (1995).

54. Guery, J.C., Sette, A., Appella, E. & Adorini, L. Constitutive presentation of dominant epitopes from endogenous naturally processed self-beta 2-microglobulin to class II-restricted T cells leads to self-tolerance. *J Immunol* **154**, 545-54 (1995).

55. Finkelman, F.D., Lees, A., Birnbaum, R., Gause, W.C. & Morris, S.C. Dendritic cells can present antigen in vivo in a tolerogenic or immunogenic fashion. *J Immunol* **157**, 1406-14 (1996).

56. Voll, R.E. et al. Immunosuppressive effects of apoptotic cells. *Nature* **390**, 350-1 (1997).

57. Urban, B.C., Willcox, N. & Roberts, D.J. A role for CD36 in the regulation of dendritic cell function. *Proc Natl Acad Sci U S A* **98**, 8750-5 (2001).

58. Gallucci, S., Lolkema, M. & Matzinger, P. Natural adjuvants: endogenous activators of dendritic cells. *Nat Med* **5**, 1249-55 (1999).

59. Stuart, L.M. et al. Inhibitory effects of apoptotic cell ingestion upon endotoxin-driven myeloid dendritic cell maturation. *J Immunol* **168**, 1627-35 (2002).

60. Takahashi, M. & Kobayashi, Y. Cytokine production in association with phagocytosis of apoptotic cells by immature dendritic cells. *Cell Immunol* **226**, 105-15 (2003).

61. Verbovetski, I. et al. Opsonization of apoptotic cells by autologous iC3b facilitates clearance by immature dendritic cells, down-regulates DR and CD86, and up-regulates CC chemokine receptor 7. *J Exp Med* **196**, 1553-61 (2002).

62. Pugh, C.W., MacPherson, G.G. & Steer, H.W. Characterization of nonlymphoid cells derived from rat peripheral lymph. *J Exp Med* **157**, 1758-79 (1983).

63. Hemmi, H. et al. Skin antigens in the steady state are trafficked to regional lymph nodes by transforming growth factor-beta1-dependent cells. *Int Immunol* **13**, 695-704 (2001).

64. Ip, W.K. & Lau, Y.L. Distinct maturation of, but not migration between, human monocyte-derived dendritic cells upon ingestion of apoptotic cells of early or late phases. *J Immunol* **173**, 189-96 (2004).

65. Huang, F.P. et al. A discrete subpopulation of dendritic cells transports apoptotic intestinal epithelial cells to T cell areas of mesenteric lymph nodes. *J Exp Med* **191**, 435-44 (2000).

66. Adler, A.J. et al. CD4+ T cell tolerance to parenchymal self-antigens requires presentation by bone marrow-derived antigen-presenting cells. *J Exp Med* **187**, 1555-64 (1998).

67. Kurts, C., Kosaka, H., Carbone, F.R., Miller, J.F. & Heath, W.R. Class I-restricted cross-presentation of exogenous self-antigens leads to deletion of autoreactive CD8(+) T cells. *J Exp Med* **186**, 239-45 (1997).

68. Liu, K. et al. Immune tolerance after delivery of dying cells to dendritic cells in situ. *J Exp Med* **196**, 1091-7 (2002).

69. Albert, M.L., Sauter, B. & Bhardwaj, N. Dendritic cells acquire antigen from apoptotic cells and induce class I-restricted CTLs. *Nature* **392**, 86-9 (1998).

70. Yrlid, U. & Wick, M.J. Salmonella-induced apoptosis of infected macrophages results in presentation of a bacteria-encoded antigen after uptake by bystander dendritic cells. *J Exp Med* **191**, 613-24 (2000).

71. Inaba, K. et al. Efficient presentation of phagocytosed cellular fragments on the major histocompatibility complex class II products of dendritic cells. *J Exp Med* **188**, 2163-73 (1998).

72. Falcone, M. & Sarvetnick, N. The effect of local production of cytokines in the pathogenesis of insulin-dependent diabetes mellitus. *Clin Immunol* **90**, 2-9 (1999).

73. Townsend, S.E. & Goodnow, C.C. Abortive proliferation of rare T cells induced by direct or indirect antigen presentation by rare B cells in vivo. *J Exp Med* **187**, 1611-21 (1998).

74. Nouri-Shirazi, M. & Guinet, E. Direct and indirect cross-tolerance of alloreactive T cells by dendritic cells retained in the immature stage. *Transplantation* **74**, 1035-44 (2002).

75. Wang, Z. et al. Use of the inhibitory effect of apoptotic cells on dendritic cells for graft survival via T-cell deletion and regulatory T cells. *Am J Transplant* **6**, 1297-311 (2006).

76. Morelli, A.E. et al. Internalization of circulating apoptotic cells by splenic marginal zone dendritic cells: dependence on complement receptors and effect on cytokine production. *Blood* **101**, 611-20 (2003).

77. Savill, J., Dransfield, I., Gregory, C. & Haslett, C. A blast from the past: clearance of apoptotic cells regulates immune responses. *Nat Rev Immunol* **2**, 965-75 (2002).

78. Stark, M.A. et al. Phagocytosis of apoptotic neutrophils regulates granulopoiesis via IL-23 and IL-17. *Immunity* **22**, 285-94 (2005).

79. Craciun, L.I. et al. Anti-inflammatory effects of UV-irradiated lymphocytes: induction of IL-1Ra upon phagocytosis by monocyte/macrophages. *Clin Immunol* **114**, 320-6 (2005).

80. Fadok, V.A., McDonald, P.P., Bratton, D.L. & Henson, P.M. Regulation of macrophage cytokine production by phagocytosis of apoptotic and post-apoptotic cells. *Biochem Soc Trans* **26**, 653-6 (1998).

81. Morimoto, K. et al. Alveolar macrophages that phagocytose apoptotic neutrophils produce hepatocyte growth factor during bacterial pneumonia in mice. *Am J Respir Cell Mol Biol* **24**, 608-15 (2001).

82. Ansari, M.J. et al. The programmed death-1 (PD-1) pathway regulates autoimmune diabetes in nonobese diabetic (NOD) mice. *J Exp Med* **198**, 63-9 (2003).

83. Bauer, T.M. et al. Studying the immunosuppressive role of indoleamine 2,3-dioxygenase: tryptophan metabolites suppress rat allogeneic T-cell responses in vitro and in vivo. *Transpl Int* **18**, 95-100 (2005).

84. Gao, W., Demirci, G., Strom, T.B. & Li, X.C. Stimulating PD-1-negative signals concurrent with blocking CD154 co-stimulation induces long-term islet allograft survival. *Transplantation* **76**, 994-9 (2003).

85. Nishimura, H., Nose, M., Hiai, H., Minato, N. & Honjo, T. Development of lupus-like autoimmune diseases by disruption of the PD-1 gene encoding an ITIM motif-carrying immunoreceptor. *Immunity* **11**, 141-51 (1999).

86. Ozkaynak, E. et al. Programmed death-1 targeting can promote allograft survival. *J Immunol* **169**, 6546-53 (2002).

87. Salama, A.D. et al. Critical role of the programmed death-1 (PD-1) pathway in regulation of experimental autoimmune encephalomyelitis. *J Exp Med* **198**, 71-8 (2003).

88. Albert, M.L., Kim, J.I. & Birge, R.B. alphavbeta5 integrin recruits the CrkII-Dock180-rac1 complex for phagocytosis of apoptotic cells. *Nat Cell Biol* **2**, 899-905 (2000).

89. Akakura, S. et al. The opsonin MFG-E8 is a ligand for the alphavbeta5 integrin and triggers DOCK180-dependent Rac1 activation for the phagocytosis of apoptotic cells. *Exp Cell Res* **292**, 403-16 (2004).

90. Rodriguez, A., Regnault, A., Kleijmeer, M., Ricciardi-Castagnoli, P. & Amigorena, S. Selective transport of internalized antigens to the cytosol for MHC class I presentation in dendritic cells. *Nat Cell Biol* **1**, 362-8 (1999).

91. Peche, H., Heslan, M., Usal, C., Amigorena, S. & Cuturi, M.C. Presentation of donor major histocompatibility complex antigens by bone marrow dendritic cell-derived exosomes modulates allograft rejection. *Transplantation* **76**, 1503-10 (2003).

92. Peche, H. et al. Induction of tolerance by exosomes and short-term immunosuppression in a fully MHC-mismatched rat cardiac allograft model. *Am J Transplant* **6**, 1541-50 (2006).

93. Harshyne, L.A., Watkins, S.C., Gambotto, A. & Barratt-Boyes, S.M. Dendritic cells acquire antigens from live cells for cross-presentation to CTL. *J Immunol* **166**, 3717-23 (2001).

94. Harshyne, L.A., Zimmer, M.I., Watkins, S.C. & Barratt-Boyes, S.M. A role for class A scavenger receptor in dendritic cell nibbling from live cells. *J Immunol* **170**, 2302-9 (2003).

95. Game, D.S., Rogers, N.J. & Lechler, R.I. Acquisition of HLA-DR and costimulatory molecules by T cells from allogeneic antigen presenting cells. *Am J Transplant* **5**, 1614-25 (2005).

96. Li, G., Kim, Y.J. & Broxmeyer, H.E. Macrophage colony-stimulating factor drives cord blood monocyte differentiation into IL-10(high)IL-12absent dendritic cells with tolerogenic potential. *J Immunol* **174**, 4706-17 (2005).

97. Bohana-Kashtan, O. & Civin, C.I. Fas ligand as a tool for immunosuppression and generation of immune tolerance. *Stem Cells* **22**, 908-24 (2004).

98. Griffin, M.D., Xing, N. & Kumar, R. Vitamin D and its analogs as regulators of immune activation and antigen presentation. *Annu Rev Nutr* **23**, 117-45 (2003).

99. Lemire, J.M. Immunomodulatory actions of 1,25-dihydroxyvitamin D3. *J Steroid Biochem Mol Biol* **53**, 599-602 (1995).

100. Rigby, W.F. The immunobiology of vitamin D. *Immunol Today* **9**, 54-8 (1988).

101. Jones, G., Strugnell, S.A. & DeLuca, H.F. Current understanding of the molecular actions of vitamin D. *Physiol Rev* **78**, 1193-231 (1998).

102. Griffin, M.D., Dong, X. & Kumar, R. Vitamin D receptor-mediated suppression of RelB in antigen presenting cells: a paradigm for ligand-augmented negative transcriptional regulation. *Arch Biochem Biophys* **460**, 218-26 (2007).

103. Carlberg, C. & Polly, P. Gene regulation by vitamin D3. *Crit Rev Eukaryot Gene Expr* **8**, 19-42 (1998).

104. Dong, X. et al. Regulation of relB in dendritic cells by means of modulated association of vitamin D receptor and histone deacetylase 3 with the promoter. *Proc Natl Acad Sci U S A* **102**, 16007-12 (2005).

105. Penna, G. et al. 1,25-Dihydroxyvitamin D3 selectively modulates tolerogenic properties in myeloid but not plasmacytoid dendritic cells. *J Immunol* **178**, 145-53 (2007).

106. Koeffler, H.P., Amatruda, T., Ikekawa, N., Kobayashi, Y. & DeLuca, H.F. Induction of macrophage differentiation of human normal and leukemic myeloid stem cells by 1,25-dihydroxyvitamin D3 and its fluorinated analogues. *Cancer Res* **44**, 5624-8 (1984).

107. Kreutz, M. & Andreesen, R. Induction of human monocyte to macrophage maturation in vitro by 1,25-dihydroxyvitamin D3. *Blood* **76**, 2457-61 (1990).

108. Walters, M.R. Newly identified actions of the vitamin D endocrine system. *Endocr Rev* **13**, 719-64 (1992).

109. Piemonti, L. et al. Vitamin D3 affects differentiation, maturation, and function of human monocyte-derived dendritic cells. *J Immunol* **164**, 4443-51 (2000).

110. Penna, G. & Adorini, L. 1 Alpha,25-dihydroxyvitamin D3 inhibits differentiation, maturation, activation, and survival of dendritic cells leading to impaired alloreactive T cell activation. *J Immunol* **164**, 2405-11 (2000).

111. Tsoukas, C.D. et al. Inhibition of interleukin-1 production by 1,25-dihydroxyvitamin D3. *J Clin Endocrinol Metab* **69**, 127-33 (1989).

112. Lemire, J.M., Adams, J.S., Sakai, R. & Jordan, S.C. 1 alpha,25-dihydroxyvitamin D3 suppresses proliferation and immunoglobulin production by normal human peripheral blood mononuclear cells. *J Clin Invest* **74**, 657-61 (1984).

113. Rigby, W.F., Denome, S. & Fanger, M.W. Regulation of lymphokine production and human T lymphocyte activation by 1,25-dihydroxyvitamin D3. Specific inhibition at the level of messenger RNA. *J Clin Invest* **79**, 1659-64 (1987).

114. Rigby, W.F., Yirinec, B., Oldershaw, R.L. & Fanger, M.W. Comparison of the effects of 1,25-dihydroxyvitamin D3 on T lymphocyte subpopulations. *Eur J Immunol* **17**, 563-6 (1987).

115. Griffin, M.D. et al. Dendritic cell modulation by 1alpha,25 dihydroxyvitamin D3 and its analogs: a vitamin D receptor-dependent pathway that promotes a persistent state of immaturity in vitro and in vivo. *Proc Natl Acad Sci U S A* **98**, 6800-5 (2001).

116. Provvedini, D.M., Tsoukas, C.D., Deftos, L.J. & Manolagas, S.C. 1,25-dihydroxyvitamin D3 receptors in human leukocytes. *Science* **221**, 1181-3 (1983).

117. Brennan, A. et al. Dendritic cells from human tissues express receptors for the immunoregulatory vitamin D3 metabolite, dihydroxycholecalciferol. *Immunology* **61**, 457-61 (1987).

118. Carlberg, C. Current understanding of the function of the nuclear vitamin D receptor in response to its natural and synthetic ligands. *Recent Results Cancer Res* **164**, 29-42 (2003).

119. Griffin, M.D. et al. Potent inhibition of dendritic cell differentiation and maturation by vitamin D analogs. *Biochem Biophys Res Commun* **270**, 701-8 (2000).

120. Suciu-Foca, N. et al. Molecular characterization of allospecific T suppressor and tolerogenic dendritic cells: review. *Int Immunopharmacol* **5**, 7-11 (2005).

121. Penna, G. et al. Expression of the inhibitory receptor ILT3 on dendritic cells is dispensable for induction of CD4+Foxp3+ regulatory T cells by 1,25-dihydroxyvitamin D3. *Blood* **106**, 3490-7 (2005).

122. Penna, G. et al. Manipulating dendritic cells to induce regulatory T cells. *Microbes Infect* **7**, 1033-9 (2005).

123. Yates, S.F. et al. Induction of regulatory T cells and dominant tolerance by dendritic cells incapable of full activation. *J Immunol* **179**, 967-76 (2007).

124. Nashold, F.E., Hoag, K.A., Goverman, J. & Hayes, C.E. Rag-1-dependent cells are necessary for 1,25-dihydroxyvitamin D(3) prevention of experimental autoimmune encephalomyelitis. *J Neuroimmunol* **119**, 16-29 (2001).

125. Nashold, F.E., Miller, D.J. & Hayes, C.E. 1,25-dihydroxyvitamin D3 treatment decreases macrophage accumulation in the CNS of mice with experimental autoimmune encephalomyelitis. *J Neuroimmunol* **103**, 171-9 (2000).

126. Lemire, J.M., Ince, A. & Takashima, M. 1,25-Dihydroxyvitamin D3 attenuates the expression of experimental murine lupus of MRL/l mice. *Autoimmunity* **12**, 143-8 (1992).

127. Linker-Israeli, M., Elstner, E., Klinenberg, J.R., Wallace, D.J. & Koeffler, H.P. Vitamin D(3) and its synthetic analogs inhibit the spontaneous in vitro immunoglobulin production by SLE-derived PBMC. *Clin Immunol* **99**, 82-93 (2001).

128. Gregori, S., Giarratana, N., Smiroldo, S., Uskokovic, M. & Adorini, L. A 1alpha,25-dihydroxyvitamin D(3) analog enhances regulatory T-cells and arrests autoimmune diabetes in NOD mice. *Diabetes* **51**, 1367-74 (2002).

129. Overbergh, L. et al. 1alpha,25-dihydroxyvitamin D3 induces an autoantigen-specific T-helper 1/T-helper 2 immune shift in NOD mice immunized with GAD65 (p524-543). *Diabetes* **49**, 1301-7 (2000).

130. van Halteren, A.G. et al. Redirection of human autoreactive T-cells Upon interaction with dendritic cells modulated by TX527, an analog of 1,25 dihydroxyvitamin D(3). *Diabetes* **51**, 2119-25 (2002).

131. Amuchastegui, S., Daniel, K.C. & Adorini, L. Inhibition of acute and chronic allograft rejection in mouse models by BXL-628, a nonhypercalcemic vitamin D receptor agonist. *Transplantation* **80**, 81-7 (2005).

132. Hullett, D.A. et al. Prolongation of allograft survival by 1,25-dihydroxyvitamin D3. *Transplantation* **66**, 824-8 (1998).

133. Johnsson, C., Binderup, L. & Tufveson, G. Immunosuppression with the vitamin D analogue MC 1288 in experimental transplantation. *Transplant Proc* **28**, 888-91 (1996).

134. Briffa, N.K., Keogh, A.M., Sambrook, P.N. & Eisman, J.A. Reduction of immunosuppressant therapy requirement in heart transplantation by calcitriol. *Transplantation* **75**, 2133-4 (2003).

135. Afzali, B., Lechler, R.I. & Hernandez-Fuentes, M.P. Allorecognition and the alloresponse: clinical implications. *Tissue Antigens* **69**, 545-56 (2007).

136. Gallon, L.G., Leventhal, J.R. & Kaufman, D.B. Pretransplant evaluation of renal transplant candidates. *Semin Nephrol* **22**, 515-25 (2002).

137. Magee, C.C. Transplantation across previously incompatible immunological barriers. *Transpl Int* **19**, 87-97 (2006).

138. Ibrahim, S., Dawson, D.V. & Sanfilippo, F. Predominant infiltration of rejecting human renal allografts with T cells expressing CD8 and CD45RO. *Transplantation* **59**, 724-8 (1995).

139. Sayegh, M.H. & Carpenter, C.B. Transplantation 50 years later--progress, challenges, and promises. *N Engl J Med* **351**, 2761-6 (2004).

140. Pascual, M., Theruvath, T., Kawai, T., Tolkoff-Rubin, N. & Cosimi, A.B. Strategies to improve long-term outcomes after renal transplantation. *N Engl J Med* **346**, 580-90 (2002).

141. Le Moine, A., Goldman, M. & Abramowicz, D. Multiple pathways to allograft rejection. *Transplantation* **73**, 1373-81 (2002).

142. Land, W. et al. The beneficial effect of human recombinant superoxide dismutase on acute and chronic rejection events in recipients of cadaveric renal transplants. *Transplantation* **57**, 211-7 (1994).

143. LaRosa, D.F., Rahman, A.H. & Turka, L.A. The innate immune system in allograft rejection and tolerance. *J Immunol* **178**, 7503-9 (2007).

144. Christopher, K., Mueller, T.F., Ma, C., Liang, Y. & Perkins, D.L. Analysis of the innate and adaptive phases of allograft rejection by cluster analysis of transcriptional profiles. *J Immunol* **169**, 522-30 (2002).

145. He, H., Stone, J.R. & Perkins, D.L. Analysis of differential immune responses induced by innate and adaptive immunity following transplantation. *Immunology* **109**, 185-96 (2003).

146. He, H., Stone, J.R. & Perkins, D.L. Analysis of robust innate immune response after transplantation in the absence of adaptive immunity. *Transplantation* **73**, 853-61 (2002).

147. Medzhitov, R. & Janeway, C.A., Jr. Decoding the patterns of self and nonself by the innate immune system. *Science* **296**, 298-300 (2002).

148. Mollen, K.P. et al. Emerging paradigm: toll-like receptor 4-sentinel for the detection of tissue damage. *Shock* **26**, 430-7 (2006).

149. Tsung, A. et al. Hepatic ischemia/reperfusion injury involves functional TLR4 signaling in nonparenchymal cells. *J Immunol* **175**, 7661-8 (2005).

150. Zhai, Y. et al. Cutting edge: TLR4 activation mediates liver ischemia/reperfusion inflammatory response via IFN regulatory factor 3-dependent MyD88-independent pathway. *J Immunol* **173**, 7115-9 (2004).

151. Shen, X.D. et al. Inflammatory responses in a new mouse model of prolonged hepatic cold ischemia followed by arterialized orthotopic liver transplantation. *Liver Transpl* **11**, 1273-81 (2005).

152. Shen, X.D. et al. Toll-like receptor and heme oxygenase-1 signaling in hepatic ischemia/reperfusion injury. *Am J Transplant* **5**, 1793-800 (2005).

153. Tesar, B.M., Zhang, J., Li, Q. & Goldstein, D.R. TH1 immune responses to fully MHC mismatched allografts are diminished in the absence of MyD88, a toll-like receptor signal adaptor protein. *Am J Transplant* **4**, 1429-39 (2004).

154. McKay, D., Shigeoka, A., Rubinstein, M., Surh, C. & Sprent, J. Simultaneous deletion of MyD88 and Trif delays major histocompatibility and minor antigen mismatch allograft rejection. *Eur J Immunol* **36**, 1994-2002 (2006).

155. Palmer, S.M. et al. The role of innate immunity in acute allograft rejection after lung transplantation. *Am J Respir Crit Care Med* **168**, 628-32 (2003).

156. Ducloux, D. et al. Relevance of Toll-like receptor-4 polymorphisms in renal transplantation. *Kidney Int* **67**, 2454-61 (2005).

157. Tsung, A. et al. The nuclear factor HMGB1 mediates hepatic injury after murine liver ischemia-reperfusion. *J Exp Med* **201**, 1135-43 (2005).

158. Moser, B. et al. Blockade of RAGE suppresses alloimmune reactions in vitro and delays allograft rejection in murine heart transplantation. *Am J Transplant* **7**, 293-302 (2007).

159. Bingaman, A.W. et al. Vigorous allograft rejection in the absence of danger. *J Immunol* **164**, 3065-71 (2000).

160. Anderson, C.C. et al. Testing time-, ignorance-, and danger-based models of tolerance. *J Immunol* **166**, 3663-71 (2001).

161. Chalasani, G. et al. The allograft defines the type of rejection (acute versus chronic) in the face of an established effector immune response. *J Immunol* **172**, 7813-20 (2004).

162. Jaeschke, H., Farhood, A. & Smith, C.W. Neutrophils contribute to ischemia/reperfusion injury in rat liver in vivo. *Faseb J* **4**, 3355-9 (1990).

163. Morita, K. et al. Early chemokine cascades in murine cardiac grafts regulate T cell recruitment and progression of acute allograft rejection. *J Immunol* **167**, 2979-84 (2001).

164. Kitchens, W.H. et al. The changing role of natural killer cells in solid organ rejection and tolerance. *Transplantation* **81**, 811-7 (2006).

165. Obara, H. et al. IFN-gamma, produced by NK cells that infiltrate liver allografts early after transplantation, links the innate and adaptive immune responses. *Am J Transplant* **5**, 2094-103 (2005).

166. Maier, S. et al. Inhibition of natural killer cells results in acceptance of cardiac allografts in CD28-/- mice. *Nat Med* **7**, 557-62 (2001).

167. McNerney, M.E. et al. Role of natural killer cell subsets in cardiac allograft rejection. *Am J Transplant* **6**, 505-13 (2006).

168. Wyburn, K.R., Jose, M.D., Wu, H., Atkins, R.C. & Chadban, S.J. The role of macrophages in allograft rejection. *Transplantation* **80**, 1641-7 (2005).

169. Grau, V., Herbst, B. & Steiniger, B. Dynamics of monocytes/macrophages and T lymphocytes in acutely rejecting rat renal allografts. *Cell Tissue Res* **291**, 117-26 (1998).

170. Hancock, W.W., Thomson, N.M. & Atkins, R.C. Composition of interstitial cellular infiltrate identified by monoclonal antibodies in renal biopsies of rejecting human renal allografts. *Transplantation* **35**, 458-63 (1983).

171. Jose, M.D., Ikezumi, Y., van Rooijen, N., Atkins, R.C. & Chadban, S.J. Macrophages act as effectors of tissue damage in acute renal allograft rejection. *Transplantation* **76**, 1015-22 (2003).

172. Roza, A.M. et al. NOX 100, a nitric oxide scavenger, enhances cardiac allograft survival and promotes long-term graft acceptance. *Transplantation* **69**, 227-31 (2000).

173. Worrall, N.K. et al. Modulation of in vivo alloreactivity by inhibition of inducible nitric oxide synthase. *J Exp Med* **181**, 63-70 (1995).

174. Game, D.S. & Lechler, R.I. Pathways of allorecognition: implications for transplantation tolerance. *Transpl Immunol* **10**, 101-8 (2002).

175. Lombardi, G., Sidhu, S., Batchelor, J.R. & Lechler, R.I. Allorecognition of DR1 by T cells from a DR4/DRw13 responder mimics self-restricted recognition of endogenous peptides. *Proc Natl Acad Sci U S A* **86**, 4190-4 (1989).

176. Baker, R.J., Hernandez-Fuentes, M.P., Brookes, P.A., Chaudhry, A.N. & Lechler, R.I. The role of the allograft in the induction of donor-specific T cell hyporesponsiveness. *Transplantation* **72**, 480-5 (2001).

177. Benichou, G., Takizawa, P.A., Olson, C.A., McMillan, M. & Sercarz, E.E. Donor major histocompatibility complex (MHC) peptides are presented by recipient MHC molecules during graft rejection. *J Exp Med* **175**, 305-8 (1992).

178. Liu, Z. et al. Indirect recognition of donor HLA-DR peptides in organ allograft rejection. *J Clin Invest* **98**, 1150-7 (1996).

179. Herrera, O.B. et al. A novel pathway of alloantigen presentation by dendritic cells. *J Immunol* **173**, 4828-37 (2004).

180. Talmage, D.W., Dart, G., Radovich, J. & Lafferty, K.J. Activation of transplant immunity: effect of donor leukocytes on thyroid allograft rejection. *Science* **191**, 385-8 (1976).

181. Lechler, R.I. & Batchelor, J.R. Restoration of immunogenicity to passenger cell-depleted kidney allografts by the addition of donor strain dendritic cells. *J Exp Med* **155**, 31-41 (1982).

182. Larsen, C.P., Austyn, J.M. & Morris, P.J. The role of graft-derived dendritic leukocytes in the rejection of vascularized organ allografts. Recent findings on the migration and function of dendritic leukocytes after transplantation. *Ann Surg* **212**, 308-15; discussion 316-7 (1990).

183. Ciubotariu, R. et al. Persistent allopeptide reactivity and epitope spreading in chronic rejection of organ allografts. *J Clin Invest* **101**, 398-405 (1998).

184. Valujskikh, A. et al. T cells reactive to a single immunodominant self-restricted allopeptide induce skin graft rejection in mice. *J Clin Invest* **101**, 1398-407 (1998).

185. Vella, J.P. et al. Indirect allorecognition of major histocompatibility complex allopeptides in human renal transplant recipients with chronic graft dysfunction. *Transplantation* **64**, 795-800 (1997).

186. Frasca, L. et al. Role of donor and recipient antigen-presenting cells in priming and maintaining T cells with indirect allospecificity. *Transplantation* **66**, 1238-43 (1998).

187. Lee, R.S. et al. Indirect allorecognition promotes the development of cardiac allograft vasculopathy. *Transplant Proc* **33**, 308-10 (2001).

188. Reznik, S.I. et al. Indirect allorecognition of mismatched donor HLA class II peptides in lung transplant recipients with bronchiolitis obliterans syndrome. *Am J Transplant* **1**, 228-35 (2001).

189. Hornick, P.I. et al. Significant frequencies of T cells with indirect anti-donor specificity in heart graft recipients with chronic rejection. *Circulation* **101**, 2405-10 (2000).

190. Dalchau, R., Fangmann, J. & Fabre, J.W. Allorecognition of isolated, denatured chains of class I and class II major histocompatibility complex molecules. Evidence for an important role for indirect allorecognition in transplantation. *Eur J Immunol* **22**, 669-77 (1992).

191. Fangmann, J., Dalchau, R. & Fabre, J.W. Rejection of skin allografts by indirect allorecognition of donor class I major histocompatibility complex peptides. *J Exp Med* **175**, 1521-9 (1992).

192. Fangmann, J., Dalchau, R., Sawyer, G.J., Priestley, C.A. & Fabre, J.W. T cell recognition of donor major histocompatibility complex class I peptides during allograft rejection. *Eur J Immunol* **22**, 1525-30 (1992).

193. Auchincloss, H., Jr. et al. The role of "indirect" recognition in initiating rejection of skin grafts from major histocompatibility complex class II-deficient mice. *Proc Natl Acad Sci U S A* **90**, 3373-7 (1993).

194. Illigens, B.M. et al. The relative contribution of direct and indirect antigen recognition pathways to the alloresponse and graft rejection depends upon the nature of the transplant. *Hum Immunol* **63**, 912-25 (2002).

195. Steele, D.J. et al. Two levels of help for B cell alloantibody production. *J Exp Med* **183**, 699-703 (1996).

196. Terasaki, P.I. Humoral theory of transplantation. *Am J Transplant* **3**, 665-73 (2003).

197. Billingham, R.E., Brent, L. & Medawar, P.B. Actively acquired tolerance of foreign cells. *Nature* **172**, 603-6 (1953).

198. Sayegh, M.H. et al. Thymic recognition of class II major histocompatibility complex allopeptides induces donor-specific unresponsiveness to renal allografts. *Transplantation* **56**, 461-5 (1993).

199. Quezada, S.A. et al. Mechanisms of donor-specific transfusion tolerance: preemptive induction of clonal T-cell exhaustion via indirect presentation. *Blood* **102**, 1920-6 (2003).

200. Lair, D. et al. Functional compartmentalization following induction of long-term graft survival with pregraft donor-specific transfusion. *Am J Transplant* **7**, 538-49 (2007).

201. Bittencourt, M.C. et al. Intravenous injection of apoptotic leukocytes enhances bone marrow engraftment across major histocompatibility barriers. *Blood* **98**, 224-30 (2001).

202. Kleinclauss, F. et al. Intravenous apoptotic spleen cell infusion induces a TGF-beta-dependent regulatory T-cell expansion. *Cell Death Differ* **13**, 41-52 (2006).

203. Perruche, S. et al. Intravenous infusion of apoptotic cells simultaneously with allogeneic hematopoietic grafts alters anti-donor humoral immune responses. *Am J Transplant* **4**, 1361-5 (2004).

204. Sykes, M. & Sachs, D.H. Mixed chimerism. *Philos Trans R Soc Lond B Biol Sci* **356**, 707-26 (2001).

205. Sun, E. et al. Allograft tolerance induced by donor apoptotic lymphocytes requires phagocytosis in the recipient. *Cell Death Differ* **11**, 1258-64 (2004).

206. Barr, M.L. et al. Photopheresis for the prevention of rejection in cardiac transplantation. Photopheresis Transplantation Study Group. *N Engl J Med* **339**, 1744-51 (1998).

207. Wang, Z. et al. In situ-targeting of dendritic cells with donor-derived apoptotic cells restrains indirect allorecognition and ameliorates allograft vasculopathy. *PLoS ONE* **4**, e4940 (2009).

208. Emmer, P.M., van der Vlag, J., Adema, G.J. & Hilbrands, L.B. Dendritic cells activated by lipopolysaccharide after dexamethasone treatment induce donor-specific allograft hyporesponsiveness. *Transplantation* **81**, 1451-9 (2006).

209. Lan, Y.Y. et al. "Alternatively activated" dendritic cells preferentially secrete IL-10, expand Foxp3+CD4+ T cells, and induce long-term organ allograft survival in combination with CTLA4-Ig. *J Immunol* **177**, 5868-77 (2006).

210. O'Connell, P.J. et al. Immature and mature CD8alpha+ dendritic cells prolong the survival of vascularized heart allografts. *J Immunol* **168**, 143-54 (2002).

211. Tang, A.L., Bingaman, A.W., Kadavil, E.A., Leeser, D.B. & Farber, D.L. Generation and functional capacity of polyclonal alloantigen-specific memory CD4 T cells. *Am J Transplant* **6**, 1275-84 (2006).

212. Turnquist, H.R. et al. Rapamycin-conditioned dendritic cells are poor stimulators of allogeneic CD4+ T cells, but enrich for antigen-specific Foxp3+ T regulatory cells and promote organ transplant tolerance. *J Immunol* **178**, 7018-31 (2007).

213. Kamath, A.T. et al. The development, maturation, and turnover rate of mouse spleen dendritic cell populations. *J Immunol* **165**, 6762-70 (2000).

214. Taner, T., Hackstein, H., Wang, Z., Morelli, A.E. & Thomson, A.W. Rapamycin-treated, alloantigen-pulsed host dendritic cells induce ag-specific T cell regulation and prolong graft survival. *Am J Transplant* **5**, 228-36 (2005).

215. Xu, D.L. et al. Marked prolongation of murine cardiac allograft survival using recipient immature dendritic cells loaded with donor-derived apoptotic cells. *Scand J Immunol* **59**, 536-44 (2004).

216. Hokey, D.A., Larregina, A.T., Erdos, G., Watkins, S.C. & Falo, L.D., Jr. Tumor cell loaded type-1 polarized dendritic cells induce Th1-mediated tumor immunity. *Cancer Res* **65**, 10059-67 (2005).

217. Mailliard, R.B. et al. alpha-type-1 polarized dendritic cells: a novel immunization tool with optimized CTL-inducing activity. *Cancer Res* **64**, 5934-7 (2004).

218. Yu, G., Xu, X., Vu, M.D., Kilpatrick, E.D. & Li, X.C. NK cells promote transplant tolerance by killing donor antigen-presenting cells. *J Exp Med* **203**, 1851-8 (2006).

219. Tiffany, L.J., Garcia-Ojeda, P.A. & Stein, K.E. Determination of the IgG2a allotype of CXB recombinant inbred mouse strains by a PCR-based method. *Immunogenetics* **50**, 71-3 (1999).

220. Yano, Y. et al. Microchimeric cells from the peripheral blood associated with cardiac grafts are bone marrow derived, long-lived and maintain acquired tolerance to minor histocompatibility antigen H-Y. *Transplantation* **71**, 1456-62 (2001).

221. Bonilla, W.V. et al. Microchimerism maintains deletion of the donor cell-specific CD8+ T cell repertoire. *J Clin Invest* **116**, 156-62 (2006).

222. Liu, K. et al. Origin of dendritic cells in peripheral lymphoid organs of mice. *Nat Immunol* **8**, 578-83 (2007).

223. Min, W.P. et al. Dendritic cells genetically engineered to express Fas ligand induce donor-specific hyporesponsiveness and prolong allograft survival. *J Immunol* **164**, 161-7 (2000).

224. Zhang, X. et al. Generation of therapeutic dendritic cells and regulatory T cells for preventing allogeneic cardiac graft rejection. *Clin Immunol* **127**, 313-21 (2008).

225. Rovere, P. et al. Bystander apoptosis triggers dendritic cell maturation and antigen-presenting function. *J Immunol* **161**, 4467-71 (1998).

226. Ronchetti, A. et al. Immunogenicity of apoptotic cells in vivo: role of antigen load, antigen-presenting cells, and cytokines. *J Immunol* **163**, 130-6 (1999).

227. Abe, M., Wang, Z., de Creus, A. & Thomson, A.W. Plasmacytoid dendritic cell precursors induce allogeneic T-cell hyporesponsiveness and prolong heart graft survival. *Am J Transplant* **5**, 1808-19 (2005).

228. Bjorck, P., Coates, P.T., Wang, Z., Duncan, F.J. & Thomson, A.W. Promotion of long-term heart allograft survival by combination of mobilized donor plasmacytoid dendritic cells and anti-CD154 monoclonal antibody. *J Heart Lung Transplant* **24**, 1118-20 (2005).

229. Fugier-Vivier, I.J. et al. Plasmacytoid precursor dendritic cells facilitate allogeneic hematopoietic stem cell engraftment. *J Exp Med* **201**, 373-83 (2005).

230. Kang, H.K., Liu, M. & Datta, S.K. Low-dose peptide tolerance therapy of lupus generates plasmacytoid dendritic cells that cause expansion of autoantigen-specific regulatory T cells and contraction of inflammatory Th17 cells. *J Immunol* **178**, 7849-58 (2007).

231. Steptoe, R.J., Ritchie, J.M., Jones, L.K. & Harrison, L.C. Autoimmune diabetes is suppressed by transfer of proinsulin-encoding Gr-1+ myeloid progenitor cells that differentiate in vivo into resting dendritic cells. *Diabetes* **54**, 434-42 (2005).

232. Dalgaard, J., Beckstrom, K.J., Jahnsen, F.L. & Brinchmann, J.E. Differential capability for phagocytosis of apoptotic and necrotic leukemia cells by human peripheral blood dendritic cell subsets. *J Leukoc Biol* **77**, 689-98 (2005).

233. Marino, E. et al. Marginal zone B cells of Non-obese diabetic mice expand with diabetes onset, invade the pancreatic lymph nodes and present auto-antigen to diabetogenic T cells. *Diabetes* (2007).

234. Menges, M. et al. Repetitive injections of dendritic cells matured with tumor necrosis factor alpha induce antigen-specific protection of mice from autoimmunity. *J Exp Med* **195**, 15-21 (2002).

235. Wise, M.P., Bemelman, F., Cobbold, S.P. & Waldmann, H. Linked suppression of skin graft rejection can operate through indirect recognition. *J Immunol* **161**, 5813-6 (1998).

236. Carvalho-Gaspar, M. et al. Location and time-dependent control of rejection by regulatory T cells culminates in a failure to generate memory T cells. *J Immunol* **180**, 6640-8 (2008).

237. Lee, R.S., Grusby, M.J., Glimcher, L.H., Winn, H.J. & Auchincloss, H., Jr. Indirect recognition by helper cells can induce donor-specific cytotoxic T lymphocytes in vivo. *J Exp Med* **179**, 865-72 (1994).

238. Mandelbrot, D.A. et al. Expression of B7 molecules in recipient, not donor, mice determines the survival of cardiac allografts. *J Immunol* **163**, 3753-7 (1999).

239. Batchelor, J.R., Welsh, K.I., Maynard, A. & Burgos, H. Failure of long surviving, passively enhanced kidney allografts to provoke T-dependent alloimmunity. I. Retransplantation of (AS X AUG)F1 kidneys into secondary AS recipients. *J Exp Med* **150**, 455-64 (1979).

240. Lechler, R.I. & Batchelor, J.R. Immunogenicity of retransplanted rat kidney allografts. Effect of inducing chimerism in the first recipient and quantitative studies on immunosuppression of the second recipient. *J Exp Med* **156**, 1835-41 (1982).

241. Welsh, K.I., Batchelor, J.R., Maynard, A. & Burgos, H. Failure of long surviving, passively enhanced kidney allografts to provoke T-dependent alloimmunity. II. Retransplantation of (AS X AUG)F1 kidneys from AS primary recipients into (AS X WF)F1 secondary hosts. *J Exp Med* **150**, 465-70 (1979).

242. Wang, Z. et al. Heart, but not skin, allografts from donors lacking Flt3 ligand exhibit markedly prolonged survival time. *J Immunol* **172**, 5924-30 (2004).

243. McKenzie, J.L., Beard, M.E. & Hart, D.N. Depletion of donor kidney dendritic cells prolongs graft survival. *Transplant Proc* **16**, 948-51 (1984).

244. McKenzie, J.L., Beard, M.E. & Hart, D.N. The effect of donor pretreatment on interstitial dendritic cell content and rat cardiac allograft survival. *Transplantation* **38**, 371-6 (1984).

245. Stegall, M.D. et al. Interstitial class II-positive cell depletion by donor pretreatment with gamma irradiation. Evidence of differential immunogenicity between vascularized cardiac allografts and islets. *Transplantation* **49**, 246-51 (1990).

246. Roussey-Kesler, G. et al. Exhaustive depletion of graft resident dendritic cells: marginally delayed rejection but strong alteration of graft infiltration. *Transplantation* **80**, 506-13 (2005).

247. Pietra, B.A., Wiseman, A., Bolwerk, A., Rizeq, M. & Gill, R.G. CD4 T cell-mediated cardiac allograft rejection requires donor but not host MHC class II. *J Clin Invest* **106**, 1003-10 (2000).

248. Qian, S. et al. Impact of donor MHC class I or class II antigen deficiency on first- and second-set rejection of mouse heart or liver allografts. *Immunology* **88**, 124-9 (1996).

249. Larsen, C.P., Morris, P.J. & Austyn, J.M. Migration of dendritic leukocytes from cardiac allografts into host spleens. A novel pathway for initiation of rejection. *J Exp Med* **171**, 307-14 (1990).

250. Lakkis, F.G., Arakelov, A., Konieczny, B.T. & Inoue, Y. Immunologic 'ignorance' of vascularized organ transplants in the absence of secondary lymphoid tissue. *Nat Med* **6**, 686-8 (2000).

251. Bronte, V. et al. IL-4-induced arginase 1 suppresses alloreactive T cells in tumor-bearing mice. *J Immunol* **170**, 270-8 (2003).

252. Bronte, V., Serafini, P., Mazzoni, A., Segal, D.M. & Zanovello, P. L-arginine metabolism in myeloid cells controls T-lymphocyte functions. *Trends Immunol* **24**, 302-6 (2003).

253. Abdi, R. et al. Differential role of CCR2 in islet and heart allograft rejection: tissue specificity of chemokine/chemokine receptor function in vivo. *J Immunol* **172**, 767-75 (2004).

254. Ochando, J.C. et al. Alloantigen-presenting plasmacytoid dendritic cells mediate tolerance to vascularized grafts. *Nat Immunol* **7**, 652-62 (2006).

255. Blasius, A.L. et al. Bone marrow stromal cell antigen 2 is a specific marker of type I IFN-producing cells in the naive mouse, but a promiscuous cell surface antigen following IFN stimulation. *J Immunol* **177**, 3260-5 (2006).

256. Serbina, N.V. & Pamer, E.G. Monocyte emigration from bone marrow during bacterial infection requires signals mediated by chemokine receptor CCR2. *Nat Immunol* **7**, 311-7 (2006).

257. Holan, V., Krulova, M., Zajicova, A. & Pindjakova, J. Nitric oxide as a regulatory and effector molecule in the immune system. *Mol Immunol* **38**, 989-95 (2002).

258. Abdallah, A.N. et al. Evaluation of plasma levels of tumour necrosis factor alpha and interleukin-6 as rejection markers in a cohort of 142 heart-grafted patients followed by endomyocardial biopsy. *Eur Heart J* **18**, 1024-9 (1997).

259. Imagawa, D.K. et al. The role of tumor necrosis factor in allograft rejection. III. Evidence that anti-TNF antibody therapy prolongs allograft survival in rats with acute rejection. *Transplantation* **51**, 57-62 (1991).

260. Fu, F. et al. Costimulatory molecule-deficient dendritic cell progenitors (MHC class II+, CD80dim, CD86-) prolong cardiac allograft survival in nonimmunosuppressed recipients. *Transplantation* **62**, 659-65 (1996).

261. Bluestone, J.A., Thomson, A.W., Shevach, E.M. & Weiner, H.L. What does the future hold for cell-based tolerogenic therapy? *Nat Rev Immunol* **7**, 650-4 (2007).

262. Hendricks, R.L., Epstein, R.J. & Tumpey, T. The effect of cellular immune tolerance to HSV-1 antigens on the immunopathology of HSV-1 keratitis. *Invest Ophthalmol Vis Sci* **30**, 105-15 (1989).

263. Tumpey, T.M., Chen, S.H., Oakes, J.E. & Lausch, R.N. Neutrophil-mediated suppression of virus replication after herpes simplex virus type 1 infection of the murine cornea. *J Virol* **70**, 898-904 (1996).

264. Shimeld, C., Whiteland, J.L., Nicholls, S.M., Easty, D.L. & Hill, T.J. Immune cell infiltration in corneas of mice with recurrent herpes simplex virus disease. *J Gen Virol* **77 (Pt 5)**, 977-85 (1996).

265. Tumpey, T.M., Cheng, H., Yan, X.T., Oakes, J.E. & Lausch, R.N. Chemokine synthesis in the HSV-1-infected cornea and its suppression by interleukin-10. *J Leukoc Biol* **63**, 486-92 (1998).

266. Yan, X.T., Tumpey, T.M., Kunkel, S.L., Oakes, J.E. & Lausch, R.N. Role of MIP-2 in neutrophil migration and tissue injury in the herpes simplex virus-1-infected cornea. *Invest Ophthalmol Vis Sci* **39**, 1854-62 (1998).

267. Hendricks, R.L. & Tumpey, T.M. Concurrent regeneration of T lymphocytes and susceptibility to HSV-1 corneal stromal disease. *Curr Eye Res* **10 Suppl**, 47-53 (1991).

268. Metcalf, J.F., Hamilton, D.S. & Reichert, R.W. Herpetic keratitis in athymic (nude) mice. *Infect Immun* **26**, 1164-71 (1979).

269. Russell, R.G., Nasisse, M.P., Larsen, H.S. & Rouse, B.T. Role of T-lymphocytes in the pathogenesis of herpetic stromal keratitis. *Invest Ophthalmol Vis Sci* **25**, 938-44 (1984).

270. Newell, C.K., Martin, S., Sendele, D., Mercadal, C.M. & Rouse, B.T. Herpes simplex virus-induced stromal keratitis: role of T-lymphocyte subsets in immunopathology. *J Virol* **63**, 769-75 (1989).

271. Thomas, J., Gangappa, S., Kanangat, S. & Rouse, B.T. On the essential involvement of neutrophils in the immunopathologic disease: herpetic stromal keratitis. *J Immunol* **158**, 1383-91 (1997).

272. Hendricks, R.L., Tumpey, T.M. & Finnegan, A. IFN-gamma and IL-2 are protective in the skin but pathologic in the corneas of HSV-1-infected mice. *J Immunol* **149**, 3023-8 (1992).

273. Stumpf, T.H., Shimeld, C., Easty, D.L. & Hill, T.J. Cytokine production in a murine model of recurrent herpetic stromal keratitis. *Invest Ophthalmol Vis Sci* **42**, 372-8 (2001).

274. Tang, Q. & Hendricks, R.L. Interferon gamma regulates platelet endothelial cell adhesion molecule 1 expression and neutrophil infiltration into herpes simplex virus-infected mouse corneas. *J Exp Med* **184**, 1435-47 (1996).

275. Tang, Q., Chen, W. & Hendricks, R.L. Proinflammatory functions of IL-2 in herpes simplex virus corneal infection. *J Immunol* **158**, 1275-83 (1997).

276. Maertzdorf, J., Osterhaus, A.D. & Verjans, G.M. IL-17 expression in human herpetic stromal keratitis: modulatory effects on chemokine production by corneal fibroblasts. *J Immunol* **169**, 5897-903 (2002).

277. Banerjee, K., Biswas, P.S., Kim, B., Lee, S. & Rouse, B.T. CXCR2-/- mice show enhanced susceptibility to herpetic stromal keratitis: a role for IL-6-induced neovascularization. *J Immunol* **172**, 1237-45 (2004).

278. Biswas, P.S., Banerjee, K., Kinchington, P.R. & Rouse, B.T. Involvement of IL-6 in the paracrine production of VEGF in ocular HSV-1 infection. *Exp Eye Res* **82**, 46-54 (2006).

279. Cohen, T., Nahari, D., Cerem, L.W., Neufeld, G. & Levi, B.Z. Interleukin 6 induces the expression of vascular endothelial growth factor. *J Biol Chem* **271**, 736-41 (1996).

280. Fenton, R.R., Molesworth-Kenyon, S., Oakes, J.E. & Lausch, R.N. Linkage of IL-6 with neutrophil chemoattractant expression in virus-induced ocular inflammation. *Invest Ophthalmol Vis Sci* **43**, 737-43 (2002).

281. Heiligenhaus, A., Li, H., Schmitz, A., Wasmuth, S. & Bauer, D. Improvement of herpetic stromal keratitis with fumaric acid derivate is associated with systemic induction of T helper 2 cytokines. *Clin Exp Immunol* **142**, 180-7 (2005).

282. Suvas, S., Azkur, A.K., Kim, B.S., Kumaraguru, U. & Rouse, B.T. CD4+CD25+ regulatory T cells control the severity of viral immunoinflammatory lesions. *J Immunol* **172**, 4123-32 (2004).

283. Tumpey, T.M., Elner, V.M., Chen, S.H., Oakes, J.E. & Lausch, R.N. Interleukin-10 treatment can suppress stromal keratitis induced by herpes simplex virus type 1. *J Immunol* **153**, 2258-65 (1994).

284. Shirane, J. et al. Corneal epithelial cells and stromal keratocytes efficently produce CC chemokine-ligand 20 (CCL20) and attract cells expressing its receptor CCR6 in mouse herpetic stromal keratitis. *Curr Eye Res* **28**, 297-306 (2004).

285. Wuest, T. et al. Intact TRL 9 and type I interferon signaling pathways are required to augment HSV-1 induced corneal CXCL9 and CXCL10. *J Neuroimmunol* **179**, 46-52 (2006).

286. Wuest, T., Farber, J., Luster, A. & Carr, D.J. CD4+ T cell migration into the cornea is reduced in CXCL9 deficient but not CXCL10 deficient mice following herpes simplex virus type 1 infection. *Cell Immunol* **243**, 83-9 (2006).

287. Carr, D.J., Chodosh, J., Ash, J. & Lane, T.E. Effect of anti-CXCL10 monoclonal antibody on herpes simplex virus type 1 keratitis and retinal infection. *J Virol* **77**, 10037-46 (2003).

288. Chen, H. & Hendricks, R.L. B7 costimulatory requirements of T cells at an inflammatory site. *J Immunol* **160**, 5045-52 (1998).

289. O'Garra, A. & Vieira, P. T(H)1 cells control themselves by producing interleukin-10. *Nat Rev Immunol* **7**, 425-8 (2007).

290. Niemialtowski, M.G. & Rouse, B.T. Predominance of Th1 cells in ocular tissues during herpetic stromal keratitis. *J Immunol* **149**, 3035-9 (1992).

291. Niemialtowski, M.G., Godfrey, V.L. & Rouse, B.T. Quantitative studies on CD4+ and CD8+ cytotoxic T lymphocyte responses against herpes simplex virus type 1 in normal and beta 2-m deficient mice. *Immunobiology* **190**, 183-94 (1994).

292. Kim, B. et al. Vascular endothelial growth factor receptor 2-based DNA immunization delays development of herpetic stromal keratitis by antiangiogenic effects. *J Immunol* **177**, 4122-31 (2006).

293. Philipp, W., Speicher, L. & Humpel, C. Expression of vascular endothelial growth factor and its receptors in inflamed and vascularized human corneas. *Invest Ophthalmol Vis Sci* **41**, 2514-22 (2000).

294. Zheng, M., Deshpande, S., Lee, S., Ferrara, N. & Rouse, B.T. Contribution of vascular endothelial growth factor in the neovascularization process during the pathogenesis of herpetic stromal keratitis. *J Virol* **75**, 9828-35 (2001).

295. Zheng, M., Schwarz, M.A., Lee, S., Kumaraguru, U. & Rouse, B.T. Control of stromal keratitis by inhibition of neovascularization. *Am J Pathol* **159**, 1021-9 (2001).

296. Lee, S., Zheng, M., Kim, B. & Rouse, B.T. Role of matrix metalloproteinase-9 in angiogenesis caused by ocular infection with herpes simplex virus. *J Clin Invest* **110**, 1105-11 (2002).

297. Wolf, S.F. et al. Cloning of cDNA for natural killer cell stimulatory factor, a heterodimeric cytokine with multiple biologic effects on T and natural killer cells. *J Immunol* **146**, 3074-81 (1991).

298. Heinzel, F.P., Rerko, R.M., Ahmed, F. & Pearlman, E. Endogenous IL-12 is required for control of Th2 cytokine responses capable of exacerbating leishmaniasis in normally resistant mice. *J Immunol* **155**, 730-9 (1995).

299. Oppmann, B. et al. Novel p19 protein engages IL-12p40 to form a cytokine, IL-23, with biological activities similar as well as distinct from IL-12. *Immunity* **13**, 715-25 (2000).

300. Aggarwal, S., Ghilardi, N., Xie, M.H., de Sauvage, F.J. & Gurney, A.L. Interleukin-23 promotes a distinct CD4 T cell activation state characterized by the production of interleukin-17. *J Biol Chem* **278**, 1910-4 (2003).

301. Ling, P. et al. Human IL-12 p40 homodimer binds to the IL-12 receptor but does not mediate biologic activity. *J Immunol* **154**, 116-27 (1995).

302. Piccotti, J.R., Chan, S.Y., Li, K., Eichwald, E.J. & Bishop, D.K. Differential effects of IL-12 receptor blockade with IL-12 p40 homodimer on the induction of CD4+ and CD8+ IFN-gamma-producing cells. *J Immunol* **158**, 643-8 (1997).

303. Khader, S.A. et al. Interleukin 12p40 is required for dendritic cell migration and T cell priming after Mycobacterium tuberculosis infection. *J Exp Med* **203**, 1805-15 (2006).

304. Russell, T.D. et al. IL-12 p40 homodimer-dependent macrophage chemotaxis and respiratory viral inflammation are mediated through IL-12 receptor beta 1. *J Immunol* **171**, 6866-74 (2003).

305. Nieuwenhuis, E.E. et al. Disruption of T helper 2-immune responses in Epstein-Barr virus-induced gene 3-deficient mice. *Proc Natl Acad Sci U S A* **99**, 16951-6 (2002).

306. Collison, L.W. et al. The inhibitory cytokine IL-35 contributes to regulatory T-cell function. *Nature* **450**, 566-9 (2007).

307. Pflanz, S. et al. IL-27, a heterodimeric cytokine composed of EBI3 and p28 protein, induces proliferation of naive CD4(+) T cells. *Immunity* **16**, 779-90 (2002).

308. Mercadal, C.M., Bouley, D.M., DeStephano, D. & Rouse, B.T. Herpetic stromal keratitis in the reconstituted scid mouse model. *J Virol* **67**, 3404-8 (1993).

309. Babu, J.S. et al. Viral replication is required for induction of ocular immunopathology by herpes simplex virus. *J Virol* **70**, 101-7 (1996).

310. Keadle, T.L. et al. Cytokine expression in murine corneas during recurrent herpetic stromal keratitis. *Ocul Immunol Inflamm* **9**, 193-205 (2001).

311. Keadle, T.L. & Stuart, P.M. Interleukin-10 (IL-10) ameliorates corneal disease in a mouse model of recurrent herpetic keratitis. *Microb Pathog* **38**, 13-21 (2005).

312. Duan, R., Remeijer, L., van Dun, J.M., Osterhaus, A.D. & Verjans, G.M. Granulocyte macrophage colony-stimulating factor expression in human herpetic stromal keratitis: implications for the role of neutrophils in HSK. *Invest Ophthalmol Vis Sci* **48**, 277-84 (2007).

313. Kanangat, S., Thomas, J., Gangappa, S., Babu, J.S. & Rouse, B.T. Herpes simplex virus type 1-mediated up-regulation of IL-12 (p40) mRNA expression. Implications in immunopathogenesis and protection. *J Immunol* **156**, 1110-6 (1996).

314. Kumaraguru, U. & Rouse, B.T. The IL-12 response to herpes simplex virus is mainly a paracrine response of reactive inflammatory cells. *J Leukoc Biol* **72**, 564-70 (2002).

315. Al-Khatib, K., Campbell, I.L. & Carr, D.J. Resistance to ocular herpes simplex virus type 1 infection in IL-12 transgenic mice. *J Neuroimmunol* **132**, 41-8 (2002).

316. Osorio, Y., Wechsler, S.L., Nesburn, A.B. & Ghiasi, H. Reduced severity of HSV-1-induced corneal scarring in IL-12-deficient mice. *Virus Res* **90**, 317-26 (2002).

317. Kim, B., Sarangi, P.P., Azkur, A.K., Kaistha, S.D. & Rouse, B.T. Enhanced viral immunoinflammatory lesions in mice lacking IL-23 responses. *Microbes Infect* **10**, 302-12 (2008).

318. Liu, T., Khanna, K.M., Chen, X., Fink, D.J. & Hendricks, R.L. CD8(+) T cells can block herpes simplex virus type 1 (HSV-1) reactivation from latency in sensory neurons. *J Exp Med* **191**, 1459-66 (2000).

319. Lepisto, A.J., Frank, G.M., Xu, M., Stuart, P.M. & Hendricks, R.L. CD8 T cells mediate transient herpes stromal keratitis in CD4-deficient mice. *Invest Ophthalmol Vis Sci* **47**, 3400-9 (2006).

320. Divito, S.J. & Hendricks, R.L. Activated inflammatory infiltrate in HSV-1-infected corneas without herpes stromal keratitis. *Invest Ophthalmol Vis Sci* **49**, 1488-95 (2008).

321. Lee, S.K. et al. MCP-1 derived from stromal keratocyte induces corneal infiltration of CD4+ T cells in herpetic stromal keratitis. *Mol Cells* **26**, 67-73 (2008).

322. Bettelli, E. et al. Reciprocal developmental pathways for the generation of pathogenic effector TH17 and regulatory T cells. *Nature* **441**, 235-8 (2006).

323. Veldhoen, M., Hocking, R.J., Atkins, C.J., Locksley, R.M. & Stockinger, B. TGFbeta in the context of an inflammatory cytokine milieu supports de novo differentiation of IL-17-producing T cells. *Immunity* **24**, 179-89 (2006).

324. Jampel, H.D., Roche, N., Stark, W.J. & Roberts, A.B. Transforming growth factor-beta in human aqueous humor. *Curr Eye Res* **9**, 963-9 (1990).

325. Wilson, S.E., Schultz, G.S., Chegini, N., Weng, J. & He, Y.G. Epidermal growth factor, transforming growth factor alpha, transforming growth factor beta, acidic fibroblast growth factor, basic fibroblast growth factor, and interleukin-1 proteins in the cornea. *Exp Eye Res* **59**, 63-71 (1994).

326. Kim, B. et al. Depletion of MCP-1 increases development of herpetic stromal keratitis by innate immune modulation. *J Leukoc Biol* **80**, 1405-15 (2006).

327. Thomas, J., Kanangat, S. & Rouse, B.T. Herpes simplex virus replication-induced expression of chemokines and proinflammatory cytokines in the eye: implications in herpetic stromal keratitis. *J Interferon Cytokine Res* **18**, 681-90 (1998).

328. Tumpey, T.M. et al. Absence of macrophage inflammatory protein-1alpha prevents the development of blinding herpes stromal keratitis. *J Virol* **72**, 3705-10 (1998).

329. Gubler, U. et al. Coexpression of two distinct genes is required to generate secreted bioactive cytotoxic lymphocyte maturation factor. *Proc Natl Acad Sci U S A* **88**, 4143-7 (1991).